

# REPORT DOCUMENTATION PAGE

Form Approved  
OMB No. 0704-0188

Instructions: This form is to be filled out by the person or persons responsible for the collection of information and is to be submitted to the person or persons responsible for reviewing instructions, searching existing data sources, gathering information, and completing and reviewing the collection of information. Send comments regarding this burden estimate or any other aspect of this collection of information, including suggestions for reducing this burden, to Washington Headquarters Services, Directorate for Information Operations and Reports, 1215 Jefferson Davis Highway, Suite 1204, Arlington, VA 22202-4302, and to the Office of Management and Budget, Paperwork Reduction Project (0704-0188), Washington, DC 20503.

1. AGENCY USE ONLY (Leave blank)		2. REPORT DATE 1990	3. REPORT TYPE AND DATES COVERED <del>THE</del> DISSERTATION	
4. TITLE AND SUBTITLE Dynamic Response of Composite Beams Using Shear-Deformable Finite Elements			5. FUNDING NUMBERS	
6. AUTHOR(S) Stephen Robert Whitehouse				
7. PERFORMING ORGANIZATION NAME(S) AND ADDRESS(ES) AFIT Student Attending: University of Illinois at Urbana-Champaign			8. PERFORMING ORGANIZATION REPORT NUMBER AFIT/CI/CIA-90-0286	
9. SPONSORING / MONITORING AGENCY NAME(S) AND ADDRESS(ES) AFIT/CI Wright-Patterson AFB OH 45433-6583			10. SPONSORING / MONITORING AGENCY REPORT NUMBER	
11. SUPPLEMENTARY NOTES				
12a. DISTRIBUTION / AVAILABILITY STATEMENT Approved for Public Release IAW 190-1 Distributed Unlimited ERNEST A. HAYGOOD, 1st Lt, USAF Executive Officer			12b. DISTRIBUTION CODE	
13. ABSTRACT (Maximum 200 words)				
<div data-bbox="941 1400 1280 1698" data-label="Text"> <p>DTIC ELECTE NOV 02 1990 S B D</p> </div>				
14. SUBJECT TERMS			15. NUMBER OF PAGES 233	
			16. PRICE CODE	
17. SECURITY CLASSIFICATION OF REPORT	18. SECURITY CLASSIFICATION OF THIS PAGE	19. SECURITY CLASSIFICATION OF ABSTRACT	20. LIMITATION OF ABSTRACT	

AD-A227 975

DTIC FILE COPY

DYNAMIC ANALYSIS OF COMPOSITE BEAMS  
USING SHEAR-DEFORMABLE FINITE ELEMENTS

BY

STEPHEN ROBERT WHITEHOUSE

B.S., United States Air Force Academy, 1978  
M.S., Columbia University, 1979

THESIS

Submitted in partial fulfillment of the requirements  
for the degree of Doctor of Philosophy in Theoretical and Applied Mechanics  
in the Graduate College of the  
University of Illinois at Urbana-Champaign, 1990

Urbana, Illinois

UNIVERSITY OF ILLINOIS AT URBANA-CHAMPAIGN

THE GRADUATE COLLEGE

AUGUST 1990

WE HEREBY RECOMMEND THAT THE THESIS BY

STEPHEN ROBERT WHITEHOUSE

ENTITLED DYNAMIC ANALYSIS OF COMPOSITE BEAMS USING SHEAR - DEFORMABLE  
FINITE ELEMENTS

BE ACCEPTED IN PARTIAL FULFILLMENT OF THE REQUIREMENTS FOR  
THE DEGREE OF DOCTOR OF PHILOSOPHY

*Robert E. Miller*

Director of Thesis Research

*Frank J. Rizzo*

Head of Department

Committee on Final Examination†

*Robert E. Miller*

Chairperson

*William K. Allen*

*I. O. Pawson*

† Required for doctor's degree but not for master's.

## DYNAMIC RESPONSE OF COMPOSITE BEAMS USING SHEAR-DEFORMABLE FINITE ELEMENTS

Stephen Robert Whitehouse, Ph.D.  
Department of Theoretical and Applied Mechanics  
University of Illinois at Urbana-Champaign  
R. Miller, Advisor

The goal of this effort is to develop shear-deformable finite elements which can be used to find the natural frequencies of composite beams. The first objective of the study is to derive the mass and stiffness matrices for the elements of interest and incorporate them into computer programs which can be used to estimate the natural frequencies of composite beams. Composite beams of interest include sandwich beams and those of fiber-reinforced laminated construction. Elements based on the beam theories of Bernoulli-Euler, Timoshenko, Levinson-Bickford, as well as a general third-order beam theory are considered. The elements ignore transverse normal strain, coupling between longitudinal and lateral motion caused by Poisson effects, and damping, and are limited to linear, elastic materials. However, both isotropic and orthotropic layers in symmetric and nonsymmetric configurations can be accommodated. In addition, the elements can impose a kinematic constraint on the entire beam or on individual layers within the beam. This study refers to elements which employ the latter approach as "stacked elements".

The second objective is to evaluate the performance of the elements to determine when higher-order elements, including stacked elements, are needed to account for the effect of shear deformation on the natural frequencies of composite beams. Efforts associated with this objective indicate all elements developed are accurate within the limits of their respective theories. All elements possess good monotonic convergence properties and do not lock in the thin-beam limit.

In addition, the evaluation reveals that the Bernoulli-Euler beam element is generally limited to cases involving the lower natural frequencies of long, slender beams made out of homogeneous materials having a low degree of orthotropy. (The degree of orthotropy is given by the ratio of

Young's modulus in the longitudinal direction to the transverse shear modulus in the plane of the beam.) The Timoshenko beam element can be used effectively for homogeneous and composite beams possessing fairly high degrees of orthotropy if the analyst is able to choose an appropriate value for the shear correction factor associated with Timoshenko's theory. The Levinson-Bickford theory does not require a correction factor, and the element based on this theory can be used with confidence as long as the degree of orthotropy is not too high. As the degree of orthotropy increases, the analyst must rely on the third-order element to attain an adequate level of accuracy.

Finally, it is found that stacked elements must be used in the analysis of sandwich beams when the shear modulus of the facings is much larger than the shear modulus of the core. In addition to this condition, the facings must be thick enough to prevent the deformation of the core from dominating the strain energy of the beam.



Accession For	
NTIS GRA&I	<input checked="" type="checkbox"/>
DTIC TAB	<input type="checkbox"/>
Unannounced	<input type="checkbox"/>
Justification	
By	
Distribution/	
Availability Codes	
Dist	Avail and/or Special
A-1	

## DEDICATION

This work is dedicated to

my Lord and Savior, Jesus Christ, in whom are hidden all the treasures of wisdom and knowledge,

my father, Robert, and mother, Dorothy, who taught me early that the fear of the Lord is the beginning of wisdom,

and to my wife, Diana, and son, John, whose love and companionship are daily reminders of God's goodness to me.

## ACKNOWLEDGMENTS

The author wishes to thank his advisor, Professor Robert E. Miller, for the expert technical guidance and encouraging personal support provided throughout the course of this research effort. The author would also like to thank Professor James W. Phillips for his kind assistance in the computer-related aspects of the preparation of the manuscript and for the contributions he made to improving the manuscript's format. A debt of gratitude is indeed owed to Ms. Janet K. Weaver, whose expert typing was indispensable in the preparation of the manuscript. In addition, the author would like to mention that the service provided by the staffs of the University Library System and the Computing Service Office was a great help during this effort.

The author is very grateful to Colonel Cary Fisher, Professor and Head, Department of Engineering Mechanics, United States Air Force Academy, for providing the author with the opportunity to pursue doctoral studies at the University of Illinois in the Department of Theoretical and Applied Mechanics. The administrative support provided by the Air Force Institute of Technology at Wright-Patterson Air Force Base, Ohio, and by the Air Force ROTC Detachment at the University of Illinois is also acknowledged with appreciation.

Finally, the author wishes to thank his wife, Diana, and son, John, whose patience, understanding and support sustained the author throughout the time spent at the University of Illinois.

## TABLE OF CONTENTS

1. INTRODUCTION . . . . .	1
1.1 Background . . . . .	1
1.2 Literature Survey . . . . .	3
1.3 Objectives, Scope and Approach . . . . .	23
2. COMPOSITE BEAM THEORIES . . . . .	25
2.1 Assumptions . . . . .	25
2.2 Coordinate System . . . . .	26
2.3 Constitutive Relations . . . . .	28
2.4 Kinematic Constraints . . . . .	33
2.5 Governing Equations . . . . .	37
3. FINITE ELEMENT FORMULATION OF COMPOSITE BEAM THEORIES . . . . .	54
3.1 The Finite Element Method . . . . .	54
3.2 Governing Equations . . . . .	63
3.3 Mass and Stiffness Matrices . . . . .	69
3.4 Mass and Stiffness Matrices for Each Simple Element . . . . .	79
3.5 Mass and Stiffness Matrices for Stacked Elements . . . . .	94
3.6 Solution Procedure for Free Vibration Problems . . . . .	119
4. EVALUATION OF FINITE ELEMENTS . . . . .	123
4.1 Accuracy . . . . .	123
4.2 Shear Locking . . . . .	148



4.3 Evaluation of Accuracy Using Published Data . . . . .	150
4.4 Conditions Requiring Stacked Elements . . . . .	165
5. SUMMARY AND CONCLUSIONS . . . . .	169
5.1 Summary . . . . .	169
5.2 Conclusions . . . . .	175
APPENDIX . . . . .	177
LIST OF REFERENCES . . . . .	223
VITA . . . . .	233

## 1. INTRODUCTION

### 1.1. Background

Modern composites, which combine high strength and stiffness with light weight, have become very important structural materials. The added flexibility of designing the construction material as well as the structure itself leads to significant reductions in weight, since material is not used in directions or locations where it is not required. Such composite materials have obvious applications in aerospace structures, but are also being used in sports equipment, automobiles, and ships as well.

However, the behavior of composites is much harder to analyze than that of more homogeneous, isotropic materials. The inherent non-homogeneity of composites may lead to coupling between various response modes, such as stretching and bending. The anisotropy designed into composites also increases the complexity of analytical efforts. In addition, both the non-homogeneity and anisotropy of composites increase the number of failure modes which must be considered in composite design.

At the same time, analysis plays a more critical role in the design of composites. The number of combinations of design variables of interest is often too numerous to test. In addition, the complexity of composite behavior increases the cost of testing these materials. Therefore, analysis is often used to supplement test data since it may not be possible to generate experimentally all the data needed to design a composite material.

One phenomenon which can complicate the bending response of materials, particularly composite materials, is shear deformation. In pure bending, the lateral deflection of the material is caused primarily by the curvature developed by the material to generate the internal moments necessary to maintain rotational equilibrium. However, if the bending is caused by laterally applied

loads, then internal shear forces are also required to maintain translational equilibrium. The deformation associated with these shear forces, called shear deformation, produces a lateral deflection in addition to the bending deflection associated with the curvature.

In general, shear deformation increases the deflection and decreases the buckling loads and natural frequencies of beams, plates, and shells. The effects of this deformation increase as the span-to-thickness ratio of the bending element decreases, as the ratio between Young's modulus and the shear modulus increases, or as the mismatch of material properties in adjacent layers of layered materials increases.

Since classical theories for beams, plates, and shells cannot account directly for shear deformation, higher-order theories are required when the effects of shear deformation must be considered. These higher-order theories generally lead to a more complicated set of governing equations. Numerical methods, such as finite difference or finite element approaches, are often used to solve problems of practical interest, since exact analytical solutions are usually restricted to highly idealized cases. Therefore, much activity has been devoted to developing numerical techniques which can account for the effects of shear deformation in the bending response of beams, plates, and shells.

The goal of this present effort is to develop shear-deformable finite elements which can be used to find the natural frequencies of composite beams. A beam is usually defined as a structural member whose dimension in one direction (i.e., its length) is significantly greater than its dimensions in the other two orthogonal directions. The study of beams is motivated by their importance as structural elements and by the insight they give into the bending behavior of more complicated components, such as plates and shells.

Finite elements capable of analyzing natural frequencies are of interest for several reasons. The desire to avoid resonance provides perhaps the strongest motivation for developing such

elements. Driving a component at one of its natural frequencies produces the condition of resonance, in which the response of the component may become unbounded. Such a condition can be caused by machinery operating near the component of interest or possibly by aeroelastic effects. Even if resonance does not cause failure immediately, it can reduce the fatigue life of a member significantly. Therefore, a knowledge of natural frequencies is essential to avoid the problems associated with this phenomenon.

In addition, once it has been established that a finite element is capable of finding natural frequencies, the element itself can be used to solve forced-vibration problems with confidence since the validity of the element's mass and stiffness matrices should not be in question.

The elements discussed in this study can be used to estimate the natural frequencies of straight, prismatic beams of sandwich or fiber-reinforced laminate construction under a variety of end conditions.

## 1.2. Literature Survey

The formulation of the classical beam theory used today started with Galileo in the early 17th century and ended with the work of Daniel Bernoulli and Leonard Euler in the 18th century [1].<sup>1</sup> Developments in the theory of elasticity, also traced in [1], have provided a more thorough understanding of beam behavior.

In elasticity, solutions must satisfy equilibrium of stresses and compatibility of displacements, as well as the stress and displacement conditions on the boundary of the beam [2]. Solutions can be obtained by choosing an assumed displacement field, stress field, or potential function (from which stresses or displacements can be derived) which satisfies the governing equations and boundary conditions just mentioned.

---

<sup>1</sup> Numbers in brackets denote references in the List of References at the end of the thesis.

The static response of a three-dimensional beam in pure bending using an assumed stress field has been treated by Timoshenko and Goodier ([2], pp. 284-288) and Love [3] for isotropic beams and by Lekhnitskii [4] for anisotropic beams. More complicated problems in three dimensions require the use of an unknown stress function in the assumed stress field (see [2], pp. 354-379).

Potential functions are often used to analyze the static behavior of beams in plane stress or plane strain. As discussed in [2] (pp. 35-53), potential functions can be expressed as polynomials of various degrees and used to solve many bending problems of interest. Expressing potential functions as Fourier-series expansions is also possible ([5] and [2], pp. 53-63). A systematic approach for picking polynomial functions was given by Neou [6] for isotropic beams and by Hashin [7] for anisotropic beams. A potential function approach was also used by Schile [8] to treat non-homogeneous beams.

Although elasticity solutions for the static response of layered beams do not seem to be in the literature, solutions for layered plates, including plates in plane strain, have been published. Pagano [9] examined the response of simply supported orthotropic composite plates in cylindrical bending caused by static sinusoidal loading by assuming an independent stress field in each layer. A method based on assuming independent displacements in each layer was also developed by Pagano [10] for simply supported rectangular plates under sinusoidal loading. This displacement-based method was used by Pagano and Hatfield [11] to examine the influence of multiple layers (i.e., more than three layers) in the response of laminated plates.

Several authors have published elasticity solutions for vibration of homogeneous, isotropic beams. Timoshenko [12] solved the governing equations taken from Articles 14(d) and 204 of [3] by assuming fields for the rotation and cubical dilatation which are sinusoidal over the length of the beam, hyperbolic through its thickness, and harmonic in time. Forcing the assumed field to satisfy the traction-free boundary conditions on the lateral surfaces of the beam provides a

transcendental equation from which natural frequencies can be extracted. Cowper [13] employed a similar approach using assumed fields for the lateral and longitudinal displacements of the beam. Both solutions were developed to check the accuracy of approximate shear-deformation theories.

Elasticity solutions for the dynamic response of composite or sandwich beams are hard to find. However, several authors have extended the work of Pagano [9,10] to the free vibrations of composite plates, including plates in cylindrical bending. In 1970, Srinivas, Joga Rao, and Rao [14] presented an elasticity solution for laminated simply supported rectangular plates having isotropic layers. That same year, the method was extended by Srinivas and Rao [15] to similar plates made of orthotropic materials. Also in 1970 Jones [16] published a paper which discusses the elasticity solution for cross-ply laminates in cylindrical bending. Two years later, Kulkarni and Pagano [17] examined cross-ply and angle-ply laminates in cylindrical bending. In an effort similar to that of [11], Noor [18] examined the natural frequencies of multilayered plates using a finite difference formulation of the elasticity solution.

Since exact elasticity solutions are limited to highly idealized loading conditions and boundary conditions, and involve fairly difficult calculations, approximate theories are often used to examine cases involving other conditions of interest or to reduce the intensity of the calculational effort required to obtain reasonable results. Most approximate techniques assume a stress or displacement field which is simpler than the fields associated with elasticity solutions and may actually involve a truncation of a series expansion of the elasticity solution. In general, the governing equations are obtained using a strength-of-materials approach or an energy method.

In the strength-of-materials approach, the constitutive relations are expressed in terms of stress resultants, such as the internal shear and moment, and the equilibrium equations are derived in terms of these stress resultants. Natural boundary conditions are usually given in terms of these

resultants as well. In an energy formulation, unknown functions in the assumed fields are chosen to satisfy some variational principle, such as the principle of minimum potential energy for statics or Hamilton's principle for dynamics (see [19]).

An approximate technique based on an assumed stress field was developed for orthotropic beams under static loading by Rehfield and Murthy [20] in 1982. The assumed field is taken from the elasticity solution for a simply supported isotropic beam under a uniform static load (see [2], pp. 46-50), and is extended to orthotropic beams under a variety of end conditions.

In 1986, Suzuki [21] presented an approximate static theory which is based on an assumed stress field which satisfies equilibrium and natural boundary conditions. Governing equations for the unknown functions in the field are obtained by forcing the internal strain energy to be a minimum.

Although assumed distributions of stress can be used to solve problems involving beams under static loading, dynamic response is usually obtained from displacement-based theories. The most elementary approximate beam theory is Bernoulli-Euler beam theory alluded to at the start of this survey. Although not necessarily formulated originally in terms of an assumed displacement field, or kinematic constraint, the development of this theory required an understanding of how a beam deforms longitudinally in bending (see [1]). Today, the kinematic constraint can be derived from the assumptions that sections which are originally plane and perpendicular to the neutral surface of the beam before bending remain plane and perpendicular to the neutral surface after bending. These assumptions allow bending deformation to occur, but ignore shear deformation.

The static response of Bernoulli-Euler beams is covered in just about any text on strength of materials (e.g., see [22]). As early as 1925, Timoshenko [23] used the theory to investigate the response of bimetallic strips used as thermostats. A more systematic treatment of Bernoulli-Euler sandwich beams is given by Allen [24], but even in this reference some estimate of the effect of shear deformation on lateral deflection is made using the shear stress obtained from equilibrium

considerations. Laminated beams have not received much attention in the literature, but many investigators have applied the analogous plate theory (Kirchoff plate theory) to problems involving laminated plates (see [25]).

Regarding the dynamic response of Bernoulli-Euler beams, Timoshenko, Young, and Weaver [26] provide a thorough review of the vibration of these beams. The effects of rotary inertia on beam vibration can be incorporated into the theory easily, which was done by Rayleigh in his classic *Theory of Sound* [27]. Although Bernoulli-Euler beam theory can be extended to treat the dynamic response of sandwich or laminated beams, its use in this area does not appear to be widespread in the literature. However, references which use Kirchoff theory to analyze the dynamic response of laminated plates are easy to find (e.g., [25] and [28]).

Bernoulli-Euler beam theory has proven to be extremely useful over the years. It is very easy to use and provides answers which are accurate enough for many engineering applications. However, when the effects of shear deformation become important, higher-order theories must be used.

The simplest improvement to Bernoulli-Euler beam theory which incorporates shear deformation, and rotary inertia as well, was presented in a paper by Timoshenko [29] in 1921. In this theory, sections which are plane and perpendicular to the neutral surface before bending remain plane but are not constrained to remain perpendicular to the neutral surface after bending occurs. Therefore, some approximate form of shear deformation is allowed explicitly by the theory.

Although this theory has come to be known as Timoshenko beam theory, it should be pointed out that the main features of the theory were outlined by others prior to the appearance of Timoshenko's paper in 1921. As stated above, the effects of rotary inertia were discussed by Rayleigh [27] in 1877. In addition, Rankine [30] addressed the influence of shear deformation on



static deflection in a work first published in 1858. Both rotary inertia and shear deformation were treated by Bresse [31] as early as 1859. The theory of Bresse, developed for curved beams, is summarized nicely in English in a history of elasticity written by Todhunter and Pearson [32].

Much of the literature on Timoshenko beams is devoted to vibrations, as was Timoshenko's paper. Both Anderson [33] and Dolph [34] investigated the free vibration of Timoshenko beams more thoroughly and identified a second mode of vibration associated with the shear deformation of the beam. A more complete examination was conducted by Huang [35] in 1961. This work provides the mode shapes and transcendental frequency equations for a variety of end conditions. Brunelle [36] extended Timoshenko beam theory to transversely isotropic beams under initial axial stress. His paper examines buckling of clamped and simply supported beams, free vibration of simply supported beams, and wave propagation in a beam of infinite length.

In 1976, Downs [37] re-examined the free vibration of isotropic Timoshenko beams and identified a third possible mode of response discarded as physically impossible by Dolph [34]. This mode involves transverse shear vibration with no transverse deflection, a mode which has been seen in finite element calculations. This mode was also discussed earlier by Mindlin and Deresiewicz [38] where it is referred to as thickness-shear motion.

Although Timoshenko beam theory can be extended easily to composite beams, references on this subject do not appear to be prevalent in the literature. However, the analogous plate theory discussed by Mindlin [39] has been extended to the vibration of composite plates by a number of investigators, including Yang, Norris, and Stavsky [40] and Whitney and Pagano [41].

The first-order estimate of shear deformation made possible by Timoshenko beam theory provides a dramatic improvement over results obtained using Bernoulli-Euler beam theory when shear deformation effects become important. This can be seen in the experimental work done by Traill-Nash and Collar [42] and Kordes and Kruszewski [43]. However, the assumptions of the

theory lead to shear strain which is constant over the depth of the beam. Since shear strain is actually distributed in some other fashion (e.g., parabolically), a correction factor is often used to allow Timoshenko beam theory to model shear deformation effects more accurately.

A number of schemes have been proposed for calculating this correction factor. Timoshenko himself suggested a value of  $2/3$  in [29]. This value allows the shear stress obtained from the theory to match the maximum stress associated with the standard parabolic distribution of shear stress for a beam of rectangular cross section. A value of  $5/6$  allows the strain energy from the Timoshenko beam theory to match the strain energy associated with the parabolic distribution of shear strain for a rectangular cross section (see [44]).

A more sophisticated treatment of the shear correction factor was given by Cowper in [45]. His expressions for this factor were obtained by accounting for the two-dimensional distribution of shear stress over the cross section of a beam given by three-dimensional elasticity theory. This approach accounts for Poisson's ratio and the shape of the cross section. The expression for a rectangular cross section with Poisson's ratio equal to zero reduces to the standard value of  $5/6$ .

Another expression for the correction factor which is popular for dynamic calculations was discussed by Mindlin and Deresiewicz in [38]. This reference states that since the distribution of shear strain varies with the mode of vibration, it may be necessary to allow the factor to vary with mode number. An expression which has proven useful at high and low frequencies for a variety of cross-sectional shapes can be derived by forcing the natural frequency of the thickness-shear mode for the Timoshenko beam to equal the natural frequency for this mode obtained using elasticity theory. The expression provides a value of  $\pi^2/12$  for a Timoshenko beam of rectangular cross section or for a Mindlin plate.

In addition to depending on Poisson's ratio, the shape of the cross section, and the mode of response, the shear correction factor is also sensitive to the non-homogeneity present in laminated materials. Methods for estimating correction factors for laminated beams and plates are presented in [46] and [47], respectively.

The desire to dispense with the necessity of calculating a correction factor for shear has provided the motivation for developing higher-order displacement-based theories that allow the shear strain to vary in some reasonable fashion over the cross section of the beam. These theories allow warping in the longitudinal direction so that initially plane sections are no longer required to remain plane after bending. This is achieved by expressing the longitudinal displacements as a truncated series involving unknown functions of the longitudinal coordinate times powers of the lateral coordinate. This concept was discussed as early as 1890 by Basset [48] in a paper on the extension and flexure of shells.

Perhaps the most general static theory for isotropic beams was given by Wang and Dickson [49]. In their paper, they suggested expressing both lateral and longitudinal displacements as power series expansions. This approach accounts for strain in the lateral direction (transverse normal strain), as well as shear deformation. The governing equations for the unknown functions in the assumed displacement field are obtained by satisfying equilibrium and enforcing boundary conditions.

Less ambitious higher-order kinematic constraints have been proposed by others. In addition to the stress-based theory discussed in [21], Suzuki [50] has developed a displacement-based theory which can be used to examine the bending and free vibration of beams. The theory, which ignores transverse normal strain and Poisson's effects, uses an approach similar to that in [21]. Suzuki claims that the advantage of his approach is that it satisfies equilibrium and energy considerations simultaneously, something most approximate methods do not do.

Another theory based on an assumed kinematic constraint has been proposed by Krishna Murty [51-55] in a series of papers. The theory allows warping in the longitudinal direction and divides the lateral deflection into bending and shear components. The governing equations are derived using an energy formulation. The theory was developed originally to examine the vibration of short beams [51], and was later extended to treat the bending and buckling of short beams [52], the free vibration of isotropic laminated beams [53], and the free vibration and steady-state response of soft-cored sandwich beams [55]. Improvements to the static theory presented in [52] are given in [54] by accounting for the static coupling between the lateral deflection caused by bending and the lateral deflection caused by shear. This coupling is ignored in [52].

Levinson beam theory [56,57] is similar to the approaches of Suzuki [50] and Krishna Murty [54], but is more straightforward in many ways. Levinson ignores transverse normal strain and Poisson's effects, but accounts for shear deformation with longitudinal displacement which varies linearly and cubically over the depth of the beam. The cubic, or third-order, variation in longitudinal displacement leads to a parabolic distribution of shear strain over the depth of the beam. In addition, the kinematic constraint is chosen to enforce the boundary condition of no shear strain on the lateral surfaces of the beam. The equations of motion are derived using a direct, or strength-of-materials approach and are very similar to the equations for a Timoshenko beam. However, no correction factor is required in Levinson beam theory.

In 1982, Bickford [58] used Levinson's kinematic constraint to develop a different set of governing equations using a variational procedure. It is interesting to note that the equations of motion for Bernoulli-Euler and Timoshenko beams are not sensitive to whether the direct method or an energy formulation is used in their derivation. This is not true for Levinson theory. As pointed out by Levinson in [59], the direct approach yields a fourth-order system of partial differential equations which can be solved fairly easily, whereas the use of energy methods yields a sixth-order system which is harder to work with.

As with Timoshenko beam theory, it appears that Levinson theory has not been applied directly to problems involving laminated or sandwich beams. However, Levinson did extend his theory to plates in [60], where the governing equations are developed using a direct strength-of-materials approach. Later, Reddy [61] formulated a plate theory based on Levinson's kinematic constraint, but used energy methods rather than the direct approach. The resulting theory was given a finite element formulation by Reddy and Khdeir [62], who used the element to examine the buckling and vibration of laminated plates. In addition to comparing the relative performance of theories of various order, this paper provides a good set of references on the response of laminated plates.

Other higher-order theories which allow a parabolic variation of shear strain over the depth of a beam have been proposed in connection with new finite elements developed for analyzing beam behavior. Included in this group are the works of Yuan and Miller [63], Kant and Gupta [64], and Kant and Manjunath [65], which are discussed in more detail later in this section.

The work of Lo, Christensen, and Wu [66] should also be mentioned. In this plate theory, higher-order kinematic constraints are used for both longitudinal and lateral displacement. This allows parabolic shear strain and linear transverse normal strain to develop through the thickness of both homogeneous and laminated plates.

In the beam and plate theories just discussed, higher-order effects are accounted for by imposing one kinematic constraint on the entire beam. Much analytical work has also been done to develop methods which allow each layer in a composite beam some degree of independent motion. This is achieved either explicitly with an independent kinematic constraint for each layer or less directly by accounting for various kinds of strain energy and kinetic energy in each layer. In the former approach, energy methods are often applied to obtain the governing equations, although some works use strength-of-materials techniques for this purpose.

The static response of sandwich plates was examined as early as 1947 by Reissner [67]. In this paper, Reissner summarized earlier work done to formulate a new theory which accounts for shear deformation (see [68,69]). Although not formulated explicitly in terms of a kinematic constraint, as is the theory of Mindlin [39], both approaches yield basically the same results and have come to be known as Reissner-Mindlin plate theory.

In addition to summarizing and clarifying his earlier work, in this paper Reissner extended his theory to sandwich plates with equal outer layers, or facings. His treatment accounts for bending, extension, and in-plane shear strain in the facings, and transverse shear strain in the core. The results show that the form of the equation for sandwich plates is identical to that for homogeneous plates provided that properties, such as the bending stiffness, are modified to account for the composite nature of the sandwich plate. Therefore, solutions obtained for homogeneous plates can be extended easily to sandwich plates simply by the proper modification of plate properties appearing in the governing equation.

In 1948, Hoff and Mautner [70] examined the bending and buckling response of sandwich beams experimentally and using an analytical technique which is quite representative of strain-energy approaches. Their theory considers the extension and bending strain energies of the facings as well as the strain energy associated with shear deformation and transverse compression of the core. This approach ignores shear deformation in the facings as well as axial extension and bending of the core. The governing equations come from application of a variational principle.

One of the earliest theories based on an explicit kinematic constraint for each layer was developed by Yu [71] in 1959 for sandwich plates in plane strain. The variational theory treats each layer essentially as a Mindlin plate, and involves the use of a correction factor. The theory is limited to symmetric sandwich beams since it assumes the rotations of each facing are equal.

Also in 1959, Kimel, Raville, Kirmser, and Patel [72] proposed a theory for the free vibration of simply supported sandwich beams based on assumptions very similar to those of Hoff and Mautner in [70]. In the theory of Kimel, et al., the facings are treated as homogeneous, isotropic thin elastic plates which can be of unequal thickness. The core is considered to be an orthotropic elastic material, but transverse normal strain in this layer is ignored. In addition, rotary inertia of all layers is ignored. Unknown stresses and displacements are expressed in terms of Fourier-series expansions and the governing equations are derived in terms of the unknown coefficients in the expansions using variational principles.

In 1961, Raville, Ueng, and Lei [73] extended this approach to fixed-fixed sandwich beams. Since the series expansion chosen for the lateral displacement does not satisfy the geometric boundary conditions for a fixed-fixed beam, the energy formulation makes use of the Lagrange multiplier method to enforce these boundary conditions.

The approach of Reissner [67] was extended to sandwich plates with orthotropic cores by Cheng [74] in 1962. A governing equation solely in terms of the lateral deflection is derived in addition to a system of equations in terms of the stress resultants, as given by Reissner [67].

Krajcinovic [75] has also developed a theory for symmetric sandwich beams which explicitly states the independent kinematic constraint for each layer. As with Yu [71], each layer is allowed an independent linear variation of longitudinal displacement. Unlike Yu, however, Krajcinovic allowed compression of the core and expressed the through-thickness variation of all displacements in terms of orthogonal mode shapes, and derived the governing equations using the principle of virtual work. In [76], Krajcinovic extended his static theory to the free vibration of undamped sandwich beams.

In 1973, DiTaranto [77] proposed a static theory for nonsymmetric sandwich beams. The theory, formulated using a variational principle, is based on assumptions very similar to other strain-energy approaches. In 1976, Rao [78] extended the work of DiTaranto [77] to cases where the core is stiff so that the strain energy associated with its extension and bending cannot be ignored.

A method for estimating the natural frequencies of cantilever sandwich beams was developed by Rubayi and Charoenree [79] in 1976. Although similar in general approach to the work of Kimel, et Al. [72], and Raville, et Al. [73] in that unknowns are expressed as series expansions, it is simpler in many respects. In particular, expressions for the shear strain of the core are obtained indirectly from equilibrium considerations, rather than directly from giving the core an independent degree of freedom which allows shear deformation to occur explicitly. As a result, all variables of interest can be expressed in terms of the lateral deflection of the beam, which is given by a power series. The series satisfies the geometric boundary conditions for a cantilever beam, but contains only three terms. Therefore, estimates for natural frequencies are limited to the first three modes. Comparisons with experimental results reveal that estimates are reliable for only the first two modes of response.

Although the present study is not concerned with damped vibrations, it should be pointed out that the damped response of sandwich beams with viscoelastic cores has generated much interest over the years. Most of the approaches employ a set of kinematic constraints and a variational method similar to those of Yu [71] or DiTaranto [77], but allow the shear modulus of the core to be complex to account for its viscoelastic properties.

One of the earliest such works is that of Kerwin [80], which provides a technique for estimating the damping provided by a constrained viscoelastic layer added to a beam. This technique, which uses a strength-of-materials approach, is limited to cases where the layer constraining the viscoelastic layer is thin relative to the thickness of the undamped layer so that the bending strain of the constraining layer can be ignored.



A less restrictive theory for nonsymmetric sandwich beams was outlined in a paper published by DiTaranto [81] in 1965. The theory, using the same assumptions as [77], accounts for the bending stiffness of both outer layers, but ignores bending in the core. In contrast to the static equations given in [77], the governing equations were derived using a strength-of-materials approach. The method was later used by DiTaranto and Blasingame [82] to get results for specific cases of interest.

Mead and Markus [83] improved upon DiTaranto's work in [81] by explicitly incorporating the lateral deflection as an unknown in the formulation of the problem. The authors show that the resulting governing equation, also obtained using a strength-of-materials approach, is more general by deriving DiTaranto's equation from it.

In 1968, Nicholas [84] examined a two-layer viscoelastic beam, rather than the standard three-layer sandwich beam. He accounted for shear deformation and rotary inertia in each layer by treating both layers as Timoshenko beams. The governing equations were derived using Hamilton's principle.

Yan and Dowell [85] developed a method in 1972 for soft-core sandwich beams which uses a kinematic constraint similar to Yu's [71], but which allows the facings to be of unequal thickness. The method was modified by the authors in 1974 [86] to extend its application to sandwich beams with stiff elastic, rather than viscoelastic, cores.

Another paper in this area is that of Sadasiva Rao and Nakra [87]. This work examines the steady-state response of unsymmetrical sandwich beams and plates with viscoelastic cores to harmonic loading. As in [72], unknown functions are expanded as Fourier series and governing equations are in terms of the unknown coefficients in the series.

Though most of the interest in the literature is directed toward three-layer sandwich beams or plates, some work has been done on multicore sandwich elements. In 1967, Liaw and Little [88] developed a static theory for multilayered plates made of orthotropic cores sandwiched between

thin isotropic facings. As in the work of Reissner [67] and Cheng [74], this treatment ignores axial deformation of the cores and shear deformation of the facings. It also assumes that all stresses within a layer are constant over the layer. The form of the governing equation is identical to that of Cheng [74] for single-core plates, indicating that all single-core solutions are valid for multicore problems as long as the properties of the multicore plate are accounted for properly.

The treatment of Liaw and Little [88] assumes that each core experiences the same amount of shear strain. In 1968, Kao and Ross [89] extended the method of Hoff and Mautner [70] to investigate multilayer sandwich beams in which each core can experience an independent shear strain.

Vibration of multicore sandwich beams was investigated by Roske and Bert [90] in 1969. The approach is similar to that of Kao and Ross [89], except that Roske and Bert ignored the bending stiffness of the facings. However, the theory includes both lateral displacement and rotary inertia in the kinetic energy. The governing equations are based on Hamilton's principle.

The plate theory of DiSciuva [91] should be mentioned in the context of methods which allow each layer to have independent kinematic constraints. In this theory, each layer is treated essentially as a Mindlin plate with the governing equations coming from an energy formulation.

The analytical techniques described so far in this literature survey have contributed greatly to an improved understanding of beam behavior, including the more complex behavior of composite beams. However, as with all analytical techniques, they suffer from being limited to highly idealized situations or require a fair amount of calculational effort to provide quantitative answers for problems of interest. Today, with the assistance of the computer, it is possible to get good approximate results numerically.

One of the most versatile methods in structural mechanics, as well as in other fields such as heat transfer and fluid mechanics, is the finite element method [92]. Bending problems are readily

treated by this method and the stiffness and mass matrices for a Bernoulli-Euler beam element are easy to find in texts on the finite element method (e.g., see Chapters 5 and 15 of [93]). Perhaps the first systematic development of the stiffness matrix for a Bernoulli-Euler beam was given by Argyris in [94]. In this work, elements of this matrix are obtained using the unit displacement method. Although the stiffness matrix for this beam element is not given explicitly, enough examples appear so that the components of the matrix can be deduced. It should be noted that [94] is one in a series of papers by Argyris in collaboration with Kelsey which appeared in the journal *Aircraft Engineering* between October 1954 and May 1955. The complete collection of papers is available in [95].

In the course of developing a stiffness matrix for a plate element, Melosh [96] presented a matrix which characterizes the stiffness of a beam element. It can be shown that this matrix is equivalent to the one given in [93]. Melosh claimed that this matrix is equivalent to one developed earlier by Turner, et Al. [97] to model spars and ribs in box wing structures. It is interesting to note that this beam element accounts for shear deformation in the web of these structural elements.

The consistent mass matrix for a Bernoulli-Euler beam element, along with an explicit expression for the stiffness matrix, can be found in a work by Archer [98] published in 1963. In the same year, Leckie and Lindberg [99] combined the stiffness and consistent mass matrices for a Bernoulli-Euler beam to obtain the dynamic stiffness matrix used to find natural frequencies of such beams.

In the standard Bernoulli-Euler beam element found in these last two works, the nodal degrees of freedom include the lateral displacement and its slope at each end of the beam. These four degrees of freedom allow the lateral deflection to have a cubic variation in the longitudinal direction of the beam. Higher-order variations are also possible, some of which are discussed in [100].

Many finite elements for Timoshenko beams have been proposed over the years. In 1965, Archer [101] applied the same techniques used in [98] to develop a finite element for analyzing the

bending, buckling, and vibration of linearly tapered Timoshenko beams. The resulting element has four degrees of freedom (two at each node) and uses cubic shape functions to interpolate the lateral displacement. The theory behind this formulation is presented in more detail for a uniform Timoshenko beam in [102].

Kapur [103] developed another finite element for analyzing the free vibrations of linearly tapered Timoshenko beams in 1966. In his approach, the lateral displacement is divided into bending and shear components. Each component is allowed a cubic variation in the longitudinal direction, requiring the element to have a total of eight degrees of freedom.

Severn [104] developed an element for static analysis in 1970 using an assumed stress distribution. The stiffness matrix was obtained using the method developed by Pian [105].

Two Timoshenko beam elements were developed by Nickel and Secor [106]. The first has seven degrees of freedom, four for lateral displacement and three for the rotation of the cross section. This combination allows a cubic variation in lateral deflection and a quadratic variation in the rotation. As a result, the contribution of both of these displacements to the shear strain has a quadratic variation over the length of the beam. This choice of shape functions is one way to avoid shear locking, a phenomenon which makes shear-deformable finite elements artificially stiff in applications involving thin beams (see [107] and [108]).

The stiffness and mass matrices for this seven degree-of-freedom (DOF) element were derived using a variational method. A four-DOF element was also developed by making use of a simplification proposed by Egle [109]. By assuming that rotary inertia has a negligible effect on shear deformation, it is possible to develop an element which accounts for shear deformation and rotary inertia, but which only requires the four degrees of freedom associated with the cubic variation of the beam's lateral deflection.

In 1972, Davis, Henshell, and Warburton [110] developed a four-DOF finite element which can be used to examine frame structures composed of Timoshenko beam segments.

In [111], Thomas, Wilson, and Wilson provided a very good summary of the development of Timoshenko-beam finite elements up to 1973. This work clears up much of the confusion evident in the literature up to this time and corrects some of the typographical errors found in the previous references. In addition, the paper proposes a new six-DOF element for a tapered beam which allows a cubic variation in lateral deflection and a linear variation in shear strain.

This reference also points out that the four-DOF element developed by Nickel and Secor [106] cannot adequately represent the clamped boundary condition in a cantilever beam because of the nodal degrees of freedom chosen for this element. This problem was corrected by Narayanaswami and Adelman [112] in 1974 by using rotation of the cross section, rather than the slope of the lateral deflection, as a nodal degree of freedom.

In 1975, Thomas and Abbas [113] proposed an eight-DOF cubic element which allows the natural boundary conditions associated with free and simply supported ends, as well as geometric boundary conditions for all end conditions, to be imposed.

An element allowing a quintic variation in the lateral displacement and a quartic variation in the rotation was developed by Dawe [114] in 1978. The eleven degrees of freedom required initially were reduced by Dawe to six degrees of freedom using a simplification similar to that of Egle [109]. The higher-order shape functions give the element a very rapid rate of convergence.

Finite elements based on higher-order kinematic constraints which allow the beam's cross section to warp are just beginning to appear in the literature. One of the first such elements was developed by Heyliger and Reddy [115]. The element is based on the third-order kinematic constraint proposed by Levinson [56], but corresponds to the theory of Bickford [58] since the element is developed using an energy formulation. The element has eight degrees of freedom which

allow a cubic variation in lateral deflection and linear variations in rotation and axial displacement. A finite element for the analogous plate theory, which can accommodate laminated plates, is discussed in [62].

A general third-order kinematic constraint forms the basis for the static element developed by Yuan and Miller [63]. The element allows a cubic variation in lateral deflection and quadratic variations in longitudinal and rotational quantities, which requires a total of sixteen degrees of freedom.

Another finite element based on a third-order kinematic constraint was developed by Kant and Gupta [64]. This kinematic constraint allows linear transverse normal strain as well as parabolic shear strain through the thickness of the beam. The element is formulated for static and dynamic calculations.

More recently, Kant and Manjunath [65] developed a family of elements for the static analysis of composite beams. This family includes elements based on first, second and third-order kinematic constraints imposed on the entire composite beam. Comparisons with the exact elasticity solution of Pagano [9] are generally favorable, but also reveal that an independent kinematic constraint for each layer may be needed to model properly the longitudinal displacement and the associated normal stress for small span-to-depth ratios.

This requirement was alluded to by Pryor and Barker [116] in 1971, but the authors were concerned that the increased number of degrees of freedom needed to allow independent motion in each layer would discourage the use of such elements. However, such approaches have enjoyed some popularity since the late 1970's.

In 1977, Epstein and Glockner [117] presented a theory which allows each layer in a multilayered shell to be modeled as a collection of straight line segments called directors. The theory, based on the use of multi-directors and formulated using a variational approach, allows a

linear variation of longitudinal displacement within layers and continuity of displacement between layers. The approach was used to study deep and multilayered beams [118] and has been used to formulate a static finite element for multilayered and thick plates [119]. An element for multilayered elastic and viscoelastic shells has been developed also [120].

In addition to this approach, the theory of DiSciuva [91] has been used to develop a static finite element for multilayered plates [121]. Also, Chaudhuri and Seide [122-125] have developed a number of static finite elements which allow a linear variation of in-plane displacements within each layer. Developed initially to investigate plates with perforations [122] or part-through holes [123], the approach was later extended to thick, laminated plates in [124] and [125].

One of the earliest multilayer beam elements was presented in a work by Khatua and Cheung [126] in 1973. The basic assumptions behind the element are very similar to those given in the analytical approach of Kao and Ross [89]. The mass and stiffness matrices are obtained from a variational procedure.

Much more recently, Yuan and Miller [127,128] developed two multilayer beam elements. These elements are obtained essentially by stacking single elements for each layer vertically using a technique discussed by Miller in [129] and [130]. References [129] and [130] apply this technique to cases involving plates stiffened by eccentric beams. As pointed out in these papers, shape functions for variables associated with lateral and longitudinal displacement must be chosen carefully. In addition to avoiding the shear locking mentioned in [107] and [108], the proper combination of shape functions is absolutely essential to prevent a mismatch in longitudinal displacement at the interface between two adjacent layers. Such a mismatch causes the errors noted by Gupta and Ma [131] and Balmer [132]. Eliminating these errors provided the motivation for the work documented in [129] and [130] and led eventually to the elements discussed in [127] and [128].

The element presented in [127] allows each layer to behave like a Timoshenko beam; in [128], the third-order kinematic constraint discussed in [63] is imposed on each layer. The latter approach appears to be the highest-order multilayer kinematic constraint presented in the literature to date.

### 1.3. Objectives, Scope and Approach

As stated in Section 1.1, the goal of this present effort is to develop shear-deformable finite elements which can be used to calculate the natural frequencies of composite beams. The first objective of this effort is to derive the stiffness and mass matrices for these elements and incorporate them into computer programs which can be used to ascertain the natural frequencies of composite beams in free vibrations. This work considers elements which impose a single kinematic constraint on the entire beam, as well as elements capable of enforcing an independent kinematic constraint on each layer within a composite beam.

This study uses the terms “simple beam element” and “stacked beam element”, respectively, to differentiate between these two kinds of elements. The term “stacked beam element” alludes to the fact that this kind of element is actually made up of a series of simple elements stacked in a vertical array. The resulting element is able to more accurately model composite beam behavior by assigning an independent kinematic constraint to each element in the stack. It should be noted that the terms “simple” and “stacked” refer only to the way in which kinematic constraints are imposed on a beam element and imply nothing regarding the homogeneity of the beam since homogeneous and composite beams can be modeled by both simple and stacked elements.

The second objective of the investigation is to evaluate the performance of the elements to determine when higher-order kinematic constraints, including the use of a stacked element rather than a simple element, are needed to account for the effects of shear deformation on the dynamic response of composite beams.



This effort is limited to free vibrations of straight composite beams of uniform cross section in a state of plane stress or plane strain. Composite beams of interest include those of sandwich or fiber-reinforced laminate construction made of linear, elastic materials. Geometric nonlinearity, damping, and transverse normal strain are not considered in this work. In addition, the coupling between longitudinal strain and lateral strain caused by Poisson effects is ignored in the two-dimensional constitutive relations used. However, both isotropic and orthotropic materials are considered and the elements can accommodate symmetric and nonsymmetric laminated configurations.

The first objective is achieved in part by extending the work of Yuan and Miller [63] for static, homogeneous beams to the dynamic analysis of composite beams. This involves deriving the stiffness and consistent mass matrices for an element capable of imposing a third-order kinematic constraint on a symmetric or nonsymmetric composite beam. The consistent mass matrices for the static stacked elements developed by the same authors in [127] and [128] are derived in this study also. In addition, dynamic simple elements based on Bernoulli-Euler, Timoshenko, and Levinson-Bickford beam theories are generated as well. Chapter 2 of this work discusses the theories associated with these beam elements. The finite element formulation of these theories is presented in Chapter 3.

The evaluations associated with the second objective involve comparisons with exact elasticity solutions similar to that of Jones [16] and Kulkarni and Pagano [17], but for composite beams in plane stress rather than plates in plane strain. In addition, comparisons against analytical, numerical, and experimental data available in the literature are made. Chapter 4 examines the accuracy and convergence properties of the elements, and presents the results of the evaluations made against data available in the literature. Finally, Chapter 5 summarizes the results and conclusions of this investigation.

## 2. COMPOSITE BEAM THEORIES

### 2.1. Assumptions

As stated in Chapter 1, this study is limited to the free vibration of straight, prismatic composite beams in a state of plane stress or plane strain. As a result of these limitations, only the inplane bending and axial responses of composite beams are considered. These inplane responses include the coupling between the bending and axial modes which is characteristic of nonsymmetric composites. Bending out of the plane and torsion are ignored. Also, the behavior of curved beams or beams of variable cross section is not addressed.

In addition, only linear, elastic response is considered. Material nonlinearity associated with non-Hookean deformation, and geometric nonlinearity associated with large displacements are not included in the formulation of the beam theories. The damping caused by viscoelastic behavior is ignored as well. Although both isotropic and orthotropic materials are treated, the coupling between longitudinal and lateral motion caused by Poisson effects is ignored, greatly simplifying the two-dimensional constitutive relations.

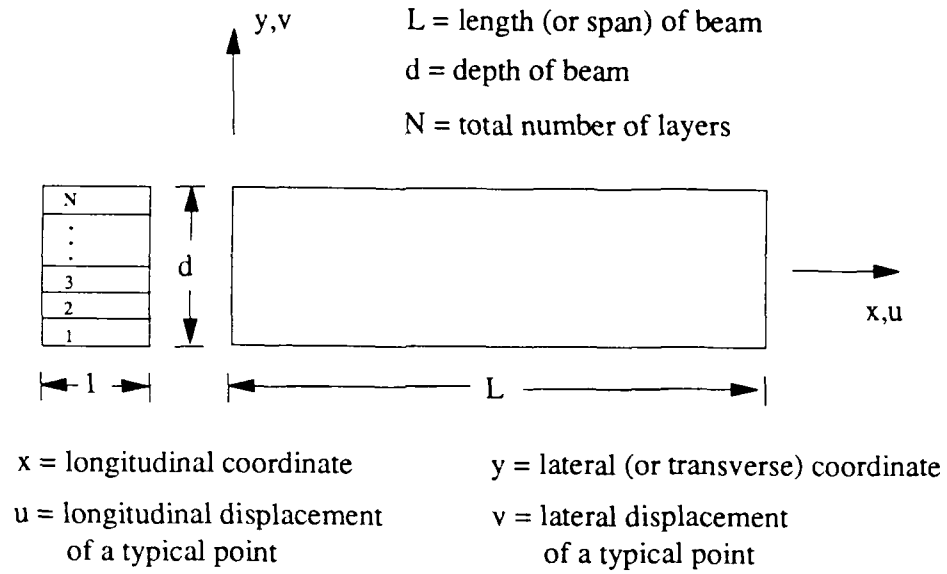
Finally, lateral displacement is assumed to be a function of the longitudinal coordinate only. This assumption eliminates the transverse normal strain associated with variations of this displacement in the lateral direction.

Although these assumptions appear to be quite restrictive, they greatly simplify the resulting theories. The effect of these assumptions on the accuracy of the results is assessed in the evaluations presented in Chapter 4.

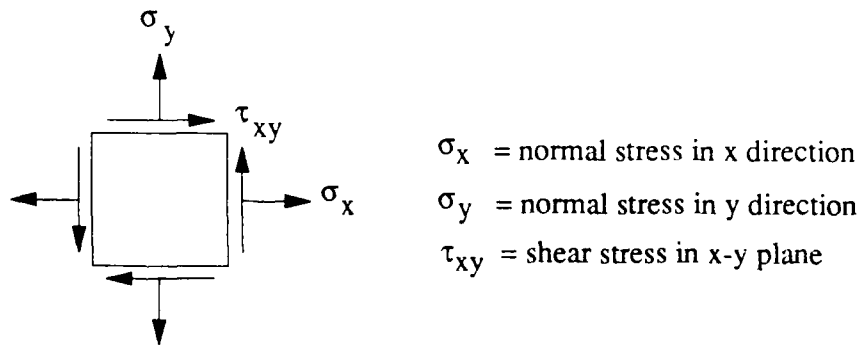
## 2.2. Coordinate System

Figure 2.1 shows the coordinate system, sign conventions, and major variables associated with the beam theories examined in this investigation. The  $x$ -axis seen in Figure 2.1a coincides with the centroidal axis of the beam. The beam is of length  $L$  and depth  $d$ , is in a state of plane stress, and has a rectangular cross section of unit width. The distance from the centroidal axis to either outer fiber is given by  $c$ , which is equal to half of the depth. The sign convention pictured in Figure 2.1b is similar to the one generally used in elasticity theory to denote positive stresses ([2], pp. 3 and 4).

In general, the beam is composed of  $N$  layers, starting with the first layer at the bottom of the beam. Both symmetric and nonsymmetric configurations are allowed. Symmetric beams must possess both geometric and material symmetry with respect to the  $x$  axis. That is, layers above the  $x$  axis must represent a mirror image of those below the axis. In addition, the material properties of matching layers above and below the axis must be identical. Any deviation from these symmetries results in a nonsymmetric beam.



(a) Displacements and geometric variables.



(b) Stresses.

- Notes:
1. Beam in state of plane stress with cross section of unit width.
  2. Positive rotation in counter-clockwise direction.

**Fig. 2.1. Beam sign convention.**

### 2.3. Constitutive Relations

The constitutive relations for an orthotropic material in a state of plane stress are given in Equations (2.1) (see [25], pp. 45-47):

$$\begin{aligned}
 \sigma_x &= \frac{E_x}{1 - \nu_{xy}\nu_{yx}}(\epsilon_x + \nu_{yx}\epsilon_y) \\
 \sigma_y &= \frac{E_y}{1 - \nu_{xy}\nu_{yx}}(\epsilon_y + \nu_{xy}\epsilon_x) \\
 \tau_{xy} &= G_{xy}\gamma_{xy} \\
 \frac{\nu_{xy}}{E_x} &= \frac{\nu_{yx}}{E_y}
 \end{aligned} \tag{2.1}$$

where

- $\sigma_x$  = normal stress in the longitudinal (x) direction
- $\sigma_y$  = normal stress in the lateral (y) direction
- $\tau_{xy}$  = shear stress in the xy plane
- $\epsilon_x$  = normal strain in the longitudinal direction
- $\epsilon_y$  = normal strain in the lateral direction
- $\gamma_{xy}$  = shear strain in the xy plane
- $E_x$  = Young's modulus in the longitudinal direction
- $E_y$  = Young's modulus in the lateral direction
- $G_{xy}$  = shear modulus in the xy plane
- $\nu_{xy}$  = Poisson's ratio for lateral strain caused by strain in the longitudinal direction

$\nu_{yx}$  = Poisson's ratio for longitudinal strain caused by strain in the lateral direction

The same equations can be used for a state of plane strain if the material properties are replaced by the starred variables defined as follows:

$$\begin{aligned}
 E_x^* &= \frac{E_x}{1 - \nu_{xz}\nu_{zx}} \\
 \nu_{xy}^* &= \frac{\nu_{xy} + \nu_{xz}\nu_{zy}}{1 - \nu_{xz}\nu_{zx}} \\
 E_y^* &= \frac{E_y}{1 - \nu_{yz}\nu_{zy}} \\
 \nu_{yx}^* &= \frac{\nu_{yx} + \nu_{yz}\nu_{zx}}{1 - \nu_{yz}\nu_{zy}} \\
 G_{xy}^* &= G_{xy}
 \end{aligned} \tag{2.2}$$

where

$E_x^*$  = equivalent  $E_x$  for material in plane strain

$E_y^*$  = equivalent  $E_y$  for material in plane strain

$\nu_{xy}^*$  = equivalent  $\nu_{xy}$  for material in plane strain

$\nu_{yx}^*$  = equivalent  $\nu_{yx}$  for material in plane strain

$\nu_{xz}$  = Poisson's ratio for longitudinal strain caused by strain perpendicular to the  $xy$  plane

$\nu_{yz}$  = Poisson's ratio for lateral strain caused by strain perpendicular to the  $xy$  plane

$\nu_{zx}$  = Poisson's ratio for strain perpendicular to the  $xy$  plane caused by strain in the longitudinal direction

$\nu_{zy}$  = Poisson's ratio for strain perpendicular to the  $xy$  plane caused by strain in the lateral direction

Similar relations for an isotropic material are given as

$$\begin{aligned}
 \sigma_x &= \frac{E}{1-\nu^2}(\epsilon_x + \nu\epsilon_y) \\
 \sigma_y &= \frac{E}{1-\nu^2}(\epsilon_y + \nu\epsilon_x) \\
 \tau_{xy} &= G \gamma_{xy} \\
 G &= \frac{E}{2(1+\nu)}
 \end{aligned} \tag{2.3}$$

where

$$\begin{aligned}
 E &= \text{Young's modulus} \\
 \nu &= \text{Poisson's ratio} \\
 G &= \text{Shear modulus}
 \end{aligned}$$

and

$$\begin{aligned}
 E^* &= \frac{E}{1-\nu^2} \\
 \nu^* &= \frac{\nu}{1-\nu} \\
 G^* &= G
 \end{aligned} \tag{2.4}$$

where

$$\begin{aligned}
 E^* &= \text{equivalent Young's modulus for material in plane strain} \\
 \nu^* &= \text{equivalent Poisson's ratio for material in plane strain} \\
 G^* &= \text{equivalent shear modulus for material in plane strain}
 \end{aligned}$$

The linear strains associated with small deformation are defined as

$$\begin{aligned}
\varepsilon_x &= u_{,x} \\
\varepsilon_y &= v_{,y} \\
\gamma_{xy} &= u_{,y} + v_{,x}
\end{aligned} \tag{2.5}$$

where

- $u$  = displacement in longitudinal direction
- $v$  = displacement in lateral direction
- $,x$  = partial derivative with respect to  $x$
- $,y$  = partial derivative with respect to  $y$

If the coupling between longitudinal and lateral strain caused by Poisson effects is ignored, the relations for plane stress or plane strain reduce to the expressions given in Equations (2.6) and (2.7) for orthotropic and isotropic materials, respectively:

$$\begin{aligned}
\sigma_x &= E_x \varepsilon_x \\
\sigma_y &= E_y \varepsilon_y \\
\tau_{xy} &= G_{xy} \gamma_{xy}
\end{aligned} \tag{2.6}$$

$$\begin{aligned}
\sigma_x &= E \varepsilon_x \\
\sigma_y &= E \varepsilon_y \\
\tau_{xy} &= G \gamma_{xy} \\
G &= E/2
\end{aligned} \tag{2.7}$$

As can be seen in these equations, all the properties for the orthotropic material are independent, whereas the isotropic material has the same Young's modulus in the longitudinal and lateral directions, and the shear modulus is related to its Young's modulus.



A final special case is given as

$$\begin{aligned}\sigma &= E\epsilon \\ \epsilon &= G\gamma\end{aligned}\tag{2.8}$$

where

$$\sigma = \sigma_x$$

$$\tau = \tau_{xy}$$

$$\epsilon = \epsilon_x$$

$$\gamma = \gamma_{xy}$$

$$E = \text{Young's modulus in longitudinal direction}$$

$$G = \text{shear modulus in } xy \text{ plane}$$

In this case, transverse normal stress and strain are ignored so that only normal stress in the longitudinal direction and shear stress are considered. As a result, the subscripts differentiating longitudinal normal stress and strain from transverse normal stress and strain can be dropped. In addition, subscripts on the shear stress and strain are also discarded, making the constitutive relations that much easier to write. This final case applies to all the beam theories examined in this investigation and the constitutive relations given by Equations (2.8) are used whenever appropriate to simplify the resulting equations somewhat.

It should be noted that even though the coupling between longitudinal and lateral strain associated with Poisson effects is ignored in all the beam theories, the relation between the shear modulus and Young's modulus for an isotropic material of arbitrary Poisson's ratio given in Equations (2.3) can still be modeled by an orthotropic beam theory. This is possible since an orthotropic theory allows these moduli to be specified independently such that the ratio given in

Equations (2.3) is satisfied. Although this approach still ignores the effect Poisson's ratio has on the normal stresses and strains, it does account for the important part this ratio plays in the relation between the shear modulus and Young's modulus for isotropic materials.

## 2.4. Kinematic Constraints

As suggested by Basset [48], variables such as the inplane displacements can be expressed as power series expansions. For the variables and coordinate system defined in Figure 2.1, expansions for longitudinal and lateral displacement take the form

$$\begin{aligned} u(x, y, t) &= A_0(x, t) + A_1(x, t)y + A_2(x, t)y^2 + \cdots \\ v(x, y, t) &= B_0(x, t) + B_1(x, t)y + B_2(x, t)y^2 + \cdots \end{aligned} \quad (2.9)$$

where

$u(x, y, t)$	=	longitudinal displacement
$v(x, y, t)$	=	lateral displacement
$x$	=	longitudinal coordinate
$y$	=	lateral coordinate
$t$	=	time
$A_i(x, t)$	=	unknown functions of $x$ and $t$
$B_i(x, t)$	=	unknown functions of $x$ and $t$

The various theories discussed in this section are obtained by assuming the actual displacements given by the series expansions can be approximated by truncating the expansions. The truncated series are then used as kinematic constraints which are imposed on the entire composite beam. Using independent kinematic constraints within each layer is discussed in conjunction with

the finite element formulation of stacked elements in Chapter 3.

As stated in the assumptions outlined in Section 2.1, all the beam theories considered in this study ignore the transverse normal strain associated with variations of the lateral displacement in the vertical direction. Therefore, the kinematic constraint for lateral displacement for all the theories contains only one term,

$$v(x, y, t) = W(x, t) \quad (2.10)$$

where

$W(x, t)$  = unknown function of  $x$  and  $t$  corresponding to displacement of beam's centroidal axis.

The difference in the theories is caused solely by changes in the kinematic constraint imposed on the longitudinal deformation of the beam.

In this study, the highest order of  $y$  present in the kinematic constraint for the longitudinal displacement is used to denote the order of the kinematic constraint and its associated theory. For example, a kinematic constraint which contains at most linear terms is referred to as a first-order kinematic constraint; a third-order constraint must contain a cubic term in addition to other possible lower-order terms.

For Bernoulli-Euler beam theory [22], the assumption that initially plane sections remain plane after bending limits the kinematic constraint for longitudinal displacement to the first two terms shown in Equations (2.9). The additional assumption that sections initially perpendicular to the neutral axis remain perpendicular after bending results in the kinematic constraints

$$\begin{aligned} u(x, y, t) &= U(x, t) - W'(x, t)y \\ v(x, y, t) &= W(x, t) \end{aligned} \quad (2.11)$$

where

$U(x, t)$  = unknown function of  $x$  and  $t$  corresponding to axial motion of the centroidal axis of the beam

$'$  = partial derivative with respect to  $x$

This equation also gives the constraint imposed on the lateral displacement as do all the kinematic-constraint equations. These assumptions lead to a theory which cannot account directly for shear deformation since shear strain is ignored:

$$\gamma = v_{,x} + u_{,y} = W'(x, t) - W'(x, t) = 0 \quad (2.12)$$

In Timoshenko beam theory [29], sections plane before bending remain so after bending; however, planes initially perpendicular to the neutral axis are not constrained to remain perpendicular after bending. Therefore, the first-order term in the kinematic constraint for longitudinal displacement is allowed to be independent of the lateral deflection:

$$\begin{aligned} u(x, y, t) &= U(x, t) - \Phi(x, t)y \\ v(x, y, t) &= W(x, t) \end{aligned} \quad (2.13)$$

where

$\Phi(x, t)$  = unknown function corresponding to rotation of beam cross sections

The resulting shear strain

$$\gamma = W'(x, t) - \Phi(x, t) \quad (2.14)$$

is constant over the depth of the beam.

Trying to model the behavior associated with some other distribution of shear strain requires the use of a correction factor, as discussed in [29] and [44-47].

Obtaining other variations of shear strain directly requires higher-order terms in the longitudinal kinematic constraint to account for the cross-sectional warping induced by shear deformation. In Levinson's beam theory [56], the third-order term is chosen such that the shear strain vanishes at the upper and lower surfaces of the beam, as prescribed by the boundary conditions for free vibrations. The kinematic constraints for this theory are:

$$\begin{aligned} u(x, y, t) &= U(x, t) - \Phi(x, t)y - \frac{1}{3c^2}[W'(x, t) - \Phi(x, t)]y^3 \\ v(x, y, t) &= W(x, t) \end{aligned} \quad (2.15)$$

where

$c$  = distance from centroidal axis to upper and lower fibers

The resulting shear strain is

$$\gamma = [W'(x, t) - \Phi(x, t)][1 - (y/c)^2] \quad (2.16)$$

The parabolic nature of the shear strain is apparent in Equation (2.16).

Finally, the general third-order theory of Yuan and Miller [63] allows warping, but includes a second-order term as well as a third-order one:

$$\begin{aligned} u(x, y, t) &= U(x, t) - \Phi_1(x, t)y - \Phi_2(x, t)y^2 - \Phi_3(x, t)y^3 \\ v(x, y, t) &= W(x, t) \end{aligned} \quad (2.17)$$

where

$\Phi_1(x, t)$  = unknown rotational function

$\Phi_2(x, t)$  = unknown function of  $x$  and  $t$  which models second-order warping of beam

$\Phi_3(x, t)$  = unknown function of  $x$  and  $t$  which models third-order warping of beam

Although no attempt is made to enforce the boundary condition for shear strain on the lateral surfaces of the beam, this kinematic constraint leads to a more general variation of shear strain which includes a constant, linear, and quadratic term

$$\gamma = W'(x, t) - \Phi_1(x, t) - 2\Phi_2(x, t)y - 3\Phi_3(x, t)y^2 \quad (2.18)$$

## 2.5. Governing Equations

As stated in Section 1.2, the governing equations for the unknown functions contained in the kinematic constraint for a beam theory can be found using either a direct strength-of-materials approach or an energy method. This investigation uses an energy method, namely Hamilton's Principle, to derive the equations for all the theories. Since the energy formulation of Levinson's beam theory was first accomplished by Bickford [58], the theory based on Levinson's kinematic constraint is referred to as Levinson-Bickford theory in this study.

According to Langhaar ([19], p. 239), Hamilton's principle for a conservative system states that "among all motions that will carry a conservative system from a given initial configuration  $\mathbf{X}_0$  to a given final configuration  $\mathbf{X}_1$  in a given time interval  $(t_0, t_1)$ , that which actually occurs provides a stationary value to the integral  $a$ ," where  $a$  is called the action and is given by

$$a = \int_{t_0}^{t_1} \mathcal{L} dt$$

$$\mathcal{L} = T - V \quad (2.19)$$

where

$\mathcal{L}$  = Lagrangian

$T$  = kinetic energy

$V$  = potential energy

$t_0$  = start of time interval

$t_1$  = end of time interval

Using this principle provides a very straightforward way of deriving the equations of motion and boundary equations for a continuous system, such as a beam. Once the kinematic constraint is chosen, the kinetic energy and potential energy can be expressed in terms of this constraint. After the expressions for these energies are substituted into the Lagrangian defined in Equation (2.19), variational calculus can be used to force the action to be stationary.

For the beam theories discussed in this study, the Lagrangian is obtained from a line integral

$$\mathcal{L} = \int_0^L F dx \quad (2.20)$$

where

$F$  = integrand of line integral used to obtain the Lagrangian,  $\mathcal{L}$

Therefore, the action involves a double integral, with integration performed once over time and once over the longitudinal coordinate. As discussed by Langhaar ([19], pp. 92-96), the action for a double integral is stationary when the differential equation

$$\frac{\partial F}{\partial \psi} - \frac{\partial}{\partial x} \left( \frac{\partial F}{\partial \psi'} \right) - \frac{\partial}{\partial t} \left( \frac{\partial F}{\partial \dot{\psi}} \right) + \frac{\partial^2}{\partial x^2} \left( \frac{\partial F}{\partial \psi''} \right) + \frac{\partial^2}{\partial x \partial t} \left( \frac{\partial F}{\partial \dot{\psi}'} \right) + \frac{\partial^2}{\partial t^2} \left( \frac{\partial F}{\partial \ddot{\psi}} \right) = 0 \quad (2.21)$$

is satisfied, where

$\psi$  = unknown function of  $x$  and  $t$  appearing in beam kinematic constraint (e.g.,  $U(x, t)$ ,  $\Phi(x, t)$ , or  $W(x, t)$ )

$'$  = partial derivative with respect to  $x$

$\dot{\phantom{x}}$  = partial derivative with respect to  $t$

subject to the boundary conditions

$$\delta \psi \left[ \frac{\partial F}{\partial \psi'} - \frac{\partial}{\partial x} \left( \frac{\partial F}{\partial \psi''} \right) - \frac{\partial}{\partial t} \left( \frac{\partial F}{\partial \dot{\psi}'} \right) \right] = 0$$

and

$$\delta \psi' \left[ \frac{\partial F}{\partial \psi''} \right] = 0$$

$$\text{at } x = 0 \quad \text{and} \quad x = L \quad (2.22)$$

where

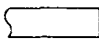
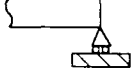


$\delta \psi$  = variation in  $\psi$

$\delta \psi'$  = variation in  $\psi'$



Applying Equation (2.21) for each dependent variable in the kinematic constraint generates the equations of motion for the beam theory. The required boundary conditions are obtained from Equations (2.22).

It should be noted that the boundary conditions specified by Equations (2.22) are expressed as the product of two terms. The first term, preceded in each equation by a variational sign, represents a forced or geometric boundary condition. The second term, placed in brackets, is a natural boundary condition.

Beam boundary conditions (at $x = L$ )		Boundary conditions for each theory			
		Bernoulli-Euler	Timoshenko	Levinson-Bickford	Third-order
Free 	No forced boundary conditions				
Simply supported 	$v(L,0,t) = 0$	$W(L,t) = 0$	$W(L,t) = 0$	$W(L,t) = 0$	$W(L,t) = 0$
Pinned 	$u(L,0,t) = 0$ $v(L,0,t) = 0$	$U(L,t) = 0$ $W(L,t) = 0$	$U(L,t) = 0$ $W(L,t) = 0$	$U(L,t) = 0$ $W(L,t) = 0$	$U(L,t) = 0$ $W(L,t) = 0$
Clamped 	$u(L,y,t) = 0$ $v(L,y,t) = 0$	$U(L,t) = 0$ $W(L,t) = 0$ $W'(L,t) = 0$	$U(L,t) = 0$ $W(L,t) = 0$ $\Phi(L,t) = 0$	$U(L,t) = 0$ $W(L,t) = 0$ $W'(L,t) = 0$ $\Phi(L,t) = 0$	$U(L,t) = 0$ $W(L,t) = 0$ $\Phi_1(L,t) = 0$ ( $i = 1,2,3$ )

**Fig. 2.2. Forced boundary conditions.**

Forced boundary conditions correspond to explicit limitations placed on the displacement at the ends of a structure. The dependent variables of the beam theories cannot violate these limitations. Figure 2.2 summarizes the forced boundary conditions for the theories and end conditions of interest in this study. Natural boundary conditions govern the stresses or stress resultants present on ends

whose displacements are not restricted. Since it is not possible to specify both kinds of conditions at a boundary, the dependent variables of a beam theory must satisfy either a forced or a natural boundary condition at each end.

The kinetic energy for general planar motion is given by

$$T = \frac{1}{2} \int_{\mathcal{V}} \rho (\dot{u}^2 + \dot{v}^2) d\mathcal{V} \quad (2.23)$$

where

$\rho$  = mass density of material

$\mathcal{V}$  = volume of material

This expression accounts for motion in the longitudinal and lateral directions and can account for the rotary inertia caused by variations of longitudinal motion in the lateral direction.

An expression for the potential energy associated with the internal strain energy of an orthotropic beam in plane stress is given as

$$\begin{aligned} V &= \frac{1}{2} \int_{\mathcal{V}} (\sigma \epsilon + \tau \gamma) d\mathcal{V} \\ &= \frac{1}{2} \int_{\mathcal{V}} [E(\epsilon)^2 + G(\gamma)^2] d\mathcal{V} \end{aligned} \quad (2.24)$$

Since transverse normal strain and the coupling between lateral and longitudinal motions caused by Poisson effects is ignored, the constitutive relations from Equations (2.8) are used. The resulting expression accounts for the strain energy caused by axial and bending response, including the effects of shear deformation.

Once a kinematic constraint for a particular beam theory is substituted into Equations (2.23) and (2.24), the variables appearing in these equations become functions of  $x$  and  $t$  only, since these variables are assumed to be constant over the width of the beam and their variations in the  $y$  direction are prescribed. Therefore, the volume integrals seen in Equations (2.23) and (2.24) can be expressed as line integrals by making use of the definitions

$$\begin{aligned} P_n &= \int_A \rho(y) y^n dA \\ Q_n &= \int_A E(y) y^n dA \\ V_n &= \int_A G(y) y^n dA \end{aligned} \quad (2.25)$$

where

$P_n, Q_n, V_n$  = composite beam properties for inertia, longitudinal stiffness, and shear stiffness, respectively.

$A$  = area of beam's cross section

$n$  = 0, 1, 2, ...

and

$$\begin{aligned} P_n &= \sum_{i=1}^N \rho_i I_i^{(n)} \\ Q_n &= \sum_{i=1}^N E_i I_i^{(n)} \\ V_n &= \sum_{i=1}^N G_i I_i^{(n)} \end{aligned} \quad (2.26)$$

$$I_i^{(n)} = \frac{1}{n+1} \{ (y_{i+1})^{n+1} - (y_i)^{n+1} \}$$

where

$\rho_i$  = mass density of  $i$ -th layer

$E_i$  = Young's modulus of  $i$ -th layer

$G_i$  = Shear modulus of  $i$ -th layer

$I_i^{(n)}$  =  $n$ -th area moment of  $i$ -th layer

$y_i$  = distance from centroidal axis to bottom of  $i$ -th layer

$y_{i+1}$  = distance from centroidal axis to top of  $i$ -th layer, or bottom of  $(i\text{-th} + 1)$  layer

$N$  = total number of layers in composite beam

Equations (2.25) correspond to a general nonhomogeneous material whose properties vary in the lateral direction only. Less general expressions for a layered composite beam with a rectangular cross section of unit width are given in Equations (2.26). The latter set of equations makes use of the numbering scheme pictured in Figure 2.1. It should be noted that  $P_n$ ,  $Q_n$ , and  $V_n$  for a symmetric beam are all zero for odd values of  $n$ .

Substituting the kinematic constraint for a Bernoulli-Euler beam given by Equations (2.11) into Equations (2.23) and (2.24) yields the expressions for kinetic energy

$$T = \frac{1}{2} \int_V \rho(y) [(\dot{U} - \dot{W}'y)^2 + \dot{W}^2] dV \quad (2.27)$$

and potential energy

$$V = \frac{1}{2} \int_V E(y) (U' - W''y)^2 dV \quad (2.28)$$

Employing the definitions given in Equations (2.26) and combining the kinetic energy and potential energy properly results in the Lagrangian

$$\begin{aligned} \mathcal{L} = \int_0^L \frac{1}{2} \{ & [P_0 \dot{U}^2 - 2P_1 \dot{U} \dot{W}' + p_2 (\dot{W}')^2 + P_0 \dot{W}^2] \\ & - [Q_0 (U')^2 - 2Q_1 U' W'' + Q_2 (W''')^2] \} dx \end{aligned} \quad (2.29)$$

Applying the operations specified in Equations (2.21) and (2.22) to the integrand of this expression yields the governing equations

$$\begin{aligned} (Q_0 U'' - P_0 \ddot{U}) - (Q_1 W''' - P_1 \ddot{W}') &= 0 \\ -(Q_1 U''' - P_1 \ddot{U}') + (Q_2 W'''' - P_2 \ddot{W}'' + P_0 \ddot{W}) &= 0 \end{aligned} \quad (2.30)$$

and boundary conditions

$$\begin{aligned} \delta U [Q_0 U' - Q_1 W''] &= 0 \\ \delta W [-(Q_1 U'' - P_1 \ddot{U}) + (Q_2 W''' - P_2 \ddot{W}')] &= 0 \\ \text{and} & \\ \delta W' [-Q_1 U' + Q_2 W''] &= 0 \\ \text{at } x = 0 \text{ and } x = L & \end{aligned} \quad (2.31)$$

A similar procedure can be used to find the governing equations and boundary conditions for the other beam theories. The results of such an effort are given in Equations (2.32) through (2.36), (2.37) through (2.41), and (2.42) through (2.46) for Timoshenko, Levinson-Bickford, and the general third-order theory, respectively. The following five equations apply to Timoshenko beam theory:

$$T = \frac{1}{2} \int_V \rho(y) [(\dot{U} - \Phi_y)^2 + \dot{W}^2] dV \quad (2.32)$$

$$V = \frac{1}{2} \int_V E(y) (U' - \Phi' y)^2 dV + \frac{1}{2} k \int_V G(y) (W' - \Phi)^2 dV \quad (2.33)$$

where

$k$  = shear correction factor

$$\begin{aligned} L = \int_0^L \frac{1}{2} [ & P_0 \dot{U}^2 - 2P_1 \dot{U} \dot{\Phi} + P_2 \dot{\Phi}^2 + P_0 \dot{W}^2 ] \\ & - [ Q_0 (U')^2 - 2Q_1 U' \Phi' + Q_2 (\Phi')^2 ] \\ & - k V_0 (W' - \Phi)^2 ] dx \end{aligned} \quad (2.34)$$

$$\begin{aligned} (Q_0 U'' - P_0 \ddot{U}) - (Q_1 \Phi'' - P_1 \ddot{\Phi}) &= 0 \\ -(Q_1 U'' - P_1 \ddot{U}) + (Q_2 \Phi'' - P_2 \ddot{\Phi}) + k V_0 (W' - \Phi) &= 0 \\ k V_0 (W'' - \Phi') - P_0 \ddot{W} &= 0 \end{aligned} \quad (2.35)$$

$$\delta U [Q_0 U' - Q_1 \Phi'] = 0$$

$$\delta \Phi [-Q_1 U' + Q_2 \Phi'] = 0$$

$$\text{and} \quad (2.36)$$

$$\delta W [W' - \Phi] = 0$$

$$\text{at } x = 0 \text{ and } x = L$$

The following five equations pertain to Levinson-Bickford beam theory:

$$T = \frac{1}{2} \int_V \rho(y) \left\{ \left[ \dot{U} - \dot{\Phi} y - \frac{1}{3c^2} (\dot{W}' - \dot{\Phi}) y^3 \right]^2 + \dot{W}^2 \right\} dV \quad (2.37)$$

$$\begin{aligned}
V &= \frac{1}{2} \int_{\mathcal{V}} E(y) \left[ U' - \Phi' y - \frac{1}{3c^2} (W'' - \Phi') y^3 \right]^2 d\mathcal{V} \\
&\quad + \frac{1}{2} \int_{\mathcal{V}} G(y) [(W' - \Phi)(1 - y^2/c^2)]^2 d\mathcal{V}
\end{aligned} \tag{2.38}$$

$$\begin{aligned}
\mathcal{L} &= \int_0^L \frac{1}{2} \left\{ [P_0 \dot{U}^2 - 2P_1 \dot{U} \dot{\Phi} - \frac{2}{3c^2} P_3 \dot{U} (\dot{W}' - \dot{\Phi}) + P_2 \dot{\Phi}^2 \right. \\
&\quad \left. + \frac{2}{3c^2} P_4 \dot{\Phi} (\dot{W}' - \dot{\Phi}) + \frac{1}{9c^4} P_6 (\dot{W}' - \dot{\Phi})^2 + P_6 \dot{W}^2] \right. \\
&\quad \left. - [Q_0 (U')^2 - 2Q_1 U' \Phi' - \frac{2}{3c^2} Q_3 U' (W'' - \Phi') + Q_2 (\Phi')^2 \right. \\
&\quad \left. + \frac{2}{3c^2} Q_4 \Phi' (W'' - \Phi') + \frac{1}{9c^4} Q_6 (W'' - \Phi')^2] \right. \\
&\quad \left. - \left[ V_0 - \frac{2}{c^2} V_2 + \frac{1}{c^4} V_4 \right] (W' - \Phi)^2 \right\} dx
\end{aligned} \tag{2.39}$$

$$\begin{aligned}
& (Q_0 U'' - P_0 \ddot{U}) - (Q_1 \Phi'' - P_1 \ddot{\Phi}) - \frac{1}{3c^2} [Q_3 (W''' - \Phi'') - P_3 (\ddot{W}' - \ddot{\Phi})] = 0 \\
& -(Q_1 U'' - P_1 \ddot{U}) + (Q_2 \Phi'' - P_2 \ddot{\Phi}) + \frac{1}{3c^2} (Q_3 U'' - P_3 \ddot{U}) \\
& + \frac{1}{3c^2} [Q_4 (W''' - 2\Phi'') - P_4 (\ddot{W}' - 2\ddot{\Phi})] \\
& - \frac{1}{9c^4} [Q_6 (W''' - \Phi'') - P_6 (\ddot{W}' - \ddot{\Phi})] \\
& + \left( V_0 - \frac{2}{c^2} V_2 + \frac{1}{c^4} V_4 \right) (W' - \Phi) = 0 \\
& \frac{1}{3c^2} (Q_3 U''' - P_3 \ddot{U}') - \frac{1}{3c^2} (Q_4 \Phi''' - P_4 \ddot{\Phi}') \\
& - \frac{1}{9c^4} [Q_6 (W'''' - \Phi''') - P_6 (\ddot{W}'' - \ddot{\Phi}')] \\
& + \left( V_0 - \frac{2}{c^2} V_2 + \frac{1}{c^4} V_4 \right) (W'' - \Phi') - P_0 \ddot{W} = 0
\end{aligned} \tag{2.40}$$

$$\begin{aligned}
& \delta U \left[ Q_0 U' - Q_1 \Phi' - \frac{1}{3c^2} Q_3 (W'' - \Phi') \right] = 0 \\
& \delta \Phi \left[ -Q_1 U' + Q_2 \Phi' + \frac{1}{3c^2} Q_3 U' + \frac{1}{3c^2} Q_4 (W'' - 2\Phi') - \frac{1}{9c^4} Q_6 (W'' - \Phi') \right] = 0 \\
& \delta W \left\{ -\frac{1}{3c^2} (Q_3 U'' - P_3 \ddot{U}) + \frac{1}{3c^2} (Q_4 \Phi'' - P_4 \ddot{\Phi}) + \frac{1}{9c^4} [Q_6 (W''' - \Phi'') - P_6 (\ddot{W}' - \ddot{\Phi})] \right. \\
& \quad \left. - \left( V_0 - \frac{2}{c^2} V_2 + \frac{1}{c^4} V_4 \right) (W' - \Phi) \right\} = 0
\end{aligned} \tag{2.41}$$

and

$$\delta W' \left[ -Q_3 U' + Q_4 \Phi' + \frac{1}{3c^2} Q_6 (W'' - \Phi') \right] = 0$$

at  $x = 0$  and  $x = L$



The following five equations are associated with the general third-order beam theory:

$$T = \frac{1}{2} \int_{\mathcal{V}} \rho(y) [(\dot{U} - \dot{\Phi}_1 y - \dot{\Phi}_2 y^2 - \dot{\Phi}_3 y^3)^2 + \dot{W}^2] d\mathcal{V} \quad (2.42)$$

$$\begin{aligned} V = & \frac{1}{2} \int_{\mathcal{V}} E(y) [U' - \Phi'_1 y - \Phi'_2 y^2 - \Phi'_3 y^3]^2 d\mathcal{V} \\ & + \frac{1}{2} \int_{\mathcal{V}} G(y) [(W' - \Phi_1) - 2\Phi_2 y - 3\Phi_3 y^2]^2 d\mathcal{V} \end{aligned} \quad (2.43)$$

$$\begin{aligned} \mathcal{L} = & \int_0^L \frac{1}{2} \{ [P_0 \dot{U}^2 - 2P_1 \dot{U} \dot{\Phi}_1 - 2P_2 \dot{U} \dot{\Phi}_2 - 2P_3 \dot{U} \dot{\Phi}_3 \\ & + P_2 \dot{\Phi}_1^2 + 2P_3 \dot{\Phi}_1 \dot{\Phi}_2 + 2P_4 \dot{\Phi}_1 \dot{\Phi}_3 \\ & + P_4 \dot{\Phi}_2^2 + 2P_5 \dot{\Phi}_2 \dot{\Phi}_3 + P_6 \dot{\Phi}_3^2 + P_0 \dot{W}^2] \\ & - [Q_0 (U')^2 - 2Q_1 U' \Phi'_1 - 2Q_2 U' \Phi'_2 - 2Q_3 U' \Phi'_3 \\ & + Q_2 \Phi_1'^2 + 2Q_3 \Phi'_1 \Phi'_2 + 2Q_4 \Phi'_1 \Phi'_3 \\ & + Q_4 \Phi_2'^2 + 2Q_5 \Phi'_2 \Phi'_3 + Q_6 \Phi_3'^2] \\ & - [V_0 (W' - \Phi_1)^2 - 4V_1 (W' - \Phi_1) \Phi_2 - 6V_2 (W' - \Phi_1) \Phi_3 \\ & + 4V_2 \Phi_2^2 + 12V_3 \Phi_3 \Phi_3 + 9V_4 \Phi_3^2] \} dx \end{aligned} \quad (2.44)$$

$$\begin{aligned}
(Q_0 U'' - P_0 \ddot{U}) - (Q_1 \Phi''_1 - P_1 \ddot{\Phi}_1) - (Q_2 \Phi''_2 - P_2 \ddot{\Phi}_2) - (Q_3 \Phi''_3 - P_3 \ddot{\Phi}_3) &= 0 \\
-(Q_1 U'' - P_1 \ddot{U}) + (Q_2 \Phi''_1 - P_2 \ddot{\Phi}_1) + (Q_3 \Phi''_2 - P_3 \ddot{\Phi}_2) \\
+(Q_4 \Phi''_3 - P_4 \ddot{\Phi}_3) + V_0(W' - \Phi_1) - 2V_1 \Phi_2 - 3V_2 \Phi_3 &= 0 \\
-(Q_2 U'' - P_2 \ddot{U}) + (Q_3 \Phi''_1 - P_3 \ddot{\Phi}_1) + (Q_4 \Phi''_2 - P_4 \ddot{\Phi}_2) &= 0 \\
+(Q_5 \Phi''_3 - P_5 \ddot{\Phi}_3) + 2V_1(W' - \Phi_1) - 4V_2 \Phi_2 - 6V_3 \Phi_3 &= 0 \\
-(Q_3 U'' - P_3 \ddot{U}) + (Q_4 \Phi''_1 - P_4 \ddot{\Phi}_1) + (Q_5 \Phi''_2 - P_5 \ddot{\Phi}_2) \\
+(Q_6 \Phi''_3 - P_6 \ddot{\Phi}_3) + 3V_2(W' - \Phi_1) - 6V_3 \Phi_2 - 9V_4 \Phi_3 &= 0 \\
V_0(W'' - \Phi'_1) - P_0 \ddot{W} - 2V_1 \Phi'_2 - 3V_2 \Phi'_3 &= 0
\end{aligned} \tag{2.45}$$

$$\begin{aligned}
\delta U [Q_0 U' - Q_1 \Phi'_1 - Q_2 \Phi'_2 - Q_3 \Phi'_3] &= 0 \\
\delta \Phi_1 [-Q_1 U' + Q_2 \Phi'_1 + Q_3 \Phi'_2 + Q_4 \Phi'_3] &= 0 \\
\delta \Phi_2 [-Q_2 U' + Q_3 \Phi'_1 + Q_4 \Phi'_2 + Q_5 \Phi'_3] &= 0 \\
\delta \Phi_3 [-Q_3 U' + Q_4 \Phi'_1 + Q_5 \Phi'_2 + Q_6 \Phi'_3] &= 0
\end{aligned} \tag{2.46}$$

and

$$\delta W [V_0(W' - \Phi_1) - 2V_1 \Phi_2 - 3V_2 \Phi_3] = 0$$

at  $x = 0$  and  $x = L$

The equations for free vibrations are obtained by assuming harmonic motion for all unknown dependent displacement variables, as shown for the generic displacement function

$$\Psi_{(x,t)} = \Psi_{(x)} e^{i\omega t} \tag{2.47}$$

where

$\omega$  = natural circular frequency of harmonic motion

This assumption reduces all the governing equations and boundary conditions to ordinary differential equations by prescribing the nature of the time dependence of variables in the equations. The resulting governing equations for Bernoulli-Euler, Timoshenko, Levinson-Bickford, and the general third-order theories are given, respectively, as follows:

$$\begin{aligned}(Q_0 U'' + \omega^2 P_0 U) - (Q_1 W'''' + \omega^2 P_1 W') &= 0 \\ (Q_1 U'''' + \omega^2 P_1 U') + (Q_2 W'''' + \omega^2 P_2 W'' - \omega^2 P_0 W) &= 0\end{aligned}\quad (2.48)$$

$$\begin{aligned}(Q_0 U'' + \omega^2 P_0 U) - (Q_1 \Phi'' + \omega^2 P_1 \Phi) &= 0 \\ -(Q_1 U'' + \omega^2 P_1 U) + (Q_2 \Phi'' + \omega^2 P_2 \Phi) + k V_0 (W' - \Phi) &= 0 \\ k V_0 (W'' - \Phi') + \omega^2 P_0 W &= 0\end{aligned}\quad (2.49)$$

$$\begin{aligned}(Q_0 U'' + \omega^2 P_0 U) - (Q_1 \Phi'' + \omega^2 P_1 \Phi) - \frac{1}{3c^2} [Q_3 (W'''' - \Phi'') + \omega^2 P_3 (W' - \Phi)] &= 0 \\ -(Q_1 U'' + \omega^2 P_1 U) + (Q_2 \Phi'' + \omega^2 P_2 \Phi) + \frac{1}{3c^2} (Q_3 U'' + \omega^2 P_3 U) \\ + \frac{1}{3c^2} [Q_4 (W'''' - 2\Phi'') + \omega^2 P_4 (W' - 2\Phi)] - \frac{1}{9c^4} [Q_6 (W'''' - \Phi'') + \omega^2 P_6 (W' - \Phi)] \\ + \left( V_0 - \frac{2}{c^2} V_2 + \frac{1}{c^4} V_4 \right) (W' - \Phi) &= 0 \\ \frac{1}{3c^2} (Q_3 U'''' + \omega^2 P_3 U') - \frac{1}{3c^2} (Q_4 \Phi'''' + \omega^2 P_4 \Phi') - \frac{1}{9c^4} [Q_6 (W'''' - \Phi''') + \omega^2 P_6 (W'' - \Phi')] \\ + \left( V_0 - \frac{2}{c^2} V_2 + \frac{1}{c^4} V_4 \right) (W'' - \Phi') + \omega^2 P_0 W &= 0\end{aligned}\quad (2.50)$$

$$\begin{aligned}
& (Q_0 U'' + \omega^2 P_0 U) - (Q_1 \Phi''_1 + \omega^2 P_1 \Phi_1) - (Q_2 \Phi''_2 + \omega^2 P_2 \Phi_2) \\
& \quad - (Q_3 \Phi''_3 + \omega^2 P_3 \Phi_3) = 0 \\
& (Q_1 U'' + \omega^2 P_1 U) + (Q_2 \Phi''_1 + \omega^2 P_2 \Phi_1) + (Q_3 \Phi''_2 + \omega^2 P_3 \Phi_2) \\
& + (Q_4 \Phi''_3 + \omega^2 P_4 \Phi_3) + V_0(W' - \Phi_1) - 2V_1\Phi_2 - 3V_2\Phi_3 = 0 \\
& (Q_2 U'' + \omega^2 P_2 U) + (Q_3 \Phi''_1 + \omega^2 P_3 \Phi_1) + (Q_4 \Phi''_2 + \omega^2 P_4 \Phi_2) \\
& + (Q_5 \Phi''_3 + \omega^2 P_5 \Phi_3) + 2V_1(W' - \Phi_1) - 4V_2\Phi_2 - 6V_3\Phi_3 = 0 \\
& - (Q_3 U'' + \omega^2 P_3 U) + (Q_4 \Phi''_1 + \omega^2 P_4 \Phi_1) + (Q_5 \Phi''_2 + \omega^2 P_5 \Phi_2) \\
& + (Q_6 \Phi''_3 + \omega^2 P_6 \Phi_3) + 3V_2(W' - \Phi_1) - 6V_3\Phi_2 - 9V_4\Phi_3 = 0 \\
& V_0(W'' - \Phi'_1) + \omega^2 P_0 W - 2V_1\Phi'_2 - 3V_2\Phi'_3 = 0
\end{aligned} \tag{2.51}$$

The natural boundary conditions for Timoshenko and the general third-order beam theories given by Equations (2.36) and (2.46), respectively, are unaffected by the assumption of harmonic motion specified by Equation (2.47). In addition, the forced boundary conditions for all beam theories remain the same. However, the natural boundary conditions for the Bernoulli-Euler theory

$$\begin{aligned}
& \delta W [-(Q_1 U'' + \omega^2 P_1 U) + (Q_2 W''' + \omega^2 P_2 W')] = 0 \\
& \text{at } x = 0 \quad \text{and } x = L
\end{aligned} \tag{2.52}$$

and Levinson-Bickford theory

$$\begin{aligned}
& \delta W \left\{ -\frac{1}{3c^2} (Q_3 U'' + \omega^2 P_3 U) + \frac{1}{3c^2} (Q_4 \Phi'' + \omega^2 P_4 \Phi) + \frac{1}{9c^4} [Q_6 (W'''' - \Phi'') + \omega^2 P_6 (W' - \Phi)] \right. \\
& \quad \left. - \left( V_0 - \frac{2}{c^2} V_2 + \frac{1}{c^4} V_4 \right) (W' - \Phi) \right\} = 0 \\
& \text{at } x = 0 \quad \text{and } x = L
\end{aligned} \tag{2.53}$$

are not the same. It should be noted that only the boundary conditions affected by the assumption of harmonic motion are given in Equations (2.52) and (2.53).

As can be seen in the governing equations for the Timoshenko beam theory, a shear correction factor,  $k$ , is incorporated into the expression for shear strain energy to allow this first-order theory to better model the strain energy associated with shear deformation [29,44-47]. Ultimately, this correction factor has some effect on the governing equations, as seen in Equations (2.35) and (2.49).

The coupling between the axial and bending responses possible in nonsymmetric beams is apparent in all the governing equations. As can be seen, this coupling exists only when the values for  $P_n$ ,  $Q_n$ , and  $V_n$ , are nonzero for odd values of  $n$ , a condition that is not possible in symmetric beams.

Finally, the increasing complexity of the theories is obvious. Simple solutions for these theories appear to be limited to two special cases. The first is symmetric or nonsymmetric beams with simply supported end conditions. For this case, solutions can be obtained fairly easily for all theories by assuming the following displacement field:

$$\begin{aligned}\psi_U(x) &= C_U \cos \frac{m\pi x}{L} \\ \psi_W(x) &= C_W \sin \frac{m\pi x}{L}\end{aligned}\tag{2.54}$$

where

- $\psi_U(x)$  = unknown function of  $x$  appearing in the kinematic constraint for longitudinal displacement
- $\psi_W(x)$  = unknown function of  $x$  appearing in the kinematic constraint for longitudinal displacement
- $C_U$  = unknown coefficient

$C_w$  = unknown coefficient

$m$  = mode number (1,2,3, etc.)

The second case is the free vibration of symmetric Bernoulli-Euler and Timoshenko beams under a variety of end conditions.

Unfortunately, none of the theories seems to admit easily obtainable solutions for all cases of interest. However, approximate solutions for both symmetric and nonsymmetric beams under simply supported and other end conditions can be obtained readily if the theories are given a finite element formulation. The desire to obtain such solutions provides the motivation for the finite element formulations discussed in Chapter 3.

### 3. FINITE ELEMENT FORMULATION OF COMPOSITE BEAM THEORIES

#### 3.1. The Finite Element Method

##### 3.1.1. Overview

In general, the finite element method assumes that the actual response of a continuous system, such as a beam, can be approximated by a collection of elements which represents a discretized model of the continuous system. This assumption transforms a problem with infinite degrees of freedom into one involving a finite number of degrees of freedom. An example of a cantilever beam model of an airplane wing is given in Figure 3.1. As can be seen in this figure, the continuous system is itself an abstract model of the actual physical system.

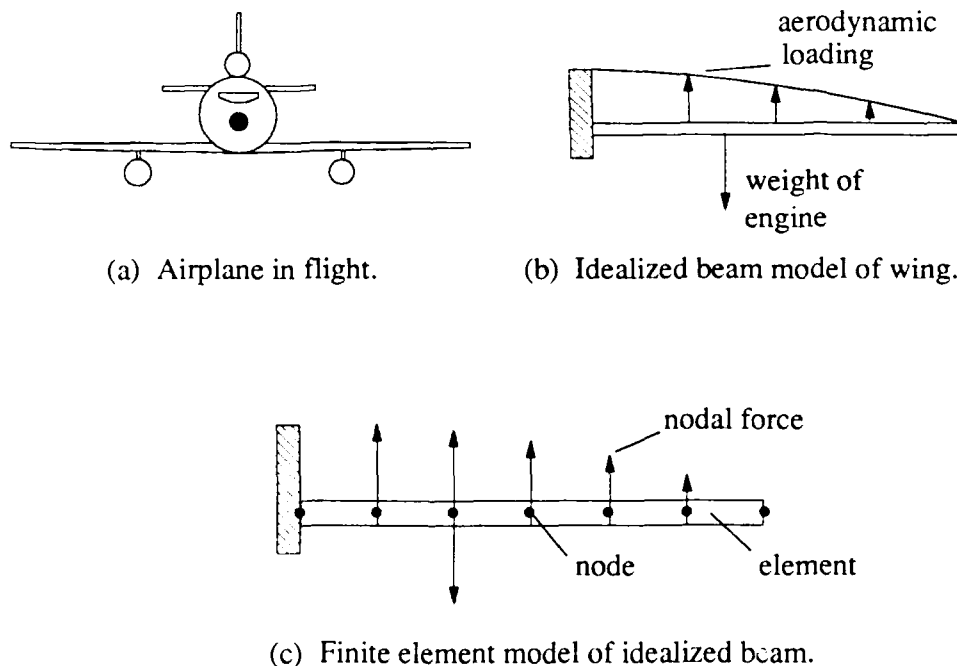


Fig. 3.1 Finite element model of idealized beam.

Many different approaches can be employed to develop the elements used in the discretized model, the most prominent of which are outlined nicely in a paper written by Pian and Tong [133] in 1969. In general, elements based on displacement methods, force methods, and mixed force-displacement methods have been formulated. In the first approach, nodal displacements are the primary unknowns, whereas forces at the nodes are the unknowns in the second approach. Both displacements and forces serve as independent unknowns in mixed formulations.

In addition to these major divisions, Pian and Tong list four different classes of elements under the general heading of displacement methods. The first is what they call the compatible model in which a displacement field which is continuous over the entire system is assumed. For statics, the principle of minimum potential energy can be used to derive the governing equations [134], although other techniques such as the unit displacement method [94,95], direct method [97], and weighted residual methods like Galerkin's method ([93], pp. 81-88) yield equivalent results.

In the equilibrium model, assumed stress fields satisfying equilibrium are used with the governing equations obtained from applying the principle of minimum complementary energy [135]. Using a modified complementary energy principle [105,136], Pian and Tong have developed so called hybrid elements in which compatible displacements are assumed at the nodes with stress fields satisfying equilibrium assumed within each element.

Finally, [133] makes mention of mixed methods. This approach assumes a continuous displacement field over the entire system and stress fields within each element. Governing equations come from a mixed variational theorem attributed to Reissner [137]. Washizu [138] attributes this principle to Hellinger [139] as well as to Reissner and shows that it is a special case of a principle which has come to be known as the Hu-Washizu principle [140,141]. The Hu-Washizu principle is a generalization of the principle of minimum potential energy in which strains and stresses, as well as displacements, appear.



It should be possible to develop mixed elements based on this three-field principle. This is alluded to by Zienkeiwicz and Lefebvre in [142], although their paper considers a mixed element in which the three fields are lateral displacement, rotation, and shear resultants, rather than stress, strain, and displacement.

Only compatible elements are examined in the present investigation. Since equilibrium, hybrid, or mixed formulations are not considered, this study refers to compatible elements simply as displacement-based elements.

### 3.1.2. Displacement-Based Elements

Two salient features of displacement-based elements are that all variables of interest, such as stress and strain, are derived from element displacements and that these displacements are assumed to vary in some prescribed manner over the element. By expressing these assumed variations in terms of shape functions, it is possible to describe displacement and all other variables of interest in terms of the displacements at the nodes of the element. Modeling a continuous system with such elements reduces the number of degrees of freedom from infinity to the finite number associated with the unknown nodal displacements in the discretized model.

As stated in Section 3.1.1, governing equations for displacement-based elements can be found using a variety of techniques, including the unit displacement method [94,95], direct method [97], variational principles ([93], pp. 78-88), or weighted residual techniques such as the Galerkin method ([93], pp. 88-91). For statics problems, this reduces a set of partial differential equations or ordinary differential equations in space to the algebraic matrix problem

$$\mathbf{Kd} = \mathbf{f} \quad (3.1)$$

where

$\mathbf{K}$  = global stiffness matrix for finite element model

$\mathbf{d}$  = global nodal displacement vector

$\mathbf{f}$  = global nodal force vector

The problem is solved by finding the unknown displacements which remain after forced, or geometric, boundary conditions are imposed. A technique such as Gaussian elimination is usually used to find the unknown displacements ([93], pp. 532-538).

For dynamics problems, the partial differential equations in space and time reduce to a linear system of ordinary differential equations in time:

$$\mathbf{M}\ddot{\mathbf{d}}(t) + \mathbf{C}\dot{\mathbf{d}}(t) + \mathbf{K}\mathbf{d}(t) = \mathbf{f}(t) \quad (3.2)$$

where

$\mathbf{M}$  = global mass matrix

$\mathbf{C}$  = global damping matrix

$\ddot{\mathbf{d}}(t)$  = global nodal acceleration vector

$\dot{\mathbf{d}}(t)$  = global nodal velocity vector

Solving Equation (3.2) for forced vibration problems usually involves the use of some numerical integration scheme ([93], pp. 476-487).

In the case of undamped free vibrations, assuming harmonic response

$$\mathbf{d}(t) = \mathbf{a}e^{i\omega t} \quad (3.3)$$

where

$\mathbf{a}$  = mode shape vector

$\omega$  = natural circular frequency of harmonic motion

yields the algebraic eigenvalue problem

$$\mathbf{K}\mathbf{a} = \omega^2 \mathbf{M}\mathbf{a} \quad (3.4)$$

As is true for statics problems, dynamics solutions are obtained after forced boundary conditions are imposed.

### 3.1.3. Convergence

In general, solutions obtained using the finite element method are rendered approximate by several kinds of error. Melosh [134] identifies three: manipulation, idealization, and discretization errors. Manipulation errors stem from the round off, truncation and other errors generated by the arithmetic operations of the computer used to solve the problem. Idealization errors occur as a result of inaccuracies associated with the simplifying assumptions required to go from the physical system to the continuous model (see Figure 3.1). Melosh cites using flat surfaces in place of curved surfaces or pinned joints instead of fixed ones as examples. Finally, discretization errors are generated by modeling a continuous system as a collection of discrete elements. This third source of error is the only kind considered further in the present study.

In general, discretization error will exist unless the assumed variation of displacements over the volume of the element happens to coincide with the actual variations given by the exact solution for the continuous system. However, it is reasonable to expect the error normally produced by discretization to become smaller as the size of the elements in the model decreases, allowing the piecewise approximation of variables afforded by the discretized finite element model to more

closely represent the true distributions of the exact solution. In fact, the discretization error approaches zero monotonically as long as the criteria of completeness and compatibility, or conformity, are satisfied (see [143], [144], and pp. 28-36 of [145]).

Elements capable of reproducing rigid-body and constant-strain modes of response possess completeness. As pointed out by Zienkeiwicz ([145], p. 29), rigid-body motion is merely a constant-strain mode with zero magnitude. Compatibility, or conformity, requires displacements to have the proper degree of continuity within and between elements. Adequate continuity within elements is established by choosing the proper shape functions. The necessary interelement continuity is obtained by forcing adjacent elements to share the appropriate nodal degrees of freedom, which also influences the selection of the proper shape functions for the element.

According to Zienkeiwicz ([145], p. 29), the proper degree of continuity can be ascertained by observing the derivatives of the displacements present in the strains for the theory being considered. The degree of continuity need not exceed one less than the maximum derivative of displacement appearing in the element's strain energy. For example, Bernoulli-Euler beam elements must be  $C^1$  continuous since second derivatives of the lateral displacement  $W(x,t)$  appear in the strain energy defined in Equation (2.28); whereas the strains in Equation (2.33) reveal that Timoshenko beam elements require only  $C^0$  continuity. Elements satisfying the minimum requirements on compatibility are referred to as conforming elements in the present study.

Although this degree of continuity in conjunction with completeness is sufficient to guarantee monotonic convergence to the exact solution, it is not a necessary condition for convergence. Less restrictive conformity requirements are spelled out by Oliveira [143,144], but it is hard to ascertain if the conditions specified are satisfied by a nonconforming element a priori. In addition, convergence for nonconforming elements is not necessarily monotonic or bounded. That is, the approximate solution does not necessarily approach the exact solution consistently from above or

below (see p. 30 and Figure 10.21, p. 205 of [145]). Therefore, it is generally desirable for elements to be conforming as well as complete, since these properties together ensure monotonic convergence to the exact solution.

Conformity is easy to achieve in line elements such as those for beams; however, it may be quite difficult to attain in plates. Doing so may require the use of complicated shape functions ([145], Chapter 10), or the use of the mixed or hybrid formulations discussed briefly in Section 3.1.1 to relax the requirements on continuity of displacement mentioned in Chapter 10 of [145]. It should be noted, however, that the bounded nature of displacement-based elements (too stiff) and equilibrium elements (too flexible) is lost when mixed or hybrid elements are used [146]. Therefore, it is impossible to tell a priori whether convergence for such elements will be from above or below the exact solution or if it will even be monotonic to begin with.

An additional means of relaxing continuity requirements in bending elements is to specify independent displacement fields for rotations and lateral displacement, as is done for Timoshenko beams. As seen in Equations (2.28) and (2.33), this not only accounts for the effects of shear deformation in some fashion, but results in strains which are defined by first derivatives of the displacements, rather than by second derivatives. Therefore, in addition to providing a better estimate of shear deformation effects, it is generally easier for shear-deformable elements to satisfy conformity requirements.

It should be noted that  $C^1$  continuity is still required in Levinson-Bickford elements, since the second derivative of  $W$  with respect to  $x$  appears in the strain energy given by Equation (2.38). In addition to requiring a higher degree of continuity, another disadvantage of such a formulation is that it forces shear strain to be continuous between elements even when it may actually be discontinuous. Discontinuities in shear strain arise naturally from abrupt changes in cross-sectional properties or when beams are used to model frame members which meet at an angle ([111], p. 319), as well as from discontinuities in applied loading.

#### 3.1.4. Shear Locking

As mentioned by Prathap, et al. in [107] and [108], a disadvantage of some shear-deformable elements is their propensity to exhibit shear locking, an artificial stiffness displayed by some bending elements in the thin-beam or thin-plate limit. Perhaps the most straightforward way to correct this problem in beam elements is to choose shape functions for the lateral and longitudinal displacements such that the contributions of these displacements to shear strain have the same variation over the length of the element. For example, Equation (2.14) reveals that a cubic variation of lateral displacement and a quadratic variation of rotation both produce quadratic contributions to the shear strain of a Timoshenko beam. The present study uses the term "consistent" to classify such a combination of shape functions. Further, the use of consistent shape functions is the only technique employed in this investigation to avoid shear locking.

However, it should be noted that the use of consistent shape functions is not favored by some since this approach requires the presence of nodes in the interior of the elements and does not result in an equal number of degrees of freedom at all nodes. These features presently make such elements unattractive for use in commercially available finite element programs. Also, the additional degrees of freedom required by consistent elements may reduce their computational efficiency somewhat. Therefore, other methods are often used to suppress shear locking in elements which are formulated using inconsistent shape functions.

The technique of reduced integration mentioned in [107] and [108] appears to be the most popular method. When a variational formulation is used to derive the governing equations for a finite element, the stiffness and mass matrices can be obtained by integrating various quantities over the volume of the element. Gaussian quadrature ([93], pp. 361-365) is often used to facilitate this integration process. Exact or approximate values of the integrals involved can be obtained depending on whether the integrand is sampled at all the required Gauss points (full integration) or

at some reduced number of points (reduced integration). In addition to saving computation time, [107] and [108] reveal that reduced integration of the stiffness matrix acts to filter out spurious constraints caused by using inconsistent shape functions that lead to locking.

Reduced integration can be applied uniformly to all components of the stiffness matrix [147] or selectively to just the shear-related terms [148]. A comparison of uniform and selective reduced integration is given by Hughes, et al. in [149] and in [150] (pp. 329-332).

The Lagrange multiplier method, also discussed in [150] (pp. 194-197, 217-226, and 323-335), is another technique which can be used to avoid shear locking. In bending applications of this method, the functional associated with potential energy for statics or the action for dynamics is augmented with a constraint which forces shear strain to go to zero as the thin-beam (or plate) limit is approached. The multipliers which enforce this constraint exactly correspond physically to shear forces and become additional unknowns in the finite element formulation of the problem. The presence of unknown forces as well as displacements requires a mixed formulation for such elements.

Malkus and Hughes [151] have demonstrated the essential equivalence between such mixed formulations and reduced integration, enhancing the legitimacy of the latter technique. In addition, Hughes actually provides several examples of equivalent mixed and reduced-integration elements on page 222 of [150].

Hughes [150] also discusses penalty functions in his treatment of the Lagrange multiplier method. These functions only enforce the shear-strain constraint in an approximate fashion, but do not increase the total number of unknowns since the functions are estimated by the analyst. As a result, a mixed formulation is not required. However, penalty-function elements may still be subject to shear locking and may require some form of reduced integration to improve their accuracy in the thin-beam or plate limit.

Apparently, shear locking is also possible in some mixed elements. One of the most recent innovations adopted to avoid shear locking in elements based on mixed formulations is the use of bubble shape functions [142,152,153]. Bubble shape functions can be employed in conjunction with an initial set of inconsistent shape functions to enforce the constraint of zero shear strain in the thin-beam or plate limit. Such an approach does not require the use of reduced integration, but does increase the number of unknowns in the problem since the bubble shape functions require extra internal nodes. In fact, the final configuration of elements which make use of bubble shape functions does not appear to be that different from those formulated using consistent shape functions to begin with.

As stated previously, consistent shape functions are employed in the formulation of all finite elements considered in the present study. Using such shape functions eliminates shear locking in a straightforward fashion while retaining the bounded monotonic convergence guaranteed for conforming, complete elements. This guarantee does not apply to elements which make use of reduced integration, mixed formulations, or bubble shape functions. In addition to ensuring bounded, monotonic convergence, utilizing consistent shape functions avoids the mismatch in interface displacements which can lead to errors in multilayered stacked elements [127-132].

### **3.2. Governing Equations**

Section 3.1.2 indicates that displacement-based finite elements are based on the following assumptions: the longitudinal and lateral displacements of the continuous beam can be approximated by the displacement field of a properly constructed discretized model, like the one depicted in Figure 3.1; all other variables, such as velocity, strain, or stress can be expressed in terms of the approximate displacement field; and prescribed spatial variations of the approximate displacement field and all related fields can be expressed in terms of a proper set of shape functions. These assumptions make it possible to recast the governing equations, derived in Chapter 2 using Hamilton's Principle, in



terms of the unknown nodal displacements of the beam elements derived in this study.

Table 3.1 Vectors and Matrices in Displacement-Based Finite Elements

Vector or Matrix	Definition
$\underline{u}$	displacement vector
$\underline{\epsilon}$	strain vector
$\underline{\sigma}$	stress vector
$\underline{q}$	local nodal displacement vector for element
$\underline{d}$	global displacement vector for finite element model
$\underline{a}$	global mode shape vector
$\underline{N}$	shape function matrix
$\underline{B}$	strain-displacement matrix
$\underline{D}$	constitutive matrix
$\underline{\rho}$	density matrix

The vectors and matrices used in the finite element formulation of the governing equations are defined in Table 3.1. Equations (3.5) express these quantities in terms of the variables discussed in Chapter 2 and reveals their functional dependence on the independent variables  $x$ ,  $y$  and  $t$ .

$$\underline{u} = \underline{u}(x, y, t) = \begin{Bmatrix} u(x, y, t) \\ v(x, y, t) \end{Bmatrix}$$

$$\underline{\epsilon} = \underline{\epsilon}(x, y, t) = \begin{Bmatrix} \epsilon(x, y, t) \\ \gamma(x, y, t) \end{Bmatrix}$$

$$\underline{\sigma} = \underline{\sigma}(x, y, t) = \begin{Bmatrix} \sigma & (x, y, t) \\ \tau & (x, y, t) \end{Bmatrix} \quad (3.5)$$

$$\mathbf{N} = \mathbf{N}(x, y)$$

$$\mathbf{B} = \mathbf{B}(x, y)$$

$$\mathbf{q} = \mathbf{q}(t)$$

The actual relations used to express the variation of the displacement, velocity, strain, and stress fields over a single element in terms of shape functions are given by Equations (3.6) through (3.9), respectively.

$$\mathbf{u} = \mathbf{N}\mathbf{q} \quad (3.6)$$

$$\dot{\mathbf{u}} = \mathbf{N}\dot{\mathbf{q}} \quad (3.7)$$

$$\underline{\varepsilon} = \mathbf{B}\mathbf{q} \quad (3.8)$$

$$\underline{\sigma} = \mathbf{D}\mathbf{B}\mathbf{q} \quad (3.9)$$

As can be seen in Equation (3.6), the displacement field is defined as the product of the shape function matrix and the nodal displacement vector for the element. Equations (3.5) indicate that the shape function matrix allows for variations in both the  $x$  and  $y$  directions. It should be noted that the variation of displacements in the  $y$  direction is actually governed by the kinematic constraints chosen for each beam element and that the  $x$  variation prescribed by the shaped functions applies only to the unknown dependent variables in the kinematic constraint. The effects of both the chosen kinematic constraint and assumed shape functions are accounted for by the shape function matrix.

It should also be noted that all time dependence is restricted to the nodal displacement vector. Therefore, the velocity field is obtained by simply premultiplying the nodal velocity vector by the shape function matrix, as shown in Equation (3.7).

Equation (3.8) reveals that the strain vector is related to the nodal displacement vector through the strain-displacement matrix. This matrix is obtained by properly applying the operations specified in Equations (2.5) to the displacement field defined by Equation (3.6). As depicted in Equation (3.9), the stress vector is obtained simply by premultiplying the strain vector by the matrix which characterizes the constitutive relations for the beam of interest.

Using these relations allows the kinetic energy ( $T_e$ ) and potential energy ( $V_e$ ) for an element to be expressed in the forms

$$T_e = \frac{1}{2} \int_V \dot{\mathbf{q}}^T \mathbf{N}^T \underline{\rho} \mathbf{N} \dot{\mathbf{q}} dV \quad (3.10)$$

$$V_e = \frac{1}{2} \int_V \mathbf{q}^T \mathbf{B}^T \mathbf{D} \mathbf{B} \mathbf{q} dV \quad (3.11)$$

It should be noted that it is not necessary to use a density matrix to define the kinetic energy for the element, as is done in Equation (3.10). The energy can be obtained by treating density as a scalar quantity, which is the standard approach usually taken. However, in some cases it becomes convenient to incorporate various inertia properties, such as lateral inertia and rotary inertia, in a density matrix. Since this treatment is more general and since it provides a certain symmetry with respect to the expression for the potential energy given in Equation (3.11), it is used in this derivation.

Substituting Equations (3.10) and (3.11) into Equation (2.19) yields the action for the element

$$a_e = \int_{t_0}^{t_1} \left\{ \frac{1}{2} \int_V \dot{\mathbf{q}}^T \mathbf{N}^T \underline{\rho} \mathbf{N} \dot{\mathbf{q}} dV - \frac{1}{2} \int_V \mathbf{q}^T \mathbf{B}^T \mathbf{D} \mathbf{B} \mathbf{q} dV \right\} dt \quad (3.12)$$

The governing equation for the element can be obtained by forcing this action to be stationary. The result makes use of the fact that the density and constitutive matrices are symmetric:

$$\left\{ \int_{\mathcal{V}} \mathbf{N}^T \underline{\rho} \mathbf{N} d\mathcal{V} \right\} \ddot{\mathbf{q}} + \left\{ \int_{\mathcal{V}} \mathbf{B}^T \mathbf{D} \mathbf{B} d\mathcal{V} \right\} \mathbf{q} = 0 \quad (3.13)$$

The local mass and stiffness matrices defined by

$$\mathbf{M}^{(e)} = \int_{\mathcal{V}} \mathbf{N}^T \underline{\rho} \mathbf{N} d\mathcal{V} \quad \mathbf{K}^{(e)} = \int_{\mathcal{V}} \mathbf{B}^T \mathbf{D} \mathbf{B} d\mathcal{V} \quad (3.14)$$

for the element allows Equation (3.13) to be rewritten as

$$\mathbf{M}^{(e)} \ddot{\mathbf{q}} + \mathbf{K}^{(e)} \mathbf{q} = 0 \quad (3.15)$$

Proper assembly of the local element matrices, namely,

$$\mathbf{M} = \sum_{i=1}^{NE} \mathbf{M}_i^{(e)} \quad \mathbf{K} = \sum_{i=1}^{NE} \mathbf{K}_i^{(e)} \quad (3.16)$$

where

$NE$  = number of elements in discretized model

allows the governing equations for the free vibration of the entire discretized system to be written in terms of the global matrices and displacement vector

$$\mathbf{M} \ddot{\mathbf{d}} + \mathbf{K} \mathbf{d} = 0 \quad (3.17)$$

Once the global mass and stiffness matrices are assembled, forced boundary conditions restricting rigid-body motion must be imposed; otherwise, the global matrices will be singular. The forced boundary conditions seen in Equations (2.31), (2.36), (2.41), and (2.46) are imposed on a

finite element model by specifying zero motion for appropriate nodal degrees of freedom at the ends of the model. This has the effect of partitioning the global mass and stiffness matrices (see [93], pp. 35-37).

For the homogeneous boundary conditions considered in the present study, the portions of the partitioned matrices required to solve free vibration problems can be obtained simply by eliminating the rows and columns of the global matrices associated with the nodal degrees of freedom which are not allowed to move. Similarly, these degrees of freedom must be eliminated from the global displacement vector as well. Only the retained portions of the partitioned global matrices and displacement vector are of interest in the following discussion.

It should be noted that, in general, the finite element method cannot satisfy the natural boundary conditions associated with simply supported or free ends unless the element contains nodal degrees of freedom which can enforce these boundary conditions explicitly as well (see [113]).

Once the global matrices and displacement vector have been modified to account for the forced boundary conditions associated with the problem of interest, the assumptions regarding harmonic motion specified by Equation (3.3) can be used to obtain the algebraic eigenvalue problem given in Equation (3.4). This eigenvalue problem can also be expressed as

$$\mathbf{K}^{-1}\mathbf{M}\mathbf{a} = \frac{1}{\omega^2}\mathbf{a} \quad (3.18)$$

$$\mathbf{M}^{-1}\mathbf{K}\mathbf{a} = \omega^2\mathbf{a} \quad (3.19)$$

The desired form depends on the approach used to solve the eigenvalue problem and the nature of the global matrices. If the lowest natural frequencies are of interest, which is usually the case, and if the method used to solve the eigenvalue problem finds the highest eigenvalues first, the form

given by Equation (3.18) is recommended. If these conditions do not apply and if one of the global matrices can be diagonalized, the approach which inverts the diagonal matrix should be used to take advantage of the computational efficiency possible in inverting such a matrix.

### 3.3. Mass and Stiffness Matrices

The fundamental task associated with developing a new finite element for dynamic analyses is deriving its mass and stiffness matrices. As can be seen in Equations (3.14), this task cannot be accomplished until the element's shape functions and the basic nature of the beam's material properties are defined. Once the shape functions and basic material behavior are defined, the fairly general treatment of the governing equations discussed in Section 3.2 can be applied easily to the beam finite elements of interest in the investigation. The definitions given in Equations (3.20) through (3.23) can be used to facilitate this process.

$$\mathbf{N} = \begin{bmatrix} \mathbf{N}_1 \\ \mathbf{N}_2 \end{bmatrix} \quad (3.20)$$

$$\mathbf{B} = \begin{bmatrix} \mathbf{B}_1 \\ \mathbf{B}_2 \end{bmatrix} = \begin{bmatrix} \frac{\partial}{\partial x} & \mathbf{N}_1 \\ \frac{\partial}{\partial x} & \mathbf{N}_2 + \frac{\partial}{\partial y} \mathbf{N}_1 \end{bmatrix} \quad (3.21)$$

$$\mathbf{D} = \begin{bmatrix} E(y) & 0 \\ 0 & G(y) \end{bmatrix} \quad (3.22)$$

$$\underline{\rho} = \begin{bmatrix} \rho(y) & 0 \\ 0 & \rho(y) \end{bmatrix} = \rho(y)\mathbf{I} \quad (3.23)$$

where

$\mathbf{I}$  = the identity matrix

Equation (3.20) partitions the shape function matrix into two submatrices which allow the shape functions for longitudinal and lateral motion to be specified independently. This partitioning also makes it easier to define the strain-displacement matrix, as shown in Equation (3.21). Finally, the constitutive and inertial properties for the simple beam elements can be stated more explicitly by the general relations given in Equations (3.22) and (3.23). These two equations reflect the nonhomogeneous nature of laminated composites in which the material properties vary discontinuously in the lateral direction.

Substituting the definitions given in Equations (3.20) through (3.23) into Equations (3.14) allows the local mass and stiffness matrices to be expressed as

$$\mathbf{M}^{(e)} = \mathbf{M}_u^{(e)} + \mathbf{M}_v^{(e)} = \int_{\mathcal{V}} \mathbf{N}_1^T \rho(y) \mathbf{N}_1 d\mathcal{V} + \int_{\mathcal{V}} \mathbf{N}_2^T \rho(y) \mathbf{N}_2 d\mathcal{V} \quad (3.24)$$

$$\mathbf{K}^{(e)} = \mathbf{K}_\epsilon^{(e)} + \mathbf{K}_\gamma^{(e)} = \int_{\mathcal{V}} \mathbf{B}_1^T E(y) \mathbf{B}_1 d\mathcal{V} + \int_{\mathcal{V}} \mathbf{B}_2^T G(y) \mathbf{B}_2 d\mathcal{V} \quad (3.25)$$

These equations reveal explicitly the contributions that longitudinal and lateral motion make to the local mass matrix, as well as the contributions of normal and shear deformation to the stiffness of the element. It should be noted that  $\mathbf{M}_u^{(e)}$  characterizes the rotational inertia of the beam as well as the translational inertia associated with its axial motion. In addition, the stiffness matrix associated with normal deformation accounts for both axial and bending response.

The shape functions for all elements examined in this investigation allow a quadratic variation of longitudinal displacement in the  $x$  direction along with a cubic variation of lateral displacement in the  $x$  direction. As stated previously, such a consistent combination of prescribed displacements avoids shear locking and leads to more compatible variations of interlayer displacements for stacked elements.

Variations for generic longitudinal and lateral displacements are defined as follows:

$$\begin{aligned}
 \psi_U(x, t) &= a_0(t) + a_1(t)x + a_2(t)x^2 \\
 &= A_1(x)q_1(t) + A_2(x)q_2(t) + A_3(x)q_3(t)
 \end{aligned} \tag{3.26}$$

where

- $a_j(t)$  = unknown coefficients in quadratic polynomial
- $q_i(t)$  = degree of freedom associated with  $i$ th node of element
- $A_i(t)$  = quadratic shape function associated with  $i$ th nodal degree of freedom,  $q_i(t)$

and

$$\begin{aligned}
 \psi_W(x, t) &= b_0(t) + b_1(t)x + b_2(t)x^2 + b_3(t)x^3 \\
 &= B_1(x)q_1(t) + B_2(x)q_2(t) + B_3(x)q_3(t) + B_4(x)q_4(t)
 \end{aligned} \tag{3.27}$$

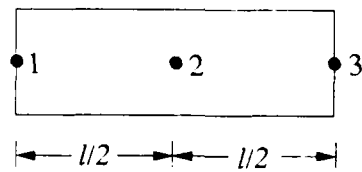
where

- $b_j(t)$  = unknown coefficients in cubic polynomial
- $B_i(x)$  = cubic shape function associated with  $i$ -th nodal degree of freedom,  $q_i(t)$

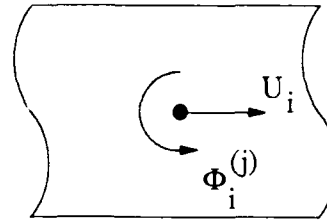
Both equations show the equivalence between expressing these variations in polynomial form and in terms of shape functions.

In general, axial motion, rotation, and second- and third-order warping of the cross section can contribute to longitudinal motion. As seen in Equation (3.26), three degrees of freedom are needed to specify a quadratic variation for any of these generalized longitudinal displacements. For all elements in this study, these three degrees of freedom correspond to generalized displacements at the end nodes and center node pictured in Figure 3.2a. Figure 3.2b shows the positive direction for axial motion, rotation, and warping deformations at a typical node.





(a) Nodes.



(b) Positive directions for longitudinal degrees of freedom at typical node.

$l$  = length of element

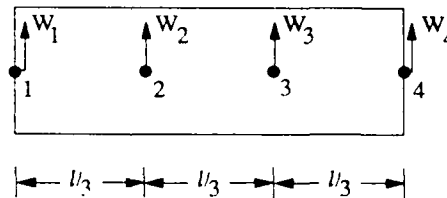
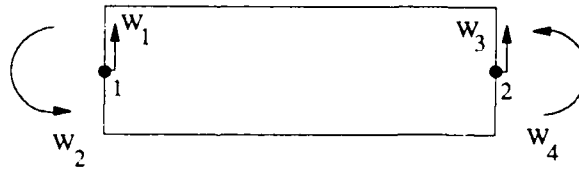
$U_i$  = axial degree of freedom (dof) at node  $i$

$\Phi_i^{(1)}$  = rotational dof at node  $i$

$\Phi_i^{(2)}$  = second-order warping dof at node  $i$

$\Phi_i^{(3)}$  = third-order warping dof at node  $i$

Fig. 3.2 Quadratic finite element.

(a)  $C^0$  element.

$w_2$  = slope at node 1

$w_4$  = slope at node 2

(b)  $C^1$  element.

Fig. 3.3 Cubic finite element.

Equation (3.27) indicates four degrees of freedom are required to specify the cubic variation in lateral motion. The nodal degrees of freedom for  $C^0$  and  $C^1$  continuity are shown in Figures 3.3a

and 3.3b, respectively. The nodes for  $C^0$  continuity are evenly spaced along the length of the element. The  $C^1$ -continuous element requires only two end nodes, but has two degrees of freedom at each node. Figure 3.3a and b also show the positive sense for all variables associated with each kind of cubic variation.

The shape functions for longitudinal,  $C^0$ -continuous lateral, and  $C^1$ -continuous lateral displacement are given in Equations (3.28), (3.29), and (3.30), respectively, as follows:

$$\begin{aligned} A_1(x) &= 1 - 3\left(\frac{x}{l}\right) + 2\left(\frac{x}{l}\right)^2 \\ A_2(x) &= 4\left(\frac{x}{l}\right) - 4\left(\frac{x}{l}\right)^2 \\ A_3(x) &= -\left(\frac{x}{l}\right) + 2\left(\frac{x}{l}\right)^2 \end{aligned} \quad (3.28)$$

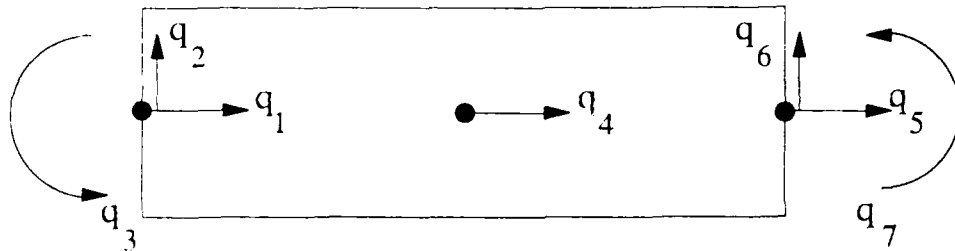
where

$l$  = length of the element

$$\begin{aligned} B_1(x) &= \frac{1}{2} \left[ 2 - 11\left(\frac{x}{l}\right) + 18\left(\frac{x}{l}\right)^2 - 9\left(\frac{x}{l}\right)^3 \right] \\ B_2(x) &= \frac{1}{2} \left[ 18\left(\frac{x}{l}\right) - 45\left(\frac{x}{l}\right)^2 + 27\left(\frac{x}{l}\right)^3 \right] \\ B_3(x) &= \frac{1}{2} \left[ -9\left(\frac{x}{l}\right) + 36\left(\frac{x}{l}\right)^2 - 27\left(\frac{x}{l}\right)^3 \right] \\ B_4(x) &= \frac{1}{2} \left[ 2\left(\frac{x}{l}\right) - 9\left(\frac{x}{l}\right)^2 + 9\left(\frac{x}{l}\right)^3 \right] \end{aligned} \quad (3.29)$$

$$\begin{aligned}
 B_1(x) &= 1 - 3\left(\frac{x}{l}\right)^2 + 2\left(\frac{x}{l}\right)^3 \\
 B_2(x) &= l\left[\left(\frac{x}{l}\right) - 2\left(\frac{x}{l}\right)^2 + \left(\frac{x}{l}\right)^3\right] \\
 B_3(x) &= 3\left(\frac{x}{l}\right)^2 - 2\left(\frac{x}{l}\right)^3 \\
 B_4(x) &= l\left[-\left(\frac{x}{l}\right)^2 + \left(\frac{x}{l}\right)^3\right]
 \end{aligned} \tag{3.30}$$

The quadratic nature of the longitudinal shape functions and the cubic nature of the longitudinal shape functions are apparent in these equations.



**Fig. 3.4 Bernoulli-Euler beam element.**

Figure 3.4 shows the nodal degrees of freedom associated with a Bernoulli-Euler beam element. The displacement vector containing the degrees of freedom seen in Figure 3.4 is given by

$$\mathbf{q}^T = [U_1 \ W_1 \ W_2 \ U_2 \ U_3 \ W_3 \ W_4] \tag{3.31}$$

The kinematic constraint for a Bernoulli-Euler beam, given initially in Equation (2.11), can be stated in terms of the nodal degrees of freedom and shape functions for this element as follows:

$$\begin{aligned}
u(x, y, t) &= U(x, t) - W'(x, t)y \\
&= \sum_{i=1}^3 A_i(x)U_i(t) - \sum_{j=1}^4 B_j'(x)W_j(t)y \\
&= \mathbf{N}_1(x, y)\mathbf{q}(t)
\end{aligned} \tag{3.32}$$

where

$U_i(t)$  = nodal degrees of freedom for axial displacement

$W_j(t)$  = nodal degrees of freedom for lateral displacement

and

$$v(x, y, t) = W(x, t) = \sum_{j=1}^4 B_j(x)W_j(t) = \mathbf{N}_2(x, y)\mathbf{q}(t) \tag{3.33}$$

The resulting shape function submatrices for longitudinal and lateral displacement are given as

$$\mathbf{N}_1 = [A_1(x) \quad B_1'(x)y \quad B_2'(x)y \quad A_2(x) \quad A_3(x) \quad B_3'(x)y \quad B_4'(x)y] \tag{3.34}$$

$$\mathbf{N}_2 = [0 \quad B_1(x) \quad B_2(x) \quad 0 \quad 0 \quad B_3(x) \quad B_4(x)] \tag{3.35}$$

As can be seen, these submatrices capture the spatial variations imposed by the kinematic constraint and prescribed by the shape functions.

The submatrices for the  $\mathbf{B}$  matrix, obtained by applying the operations specified in Equation (3.21) to the shape function submatrices given by Equations (3.34) and (3.35), are

$$\mathbf{B}_1 = [A_1'(x) \quad B_1''(x)y \quad B_2''(x)y \quad A_2'(x) \quad A_3'(x) \quad B_3''(x)y \quad B_4''(x)y] \tag{3.36}$$

$$\mathbf{B}_2 = \mathbf{0} \tag{3.37}$$

The zero submatrix seen in Equation (3.37) reflects the inability of the Bernoulli-Euler beam to model shear strain directly.

Substituting the shape functions given in Equations (3.28) and (3.30) into Equations (3.34) through (3.37), substituting these in turn into Equations (3.24) and (3.25), and carrying out the required integration over the volume of the element results in the local mass and stiffness matrices given in Equations (3.38) and (3.39), respectively:

where

$$\mathbf{M}^{(e)} = \begin{pmatrix} 8\gamma_0 l^2 & 6\gamma_1 l & -7\gamma_1 l^2 & 4\gamma_0 l^2 & -2\gamma_0 l^2 & -6\gamma_1 l & 3\gamma_1 l^2 \\ \cdot & 72\gamma_2 + 156\delta & 6\gamma_2 l + 22\delta l & 48\gamma_1 l & 6\gamma_1 l & -72\gamma_2 + 54\delta & 6\gamma_2 l - 13\delta l \\ \cdot & \cdot & 8\gamma_2 l^2 + 4\delta l^2 & 4\gamma_1 l^2 & 3\gamma_1 l^2 & -6\gamma_2 l + 13\delta l & -2\gamma_2 l^2 - 3\delta l^2 \\ \cdot & \cdot & \cdot & 32\gamma_0 l^2 & 4\gamma_0 l^2 & -48\gamma_1 l & 4\gamma_1 l^2 \\ \cdot & \cdot & \cdot & \cdot & 8\gamma_0 l^2 & -6\gamma_1 l & -7\gamma_1 l^2 \\ \cdot & \cdot & \cdot & \cdot & \cdot & 72\gamma_2 + 156\delta & -6\gamma_2 l - 22\delta l \\ \cdot & \cdot & \cdot & \cdot & \cdot & \cdot & 8\gamma_2 l^2 + 4\delta l^2 \end{pmatrix}$$

$\mathbf{M}^{(e)}$

$$\gamma_n = \frac{P_n}{60l} \quad \delta = \frac{P_0 l}{420}$$

$$\mathbf{K}^{(c)} = \left( \frac{1}{l^3} \right) \begin{pmatrix} \frac{7}{3}Q_0l^2 & -4Q_1l & -3Q_2l^2 & -\frac{8}{3}Q_0l^2 & \frac{1}{3}Q_0l^2 & 4Q_1l & -Q_2l^2 \\ \cdot & 12Q_2 & 6Q_2l & 8Q_1l & -4Q_1l & -12Q_2 & 6Q_2l \\ \cdot & \cdot & 4Q_2l^2 & 4Q_1l^2 & -Q_1l^2 & -6Q_2l & 2Q_2l^2 \\ \cdot & \cdot & \cdot & \frac{16}{3}Q_0l^2 & -\frac{8}{3}Q_0l^2 & -8Q_1l & 4Q_1l^2 \\ \cdot & \cdot & \cdot & \cdot & \frac{7}{3}Q_0l^2 & 4Q_1l & -3Q_1l^2 \\ \cdot & \cdot & \cdot & \cdot & \cdot & 12Q_2 & -6Q_2l \\ \cdot & \cdot & \cdot & \cdot & \cdot & \cdot & 4Q_2l^2 \end{pmatrix}$$

(3.39)

Several features of these matrices should be noted. First, only components in the upper triangle of each matrix are specified since both matrices are symmetric. Second, the nonhomogeneity possible in composite beams requires the use of the composite properties defined in Equations (2.25) and (2.26). Finally, the odd-numbered composite terms (e.g.,  $P_1$ ) are necessary to account for the coupling between the axial and bending responses exhibited by nonsymmetric composite beams. These components have a value of zero for symmetric beams.

The mass and stiffness matrices for all the remaining elements can be found in a similar manner. The results for the Bernoulli-Euler beam element just discussed as well as for the remaining elements are summarized in Section 3.3.2. It should be noted that the Bernoulli-Euler beam element and the Levinson-Bickford element require  $C^1$  continuity in lateral displacement. Therefore, these elements use the nodal degrees of freedom pictured in Figure 3.3b and shape functions specified in Equations (3.30) to interpolate lateral displacement. The other elements use the nodal degrees of freedom shown in Figure 3.3a and the shape functions given in Equations (3.29).

It should also be noted that  $C^1$  continuity is easy to attain in the Levinson-Bickford beam element, but more difficult in the associated plate element developed by Reddy and Khdir [62], which requires Hermite cubic shape functions to interpolate lateral displacement. In addition, the  $C^1$  continuity required by the Levinson-Bickford beam element does not allow shear strain to be discontinuous between elements. As discussed in Section 3.1.3, this can be a drawback in cases where the shear strain actually is discontinuous.

### 3.4. Mass and Stiffness Matrices for Each Simple Element

This section specifies the nodal degrees of freedom, the kinematic constraints in terms of these degrees of freedom, and the resulting local mass and stiffness matrices for each simple element developed in this investigation. The general approach outlined in Section 3.3 is used and results



are presented for elements associated with Bernoulli-Euler, Timoshenko, Levinson-Bickford, and the general third-order beam theories, in that order. The figures and equations used in Section 3.3 for the Bernoulli-Euler beam element are repeated here for completeness.

### 3.4.1. Bernoulli-Euler Beam Element

The nodal degrees of freedom for the Bernoulli-Euler element are given in Figure 3.5 and Equation (3.40). The kinematic constraints for the element are specified in Equations (3.41) and (3.42). The resulting mass and stiffness matrices are given in Equations (3.43) and (3.44), respectively.

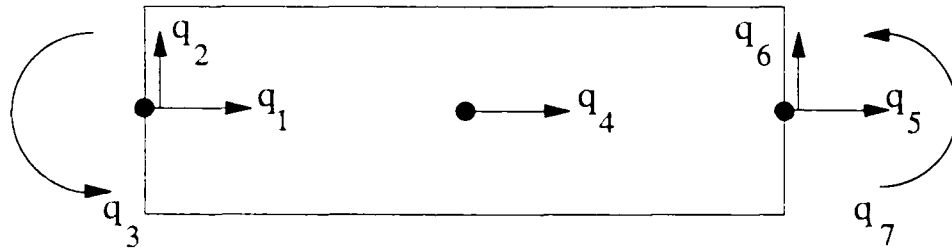


Fig. 3.5 Bernoulli-Euler beam element.

$$\mathbf{q}^T = [U_1 \ W_1 \ W_2 \ U_2 \ U_3 \ W_3 \ W_4] \quad (3.40)$$

$$\begin{aligned} u(x, y, t) &= U(x, t) - W'(x, t)y \\ &= \sum_{i=1}^3 A_i(x)U_i(t) - \sum_{j=1}^4 B_j'(x)W_j(t)y \\ &= \mathbf{N}_1(x, y)\mathbf{q}(t) \end{aligned} \quad (3.41)$$

$$v(x, y, t) = W(x, t) = \sum_{j=1}^4 B_j(x)W_j(t) = \mathbf{N}_2(x, y)\mathbf{q}(t) \quad (3.42)$$

$$\mathbf{M}^{(c)} = \begin{pmatrix} 8\gamma_0 l^2 & 6\gamma_1 l & -7\gamma_1 l^2 & 4\gamma_0 l^2 & -2\gamma_0 l^2 & -6\gamma_1 l & 3\gamma_1 l^2 \\ \cdot & 72\gamma_2 + 156\delta & 6\gamma_2 l + 22\delta l & 48\gamma_1 l & 6\gamma_1 l & -72\gamma_2 + 54\delta & 6\gamma_2 l - 13\delta l \\ \cdot & \cdot & 8\gamma_2 l^2 + 4\delta l^2 & 4\gamma_1 l^2 & 3\gamma_1 l^2 & -6\gamma_2 l + 13\delta l & -2\gamma_2 l^2 - 3\delta l^2 \\ \cdot & \cdot & \cdot & 32\gamma_0 l^2 & 4\gamma_0 l^2 & -48\gamma_1 l & 4\gamma_1 l^2 \\ \cdot & \cdot & \cdot & \cdot & 8\gamma_0 l^2 & -6\gamma_1 l & -7\gamma_1 l^2 \\ \cdot & \cdot & \cdot & \cdot & \cdot & 72\gamma_2 + 156\delta & -6\gamma_2 l - 22\delta l \\ \cdot & \cdot & \cdot & \cdot & \cdot & \cdot & 8\gamma_2 l^2 + 4\delta l^2 \end{pmatrix}$$

where

$$\gamma_n = \frac{P_n}{60l} \quad \delta = \frac{P_0 l}{420}$$

$$\mathbf{K}^{(e)} = \left( \frac{1}{l^3} \right) \begin{pmatrix} \frac{7}{3}Q_0l^2 & -4Q_1l & -3Q_1l^2 & -\frac{8}{3}Q_0l^2 & \frac{1}{3}Q_0l^2 & 4Q_1l & -Q_1l^2 \\ \cdot & 12Q_2 & 6Q_2l & 8Q_1l & -4Q_1l & -12Q_2 & 6Q_2l \\ \cdot & \cdot & 4Q_2l^2 & 4Q_1l^2 & -Q_1l^2 & -6Q_2l & 2Q_2l^2 \\ \cdot & \cdot & \cdot & \frac{16}{3}Q_0l^2 & -\frac{8}{3}Q_0l^2 & -8Q_1l & 4Q_1l^2 \\ \cdot & \cdot & \cdot & \cdot & \frac{7}{3}Q_0l^2 & 4Q_1l & -3Q_1l^2 \\ \cdot & \cdot & \cdot & \cdot & \cdot & 12Q_2 & -6Q_2l \\ \cdot & \cdot & \cdot & \cdot & \cdot & \cdot & 4Q_2l^2 \end{pmatrix}$$

(3.44)

### 3.4.2. Timoshenko Beam Element

The nodal degrees of freedom for the Timoshenko element are given in Figure 3.6 and Equation (3.45). The kinematic constraints for the element are specified in Equations (3.46) and (3.47). The resulting mass and stiffness matrices are given in Equations (3.48) and (3.49), respectively.

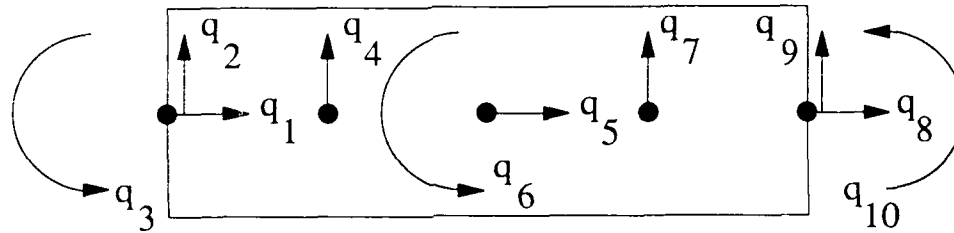


Fig. 3.6 Timoshenko beam element.

$$\mathbf{q}^T = [U_1 \ W_1 \ \Phi_1 \ W_2 \ U_2 \ \Phi_2 \ W_3 \ U_3 \ W_4 \ \Phi_3] \quad (3.45)$$

$$\begin{aligned} u(x, y, t) &= U(x, t) - \Phi(x, t)y \\ &= \sum_{i=1}^3 A_i(x)U_i(t) - \sum_{i=1}^3 A_i(x)\Phi_i(t) \\ &= \mathbf{N}_1(x, y)\mathbf{q}(t) \end{aligned} \quad (3.46)$$

where

$\Phi_i(t)$  = nodal degrees of freedom for rotation of cross section

$$v(x, y, t) = W(x, t) = \sum_{j=1}^4 B_j(x)W_j(t) = \mathbf{N}_2(x, y)\mathbf{q}(t) \quad (3.47)$$

$$\mathbf{M}^{(e)} = \begin{pmatrix} 4\gamma_0 & 0 & -4\gamma_1 & 0 & 2\gamma_0 & -2\gamma_1 & 0 & -\gamma_0 & 0 & \gamma_1 \\ \cdot & 128\delta & 0 & 99\delta & 0 & 0 & -36\delta & 0 & 19\delta & 0 \\ \cdot & \cdot & 4\gamma_2 & 0 & -2\gamma_1 & 2\gamma_2 & 0 & \gamma_1 & 0 & -\gamma_2 \\ \cdot & \cdot & \cdot & 648\delta & 0 & 0 & -81\delta & 0 & -36\delta & 0 \\ \cdot & \cdot & \cdot & \cdot & 16\gamma_0 & -16\gamma_1 & 0 & 2\gamma_0 & 0 & -2\gamma_1 \\ \cdot & \cdot & \cdot & \cdot & \cdot & 16\gamma_2 & 0 & -2\gamma_1 & 0 & 2\gamma_2 \\ \cdot & \cdot & \cdot & \cdot & \cdot & \cdot & 648\delta & 0 & 99\delta & 0 \\ \cdot & \cdot & \cdot & \cdot & \cdot & \cdot & \cdot & 4\gamma_0 & 0 & -4\gamma_1 \\ \cdot & \cdot & \cdot & \cdot & \cdot & \cdot & \cdot & \cdot & 128\delta & 0 \\ \cdot & \cdot & \cdot & \cdot & \cdot & \cdot & \cdot & \cdot & \cdot & 4\gamma_2 \end{pmatrix} \quad (3.48)$$

where

$$\gamma_n = \frac{P_n l}{30} \quad \delta = \frac{P_0 l}{1680}$$

$$\mathbf{K}^{(e)} = \begin{pmatrix}
 7\alpha_0 & 0 & -7\alpha_1 & 0 & -8\alpha_0 & 8\alpha_1 & 0 & \alpha_0 & 0 & -\alpha_1 \\
 \cdot & 444\beta & 83\beta l & -567\beta & 0 & 44\beta l & 162\beta & 0 & -39\beta & -7\beta l \\
 \cdot & \cdot & 7\alpha_2 + 13\beta l^2 & -99\beta l & 8\alpha_1 & -8\alpha_2 + 8\beta l^2 & 9\beta l & -\alpha_1 & 7\beta l & \alpha_2 - 4\beta l^2 \\
 \cdot & \cdot & \cdot & 1296\beta & 0 & 108\beta l & -891\beta & 0 & 162\beta & -9\beta l \\
 \cdot & \cdot & \cdot & \cdot & 16\alpha_0 & -16\alpha_1 & 0 & -8\alpha_0 & 0 & 8\alpha_1 \\
 \cdot & \cdot & \cdot & \cdot & \cdot & 16\alpha_2 + 64\beta l^2 & -108\beta l & 8\alpha_1 & -44\beta l & -8\alpha_2 + 8\beta l^2 \\
 \cdot & \cdot & \cdot & \cdot & \cdot & \cdot & 1296\beta & 0 & -567\beta & 99\beta l \\
 \cdot & \cdot & \cdot & \cdot & \cdot & \cdot & \cdot & 7\alpha_0 & 0 & -7\alpha_1 \\
 \cdot & \cdot & \cdot & \cdot & \cdot & \cdot & \cdot & \cdot & 44\beta & -83\beta l \\
 \cdot & \cdot & \cdot & \cdot & \cdot & \cdot & \cdot & \cdot & \cdot & 7\alpha_2 + 16\beta l^2
 \end{pmatrix} \quad (3.49)$$

where

$$\alpha_n = \frac{Q_n}{3l} \quad \beta = \frac{kV_0}{120l}$$

### 3.4.3. Levinson-Bickford Beam Element

The nodal degrees of freedom for the Levinson-Bickford element are given in Figure 3.7 and Equation (3.50). The kinematic constraints for the element are specified in Equations (3.51) and (3.52). The resulting mass and stiffness matrices are given in Equations (3.53) and (3.54), respectively.

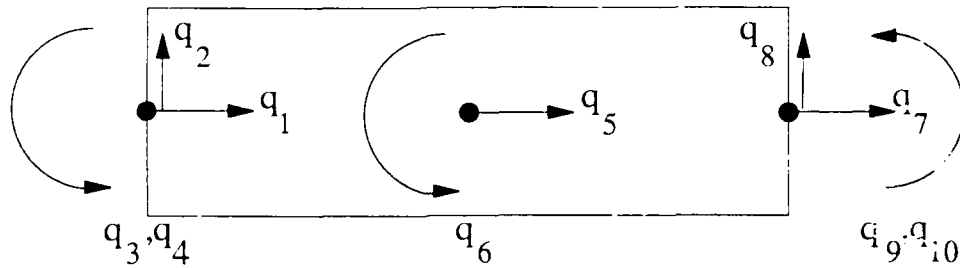


Fig. 3.7 Levinson-Bickford beam element.

$$\mathbf{q}^T = [U_1 \ W_1 \ \Phi_1 \ W_2 \ U_2 \ \Phi_2 \ U_3 \ W_4 \ \Phi_3 \ W_3] \quad (3.50)$$

$$\begin{aligned} u(x, y, t) &= U(x, t) - \Phi(x, t)y - \left\{ \frac{1}{3c^2} [W'(x, t) - \Phi(x, t)] \right\} y^3 \\ &= U(x, t) - \Phi(x, t) \left[ y - \frac{y^3}{3c^2} \right] - \frac{1}{3c^2} W'(x, t) y^3 \\ &= \sum_{i=1}^3 A_i(x) U_i(t) - \sum_{i=1}^3 A_i(x) \Phi_i(t) \left( y - \frac{y^3}{3c^2} \right) - \frac{1}{3c^2} \sum_{j=1}^4 B_j'(x) W_j(t) y^3 \\ &= \mathbf{N}_1(x, y) \mathbf{q}(t) \end{aligned} \quad (3.51)$$

$$v(x, y, t) = W(x, t) = \sum_{j=1}^4 B_j(x) W_j(t) = \mathbf{N}_2(x, y) \mathbf{q}(t) \quad (3.52)$$

$$\mathbf{M}^{(c)} = \begin{pmatrix}
4\gamma_0 & 6\eta_3 & -4\gamma_1 & -7\eta_3 l & 2\gamma_0 & -2\gamma_1 & -\gamma_0 & -6\eta_3 & \gamma_1 & 3\eta_3 l \\
\cdot & 72\eta_6 + 156\delta & -6\eta_4 & 6\eta_6 l + 22\delta l & 48\eta_3 & -48\eta_4 & 6\eta_3 & -72\eta_6 + 54\delta & -6\eta_4 & 6\eta_6 l - 13\delta l \\
\cdot & \cdot & 4\gamma_2 & 7\eta_4 l & -2\gamma_1 & 2\gamma_2 & \gamma_1 & 6\eta_4 & -\gamma_2 & -3\eta_4 l \\
\cdot & \cdot & \cdot & 8\eta_6 l^2 + 4\delta l^2 & 4\eta_3 l & -4\eta_4 l & 3\eta_3 l & -6\eta_6 l + 13\delta l & -3\eta_4 l & -2\eta_6 l^2 - 3\delta l^2 \\
\cdot & \cdot & \cdot & \cdot & 16\gamma_0 & -16\gamma_1 & 2\gamma_0 & -48\eta_3 & -2\gamma_1 & 4\eta_3 l \\
\cdot & \cdot & \cdot & \cdot & \cdot & 16\gamma_2 & -2\gamma_1 & 48\eta_4 & 2\gamma_2 & -4\eta_4 l \\
\cdot & \cdot & \cdot & \cdot & \cdot & \cdot & 4\gamma_0 & -6\eta_3 & -4\gamma_1 & -7\eta_3 l \\
\cdot & \cdot & \cdot & \cdot & \cdot & \cdot & \cdot & 72\eta_6 + 156\delta & 6\eta_4 & -6\eta_6 l - 22\delta l \\
\cdot & \cdot & \cdot & \cdot & \cdot & \cdot & \cdot & \cdot & 4\gamma_2 & 7\eta_4 l \\
\cdot & \cdot & \cdot & \cdot & \cdot & \cdot & \cdot & \cdot & \cdot & 8\eta_6 l^2 + 4\delta l^2
\end{pmatrix} \quad (3.53)$$

where

$$\begin{aligned}
\frac{1}{3c^2} \gamma_0 &= \frac{P_0 l}{30} & \gamma_1 &= \frac{l}{30}(P_1 - zP_3) & \gamma_2 &= \frac{l}{30}(P_2 - 2zP_4 + z^2P_6) \\
\eta_3 &= \frac{z}{60}P_3 & \eta_4 &= \frac{z}{60}(P_4 - zP_6) & \eta_6 &= \frac{z^2}{60l}P_6 & \delta &= \frac{P_0 l}{420}
\end{aligned}$$



$$\mathbf{K}^{(e)} = \begin{pmatrix} 7\alpha_0 & -12\xi_3 & -7\alpha_1 & -9\xi_3 l & -8\alpha_0 & 8\alpha_1 & \alpha_0 & 12\xi_3 & -\alpha_1 & -3\xi_3 l \\ \cdot & 36\xi_6 + 72\beta & 12\xi_4 + 6\beta l & 18\xi_8 l + 6\beta l & 24\xi_3 & -24\xi_4 + 48\beta l & -12\xi_3 & -36\xi_6 - 72\beta & 12\xi_4 + 6\beta l & 18\xi_8 l + 6\beta l \\ \cdot & \cdot & 7\alpha_2 + 8\beta l^2 & 9\xi_4 l - 7\beta l^2 & 8\alpha_1 & -8\alpha_2 + 4\beta l^2 & -\alpha_1 & -12\xi_4 - 6\beta l & \alpha_2 - 2\beta l^2 & 3\xi_4 l + 3\beta l^2 \\ \cdot & \cdot & \cdot & 12\xi_8 l^2 + 8\beta l^2 & 12\xi_3 l & -12\xi_4 l + 4\beta l^2 & -3\xi_3 l & -18\xi_8 l - 6\beta l & 3\xi_4 l + 3\beta l^2 & 6\xi_8 l^2 - 2\beta l^2 \\ \cdot & \cdot & \cdot & \cdot & 16\alpha_0 & -16\alpha_1 & -8\alpha_0 & -24\xi_3 & 8\alpha_1 & 12\xi_3 l \\ \cdot & \cdot & \cdot & \cdot & \cdot & 16\alpha_2 + 32\beta l^2 & 8\alpha_1 & 24\xi_4 - 48\beta l & -8\alpha_2 + 4\beta l^2 & -12\xi_4 l + 4\beta l^2 \\ \cdot & \cdot & \cdot & \cdot & \cdot & \cdot & 7\alpha_0 & 12\xi_3 & -7\alpha_1 & -9\xi_3 l \\ \cdot & \cdot & \cdot & \cdot & \cdot & \cdot & \cdot & 36\xi_6 + 72\beta & -12\xi_4 - 6\beta l & -18\xi_8 l - 6\beta l \\ \cdot & \cdot & \cdot & \cdot & \cdot & \cdot & \cdot & \cdot & 7\alpha_2 + 8\beta l^2 & 9\xi_4 l - 7\beta l^2 \\ \cdot & \cdot & \cdot & \cdot & \cdot & \cdot & \cdot & \cdot & \cdot & 12\xi_8 l^2 + 8\beta l^2 \end{pmatrix} \quad (3.54)$$

where

$$\begin{aligned} \alpha_0 &= \frac{Q_0}{3l} & \alpha_1 &= \frac{1}{3l}(Q_1 - zQ_3) & \alpha_2 &= \frac{1}{3l}(Q_2 - 2zQ_4 + z^2Q_6) \\ \xi_3 &= \frac{z}{3l^2}Q_3 & \xi_4 &= \frac{z}{3l^2}(Q_4 - zQ_6) & \xi_6 &= \frac{z^2}{3l^3}Q_6 & \beta &= \frac{k}{60l}\left(V_0 - \frac{2}{c^2}V_2 + \frac{1}{c^4}V_4\right) \end{aligned}$$

### 3.4.4. Third-Order Beam Element

The nodal degrees of freedom for the third-order element are given in Figure 3.8 and Equation (3.55). The kinematic constraints for the element are specified in Equations (3.56) and (3.57). The resulting mass and stiffness matrices are given in Equations (3.58) and (3.59), respectively.

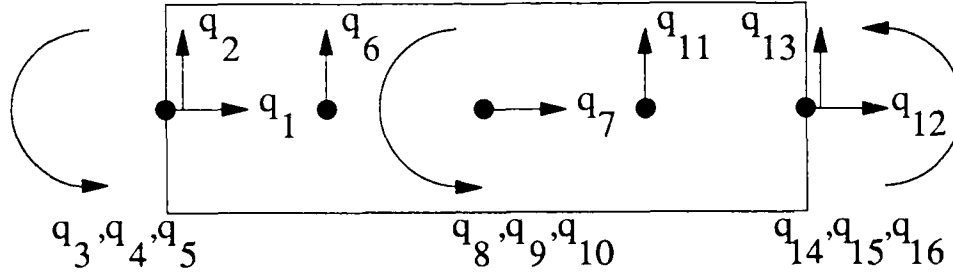


Fig. 3.8 General third-order beam element.

$$\mathbf{q}^T = [U_1 \quad W_1 \quad \Phi_1^{(1)} \quad \Phi_1^{(2)} \quad \Phi_1^{(3)} \quad W_2 \quad U_2 \quad \Phi_2^{(1)} \quad \Phi_2^{(2)} \quad \Phi_2^{(3)} \quad W_3 \quad U_3 \quad W_4 \quad \Phi_3^{(1)} \quad \Phi_3^{(2)} \quad \Phi_3^{(3)}] \quad (3.55)$$

$$\begin{aligned} u(x, y, t) &= U(x, t) - \Phi^{(1)}(x, t)y - \Phi^{(2)}(x, t)y^2 - \Phi^{(3)}(x, t)y^3 \\ &= \sum_{i=1}^3 A_i(x)U_i(t) - \sum_{i=1}^3 A_i(x)\Phi_i^{(1)}(t)y - \sum_{i=1}^3 A_i(x)\Phi_i^{(2)}(t)y^2 \\ &\quad - \sum_{i=1}^3 A_i(x)\Phi_i^{(3)}(t)y^3 = \mathbf{N}_1(x, y)\mathbf{q}(t) \end{aligned} \quad (3.56)$$

where

$$\begin{aligned} \Phi_i^{(1)}(t) &= \text{nodal degrees of freedom for rotation of the cross section} \\ \Phi_i^{(2)}(t) &= \text{nodal degrees of freedom for second-order warping of the cross section} \\ \Phi_i^{(3)}(t) &= \text{nodal degrees of freedom for third-order warping of the cross section} \end{aligned}$$

$$v(x, y, t) = W(x, t) = \sum_{j=1}^4 B_j(x)W_j(t) = \mathbf{N}_2(x, y)\mathbf{q}(t) \quad (3.57)$$

$$\mathbf{M}^{(e)} = \begin{pmatrix}
4\gamma_0 & 0 & -4\gamma_1 & -4\gamma_2 & -4\gamma_3 & 0 & 2\gamma_0 & -2\gamma_1 & -2\gamma_2 & -2\gamma_3 & 0 & -\gamma_0 & 0 & \gamma_1 & \gamma_2 & \gamma_3 \\
\cdot & 128\delta & 0 & 0 & 0 & 99\delta & 0 & 0 & 0 & 0 & -36\delta & 0 & 19\delta & 0 & 0 & 0 \\
\cdot & \cdot & 4\gamma_2 & 4\gamma_3 & 4\gamma_4 & 0 & -2\gamma_1 & 2\gamma_2 & 2\gamma_3 & 2\gamma_4 & 0 & \gamma_1 & 0 & -\gamma_2 & -\gamma_3 & -\gamma_4 \\
\cdot & \cdot & \cdot & 4\gamma_4 & 4\gamma_5 & 0 & -2\gamma_2 & 2\gamma_3 & 2\gamma_4 & 2\gamma_5 & 0 & \gamma_2 & 0 & -\gamma_3 & -\gamma_4 & -\gamma_5 \\
\cdot & \cdot & \cdot & \cdot & 4\gamma_6 & 0 & -2\gamma_3 & 2\gamma_4 & 2\gamma_5 & 2\gamma_6 & 0 & \gamma_3 & 0 & -\gamma_4 & -\gamma_5 & -\gamma_6 \\
\cdot & \cdot & \cdot & \cdot & \cdot & 648\delta & 0 & 0 & 0 & 0 & -81\delta & 0 & -36\delta & 0 & 0 & 0 \\
\cdot & \cdot & \cdot & \cdot & \cdot & \cdot & 16\gamma_0 & -16\gamma_1 & -16\gamma_2 & -16\gamma_3 & 0 & 2\gamma_0 & 0 & -2\gamma_1 & -2\gamma_2 & -2\gamma_3 \\
\cdot & \cdot & \cdot & \cdot & \cdot & \cdot & \cdot & 16\gamma_2 & 16\gamma_3 & 16\gamma_4 & 0 & -2\gamma_1 & 0 & 2\gamma_2 & 2\gamma_3 & 2\gamma_4 \\
\cdot & \cdot & \cdot & \cdot & \cdot & \cdot & \cdot & \cdot & 16\gamma_4 & 16\gamma_5 & 0 & -2\gamma_2 & 0 & 2\gamma_3 & 2\gamma_4 & 2\gamma_5 \\
\cdot & \cdot & \cdot & \cdot & \cdot & \cdot & \cdot & \cdot & \cdot & 16\gamma_6 & 0 & -2\gamma_3 & 0 & 2\gamma_4 & 2\gamma_5 & 2\gamma_6 \\
\cdot & \cdot & \cdot & \cdot & \cdot & \cdot & \cdot & \cdot & \cdot & \cdot & 648\delta & 0 & 99\delta & 0 & 0 & 0 \\
\cdot & \cdot & \cdot & \cdot & \cdot & \cdot & \cdot & \cdot & \cdot & \cdot & \cdot & 4\gamma_0 & 0 & -4\gamma_1 & -4\gamma_2 & -4\gamma_3 \\
\cdot & \cdot & \cdot & \cdot & \cdot & \cdot & \cdot & \cdot & \cdot & \cdot & \cdot & \cdot & 128\delta & 0 & 0 & 0 \\
\cdot & \cdot & \cdot & \cdot & \cdot & \cdot & \cdot & \cdot & \cdot & \cdot & \cdot & \cdot & \cdot & 4\gamma_2 & 4\gamma_3 & 4\gamma_4 \\
\cdot & \cdot & \cdot & \cdot & \cdot & \cdot & \cdot & \cdot & \cdot & \cdot & \cdot & \cdot & \cdot & \cdot & 4\gamma_4 & 4\gamma_5 \\
\cdot & \cdot & \cdot & \cdot & \cdot & \cdot & \cdot & \cdot & \cdot & \cdot & \cdot & \cdot & \cdot & \cdot & \cdot & 4\gamma_6
\end{pmatrix}$$

(3.58)

where

$$\gamma_n = \frac{P_n l}{30} \quad \delta = \frac{P_0 l}{1680}$$

$$\mathbf{K}^{(e)} = \begin{pmatrix} \mathbf{K}_{11} & \mathbf{K}_{12} \\ \cdot & \mathbf{K}_{22} \end{pmatrix} \quad (3.59)$$

where

$$\mathbf{K}_{11} = \begin{pmatrix} 7\alpha_0 & 0 & -7\alpha_1 & -7\alpha_2 & -7\alpha_3 & 0 & -8\alpha_0 & 8\alpha_1 \\ \cdot & 444\beta_0 & 83\beta_1 l & 166\beta_1 l & 249\beta_2 l & -567\beta_0 & 0 & 44\beta_0 l \\ \cdot & \cdot & 7\alpha_2 + 16\beta_0 l^2 & 7\alpha_3 + 32\beta_1 l^2 & 7\alpha_4 + 48\beta_2 l^2 & -99\beta_0 l & 8\alpha_1 & -8\alpha_2 + 8\beta_0 l^2 \\ \cdot & \cdot & \cdot & 7\alpha_4 + 64\beta_2 l^2 & 7\alpha_5 + 96\beta_3 l^2 & -198\beta_1 l & 8\alpha_2 & -8\alpha_3 + 16\beta_1 l^2 \\ \cdot & \cdot & \cdot & \cdot & 7\alpha_6 + 144\beta_4 l^2 & -297\beta_2 l & 8\alpha_3 & -8\alpha_4 + 24\beta_2 l^2 \\ \cdot & \cdot & \cdot & \cdot & \cdot & 1296\beta_0 & 0 & 108\beta_0 l \\ \cdot & \cdot & \cdot & \cdot & \cdot & \cdot & 16\alpha_0 & -16\alpha_1 \\ \cdot & \cdot & \cdot & \cdot & \cdot & \cdot & \cdot & 16\alpha_2 + 64\beta_0 l^2 \end{pmatrix} \quad (3.59a)$$

$$\mathbf{K}_{12} = \begin{pmatrix}
8\alpha_2 & 8\alpha_3 & 0 & \alpha_0 & 0 & -\alpha_1 & -\alpha_2 & -\alpha_3 \\
88\beta_1 l & 132\beta_2 l^2 & 162\beta_0 & 0 & -39\beta_0 & -7\beta_0 l & -14\beta_1 l & -21\beta_2 l \\
-8\alpha_3 + 16\beta_1 l^2 & -8\alpha_4 + 24\beta_2 l^2 & 9\beta_0 l & -\alpha_1 & 7\beta_0 l & \alpha_2 - 4\beta_0 l^2 & \alpha_3 - 8\beta_1 l^2 & \alpha_4 - 12\beta_2 l^2 \\
-8\alpha_4 + 32\beta_2 l^2 & -8\alpha_5 + 48\beta_3 l^2 & 18\beta_1 l & -\alpha_2 & 14\beta_1 l & \alpha_3 - 8\beta_1 l^2 & \alpha_4 - 16\beta_2 l^2 & \alpha_5 - 24\beta_3 l^2 \\
-8\alpha_5 + 48\beta_3 l^2 & -8\alpha_6 + 72\beta_4 l^2 & 27\beta_2 l & -\alpha_3 & 21\beta_2 l & \alpha_4 - 12\beta_2 l^2 & \alpha_5 - 24\beta_3 l^2 & \alpha_6 - 36\beta_4 l^2 \\
216\beta_1 l & 324\beta_2 l & -891\beta_0 & 0 & 162\beta_0 & -9\beta_0 l & -18\beta_1 l & -27\beta_2 l \\
-16\alpha_2 & -16\alpha_3 & 0 & -8\alpha_0 & 0 & 8\alpha_1 & 8\alpha_2 & 8\alpha_3 \\
16\alpha_3 + 128\beta_1 l^2 & 16\alpha_4 + 192\beta_2 l^2 & -108\beta_0 l & 8\alpha_1 & -44\beta_0 l & -8\alpha_2 + 8\beta_0 l^2 & -8\alpha_3 + 16\beta_1 l^2 & -8\alpha_4 + 24\beta_2 l^2
\end{pmatrix} \quad (3.59b)$$

$$\mathbf{K}_{22} = \begin{pmatrix}
 16\alpha_4 + 256\beta_2 l^2 & 16\alpha_5 + 384\beta_3 l^2 & -216\beta_1 l & 8\alpha_2 & -88\beta_1 l & -8\alpha_3 + 16\beta_1 l^2 & -8\alpha_4 + 32\beta_2 l^2 & -8\alpha_5 + 48\beta_3 l^2 \\
 \cdot & 16\alpha_6 + 576\beta_4 l^2 & -327\beta_2 l & 8\alpha_3 & -132\beta_2 l & -8\alpha_4 + 24\beta_2 l^2 & -8\alpha_5 + 48\beta_3 l^2 & -8\alpha_6 + 72\beta_4 l^2 \\
 \cdot & \cdot & 1296\beta_0 & 0 & -567\beta_0 & 99\beta_0 l & 198\beta_1 l & 297\beta_2 l \\
 \cdot & \cdot & \cdot & 7\alpha_0 & 0 & -7\alpha_1 & -7\alpha_2 & -7\alpha_3 \\
 \cdot & \cdot & \cdot & \cdot & 444\beta_0 & -83\beta_0 l & -166\beta_1 l & -249\beta_2 l \\
 \cdot & \cdot & \cdot & \cdot & \cdot & 7\alpha_2 + 16\beta_0 l^2 & 7\alpha_3 + 32\beta_1 l^2 & 7\alpha_4 + 48\beta_2 l^2 \\
 \cdot & \cdot & \cdot & \cdot & \cdot & \cdot & 7\alpha_4 + 64\beta_2 l^2 & 7\alpha_5 + 96\beta_3 l^2 \\
 \cdot & \cdot & \cdot & \cdot & \cdot & \cdot & \cdot & 7\alpha_6 + 144\beta_4 l^2
 \end{pmatrix} \quad (3.59c)$$

where

$$\alpha_n = \frac{Q_n}{3l} \quad \beta_n = \frac{V_n}{120l}$$

### 3.5. Mass and Stiffness Matrices for Stacked Elements

The procedure for finding the mass and stiffness matrices for stacked elements is outlined by Miller in [129] and [130] and discussed in detail by Yuan and Miller in [127] and [128]. Basically, a stacked element is made by simply placing a series of individual elements on top of each other. The matrices for this vertical array of elements are obtained by performing a sequence of transformations that relate the nodal degrees of freedom in each layer to the master degrees of freedom chosen for the stacked element. In this process, some degrees of freedom in individual layers are considered to be slave variables of the master variables associated with the stacked element. The transformations eliminate the slave variables, resulting in a more efficient element still capable of modeling the deformation of individual layers explicitly.

#### 3.5.1. General Matrix Transformations for any Finite Element

Before discussing this process in detail for the two stacked elements developed in this study, some general comments regarding matrix transformations are in order. Figure 3.9 pictures two essentially identical finite elements each possessing a different set of equivalent degrees of freedom or generalized coordinates. The difference in generalized coordinates could be due to eliminating slave variables in one element, rearranging the order or location of an element's degrees of freedom, or some other change. Whatever the difference in the degrees of freedom for each element, it is assumed that they can be related by a transformation as shown in Equation (3.60).

$q$ = nodal displacement vector $f$ = nodal force vector $A$ = mass or stiffness matrix
---

(a) Original element.

$p$ = nodal displacement vector $g$ = nodal force vector $A^*$ = mass or stiffness matrix
---

(b) Transformed element.

**Fig. 3.9 Element transformation.**

$$q = Tp \quad (3.60)$$

where

$q$  = nodal displacement vector for original finite element  
 $p$  = nodal displacement vector for transformed finite element  
 $T$  = generic transformation matrix

Since both systems are equivalent, the external work done by nodal forces acting through the associated nodal displacements should be equal for each system. This is stated mathematically as

$$f^T q - g^T p = 0 \quad (3.61)$$

where

$f$  = nodal force vector for original finite element



$g$  = nodal force vector for transformed finite element

Substituting Equation (3.60) into this equation yields the result

$$f^T T p - g^T p = [f^T T - g^T] p = 0 \quad (3.62)$$

Hence

$$g = T^T f \quad (3.63)$$

A final relationship of interest is that between the nodal forces and the nodal displacements, namely,

$$a) \quad f = A q \quad b) \quad g = A^* p \quad (3.64)$$

For static nodal forces, the  $A$  and  $A^*$  matrices correspond to stiffness matrices; in the case of nodal inertial forces which can be derived from acceleration via D'Alembert's principle ([19], p. 235),  $A$  and  $A^*$  represent mass matrices.

Substituting Equation (3.60) into Equation (3.64a) and substituting this in turn into Equation (3.63) yields the result

$$g = T^T f = T^T A q = T^T A T p \quad (3.65)$$

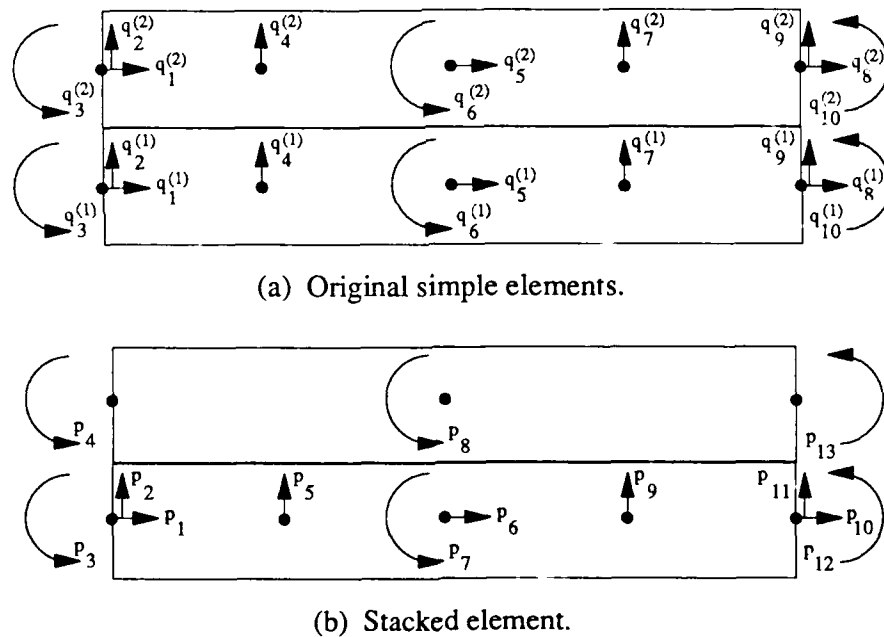
Comparing this result with Equation (3.64b) yields the matrix transformation

$$A^* = T^T A T \quad (3.66)$$

This equation shows how a matrix for the transformed system can be derived from the equivalent matrix associated with the original system. This transformation is applicable to either mass or stiffness matrices.

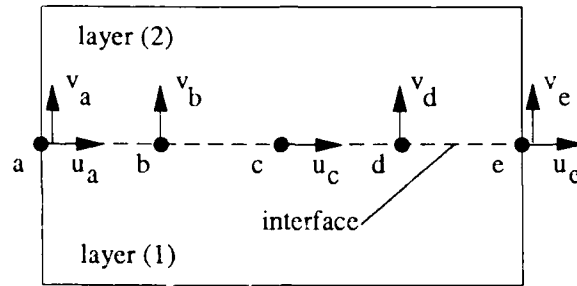
### 3.5.2. General Matrix Transformations for Stacked Elements

The transformation for a stacked element starts by considering a two-lamina configuration, such as the stacked Timoshenko beam depicted in Figure 3.10. As seen in this figure, the original system comprises two elements simply stacked on top of each other and includes all the degrees of freedom associated with the two elements. The transformed system represents a stacked element in which redundant degrees of freedom in the original two-lamina configuration have been eliminated by enforcing the continuity of longitudinal and vertical displacements at the interface between the two layers.



**Fig. 3.10 Two-lamina stacked Timoshenko beam element.**

In general, the original configuration can be made up of elements based on either Timoshenko beam or the general third-order beam theory. Levinson-Bickford beam elements are not amenable to this treatment since the assumption of zero shear strain on the lateral surfaces of the beam inherent in the associated theory precludes stacking such elements vertically.



(c) Displacements at interface.

**Fig. 3.10 Concluded.**

The equations defining continuity of displacement for the points on the interface pictured in Figure 3.10c are

$$\begin{aligned} u_a^{(1)} &= u_a^{(2)} & u_c^{(1)} &= u_c^{(2)} & u_e^{(1)} &= u_e^{(2)} \\ v_a^{(1)} &= v_a^{(2)} & v_b^{(1)} &= v_b^{(2)} & v_d^{(1)} &= v_d^{(2)} & v_e^{(1)} &= v_e^{(2)} \end{aligned} \quad (3.6i)$$

where

$$\begin{aligned} u_j^{(i)} &= \text{longitudinal displacement of layer } i \text{ at point } j \\ v_j^{(i)} &= \text{lateral displacement of layer } i \text{ at point } j \end{aligned}$$

As seen in these equations, compatibility of longitudinal displacement provides three equations, which are used to eliminate the three degrees of freedom associated with pure axial motion of the top layer. Similarly, the continuity of vertical displacement allows the four degrees of freedom for lateral displacement of the top layer to be eliminated as well.

The transformation from the original set of generalized coordinates associated with the two individual elements in the stack to the master variables retained in the final stacked element is

achieved one layer at a time. General expressions for these layerwise transformations are shown in Equations (3.68) and (3.69) and, in accordance with Equation (3.66), lead to the general matrix transformations shown in Equations (3.70).

$$\begin{aligned} \mathbf{q}^{(1)} &= \mathbf{R}^{(1)} \mathbf{p} \\ \mathbf{q}^{(2)} &= \mathbf{T}^{(2)} \mathbf{p} \end{aligned} \quad (3.68)$$

where

- $\mathbf{q}^{(i)}$  = nodal displacements in layer  $i$  of original element
- $\mathbf{p}$  = nodal displacement vector for stacked element
- $\mathbf{R}^{(1)}$  = transformation matrix for lower layer in a two-layer stacked element
- $\mathbf{T}^{(2)}$  = transformation matrix for upper layer in a two-layer stacked element

$$\begin{aligned} \mathbf{g}^{(1)} &= \mathbf{R}^{(1)T} \mathbf{f}^{(1)} \\ \mathbf{g}^{(2)} &= \mathbf{T}^{(2)T} \mathbf{f}^{(2)} \end{aligned} \quad (3.69)$$

where

- $\mathbf{f}^{(i)}$  = nodal forces in layer  $i$  associated with nodal displacements  $\mathbf{q}^{(i)}$
- $\mathbf{g}$  = nodal forces for stacked element
- $\mathbf{g}^{(i)}$  = portion of  $\mathbf{g}$  associated with layer  $i$

$$\begin{aligned} \mathbf{A}^{*(1)} &= \mathbf{R}^{(1)T} \mathbf{A}^{(1)} \mathbf{R}^{(1)} \\ \mathbf{A}^{*(2)} &= \mathbf{T}^{(2)T} \mathbf{A}^{(2)} \mathbf{T}^{(2)} \end{aligned} \quad (3.70)$$

where

- $\mathbf{A}^{(i)}$  = mass or stiffness matrix for layer  $i$
- $\mathbf{A}^*$  = mass or stiffness matrix for stacked element

$A^{*(i)}$  = portion of  $A^*$  associated with layer  $i$

The equivalent matrix for the stacked element is given by the summation of the transformed matrices for the top and bottom layers:

$$A^* = A^{*(1)} + A^{*(2)} \quad (3.71)$$

For a three-lamina element, the procedure just described is used to combine the top two laminae into a single layer. The result of this operation is then treated as a single layer which is combined with the remaining lower layer by repeating the same basic transformation procedure one more time. The resulting matrix transformation is described mathematically as

$$A^* = T^{(2)T} (T^{(3)T} A^{(3)} T^{(3)} + R^{(2)T} A^{(2)} R^{(2)}) T^{(2)} + R^{(1)T} A^{(1)} R^{(1)} \quad (3.72)$$

where

$A^{*(i)}$  = mass or stiffness matrix for layer  $i$

$A^*$  = mass or stiffness matrix for stacked element

$R^{(j)}$  = transformation matrices for the two-layer stack containing layer  $j$  as the bottom layer

$T^{(j)}$  = transformation matrices for the two-layer stack containing layer  $j$  as the upper layer

The generalized process for an  $N$ -lamina beam is given as

$$A^* = T^{(2)T} (T^{(3)T} (.... T^{(n)T} A^{(n)} T^{(n)} + R^{(n-1)T} A^{(n-1)} R^{(n-1)} ....) T^{(3)} + R^{(2)T} A^{(2)} R^{(2)}) T^{(2)} + R^{(1)T} A^{(1)} R^{(1)} \quad (3.73)$$

As can be seen in this equation, the procedure just described for a three-lamina beam is continued in a cascading fashion until all the layers are combined in a single stacked element with the bottom layer acting as the key layer. This layer has the distinction of being the one in which the degrees of freedom associated with lateral and pure axial displacements have not been eliminated.

Obviously, defining the **R** and **T** matrices properly is essential in the transformation procedure. Obtaining the **R** matrix for the two-lamina configuration pictured in Figure 3.10 is very straightforward since the degrees of freedom for the bottom layer represent a subset of the master variables of the stacked element. Therefore, this matrix must contain the proper combination of zeros and ones required to filter out the master degrees of freedom not present in the bottom layer.

The components of the **T** matrix for the configuration seen in Figure 3.10 are also obtained in a straightforward fashion; however, finding some of these components involves a little more algebra. In addition to the zeros and ones needed to filter out the appropriate master variables of the stacked element, the **T** matrix contains the components necessary to eliminate the slave variables in the upper layer by enforcing the compatibility conditions given by Equations (3.67).

These general remarks regarding the **R** and **T** matrices apply to all steps in the cascading procedure defined by Equation (3.73) and are valid for stacked elements based on both Timoshenko beam and the general third-order beam theory. Specific matrices for each kind of element and for each step encountered in the cascading transformation procedure are provided in Section 3.4.3.

### 3.5.3. Transformation Matrices for Stacked Timoshenko Beam and Third-Order Beam Elements

Figure 3.10b shows a two-lamina stacked element made up of Timoshenko beam elements. The  $10 \times 13$  **R**<sup>(1)</sup> matrix for this element is given as

$$\begin{Bmatrix} q_1^{(1)} \\ q_2^{(1)} \\ q_3^{(1)} \\ q_4^{(1)} \\ q_5^{(1)} \\ q_6^{(1)} \\ q_7^{(1)} \\ q_8^{(1)} \\ q_9^{(1)} \\ q_{10}^{(1)} \end{Bmatrix} = \begin{pmatrix} 1 & 0 & 0 & 0 & 0 & 0 & 0 & 0 & 0 & 0 & 0 & 0 & 0 \\ 0 & 1 & 0 & 0 & 0 & 0 & 0 & 0 & 0 & 0 & 0 & 0 & 0 \\ 0 & 0 & 1 & 0 & 0 & 0 & 0 & 0 & 0 & 0 & 0 & 0 & 0 \\ 0 & 0 & 0 & 0 & 1 & 0 & 0 & 0 & 0 & 0 & 0 & 0 & 0 \\ 0 & 0 & 0 & 0 & 0 & 1 & 0 & 0 & 0 & 0 & 0 & 0 & 0 \\ 0 & 0 & 0 & 0 & 0 & 0 & 1 & 0 & 0 & 0 & 0 & 0 & 0 \\ 0 & 0 & 0 & 0 & 0 & 0 & 0 & 1 & 0 & 0 & 0 & 0 & 0 \\ 0 & 0 & 0 & 0 & 0 & 0 & 0 & 0 & 1 & 0 & 0 & 0 & 0 \\ 0 & 0 & 0 & 0 & 0 & 0 & 0 & 0 & 0 & 1 & 0 & 0 & 0 \\ 0 & 0 & 0 & 0 & 0 & 0 & 0 & 0 & 0 & 0 & 1 & 0 & 0 \end{pmatrix} \begin{Bmatrix} p_1 \\ p_2 \\ \cdot \\ \cdot \\ \cdot \\ \cdot \\ \cdot \\ \cdot \\ \cdot \\ p_{13} \end{Bmatrix} \quad (3.74)$$

As can be seen, the matrix acts to filter out the master variables not present in the lower lamina of the element.

In addition to filtering out similar variables not present in the upper lamina, the  $10 \times 13 \mathbf{T}^{(2)}$  matrix enforces the compatibility conditions given in Equations (3.67). These conditions are enforced by expressing the generalized coordinates associated with lateral displacement and pure axial motion of the upper layer in terms of the master variables retained in the stacked element. The relations required for this operation are derived from Equations (3.67). The appropriate formulae for the stacked Timoshenko beam element depicted in Figure 3.10 are given by

$$\begin{aligned}
q_1^{(2)} &= q_1^{(1)} - \left[ q_3^{(1)} \frac{t^{(1)}}{2} + q_3^{(2)} \frac{t^{(2)}}{2} \right] \\
q_5^{(2)} &= q_5^{(1)} - \left[ q_6^{(1)} \frac{t^{(1)}}{2} + q_6^{(2)} \frac{t^{(2)}}{2} \right] \\
q_8^{(2)} &= q_8^{(1)} - \left[ q_{10}^{(1)} \frac{t^{(1)}}{2} + q_{10}^{(2)} \frac{t^{(2)}}{2} \right]
\end{aligned} \tag{3.75}$$

where

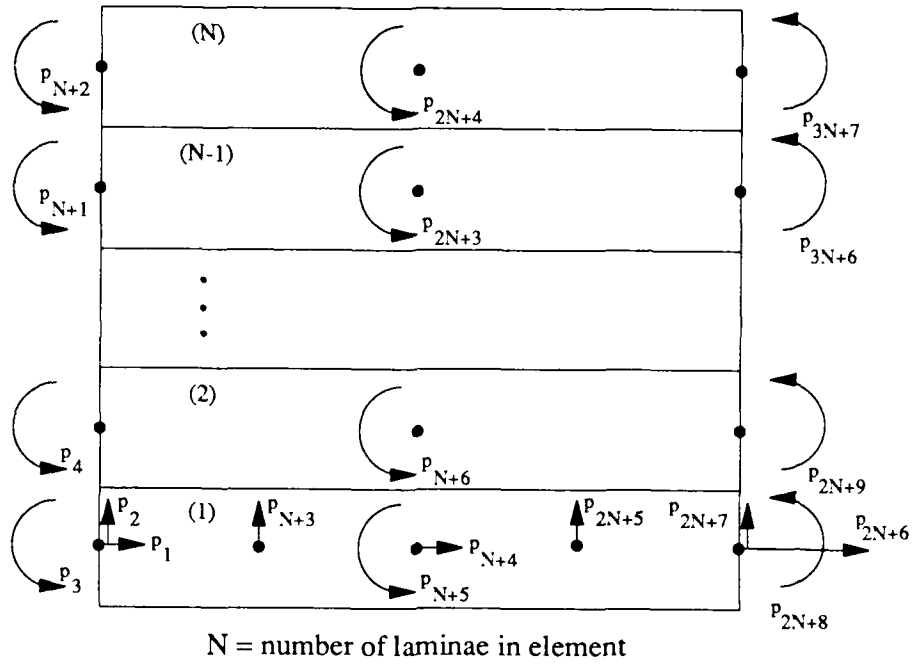
$$\begin{aligned}
q_j^{(i)} &= j\text{-th degree of freedom in layer } i \\
t^{(i)} &= \text{thickness of layer } i
\end{aligned}$$

These relations are incorporated into the  $\mathbf{T}^{(2)}$  matrix, which becomes



$$\begin{Bmatrix} q_1^{(2)} \\ q_2^{(2)} \\ q_3^{(2)} \\ q_4^{(2)} \\ q_5^{(2)} \\ q_6^{(2)} \\ q_7^{(2)} \\ q_8^{(2)} \\ q_9^{(2)} \\ q_{10}^{(2)} \end{Bmatrix} = \begin{pmatrix} 1 & 0 & \frac{-t^{(1)}}{2} & \frac{-t^{(2)}}{2} & 0 & 0 & 0 & 0 & 0 & 0 & 0 & 0 & 0 \\ 0 & 1 & 0 & 0 & 0 & 0 & 0 & 0 & 0 & 0 & 0 & 0 & 0 \\ 0 & 0 & 0 & 1 & 0 & 0 & 0 & 0 & 0 & 0 & 0 & 0 & 0 \\ 0 & 0 & 0 & 0 & 1 & 0 & 0 & 0 & 0 & 0 & 0 & 0 & 0 \\ 0 & 0 & 0 & 0 & 0 & 1 & \frac{-t^{(1)}}{2} & \frac{-t^{(2)}}{2} & 0 & 0 & 0 & 0 & 0 \\ 0 & 0 & 0 & 0 & 0 & 0 & 0 & 1 & 0 & 0 & 0 & 0 & 0 \\ 0 & 0 & 0 & 0 & 0 & 0 & 0 & 0 & 1 & 0 & 0 & 0 & 0 \\ 0 & 0 & 0 & 0 & 0 & 0 & 0 & 0 & 0 & 1 & 0 & \frac{-t^{(1)}}{2} & \frac{-t^{(2)}}{2} \\ 0 & 0 & 0 & 0 & 0 & 0 & 0 & 0 & 0 & 0 & 1 & 0 & 0 \\ 0 & 0 & 0 & 0 & 0 & 0 & 0 & 0 & 0 & 0 & 0 & 0 & 1 \end{pmatrix} \begin{Bmatrix} p_1 \\ p_2 \\ \cdot \\ \cdot \\ \cdot \\ \cdot \\ \cdot \\ \cdot \\ \cdot \\ p_{13} \end{Bmatrix} \quad (3.76)$$

Figure 3.11 shows a stacked element containing  $N$  laminae, each of which is allowed to act like a Timoshenko beam. The formulae for the general **R** and **T** matrices required for such a stacked Timoshenko element are given in Equations (3.77) and (3.78), respectively.



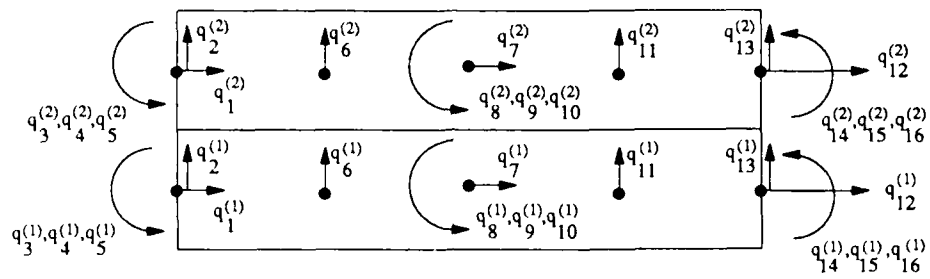
**Fig. 3.11 Multilayered stacked Timoshenko beam element.**

$$\begin{aligned}
 &\text{All } R_{j,k}^{(i)} = 0 \text{ except} \\
 &R_{j,j}^{(i)} = 1 \text{ for } j = 1, 2, 3 \\
 &R_{j,j+N-i}^{(i)} = 1 \text{ for } j = 4, 5, 6 \\
 &R_{j,j+2(N-i)}^{(i)} = 1 \text{ for } j = 7, 8, 9, 10 \\
 &i = 1, N-1
 \end{aligned} \tag{3.77}$$

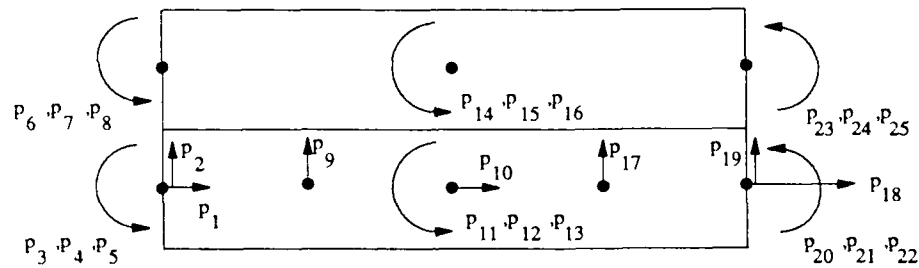
$$\begin{aligned}
&\text{All } T_{j,k}^{(i)} = 0 \text{ except} \\
&T_{j,j}^{(i)} = 1 \quad j = 1, 2 \\
&T_{j,j+1}^{(i)} = 1 \quad j = 3, 5 + (N - i) \\
&T_{j,j+2}^{(i)} = 1 \quad j = 6 + (N - i), 9 + 2(N - i) \\
&T_{j,j+3}^{(i)} = 1 \quad j = 10 + 2(N - i), 10 + 3(N - i) \\
&T_{j,k}^{(i)} = -\frac{t^{(i-1)}}{2} \quad \text{for } j = 1, k = 3 \\
&\quad \quad \quad j = 5 + (N - i), k = 7 + (N - i) \\
&\quad \quad \quad j = 8 + 2(N - i), k = 12 + 2(N - i) \\
&T_{j,k}^{(i)} = -\frac{t^{(i)}}{2} \quad \text{for } j = 1, k = 4 \\
&\quad \quad \quad j = 5 + (N - i), k = 8 + (N - i) \\
&\quad \quad \quad j = 8 + 2(N - i), k = 13 + 2(N - i) \\
&i = 2, N
\end{aligned} \tag{3.78}$$

The typical  $\mathbf{R}^{(i)}$  matrix for the  $i$ -th layer of this element has dimensions of  $10 \times [10 + 3(N - i)]$ ; the dimensions for the typical  $\mathbf{T}^{(i)}$  matrix are  $[10 + 3(N - i)] \times [13 + 3(N - i)]$ .

A stacked element composed of two third-order beam elements is pictured in Figures 3.12a and 3.12b. The  $16 \times 25 \mathbf{R}^{(1)}$  matrix for this element is given by Equations (3.79).

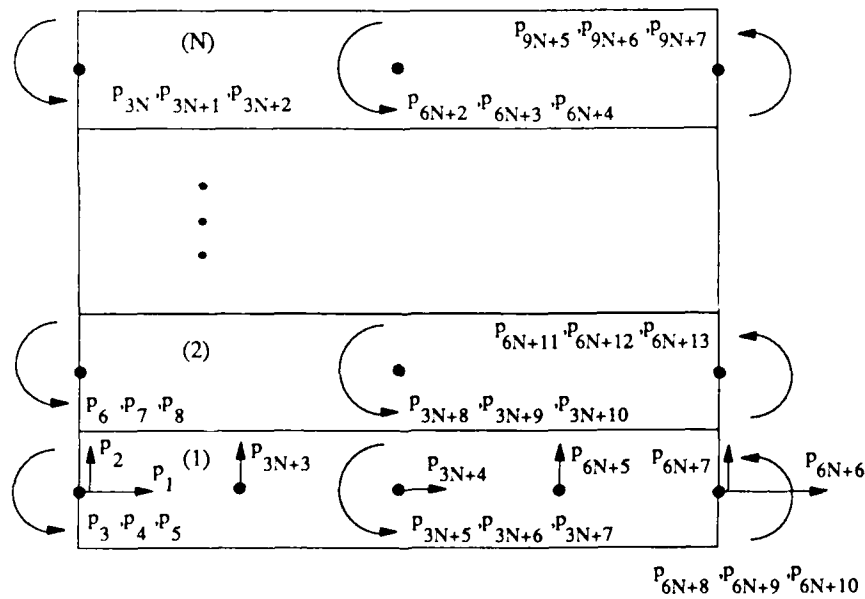


(a) Original simple elements.



(b) Stacked element.

Fig. 3.12 Third-order beam element.



(c) Multilayered stacked element.

Fig. 3.12 Concluded.

$$\begin{aligned}
\text{All } \mathbf{R}_{j,k}^{(1)} &= 0 \text{ except} \\
R_{j,j}^{(1)} &= 1 \text{ for } j = 1, 5 \\
R_{j,j+3}^{(1)} &= 1 \text{ for } j = 6, 10 \\
R_{j,j+6}^{(1)} &= 1 \text{ for } j = 11, 16
\end{aligned} \tag{3.79}$$

Equations (3.80) provide the compatibility conditions which can be derived from Equations (3.67) for the configuration shown in Figures 3.12a and b.

$$\begin{aligned}
q_1^{(2)} &= q_1^{(1)} - q_3^{(1)}t^{(1)}/2 - q_4^{(1)}(t^{(1)}/2)^2 - q_5^{(1)}(t^{(1)}/2)^3 \\
&\quad - q_3^{(2)}t^{(2)}/2 + q_4^{(2)}(t^{(2)}/2)^2 - q_5^{(2)}(t^{(2)}/2)^3 \\
q_7^{(2)} &= q_7^{(1)} - q_8^{(1)}t^{(1)}/2 - q_9^{(1)}(t^{(1)}/2)^2 - q_{10}^{(1)}(t^{(1)}/2)^3 \\
&\quad - q_8^{(2)}t^{(2)}/2 + q_9^{(2)}(t^{(2)}/2)^2 - q_{10}^{(2)}(t^{(1)}/2)^3 \\
q_{12}^{(2)} &= q_{12}^{(1)} - q_{14}^{(1)}t^{(1)}/2 - q_{15}^{(1)}(t^{(1)}/2)^2 - q_{16}^{(1)}(t^{(1)}/2)^3 \\
&\quad - q_{14}^{(2)}t^{(2)}/2 + q_{15}^{(2)}(t^{(2)}/2)^2 - q_{16}^{(2)}(t^{(1)}/2)^3
\end{aligned} \tag{3.80}$$

Elements of the  $16 \times 25 \mathbf{T}^{(2)}$  matrix which enforces these conditions are given as follows:

$$\begin{aligned}
&\text{All } T_{j,k}^{(2)} = 0 \text{ except} \\
&T_{j,j}^{(2)} = 1 \text{ for } j = 1, 2 \\
&T_{j,j+3}^{(2)} = 1 \text{ for } j = 3, 7 \\
&T_{j,j+6}^{(2)} = 1 \text{ for } j = 8, 13 \\
&T_{j,j+9}^{(2)} = 1 \text{ for } j = 14, 16 \\
&T_{j,j+k+m}^{(2)} = -(t^{(1)}/2)^m \tag{3.81} \\
&\text{for } j = 1, k = 1, m = 1, 3 \\
&\text{for } j = 7, k = 3, m = 1, 3 \\
&\text{for } j = 12, k = 7, m = 1, 3 \\
&T_{j,j+k+m}^{(2)} = (-t^{(2)}/2)^m \\
&\text{for } j = 1, k = 4, m = 1, 3 \\
&\text{for } j = 7, k = 6, m = 1, 3 \\
&\text{for } j = 12, k = 10, m = 1, 3
\end{aligned}$$

Formulae for the general **R** and **T** matrices associated with the  $N$ -lamina configuration pictured in Figure 3.12c are given as follows:

$$\begin{aligned}
&\text{All } R_{j,k}^{(i)} = 0 \text{ except} \\
&R_{j,j}^{(i)} = 1 \text{ for } j = 1, 5 \\
&R_{j,j+3(N-i)}^{(i)} = 1 \text{ for } j = 6, 10 \\
&R_{j,j+6(N-i)}^{(i)} = 1 \text{ for } j = 11, 16 \\
&i = 1, N-1
\end{aligned} \tag{3.82}$$

$$\begin{aligned}
&\text{All } T_{j,k}^{(i)} = 0 \text{ except} \\
&T_{j,j}^{(i)} = 1 \quad j = 1, 2 \\
&T_{j,j+3}^{(i)} = 1 \quad j = 3, 7 + 3(N-i) \\
&T_{j,j+6}^{(i)} = 1 \quad j = 8 + 3(N-i), 13 + 6(N-i) \\
&T_{j,j+9}^{(i)} = 1 \quad j = 14 + 6(N-i), 16 + 9(N-i) \\
&T_{j,k}^{(i)} = -(t^{(i-1)}/2)^m \quad j = 1, k = 2 + m \\
&\quad \quad \quad j = 7 + 3(N-i), k = 10 + m + 3(N-i) \\
&\quad \quad \quad j = 12 + 6(N-i), k = 19 + m + 6(N-i) \\
&T_{j,k}^{(i)} = (-t^{(i)}/2)^m \quad j = 1, k = 5 + m \\
&\quad \quad \quad j = 7 + 3(N-i), k = 13 + m + 3(N-i) \\
&\quad \quad \quad j = 12 + 6(N-i), k = 22 + m + 6(N-i) \\
&m = 1, 3; \quad i = 2, N
\end{aligned} \tag{3.83}$$

Typical matrices for the  $i$ -th layer of the third-order stacked element have dimensions of  $16 \times [16 + 9(N-i)]$  for  $\mathbf{R}^{(i)}$  and  $[16 + 9(N-i)] \times [25 + 9(N-i)]$  for  $\mathbf{T}^{(i)}$ .

Once the formulae for computing the mass and stiffness matrices of individual layers as well as the general  $\mathbf{R}$  and  $\mathbf{T}$  matrices are automated for use on the computer, they can be used to assemble the overall mass and stiffness matrices for a stacked element using the cascading procedure specified by Equation (3.73).

The mass and stiffness matrices for individual layers in stacked Timoshenko beam elements are derived from Equations (3.48) and (3.49), respectively. Equations (3.58) and (3.59) provide the bases for the matrices associated with individual layers in stacked third-order beam elements. However, since each layer in a stacked element is homogeneous, the composite properties defined by Equations (2.25) or (2.26) reduce to those given by Equations (3.84).

$$\begin{aligned}
 P_n &= \rho I_n \\
 Q_n &= EI_n \\
 V_n &= GI_n
 \end{aligned}
 \tag{3.84}$$

where

$$I_n = \int_A y^n dA = \begin{cases} \frac{2c^{n+1}}{n+1} & n \text{ even} \\ 0 & n \text{ odd} \end{cases}$$

In addition, a value of  $k=1$  is assumed for each layer in a stacked Timoshenko beam element since the actual variation of shear strain over each layer is not known a priori.

#### 3.5.4. Arbitrary Key Layer

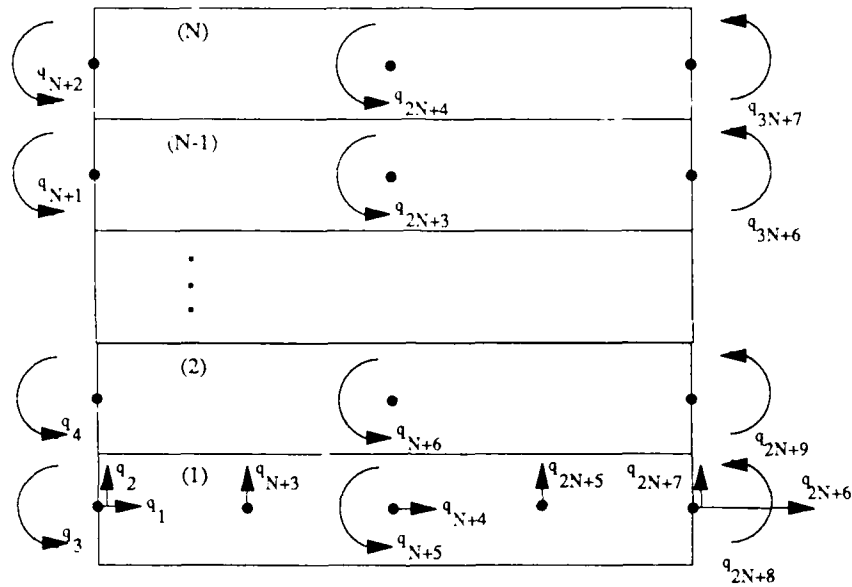
Finally, it should be pointed out that this treatment assumes the bottom layer is the key layer, which may influence the effects the forced boundary conditions have on the response calculated by stacked elements. For most end conditions, the location of the key layer has no effect. However, in the case of beams with a pinned end, that is an end which is unable to move in either the  $x$  or  $y$  direction but is free to rotate, the location of the key layer influences the basic nature of the beam's response.

If the bottom layer is retained as the key layer, the finite element model of the beam assumes that the pin enforcing this end condition is physically located in the bottom lamina. This nonsymmetric boundary condition leads to coupling between axial and bending response, even in beams with symmetric lamination configurations.

Although being able to model a pinned boundary condition in any layer may not be essential to analyzing actual physical systems given the highly idealized nature of this boundary condition,



many exact analytical solutions [12-18] are based on simple supports which possess geometric symmetry relative to the midplane of a beam or plate. Therefore, an evaluation of the performance of stacked elements made using such analytical solutions requires the ability to move the key layer to avoid or minimize the coupling induced by a nonsymmetric pinned boundary condition.

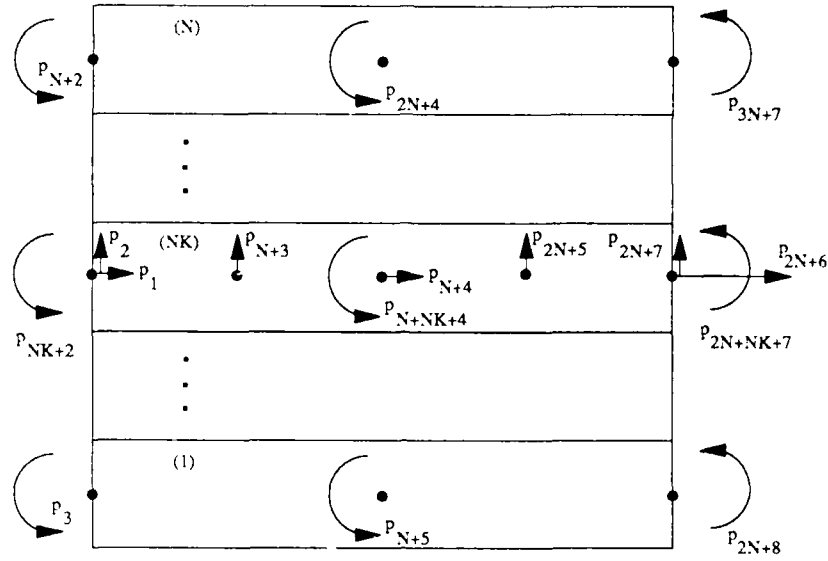


(a) Original element with key layer at the bottom.

**Fig. 3.13 Stacked element with arbitrary key layer.**

Moving the key layer to any specified lamina within the stacked element can be done simply by treating the problem as a transformation from a finite element with an initial set of generalized coordinates to one with a new set of generalized coordinates. As seen in the stacked Timoshenko beam pictured in Figure 3.13, this transformation moves the degrees of freedom associated with pure axial displacement and lateral displacement from the bottom layer to the newly specified key layer.

Actually, no transformation is necessary to move the degrees of freedom for the lateral displacement. Since all elements considered in this study ignore transverse normal strain, the actual



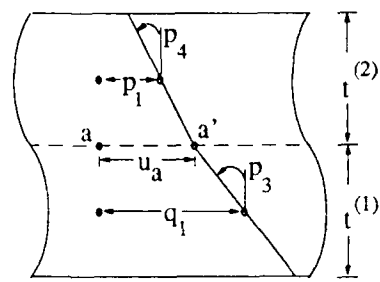
NK = layer number of key layer

(b) Transformed element with arbitrary key layer.

**Fig. 3.13 Concluded.**

location of these degrees of freedom has no effect on the mass and stiffness matrices. Therefore, they can be considered to reside in any lamina desired as long as the order in which they appear in the element's nodal displacement vector does not change.

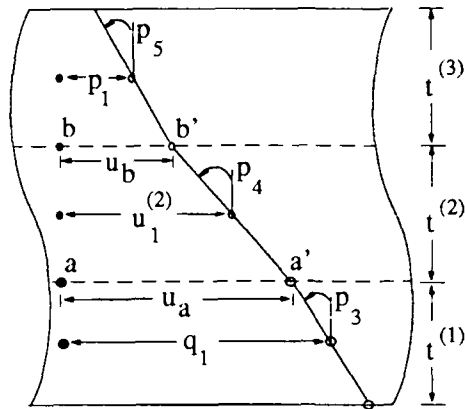
The degrees of freedom for pure axial motion for the original stacked Timoshenko beam shown in Figure 3.13a can be "moved" by expressing them in terms of the degrees of freedom associated with the modified stacked element shown in Figure 3.13b. The equations required for this process are based on continuity of displacement between adjacent layers and the kinematic constraints for each layer between the bottom lamina and the new key layer.



a, b, and n are points on interface in line with node 1 before deformation

a', b', and n' are locations of these points after deformation

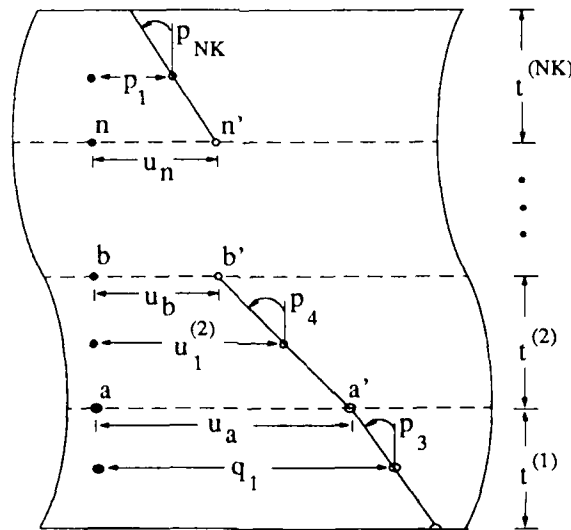
(a) Key layer = lamina (2).



$u_1^{(j)}$  = axial motion at node 1 in layer (j)

(b) Key layer = lamina (3).

Fig. 3.14 Geometry associated with moving the key layer.



(c) Arbitrary key layer.

Fig. 3.14 Concluded.

Figure 3.14a shows the geometry at node 1 associated with moving the key layer up one lamina. The analytical expressions related to this geometry for all node points become

$$\begin{aligned}
q_1 &= p_1 + p_3 t^{(1)}/2 + p_4 t^{(2)}/2 \\
q_{N+4} &= p_{N+4} + p_{N+5} t^{(1)}/2 + p_{N+6} t^{(2)}/2 \\
q_{2N+6} &= p_{2N+6} + p_{2N+8} t^{(1)}/2 + p_{2N+9} t^{(2)}/2
\end{aligned} \tag{3.85}$$

These equations are similar to Equations (3.75), which are associated with the stacked Timoshenko beam's **T** matrix.

A two-layer move of the key layer is portrayed in Figure 3.14b and the following relations:

$$\begin{aligned}
q_1 &= p_1 + p_3 t^{(1)}/2 + p_4 t^{(2)} + p_5 t^{(3)}/2 \\
q_{N+4} &= p_{N+4} + p_{N+5} t^{(1)}/2 + p_{N+6} t^{(2)} + p_{N+7} t^{(3)}/2 \\
q_{2N+6} &= p_{2N+6} + p_{2N+8} t^{(1)}/2 + p_{2N+9} t^{(2)} + p_{2N+10} t^{(3)}/2
\end{aligned} \tag{3.86}$$

Essentially, these equations are obtained by using the continuity of displacement at the interface between lamina 2 and lamina 3 (point b for node 1) to relate the axial displacement in the second lamina ( $U_1^{(2)}$  for node 1) to  $p_1$ , and using Equations (3.85) to relate this displacement to  $q_1$ .

The generalized problem is depicted geometrically in Figure 3.14c and analytically as follows:

$$\begin{aligned}
q_1 &= p_1 + \sum_{i=1}^{NK-1} \left( p_{i+2} \frac{t^{(i)}}{2} + p_{i+3} \frac{t^{(i+1)}}{2} \right) \\
q_{N+4} &= p_{N+4} + \sum_{i=1}^{NK-1} \left( p_{i+N+4} \frac{t^{(i)}}{2} + p_{i+N+5} \frac{t^{(i+1)}}{2} \right) \\
q_{2N+6} &= p_{2N+6} + \sum_{i=1}^{NK-1} \left( p_{i+2N+7} \frac{t^{(i)}}{2} + p_{i+2N+8} \frac{t^{(i+1)}}{2} \right)
\end{aligned} \tag{3.87}$$

where

$NK$  = layer number of key layer

These equations generalize the results given in Equations (3.85) and (3.86) and Figures 3.14a and b.

The transformation matrix involved in moving the key layer up to any specified lamina acts to retain all degrees of freedom not affected by this change, including those associated with lateral displacement. In addition, this matrix enforces the generalized relations given by Equations (3.87). The elements of the resulting matrix for a stacked Timoshenko beam element are given as

$$\begin{aligned}
 &\text{All } L_{j,k} = 0 \text{ except} \\
 &L_{j,j} = 1 \quad \text{for } j = 1, 2, \dots, 3N + 7 \\
 &L_{j,k} = t^{(1)}/2 \quad \text{for } j = 1, k = 3 \\
 &\qquad\qquad\qquad j = N + 4, k = N + 5 \\
 &\qquad\qquad\qquad j = 2N + 6, k = 2N + 8 \\
 &L_{j,k} = t^{(NK)}/2 \quad j = 1, k = 2 + NK \\
 &\qquad\qquad\qquad j = N + 4, k = N + 4 + NK \\
 &\qquad\qquad\qquad j = 2N + 6, k = 2N + 7 + NK \\
 &L_{j,k} = t^{(i)} \quad \text{for } j = 1, k = 2 + i \\
 &\qquad\qquad\qquad j = N + 4, k = N + 4 + i \\
 &\qquad\qquad\qquad j = 2N + 6, k = 2N + 7 + i \\
 &\qquad\qquad\qquad i = 2, 3, \dots, NK - 1
 \end{aligned} \tag{3.88}$$

where

$\mathbf{L}$  = transformation matrix associated with moving the key layer to layer  $NK$

This square matrix has dimensions of  $r \times r$ , where  $r = 3N + 7$ .

The transformation matrix for a stacked third-order element is very similar. The only difference is that Equations (3.87) must be replaced by the following:

$$\begin{aligned}
 q_1 &= p_1 + \sum_{i=1}^{NK-1} \left[ p_{3i} \left( \frac{t^{(i)}}{2} \right) + p_{3i+1} \left( \frac{t^{(i)}}{2} \right)^2 + p_{3i+2} \left( \frac{t^{(i)}}{2} \right)^3 \right. \\
 &\quad \left. + p_{3i+3} \frac{t^{(i+1)}}{2} - p_{3i+4} \left( \frac{t^{(i+1)}}{2} \right)^2 + p_{3i+5} \left( \frac{t^{(i+1)}}{2} \right)^3 \right] \\
 q_{3N+4} &= p_{3N+4} + \sum_{i=1}^{NK-1} \left[ p_{3i+3N+2} \left( \frac{t^{(i)}}{2} \right) + p_{3i+3N+3} \left( \frac{t^{(i)}}{2} \right)^2 \right. \\
 &\quad \left. + p_{3i+3N+4} \left( \frac{t^{(i)}}{2} \right)^3 + p_{3i+3N+5} \left( \frac{t^{(i+1)}}{2} \right) \right. \\
 &\quad \left. - p_{3i+3N+6} \left( \frac{t^{(i+1)}}{2} \right)^2 + p_{3i+3N+7} \left( \frac{t^{(i+1)}}{2} \right)^3 \right] \\
 q_{6N+6} &= p_{6N+6} + \sum_{i=1}^{NK-1} \left[ p_{3i+6N+5} \left( \frac{t^{(i)}}{2} \right) + p_{3i+6N+6} \left( \frac{t^{(i)}}{2} \right)^2 \right. \\
 &\quad \left. + p_{3i+6N+7} \left( \frac{t^{(i)}}{2} \right)^3 + p_{3i+6N+8} \left( \frac{t^{(i+1)}}{2} \right) \right. \\
 &\quad \left. - p_{3i+6N+9} \left( \frac{t^{(i+1)}}{2} \right)^2 + p_{3i+6N+10} \left( \frac{t^{(i+1)}}{2} \right)^3 \right]
 \end{aligned} \tag{3.89}$$

These equations, which reflect the higher-order kinematic constraints associated with the third-order element, lead to the transformation matrix

$$\begin{aligned}
&\text{All } L_{j,k} = 0 \text{ except} \\
&L_{j,j} = 1 \text{ for } j = 1, 2, \dots, 9N + 7 \\
&L_{j,k} = \left( \frac{t^{(1)}}{2} \right) \text{ for } j = 1, k = 2 + m \\
&\quad j = 3N + 4, k = 3N + 4 + m \\
&\quad j = 6N + 6, k = 6N + 7 + m \\
&\quad m = 1, 2, 3 \\
&L_{j,k} = - \left( -\frac{t^{(NK)}}{2} \right)^m \text{ for } j = 1, k = 3NK - 1 + m \\
&\quad j = 3N + 4, k = 3(NK + N) + 1 + m \\
&\quad j = 6N + 6, k = 3(NK + 2N) + 4 + m \\
&\quad m = 1, 2, 3 \\
&L_{j,k} = 2 \left( \frac{t^{(i)}}{2} \right)^m \text{ for } j = 1, k = 3i - 1 + m \\
&\quad j = 3N + 4, k = 3(i + N) + 1 + m \\
&\quad j = 6N + 6, k = 3(i + 2N) + 4 + m \\
&\quad m = 1 \text{ and } 3 \\
&\quad i = 2, 3, \dots, NK - 1
\end{aligned} \tag{3.90}$$

The dimensions for this matrix are  $r \times r$ , where  $r = 9N + 7$ .

Once the proper transformation matrix is defined, the local mass and stiffness matrices associated with moving the key layer up to the desire lamina are found using the general matrix transformation given by Equation (3.66). The transformations for these matrices are given explicitly as

$$\mathbf{M}^* = \mathbf{L}^T \mathbf{M} \mathbf{L} \quad \mathbf{K}^* = \mathbf{L}^T \mathbf{K} \mathbf{L} \tag{3.91}$$

where

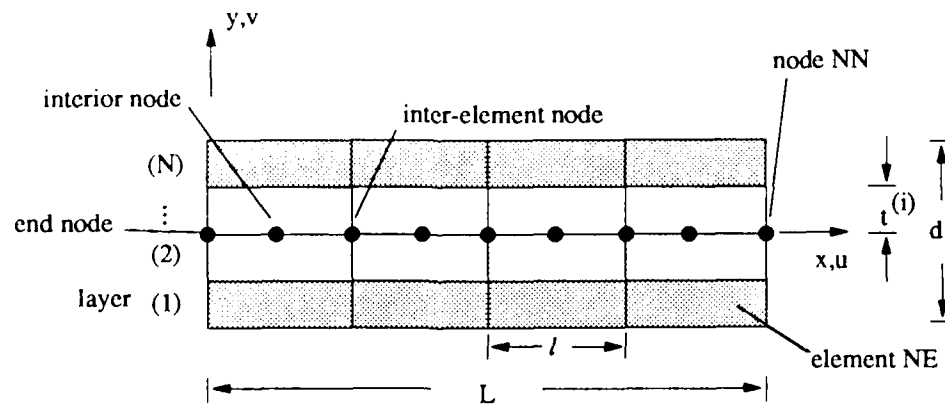
$\mathbf{M}^*$  = mass matrix for element with new key layer

$\mathbf{K}^*$  = stiffness matrix for element with new key layer

It should be noted that all transformations allow the key layer to move in the positive vertical direction only.

### 3.6. Solution Procedure for Free Vibration Problems

Figure 3.15 shows the kind of discretized beam model used in this study to find the natural frequencies of composite beams. As can be seen, the model is made up of a series of finite elements capable of accounting for the nonhomogeneous nature of composite beams. A requirement not portrayed explicitly in Figure 3.15 is that the elements on the ends of the model must be restrained in some way to prevent rigid-body motion.



$L$  = length of beam

$l$  = length of element

$t(i)$  = thickness of lamina (i)

$d$  = depth of beam

$N$  = total number of layers

$NK$  = layer number of key layer

$NE$  = total number of elements

$NN$  = total number of nodes

Fig. 3.15 Discretized composite beam model.



Although it is certainly possible to restrain the motion at interior points of a finite element beam model, this feature is not generally required for the problems of interest in this investigation. However, calculations associated with exact elasticity solutions require restrained nodes in the interior of the beam. This exception is discussed in detail in Chapter 4.

The end conditions considered in this study are restricted to a pinned or fixed condition on the left end of the beam and free, simply supported, pinned, or fixed conditions on the beam's right end. The constraints each condition places on the motion of the end of the beam are summarized in Figure 3.16. The effects of these constraints on the degrees of freedom associated with each finite element developed for this effort are also specified in this figure. It should be noted that these effects are expressed in terms of local degrees of freedom for the right end of each beam element, not the global ones associated with the actual discretized beam model. It should also be noted that any combination of left and right end conditions is valid with the exception of the pinned-free combination.

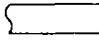

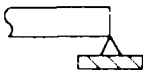
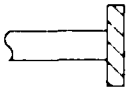
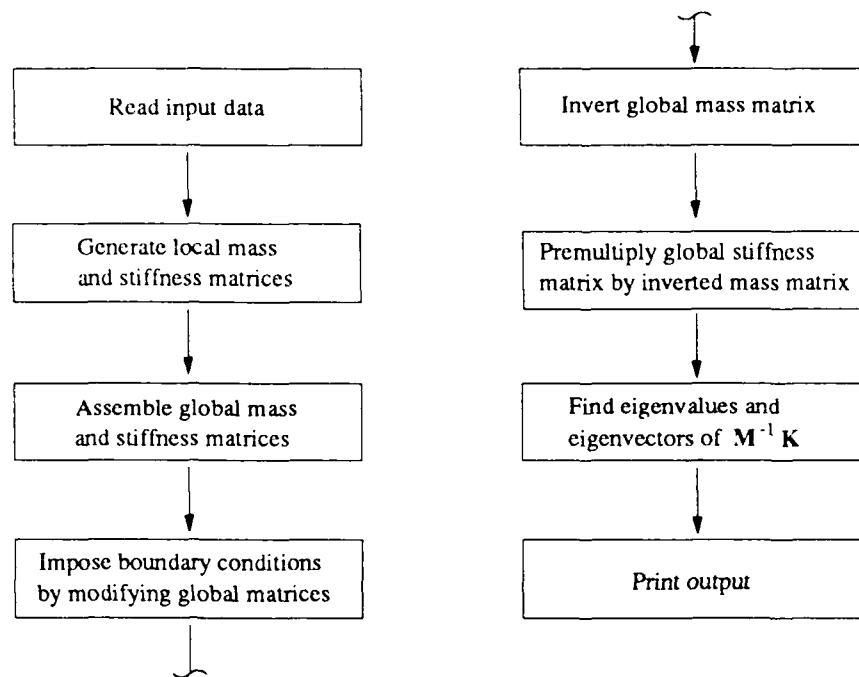
Beam boundary conditions (at $x = L$ )		Finite element boundary conditions			
		Bernoulli-Euler	Timoshenko	Levinson-Bickford	Third-order
Free 	No forced boundary conditions				
Simply supported 	$v(L,0,t) = 0$	$w_3 = 0$	$w_4 = 0$	$w_3 = 0$	$w_4 = 0$
Pinned 	$u(L,0,t) = 0$ $v(L,0,t) = 0$	$U_3 = 0$ $w_3 = 0$	$U_3 = 0$ $w_4 = 0$	$U_3 = 0$ $w_3 = 0$	$U_3 = 0$ $w_4 = 0$
Clamped 	$u(L,y,t) = 0$ $v(L,y,t) = 0$	$U_3 = 0$ $w_3 = 0$ $w_4 = 0$	$U_3 = 0$ $w_4 = 0$ $\Phi_3 = 0$	$U_3 = 0$ $w_3 = 0$ $w_4 = 0$ $\Phi_3 = 0$	$U_3 = 0$ $w_4 = 0$ $\Phi_3^{(i)} = 0$ ( $i = 1,2,3$ )

Fig. 3.16 Finite element boundary conditions.

All finite element programs developed in this effort to solve the free vibration problem pictured in Figure 3.15 follow the procedure outlined in Figure 3.17. As can be seen, the first step is to read the input data required to derive the local mass and stiffness matrices. After the local matrices are derived using the input data, these matrices are assembled to generate the global mass and stiffness matrices. Then the global matrices are modified to account for the forced boundary conditions associated with the problem of interest.



**Fig. 3.17** Flowchart for free-vibration programs.

Once the forced boundary conditions are imposed, the modified mass matrix is inverted. Subsequently, the modified stiffness matrix is premultiplied by the inverted mass matrix. A subroutine contained in the International Mathematical Subroutine Library (IMSL) is then used to find the eigenvalues and eigenvectors of the resulting matrix. Finally, the natural frequencies and mode shapes obtained from this procedure are stored in the output file and printed as required.

The programs written to perform the calculations just described run on the UXH Mainframe computer at the University of Illinois at Urbana-Champaign. This machine, a CONVEX Computer

Corporation C1/C120/C210A series supercomputer, runs on the UNIX operating system and performs calculations in 64-bit double precision and 32-bit single precision. All the results discussed in the present study are based on double-precision calculations.

Finally, all programs make use of the IMSL subroutine call DEVCRG, which can be used to find the eigenvalues and eigenvectors of any general, real matrix. According to the IMSL User's Manual [154], this subroutine balances the matrix of interest, reduces the balanced matrix to a real upper Hessenberg matrix, and computes the eigenvalues and eigenvectors associated with this matrix. More details regarding this subroutine can be found in [154].

## 4. EVALUATION OF FINITE ELEMENTS

This chapter documents the results of calculations made to evaluate the performance of the elements developed in this study. These calculations provide the data necessary to investigate the accuracy and convergence properties of the elements, ensure the absence of shear locking in the shear-deformable elements, assess the accuracy of the elements using analytical and experimental data available in the literature, and identify conditions in which stacked elements are required to obtain reasonably accurate estimates of natural frequency. Table 4.1<sup>1</sup> provides a summary of the calculations made in this effort. In addition, abbreviations used throughout this chapter are defined in Table 4.2.

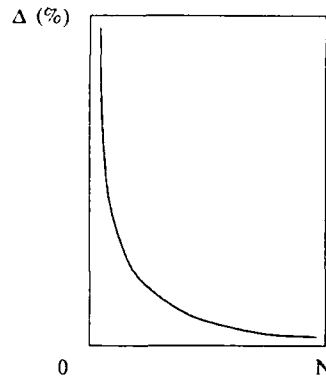
### 4.1. Accuracy

As stated in Chapter 3, complete, conforming elements for a given theory are guaranteed to generate results which converge monotonically to the values associated with the exact solution for that theory. The convergence properties of such elements can be portrayed graphically by plotting the error associated with the finite element results as a function of the number of elements or the number of degrees of freedom used in the finite element model. Figure 4.1a provides an example of such a convergence curve. It should be noted that although the error is actually a function of a discrete variable rather than a continuous one, Figure 4.1a presents this curve schematically as a smooth, continuous function of a continuous variable.

As can be seen in this figure, the error converges monotonically to zero since the error is calculated with respect to the exact solution for the theory upon which the element is based. However, if the error is calculated relative to a higher-order theory, such as the theory of elasticity,

---

<sup>1</sup> All tables for this chapter are contained in the Appendix.

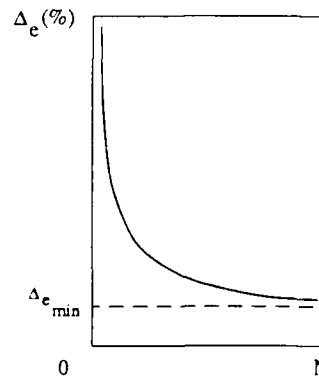


(a) Error calculated with respect to exact solution for theory upon which finite element based.

$$\Delta(\%) = [(V_f - V_s) / V_s] \times 100$$

$$\Delta_e(\%) = [(V_f - V_e) / V_e] \times 100$$

$$\Delta_{e_{\min}} = [(V_s - V_e) / V_e] \times 100$$



(b) Error calculated with respect to higher-order exact solution.

$N$  = number of elements or dof in finite element model

$V_f$  = value from finite element solution

$V_s$  = exact value from theory on which element is based

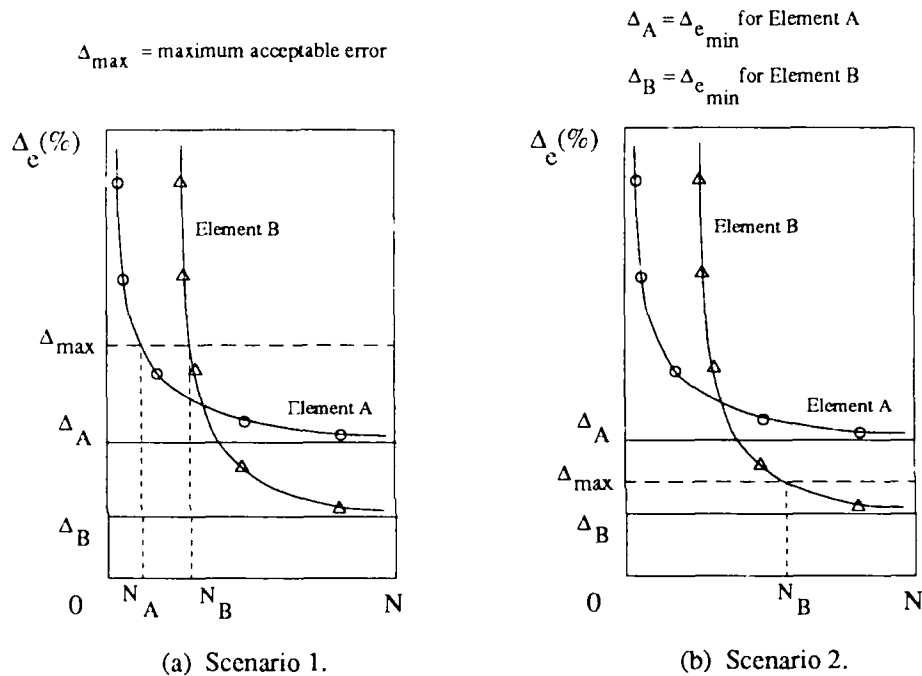
$V_e$  = exact value from higher-order theory

**Fig. 4.1 Accuracy and convergence of finite element solutions.**

a curve like the one given in Figure 4.1b results. In this case, the error converges to a value which represents the error inherent in the lower-order theory relative to the higher-order one. This inherent error represents the minimum error attainable with a particular element.

It should be noted that applying the term “convergence” to the reduction in error depicted by the curve shown in Figure 4.1b is not correct, strictly speaking. In a strict mathematical sense, the term convergence should be used only when the error is measured relative to the exact solution for the theory on which the element is based, as is the case in Figure 4.1a. When studying true convergence, the analyst is not concerned with the accuracy of an element, only with the manner in which its discretization error decreases as a larger number of elements is used in the finite element model.

However, from an engineering point of view, the analyst is usually interested in both convergence and accuracy when evaluating the relative merits of various finite elements. The proper element for a calculation can be chosen only after evaluating the tradeoffs between accuracy and the rate of convergence for the various elements being considered for use.



**Fig. 4.2 Tradeoffs in the convergence of finite element solutions.**

Two possible scenarios for such an evaluation are pictured in Figures 4.2a and b. Both these figures present “convergence” curves for different elements (elements A and B) along with the maximum error which the analyst can accept in each case. In the first scenario, both elements possess adequate accuracy for the desired calculation. Therefore, element A is the most efficient element in this case. Even though it is a less accurate element than element B, it yields results which attain an adequate level of accuracy using fewer degrees of freedom. This reduction in the required number of degrees of freedom leads to lower computer storage requirements and computation time, and hence, to cheaper calculations.

In the second scenario, a more stringent accuracy requirement makes element B the only option. Even though it appears to have a slower rate of convergence, it is the only element capable of providing the accuracy specified in this case.

Once again, the curves pictured in Figures 4.2a and b are not true convergence curves since the error in these figures is measured with respect to a higher-order theory, rather than the exact solution on which the elements are based. Therefore, the error includes that which is inherent in the lower-order theory as well as the discretization error. However, calculating error with respect to a higher-order solution, such as an elasticity solution, provides a convenient way to assess both the accuracy of the various elements examined in this study and how many degrees of freedom are required to attain this accuracy.

As a result, this approach is used throughout most of Section 4.1. In addition, the term “convergence” is used to refer to the reduction in error associated with using more elements (and hence more degrees of freedom) in the finite element model regardless of whether the error is measured relative to the appropriate beam theory for the element or with respect to a higher-order theory. This usage gives the term a broader meaning than is usually the case, but facilitates the discussion which follows.

This report also makes use of the following definitions to facilitate the comparison of the accuracy of the various elements presented in this section. If an element is capable of estimating natural frequencies to within 10% of the value obtained from an exact elasticity solution, it is said to have first-order accuracy. Similarly, second- and third-order accuracy are defined as being able to estimate natural frequencies to within 1% and 0.1%, respectively, of the values associated with the exact elasticity solution.

In general, techniques capable of generating between first-order and second-order accuracy are adequate for most engineering purposes. As is pointed out by Biggs [155], sophisticated

techniques capable of providing greater accuracy are not required in most cases since input data, such as geometric or material properties, are not usually known with enough precision to justify the use of such techniques [155]. Therefore, third-order accuracy is seldom required, but it is used in this study to identify elements capable of generating extremely accurate results.

#### 4.1.1. Accuracy of Present Elements

This section examines the accuracy and convergence behavior of all elements developed in this study when used to model the free vibrations of homogeneous isotropic and orthotropic beams as well as composite beams of fiber-reinforced and sandwich construction. As specified in Table 4.1, all calculations related to accuracy and convergence are identified by a “C” prefix to distinguish them from the accuracy calculations discussed in Section 4.3. In addition, all calculations discussed in this section are labeled with the “C1” prefix. The homogeneous, isotropic beam associated with case C1-IS is assumed to be made out of aluminum. The homogeneous, orthotropic beam, case C1-OR, is made of a material with the properties of graphite-epoxy. Finally, cases C1-L3 and C1-S3 correspond to the three-lamina graphite-epoxy beam and aluminum-balsa sandwich beam, respectively, used in the study of convergence for composite beams.

The material and geometric properties, as well as the boundary conditions, for each case are specified in Table 4.3. As can be seen, all calculations involve beams with a span-to-depth ( $L/d$ ) ratio of 10. The material properties listed are not associated with any particular kind of aluminum, graphite epoxy, or balsa wood, but are meant to be representative values for these materials. The properties chosen for the aluminum are based on values given by Beer and Johnston in [156]. The elastic constants for the graphite-epoxy beams were obtained from a paper by Whitney and Sun [157]; the density was acquired from work done by Khdir and Reddy [158]. Finally, the properties of the balsa wood were chosen based on information found on page 252 of Allen’s text [24]. In



many of the cases investigated in Chapter 4, only a Young's modulus or a shear modulus could be found. In such cases, the remaining modulus is estimated using the relation found in Equation (2.3) in conjunction with a Poisson's ratio of 0.25.

Data required to generate convergence curves for all the elements developed in this effort were obtained for the four cases of interest from calculations which employed 1,2,4,8,12, and 16 elements in the finite element model of the beam. Only data for the first and fifth modes of bending are examined in this study of accuracy and convergence. Since the beams have an  $L/d$  ratio of 10, the first mode is associated with a fairly thin beam. However, because simply supported boundary conditions are employed in all calculations, the fifth mode can be thought to represent the fundamental mode of a beam with a span-to-depth ratio of 2, a condition in which shear deformation should have a significant influence on the natural frequencies for all the cases considered in this study.

The data from this study are summarized in Tables 4.4 through 4.7. These tables provide the actual frequencies obtained from each calculation, and specify both the number of elements and number of degrees of freedom contained in the finite element models from which the data were obtained. The number of degrees of freedom refers to the number which remain after the pinned-simply supported boundary conditions are imposed on the finite element model.

Elements considered in this study include the Bernoulli-Euler element, which accounts for rotary inertia, as well as the Timoshenko, Levinson-Bickford, and general third-order elements. In addition, the stacked Timoshenko element and stacked third-order element are examined. Shear correction factors of  $k=5/6$  and  $k=1$  are employed in an effort to bound the response of the Timoshenko beam model using fairly standard values for this factor. This study uses the terms "corrected Timoshenko element" and "basic Timoshenko element" to differentiate between simple Timoshenko elements which use a correction factor of  $k=5/6$  and  $k=1$ , respectively.

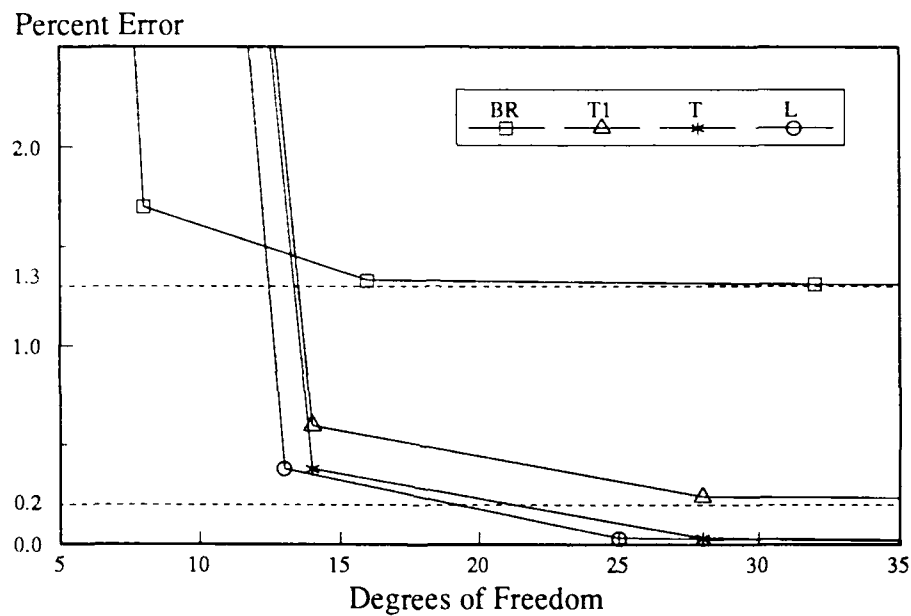
The stacked elements are used to estimate the response of the homogeneous beams, as well as the composite beams, to see if the increased number of degrees of freedom associated with these elements gives them any advantage over the simple elements in the homogeneous cases. The stacked finite element model for these cases divides the beam into three equal layers and imposes an independent kinematic constraint on each of these layers.

As can be seen, error with respect to an exact elasticity solution is provided in these tables. The elasticity solution is a plane-stress solution similar to the plane-strain solutions developed by Jones [16] and Kulkarni and Pagano [17]. All elasticity solutions ignore the coupling between longitudinal and lateral motion caused by Poisson effects, and attempt to suppress transverse normal strain by using values for the transverse Young's modulus which are three orders of magnitude larger than the associated longitudinal modulus. These conventions were adopted to allow differences between the finite element solutions and the elasticity solution to be attributable to discretization error and approximate kinematic constraints only. The importance of ignoring Poisson's effects and transverse normal strain is addressed in the study of element accuracy discussed in Section 4.3.1 of this report.

In addition to error relative to an exact elasticity solution, error with respect to the associated beam theory is provided for the Bernoulli-Euler and Timoshenko elements. The exact solutions for these theories were obtained using the technique presented by Huang in [35] modified to account for the properties of composite beams. The data in these comparisons represent true convergence data in the strict mathematical sense of the word.

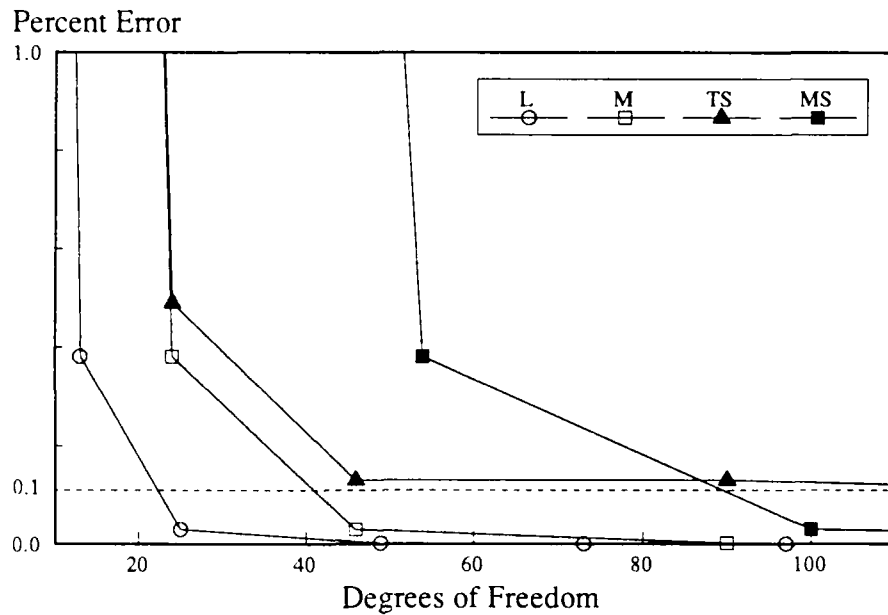
The information given in these tables is presented in a graphical form in Figures 4.3 through 4.6. These figures plot the error relative to the exact elasticity solution as a function of the number of degrees of freedom contained in the finite element model after the boundary conditions are imposed.

As can be seen in Figures 4.3a and b, all elements developed in this study are capable of first-order accuracy for the first mode of the homogeneous, isotropic aluminum beam. In addition, all elements except the Bernoulli-Euler element and stacked Timoshenko beam possess second-order accuracy. The fact that even this element comes very close to this level of accuracy indicates shear deformation does not have a significant influence on the natural frequency in this case.



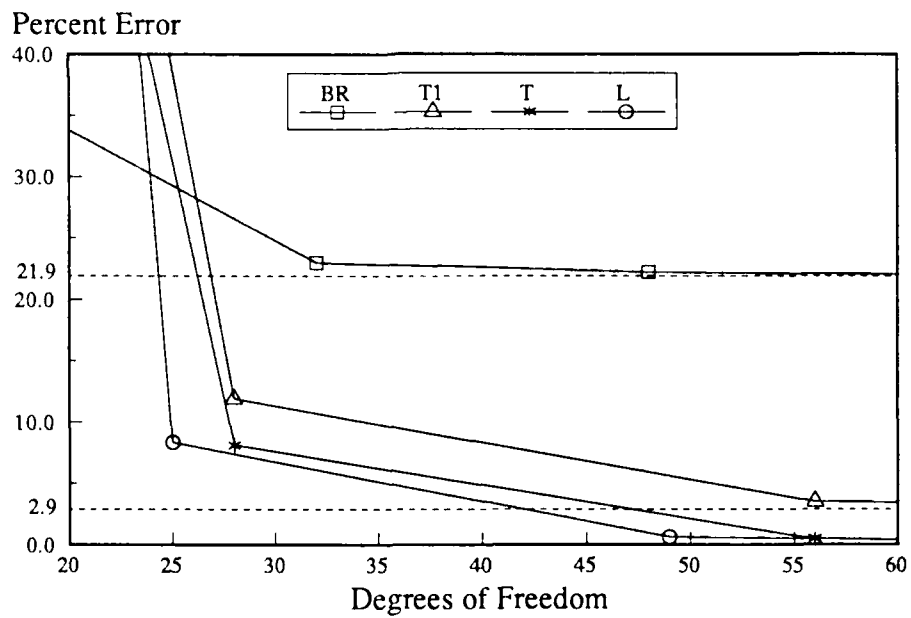
(a) Mode 1 (Elements BR,T1,T & L).

Fig. 4.3 Accuracy data, Case C1-IS.



(b) Mode 1 (Elements L,M,TS &amp; MS).

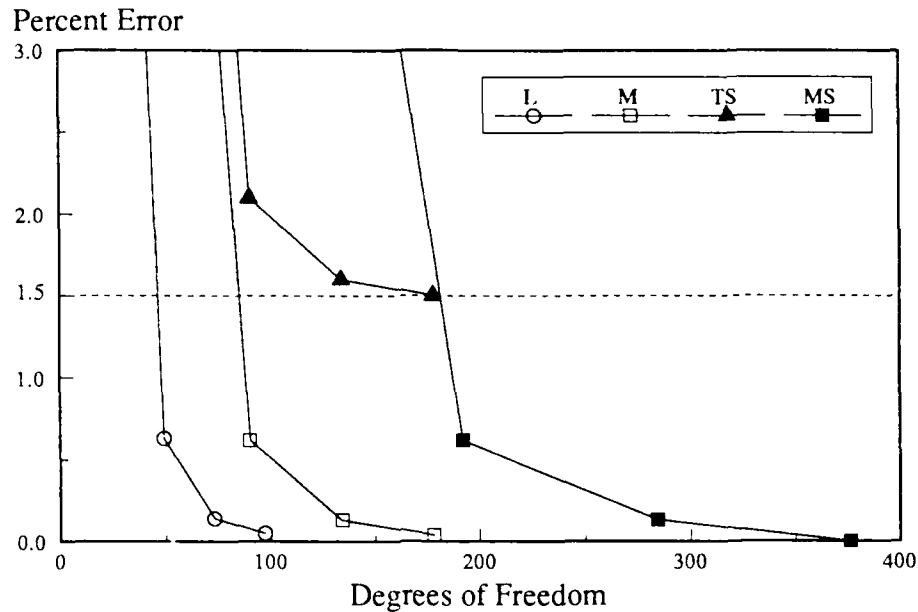
Fig. 4.3 Continued.



(c) Mode 5 (Elements BR,T1,T &amp; L).

Fig. 4.3 Continued.

Of the elements capable of second-order accuracy, the Levinson-Bickford element has a slightly faster rate of convergence than the corrected Timoshenko beam, its closest competitor. This



(d) Mode 5 (Elements L,M,TS &amp; MS).

**Fig. 4.3 Concluded.**

slight advantage is probably due to the fact that all degrees of freedom associated with lateral motion of the Levinson-Bickford element must be at the end nodes to enforce  $C^1$  continuity. As a result, the degrees of freedom for this element do not proliferate as rapidly with an increase in the number of elements as do the degrees of freedom associated with the other higher-order elements.

Figure 4.3a reveals that the Levinson-Bickford and simple third-order elements are both capable of third-order accuracy, as is the Timoshenko element as long as the proper shear correction factor is chosen. However, both the Levinson-Bickford and third-order elements achieve this accuracy without recourse to a correction factor. Of these two elements, the Levinson-Bickford element is clearly the more efficient one.

It should be noted that the value of  $k=5/6$  actually makes the corrected Timoshenko beam more flexible than the beam associated with the exact elasticity solution, a result which manifests itself in the negative errors listed for this beam in Table 4.4. It should also be noted that even though the exact solution for the corrected Timoshenko beam generates a natural frequency slightly lower

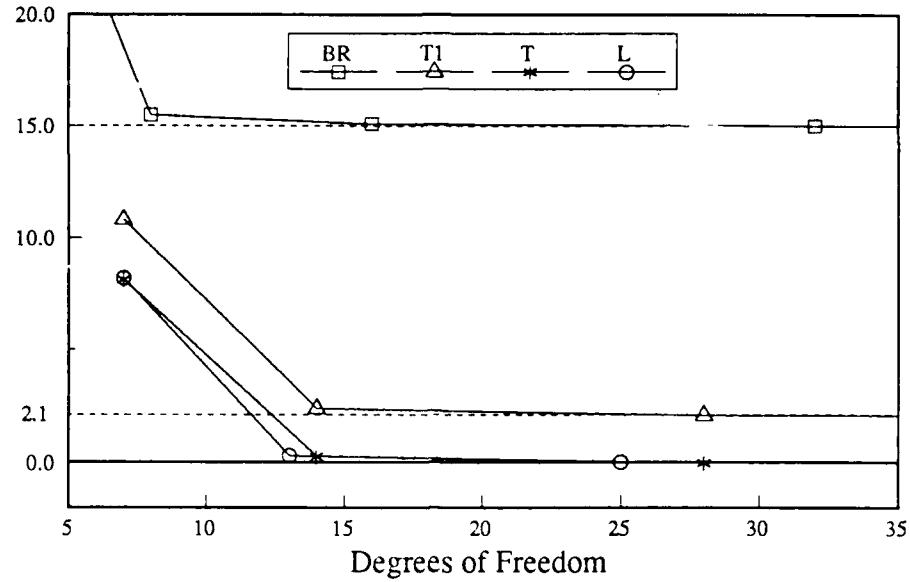
than that of the exact elasticity solution, the natural frequencies obtained from the beam model composed of corrected Timoshenko elements always approach the value for the exact Timoshenko solution monotonically from above.

The stacked Timoshenko element is fairly competitive with the simple third-order element, but appears to be slightly stiffer in that it converges to an error slightly larger than 0.1%. The data in Table 4.4 reveal that the stacked third-order element should not be used in situations similar to case C1-IS since its accuracy is identical to that of the simple third-order beam, but is achieved with a much greater number of degrees of freedom.

Figures 4.3c and d show that the results for the fifth mode in this case are generally similar to those observed for vibration in the first mode. Notable exceptions include the inability of the Bernoulli-Euler element and Timoshenko element ( $k=1$ ) to achieve first-order and second-order accuracy, respectively. These results indicate that shear deformation plays a greater role in this mode of vibration.

The influence of shear deformation can be seen at lower modes in the orthotropic beam examined in case C1-OR. Table 4.5 and Figure 4.4a reveal that the Bernoulli-Euler element is incapable of first-order accuracy even for the first mode in this case. In addition, the basic Timoshenko element ( $k=1$ ) does not possess second-order accuracy. Once again, using corrected Timoshenko elements leads to a beam model which appears to be more flexible than the beam associated with the elasticity solution. However, the magnitude of the error associated with this model is still within the range of third-order accuracy.

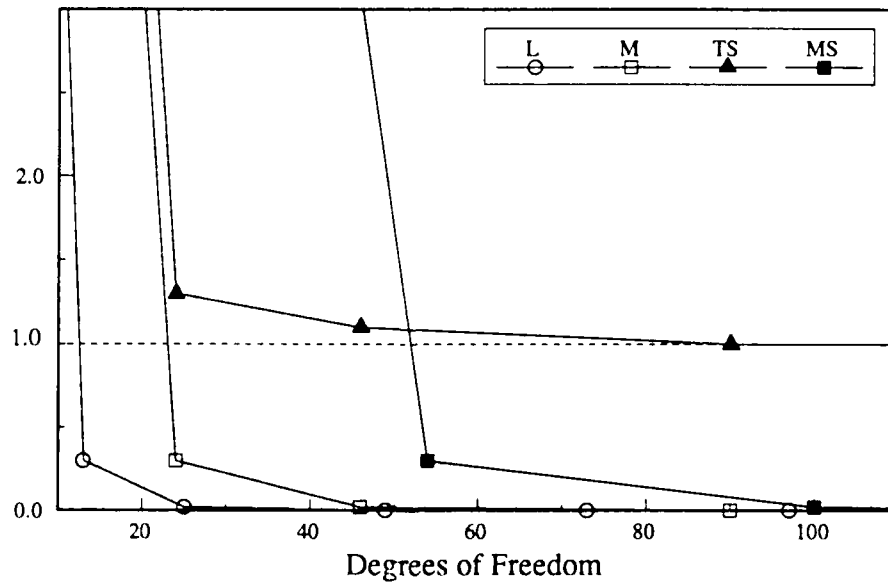
Percent Error



(a) Mode 1 (Elements BR,T1,T &amp; L).

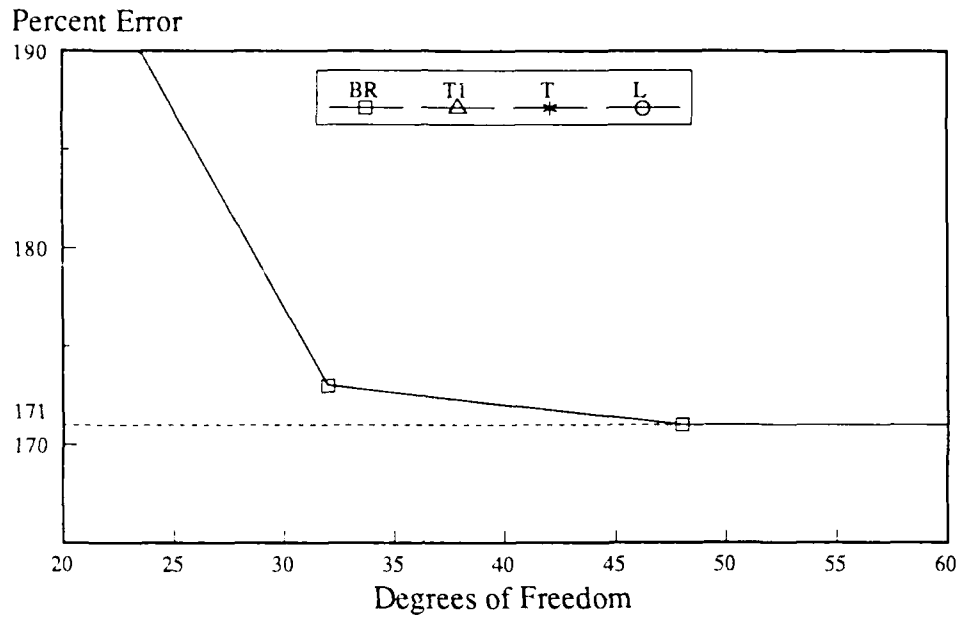
Fig. 4.4 Accuracy data, Case C1-OR.

Percent Error



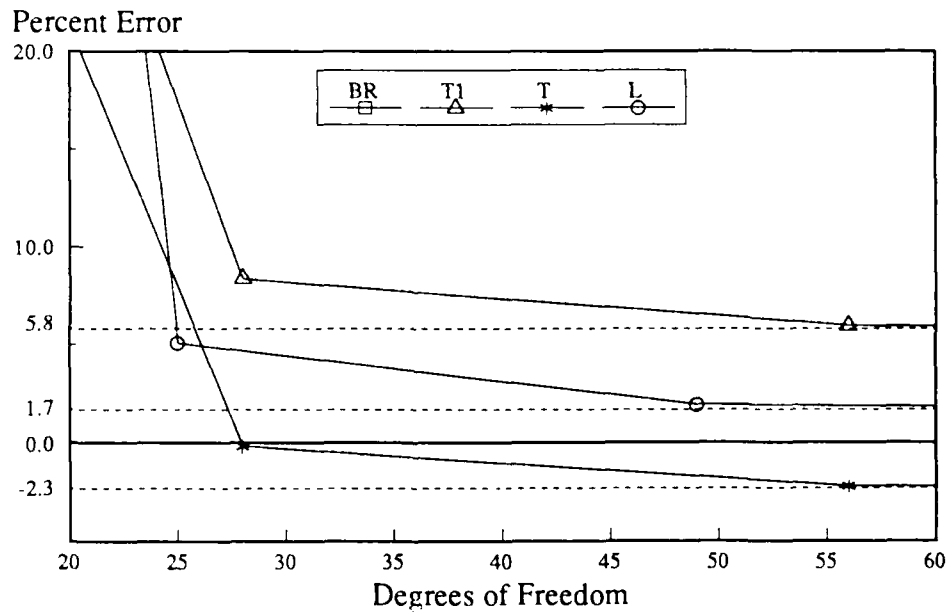
(b) Mode 1 (Elements L,M,TS &amp; MS).

Fig. 4.4 Continued.



(c) Mode 5 (Element BR).

Fig. 4.4 Continued.

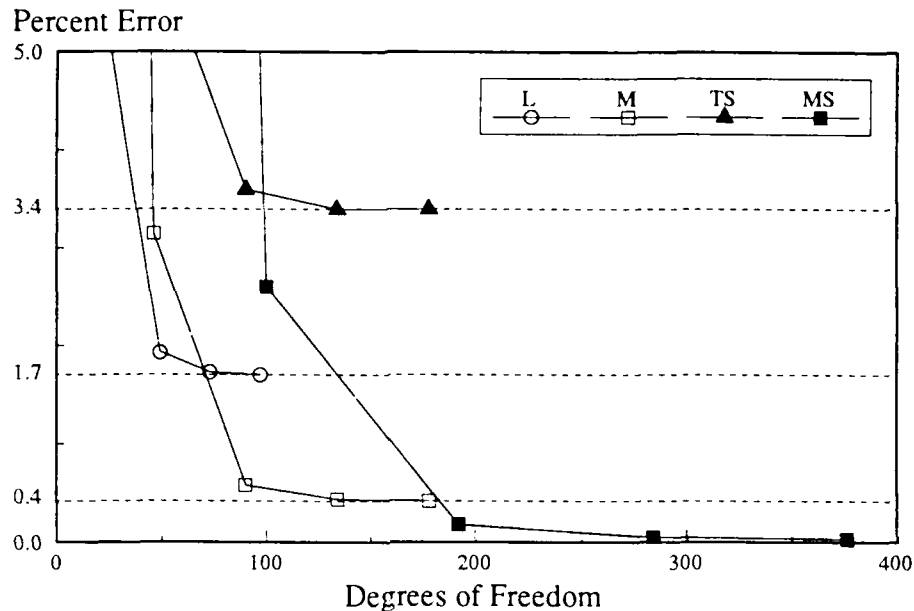


(d) Mode 5 (Elements T1, T &amp; L).

Fig. 4.4 Continued.

The Levinson-Bickford and simple third-order elements (Figure 4.4b) are also capable of this accuracy with the former element attaining this level of performance with the fewest degrees of





(e) Mode 5 (Elements L,M,TS &amp; MS).

**Fig. 4.4 Concluded.**

freedom. As in the isotropic case, this element enjoys a slight advantage in terms of convergence over the corrected Timoshenko element and a fairly substantial advantage relative to the simple third-order element.

The stacked Timoshenko beam is not as competitive with the simple third-order element in this case in that it barely achieves second-order accuracy. In addition, the accuracy of the stacked third-order element is similar to that of its simple counterpart, but attains this accuracy with a much larger number of degrees of freedom.

In the fifth mode (Figures 4.4c-e), trends seen in the progression from the isotropic to the orthotropic case are even more pronounced. The Bernoulli-Euler element is not even capable of zero-order accuracy, producing an error around 170%. In addition, neither the corrected nor the basic Timoshenko element can attain second-order accuracy. The fact that the results obtained with these elements bound the exact elasticity solution may indicate that the actual distribution of shear strain over the depth of the beam for this mode is somewhere between the parabolic distribution

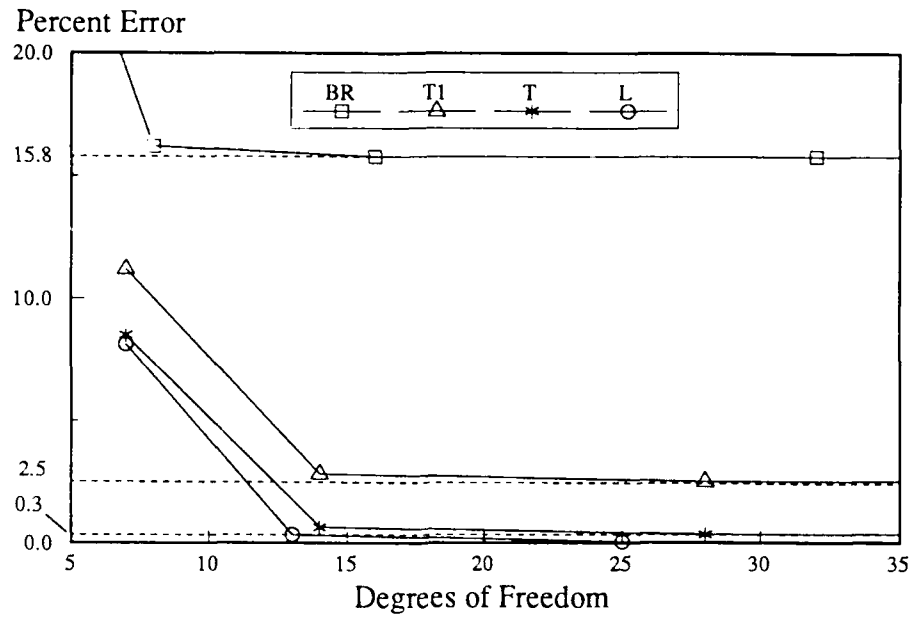
associated with  $k=5/6$  and the uniform distribution related to  $k=1$ . The fact that the corrected element appears to be too flexible and the basic element too stiff also implies greater accuracy may be obtained by using a shear correction factor between these values. However, determining this value a priori may prove difficult.

One major difference seen in the data presented in Figure 4.4e is that the Levinson-Bickford element is no longer the most efficient element if second-order accuracy is required since the error for this element converges to a value of 1.7% for this case. Of the simple elements, only the third-order element is capable of this level of accuracy. It should be noted that the element achieves this level of performance without resorting to the use of a correction factor.

A continued deterioration in the performance of the stacked Timoshenko element relative to the simple third-order beam is apparent. Although the error for the stacked element converges to 3.4%, a value probably adequate for many engineering purposes, the error for the simple third-order element is an order of magnitude lower and is achieved with the same number of degrees of freedom as used by the stacked Timoshenko beam model.

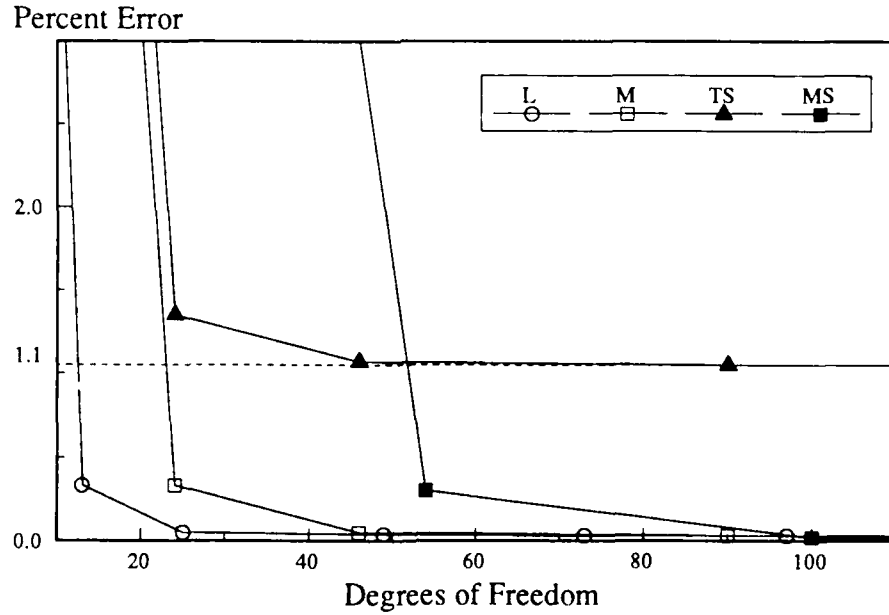
It should be noted that the stacked third-order element is the only one capable of third-order accuracy. However, the large number of degrees of freedom required to attain this level of performance still make this element unattractive to use in cases involving homogeneous beams.

The results for the three-lamina graphite-epoxy beam, presented in Table 4.6 and Figure 4.5, are very similar to those just discussed with the exception that the corrected and basic Timoshenko elements appear to be stiffer relative to the exact elasticity solution than was the case for the homogeneous orthotropic beam.



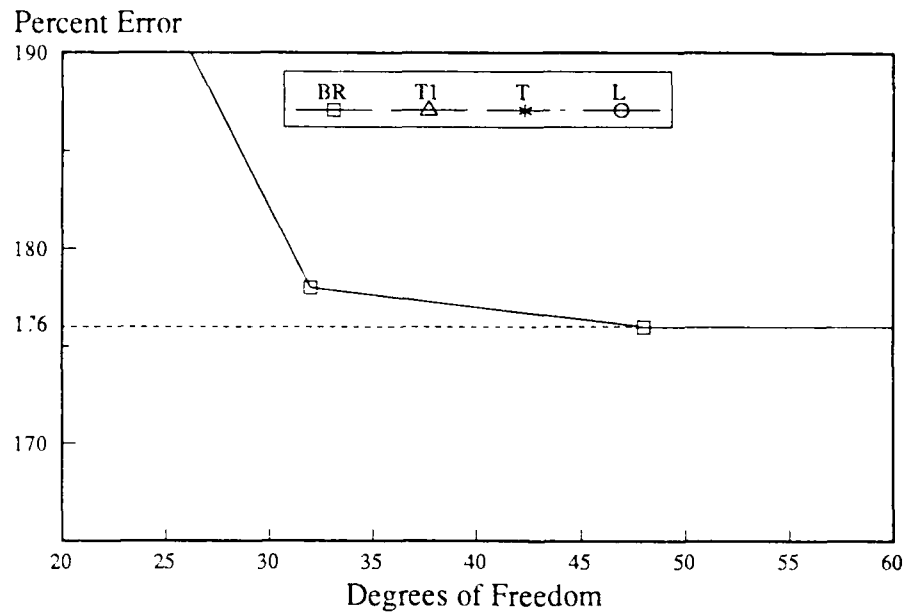
(a) Mode 1 (Elements BR,T1,T &amp; L).

Fig. 4.5 Accuracy data, Case C1-L3.



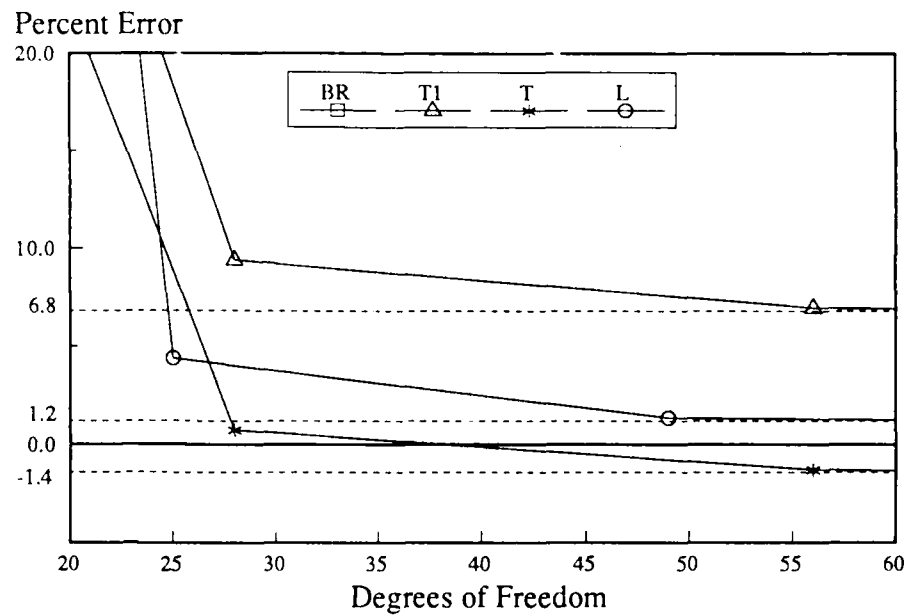
(b) Mode 1 (Elements L,M,TS &amp; MS).

Fig. 4.5 Continued.



(c) Mode 5 (Element BR).

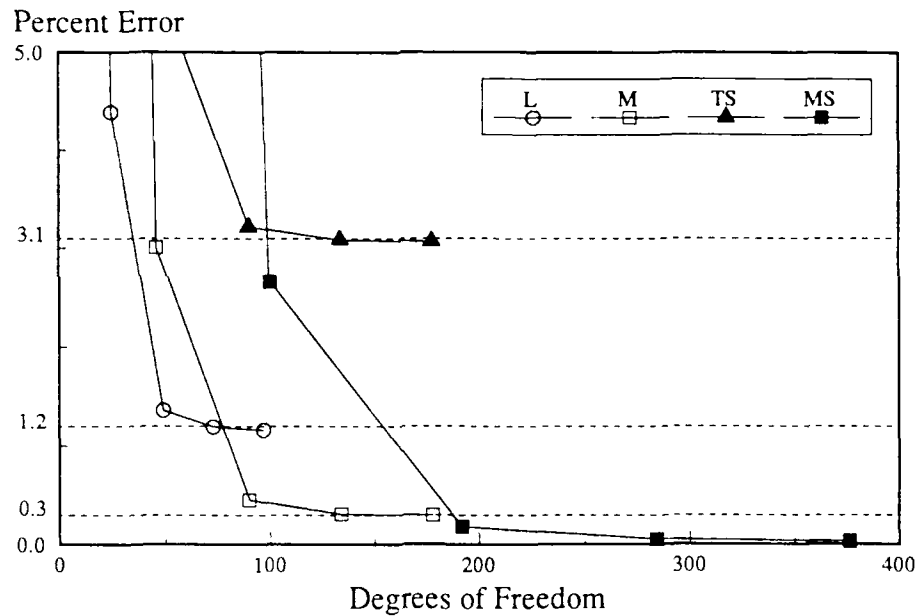
Fig. 4.5 Continued.



(d) Mode 5 (Elements T1, T &amp; L).

Fig. 4.5 Continued.

In addition, the fifth mode for the laminated case is the first situation encountered in this investigation in which the simple third-order element cannot attain third-order accuracy (Figure



(e) Mode 5 (Elements L,M,TS &amp; MS).

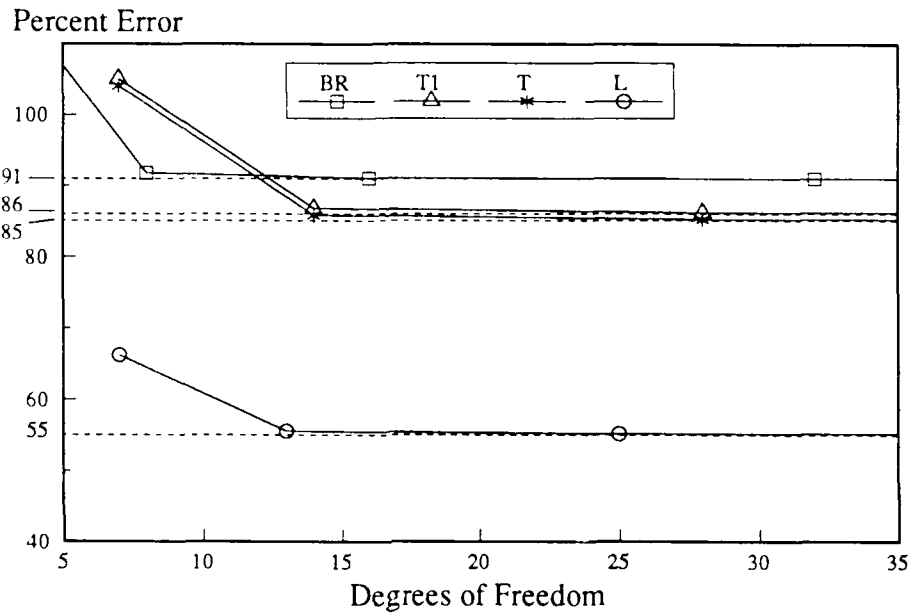
**Fig. 4.5 Concluded.**

4.5e). However, this simple element is still more accurate than the stacked Timoshenko beam. Evidently, the piecewise-linear profile of shear strain over the depth of the composite beam afforded by the latter element leads to a finite element beam model which is stiffer and less accurate than the one associated with the simple third-order element, in which the distribution of shear strain is continuous and quadratic.

Although the stacked third-order element is capable of third-order accuracy, it is still not an attractive alternative since the level of performance achieved by the simple third-order element and even the Levinson-Bickford element are probably adequate for most engineering applications and are attained with far fewer degrees of freedom.

However, Table 4.7 and Figure 4.6 reveal that stacked elements are absolutely essential for estimating the response of the three-layer aluminum-balsa sandwich beam considered in case C1-S3. In this case, the Bernoulli-Euler and Timoshenko elements yield errors of about 90% for the first mode. Although the errors for the Levinson-Bickford and simple third-order theories are lower

(55% and 37%, respectively), these errors are still far greater than the 10% error associated with first-order accuracy in this study. However, both stacked elements are capable of third-order accuracy for the first mode. In addition, the stacked third-order element can achieve this level of performance in the fifth mode of vibration (see Table 4.7).

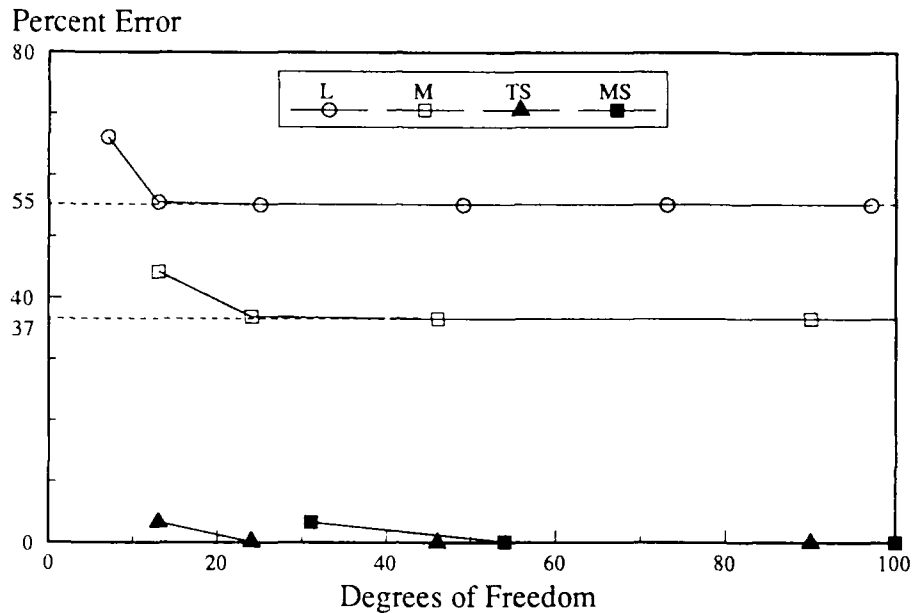


(a) Mode 1 (Elements BR,T1,T & L).

**Fig. 4.6 Accuracy data, Case C1-S3.**

However, the higher rate of convergence of the stacked Timoshenko beam probably makes it the element of choice in cases involving sandwich beams made up of highly dissimilar materials. The combination of material and geometric properties which lead to the requirement for stacked elements is discussed in detail in Section 4.4.

Several conclusions can be drawn from the study just discussed. For one thing, it is apparent that shear deformation restricts the use of Bernoulli-Euler elements to the fairly benign conditions associated with the lower modes of fairly long and slender isotropic beams. Higher-order elements are required for other cases in which shear deformation has a larger influence on beam vibration.



(b) Mode 1 (Elements L,M,TS &amp; MS).

**Fig. 4.6 Concluded.**

The Timoshenko element can be quite accurate in such cases if the proper shear correction factor is chosen. The standard value of  $k=5/6$  appears to be adequate for the lower modes of isotropic, orthotropic, and laminated composite beams. However, it leads to a beam which is more flexible than the one associated with the exact elasticity solution. The attendant underestimation of natural frequency becomes more pronounced as the degree of orthotropy of the beam increases (i.e., as the ratio of Young's modulus in the longitudinal direction to the transverse shear modulus increases), and as higher modes are encountered.

The Levinson-Bickford element turns out to be a very good element for most cases examined in this portion of the convergence study. Its accuracy is probably adequate for most engineering purposes, except for the sandwich beam considered in case C1-S3. In addition, its rate of convergence is higher than the other higher-order elements developed in this effort. It also enjoys the advantage of achieving these results without recourse to a shear correction factor.

The simple third-order element also has the advantage of not requiring a shear correction factor. In general, it can attain a higher level of accuracy than the Levinson-Bickford element, but pays for this accuracy with a much lower rate of convergence. The stacked Timoshenko element with three layers has a similar rate of convergence, but is outperformed slightly in terms of accuracy by the simple third-order elements for all cases except the sandwich beam. In the cases not involving the sandwich beam, the accuracy of the stacked third-order element is equal to or better than that of its simple counterpart, but is attained with a much larger number of degrees of freedom, a fact which makes it an unattractive alternative in these cases.

However, the stacked elements are essential in cases similar to the sandwich beam in which the properties in adjacent layers are quite dissimilar. For cases requiring these elements, the stacked Timoshenko element appears to be more efficient. It is not as accurate as the stacked third-order element, but is capable of providing adequate accuracy with less degrees of freedom.

It should be noted that natural frequency is the only parameter discussed in this study of accuracy. For cases in which the stresses associated with free or forced vibration of a sandwich or fiber-reinforced composite beam are of interest, the higher-order kinematic constraint of the stacked third-order element may be required to estimate the magnitude and distribution of these stresses adequately. The comparison made by Yuan and Miller [128] with the exact elasticity solution of Pagano [9] for static loading supports this conjecture.

Finally, the data in Tables 4.4 through 4.7 reveal that all elements appear to converge to within 1% of the associated exact solution for the first and fifth modes when eight or more elements are used. Based on this conclusion, all calculations made to evaluate the accuracy of these elements against data found in the literature involve finite element beam models made up of eight or more elements.



#### 4.1.2. Comparison of Present Elements with Other Elements

In addition to the accuracy study just discussed, calculations were made to compare the accuracy and convergence of elements developed in this effort to the accuracy and convergence of elements which appear in the literature. The elements considered in this subsequent set of calculations include Timoshenko beams discussed in the work of Thomas, et al. in [111] and the third-order element developed by Kant and Gupta [64].

Calculations associated with the elements examined in [111] include cases C2-IA and C2-IB; cases C3-IA and C3-IB are associated with the elements described in [64]. Table 4.8 summarizes the properties of the homogeneous, isotropic beams considered in these cases. As can be seen, cases C2-IA and B involve cantilever steel beams. The simply supported aluminum beam of interest in case C1-IS is also investigated in cases C3-IA and B. The results of the calculations associated with these cases are in Tables 4.9 and 4.10, and Figures 4.7 through 4.9.

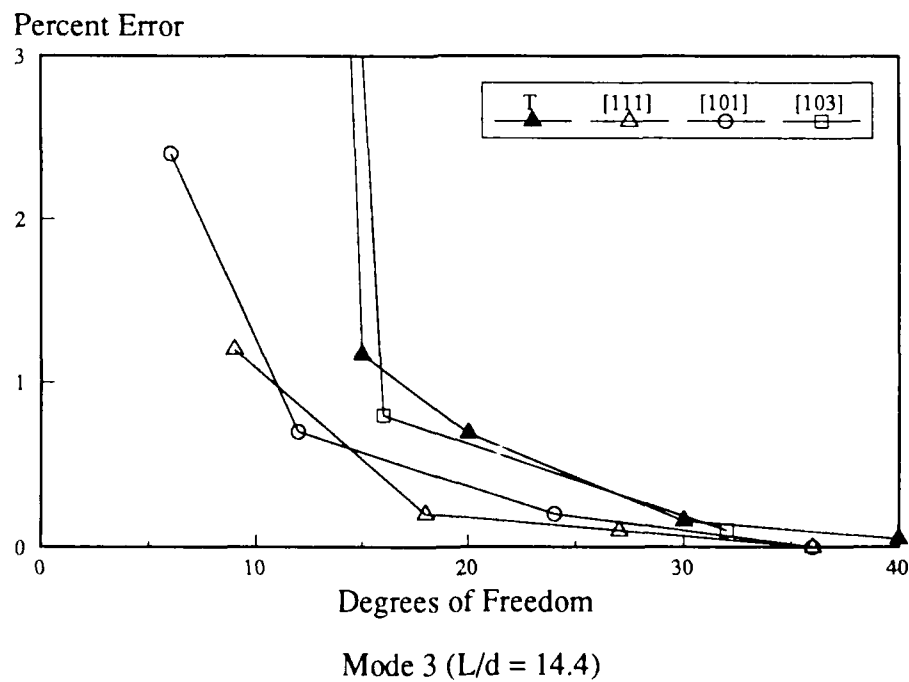


Fig. 4.7 Convergence data, Case C2-IA.<sup>2</sup>

<sup>2</sup>Values from [111] obtained from a graph.

Figure 4.7 compares the Timoshenko beam developed in the present effort to elements discussed in [111]. It should be noted that the axial degrees of freedom of the Timoshenko element developed in the present effort are not included in the data used to generate the convergence curves for this element seen in Figures 4.7 and 4.8.

As can be seen in Figure 4.7, this element is very competitive with the elements examined by Thomas, et al., in terms of accuracy, but has a rate of convergence which is generally lower than the element of Archer [101] and Thomas, et al. [111]. Figure 4.7 shows the elements of Kapur [103] and Nickel and Secor [106] to be slightly more efficient than the Timoshenko element of the present effort.

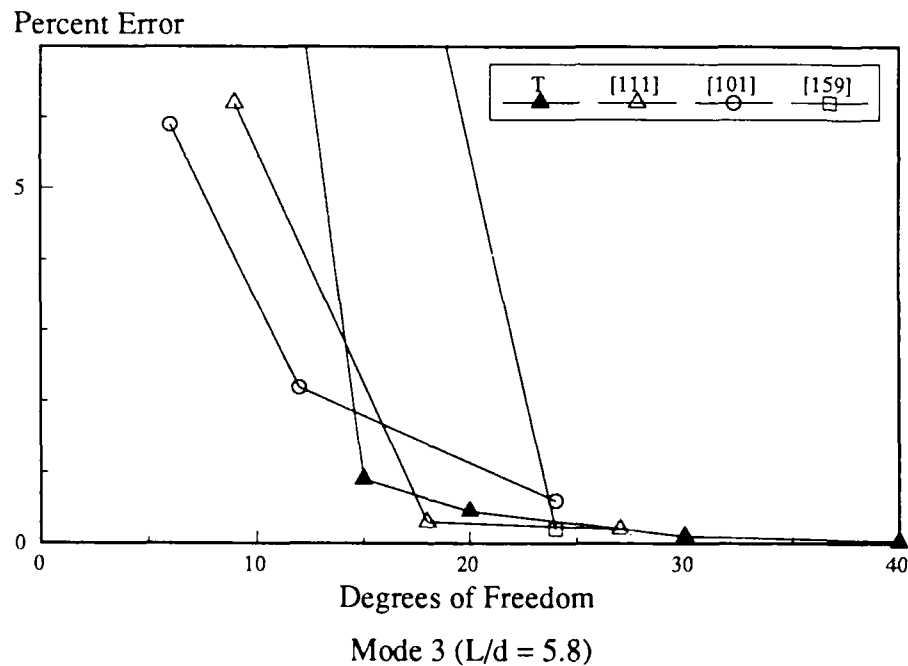


Fig. 4.8 Convergence data, Case C2-IB.<sup>3</sup>

Figure 4.8 reveals that the present element outperforms the element of Carnegie, et al. [159]. In addition, it compares more favorably with the elements of Archer [103] and Thomas, et al. [111]

<sup>3</sup> Values from [111] obtained from a graph.

for case C2-IB where the effects of shear deformation are more pronounced than they are in Case C2-IA. It should be noted that the present Timoshenko element also has the advantage of being able to model axial motion and composite beam behavior. However, it cannot model the response of linearly tapered beams as some of the elements discussed in [111] can.

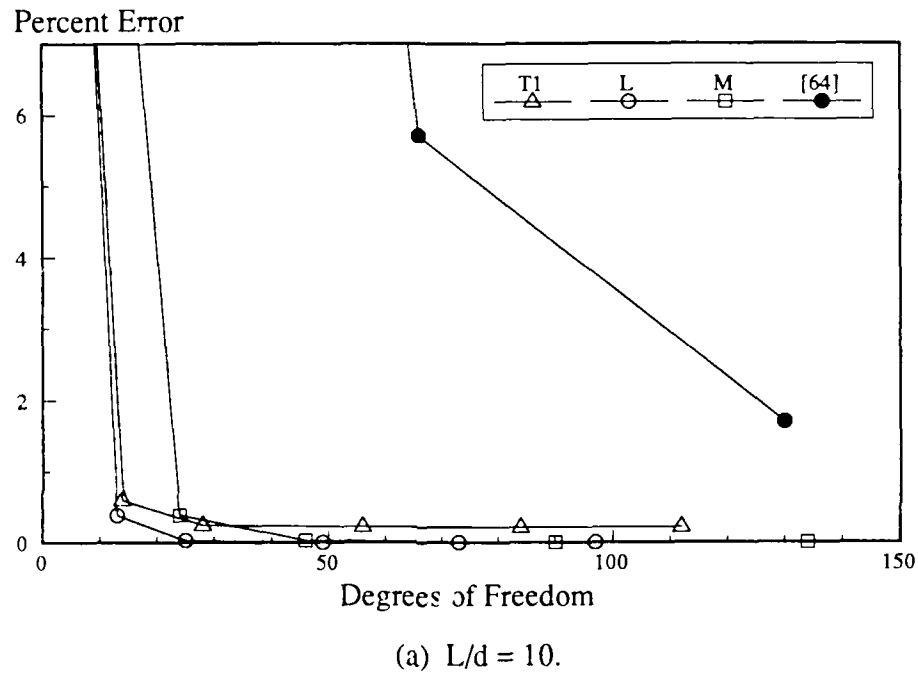
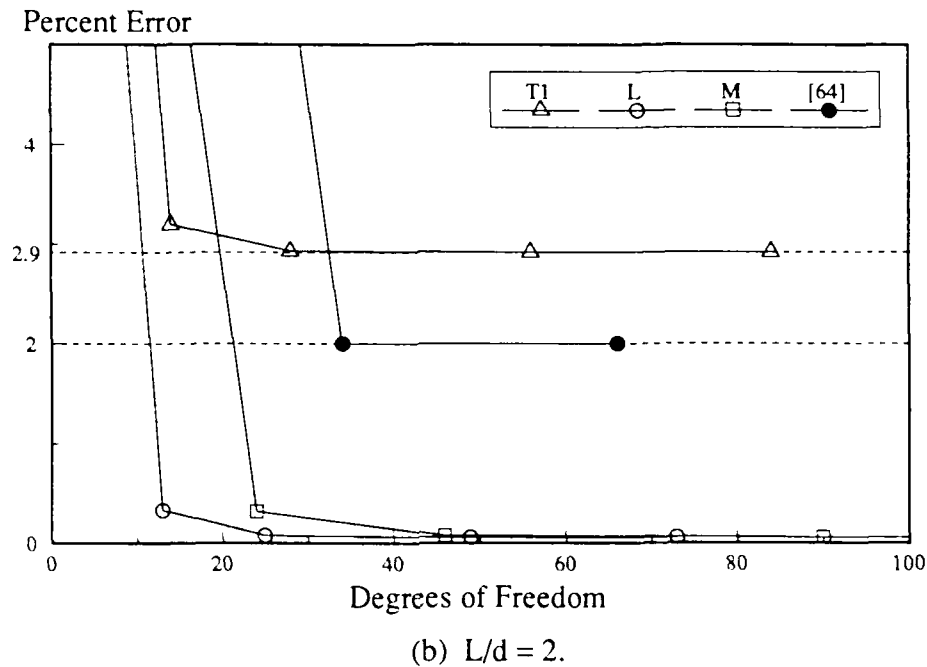


Fig. 4.9 Accuracy data, Case C3-IA.<sup>4</sup>

The comparisons given in Figure 4.9 indicate that the higher-order elements developed in this effort appear to be more robust than the third-order element of Kant and Gupta [64]. Figure 4.9a presents data for the first mode for a beam with a span-to-depth ratio of 10. As can be seen, the element of Kant and Gupta converges very slowly relative to the elements of the present effort. Kant and Gupta's element does much better for the thicker beam with  $L/d = 2$  associated with Figure 4.9b; however, it is still outperformed by all elements in the present effort in terms of rate of convergence, and by all save the basic Timoshenko element ( $k=1$ ) in terms of accuracy. It should be noted that the axial degrees of freedom of the present elements are retained in these comparisons.

<sup>4</sup> Values from [64] obtained from a graph.



**Fig. 4.9 Concluded.**

Although it cannot be stated with certainty, the convergence data seen in Figure 4.9 as well as other convergence curves presented in [64] indicate the element of Kant and Gupta may be subject to shear locking. All displacements in this element are interpolated with linear shape functions; therefore, the conditions for shear locking specified by Prathap, et al. [107,108] are present. In addition, a deterioration in convergence is evident when this element is used to examine a fairly thin beam (Figure 4.9a) rather than the thick beam of interest in Figure 4.9b. Finally, data in [64] (Figure 10 on p. 199 of [64]) seem to indicate the natural frequencies calculated by this element converge to values greater than those obtained from Bernoulli-Euler theory when even thinner beams ( $L/d = 20$ ) are examined.

Regardless of whether shear locking is present or not, the higher-order elements developed in the present effort are superior to the element proposed by Kant and Gupta in the cases considered in this section. In addition, the present elements appear to be more robust in that their performance does not deteriorate when thinner beams are examined.

## 4.2. Shear Locking

To ensure that all elements developed in this effort do not lock in the thin-beam limit, calculations were performed to evaluate the performance of these elements as  $L/d$  becomes large. These calculations involve all the cases considered in Section 4.1.1 and include beams with span-to-depth ratios of 10, 100, 1000, and 10,000. All the data for this study of shear locking were obtained from finite element beam models containing eight elements. Only data for the fundamental mode of vibration are considered in this study.

Table 4.11 summarizes the data from this study. In this table, all natural frequencies are normalized with respect to the natural frequencies obtained from the exact solution for a Bernoulli-Euler beam with rotary inertia. As in the convergence study documented in Section 4.1.1, natural frequencies associated with this theory were obtained using the method of Huang [35] modified to account for the properties of composite beams.

For fairly thick beams, normalized natural frequencies having a value less than one reveal the influence of shear deformation on the vibration of the beam. If shear locking exists, it should manifest itself by producing normalized natural frequencies greater than one as the thin-beam limit is approached.

As can be seen in Table 4.11, shear deformation does have an effect on the fundamental mode of vibration at the lowest span-to-depth ratio ( $L/d = 10$ ), as might be expected from the information presented in Section 4.1.1. In addition, this effect is more pronounced for the orthotropic, composite, and sandwich beams than for the homogeneous, isotropic beam considered. However, all solutions presented in Table 4.11 converge to the Bernoulli-Euler solution for span-to-depth ratios of 100 and 1000. The only case in which a very minor shear-deformation effect can be detected at these  $L/d$  ratios is the sandwich beam for  $L/d = 100$ , in which the most powerful elements estimate

normalized natural frequencies about 1% below unity. These results indicate that shear locking is not present in the finite element models for very thin beams with span-to-depth ratios of 1000 or less.

However, this good performance does not extend to even thinner beams having  $L/d$  ratios of 10,000. In this range, anomalous results are evident in the data for some of the elements. At present, the source of these anomalies is not known, but they do not appear to be caused by shear locking since some of the elements register natural frequencies lower than those obtained from the Bernoulli-Euler beam theory. In fact, some of the eigenvalues calculated at this  $L/d$  ratio are actually negative. Such eigenvalues are obviously in error since the positive-definite nature of both the mass and stiffness matrices prohibits the existence of such eigenvalues.

As stated above, the cause of these anomalous results is not known currently, although they may be numerical in nature. One feature of the IMSL subroutine used in the finite element programs for the present elements is that it provides a performance parameter which can be used to judge the validity of the results generated by the subroutine (see p. 298 of [154]). Confidence in the results decreases as the value of the parameter increases. The value of this parameter does increase as the thin-beam limit is approached, indicating that numerical problems are more likely. However, it should be noted that all performance parameters examined in this study are well within the range in which acceptable results can be expected. Therefore, the cause of the anomalous values seen at  $L/d=10,000$  cannot be identified positively with the data available at the present time.

The questionable data seen at the highest  $L/d$  ratio indicate the elements cannot be used with confidence for span-to-depth ratios greater than 1000. However, the other results listed in Table 4.11 lead to the conclusion that shear locking does not appear to be a problem at or below span-to-depth ratios of 1000. Therefore, the elements should produce results which are valid, within the limits of their respective theories, in this range of the  $L/d$  ratio. This range should cover most, if not all, situations of practical interest.

### 4.3. Evaluation of Accuracy Using Published Data

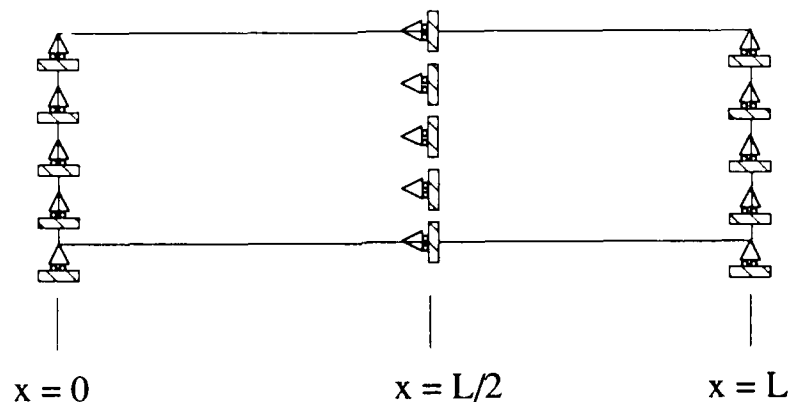
The purpose of this section is to evaluate the performance of the elements developed in this study against data available in the literature, including data from exact elasticity solutions (Section 4.3.1), higher-order analytical solutions (Section 4.3.2), and experimental efforts (Section 4.3.3). All finite element calculations for this portion of the evaluation effort were made using ten-element beam models. This number of elements was chosen in an attempt to attain third-order accuracy (relative to the appropriate beam theory) for modes as high as the fifth mode. This appears to be a reasonable expectation in light of the results obtained in the convergence study discussed in Section 4.1.1.

#### 4.3.1. Exact Elasticity Solutions

The first set of accuracy calculations compares results obtained using the present elements against data for composite plates in cylindrical bending obtained by Kulkarni and Pagano [17] and Jones [16] using a plane-strain elasticity solution. In both these references, a solution is obtained by assuming sinusoidal fields for longitudinal and lateral displacements similar to those specified for beam theories in Equations (2.54). The sinusoidal fields are chosen to satisfy the boundary conditions associated with simple supports. The resulting solution yields an infinite number of natural frequencies for each assumed mode shape. For symmetric composites, the first and second natural frequencies correspond to flexural and extensional responses, respectively. For composites of nonsymmetric configuration, these responses are coupled for each assumed mode shape, and distinct flexural and extensional responses do not exist, strictly speaking. However, both references still associate the first natural frequency for a given mode of a nonsymmetric composite with the term "flexural" response and the second such natural frequency with the term "extensional" response.

The material properties, geometric properties, and boundary conditions for the cases considered in this evaluation are detailed in Table 4.12. As can be seen in this table, all cases involve simply supported composite beams made of fiber-reinforced laminates. The two cases from [17] involve mildly orthotropic layers arranged in symmetric and nonsymmetric configurations. Both cases taken from Jones [16] deal with nonsymmetric composites, but consider a strongly orthotropic material in addition to a mildly orthotropic material. The latter material is similar, though not identical, to the material used in the cases taken from [17].

It should be noted that the solutions discussed in [17] and [16] are for two-dimensional problems in plane strain whereas the finite elements developed in this effort assume conditions of plane stress. Plane-stress techniques can be used to analyze plane-strain problems simply by modifying the material properties used in the plane-stress method, as outlined in Equations (2.2). However, these modifications were deemed unnecessary in this set of calculations since material properties affected by this modification increase by at most 2% for the cases considered in this section.



**Fig. 4.10 Elasticity boundary conditions.**

However, all finite element programs were modified to account for the boundary conditions actually associated with the sinusoidal displacement fields assumed in the exact elasticity solution



for the first mode shape. As shown in Figure 4.10, these boundary conditions involve two sets of distributed rollers. One set acts at  $x = 0$  and  $x = L$  to restrict the vertical motion of all points located at the ends of the beam while allowing these points total freedom in the longitudinal direction. The other set acts at  $x = L/2$  and restricts the longitudinal motion of all points along the centerline of the beam, but allows these points to move freely in the vertical direction. Therefore, the modified finite element programs restrict all vertical motion at  $x = 0$  and  $x = L$  and all longitudinal motion at  $x = L/2$ , but do not constrain the remaining degrees of freedom. Although the former restriction can be approximated accurately with the pinned-simply supported boundary condition already available in the programs, the latter restriction cannot be enforced without modifying the programs.

The results from references [17] and [16] are given in the form of dispersion curves which plot nondimensional natural frequency as a function of  $md/L$ , where  $m$  is the mode number,  $d$  is the depth of the beam or one-way plate, and  $L$  is its length. The nondimensional natural frequency used by Kulkarni and Pagano [17] is given in Equation (4.1).

$$\begin{aligned} \text{Frequency} &= \omega/\omega_0 \\ \omega_0 &= \frac{m\pi}{L} \sqrt{\frac{E_x}{\rho}} \end{aligned} \quad (4.1)$$

where

$E_x$  = Young's modulus in the longitudinal direction (i.e., in the direction the fibers are aligned)

$\rho$  = mass density

Equation (4.2) gives a similar expression used by Jones in [16].

$$\begin{aligned}
 \text{Frequency} &= \frac{\omega}{\omega_0} \\
 \omega_0 &= \frac{m\pi}{L} \sqrt{\frac{R_{11}}{\rho}} \\
 R_{11} &= \frac{E_z}{1 - \nu_{xy}\nu_{yx}}
 \end{aligned} \tag{4.2}$$

where

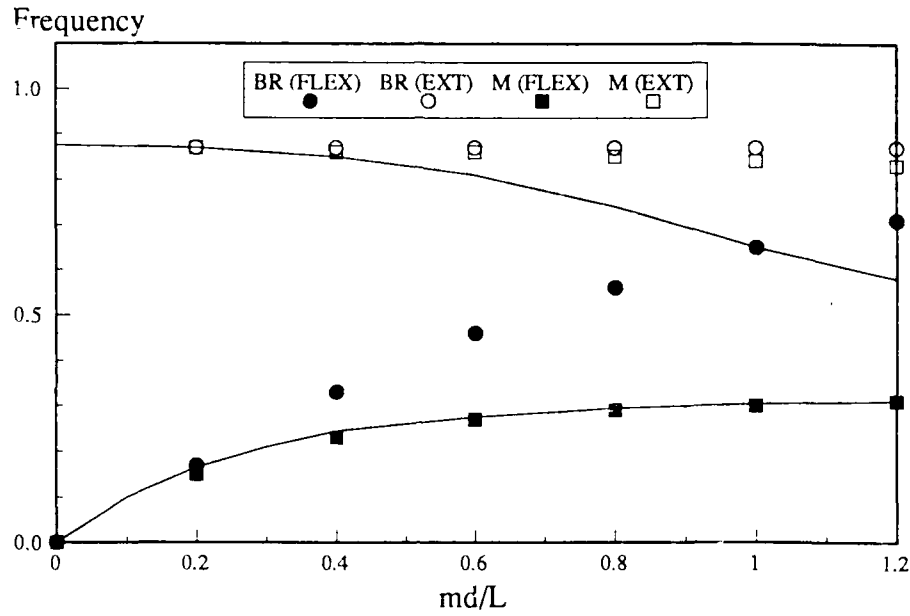
$\nu_{xy}$  = Poisson's ratio for lateral strain caused by strain in the longitudinal direction

$\nu_{yx}$  = Poisson's ratio for longitudinal strain caused by strain in the lateral direction

Once again, the longitudinal direction is the direction in which the fibers run.

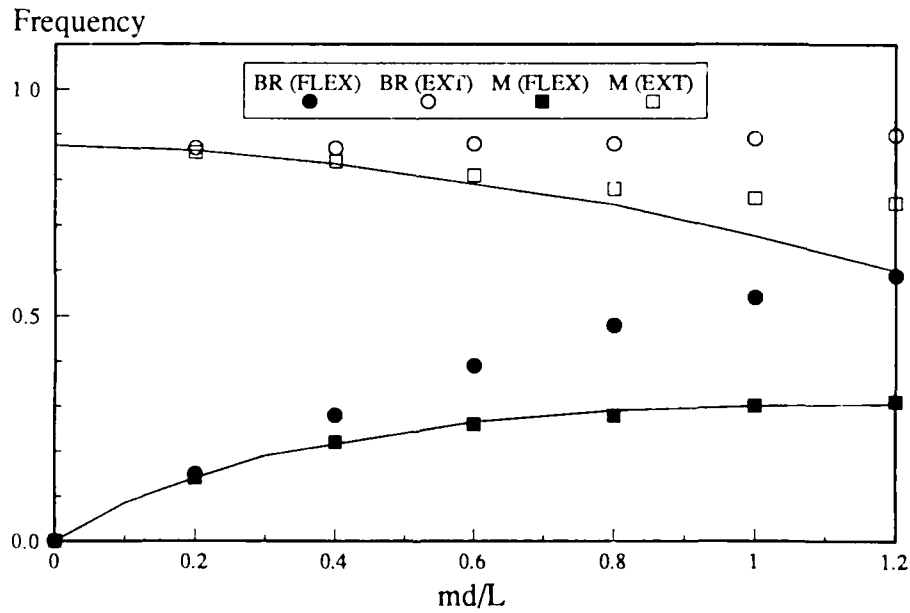
It should be noted that the dispersion curves obtained by Kulkarni and Pagano and by Jones account for Poisson's effects as well as transverse normal strain, two phenomena ignored in the exact elasticity solutions generated for the convergence studies discussed in Section 4.1.1. Therefore, comparisons of finite element results against data from [17] and [16] should indicate if and when the importance of these effects render the present finite elements unusable.

Dispersion curves for the cases considered in this evaluation are given in Figures 4.11 and 4.12. Data obtained from the finite element calculations associated with this evaluation are tabulated in Tables 4.13 and 4.14 and plotted in Figures 4.11 and 4.12 as well.



(a) Case A1-L3-KP.

Fig. 4.11 Comparison with Kulkarni and Pagano [17].



(b) Case A1-L2-KP.

Fig. 4.11 Concluded.

Figure 4.11a compares the results for the symmetric case of Kulkarni and Pagano [17] to the data obtained using the Bernoulli-Euler and simple third-order elements. Only data from these two

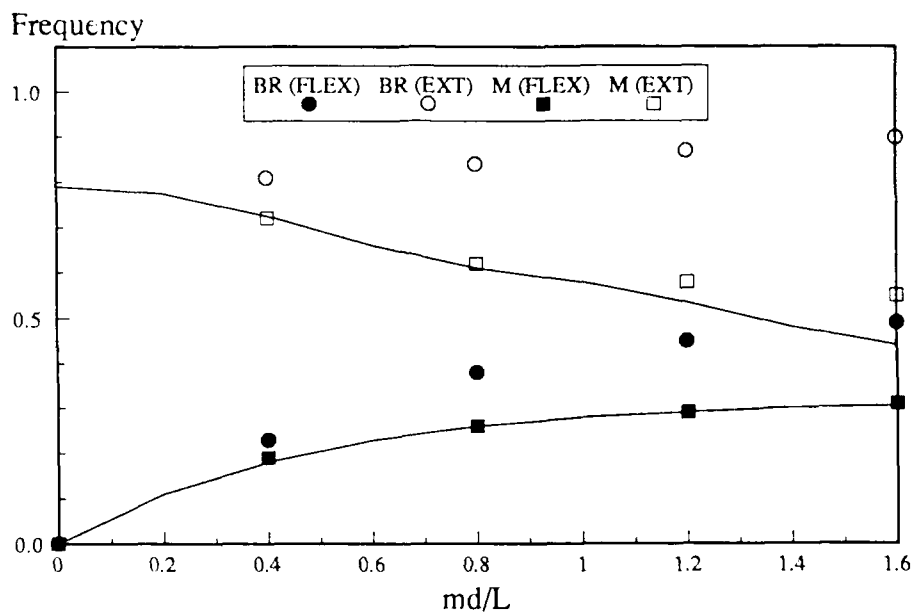
elements are plotted in Figure 4.11 since all other elements provide data almost identical to those of the simple third-order element. As can be seen, the higher-order element does an excellent job matching the dispersion curve associated with flexural response. The results for the Bernoulli-Euler element show the necessity of accounting for shear deformation in these calculations as the magnitude of  $md/L$  increases (i.e., as the mode number increases or as the span-to-depth ratio decreases). The effects of shear deformation significantly reduce the accuracy of the Bernoulli-Euler element above a value of  $md/L$  equal to 0.2. This value can be thought of as corresponding to the first mode of vibration for a beam with an  $L/d$  ratio of 5, or to the second mode for a beam having a span-to-depth ratio of 10.

The good agreement seen in the bending data from the third-order element reveals that ignoring Poisson's effects and transverse normal strain does not adversely affect the accuracy of the higher-order elements in this case.

Results for the extensional response indicate that the simple third-order element, though slightly more flexible than the Bernoulli-Euler element in axial response in this case, estimates extensional natural frequencies much higher than those of the exact solution of Kulkarni and Pagano at values of  $md/L$  above 0.4. Apparently, the kinematic constraint of the third-order element is not capable of modeling the effect shear deformation has on the axial motion as the composite considered by Kulkarni and Pagano in this case gets thicker relative to its length.

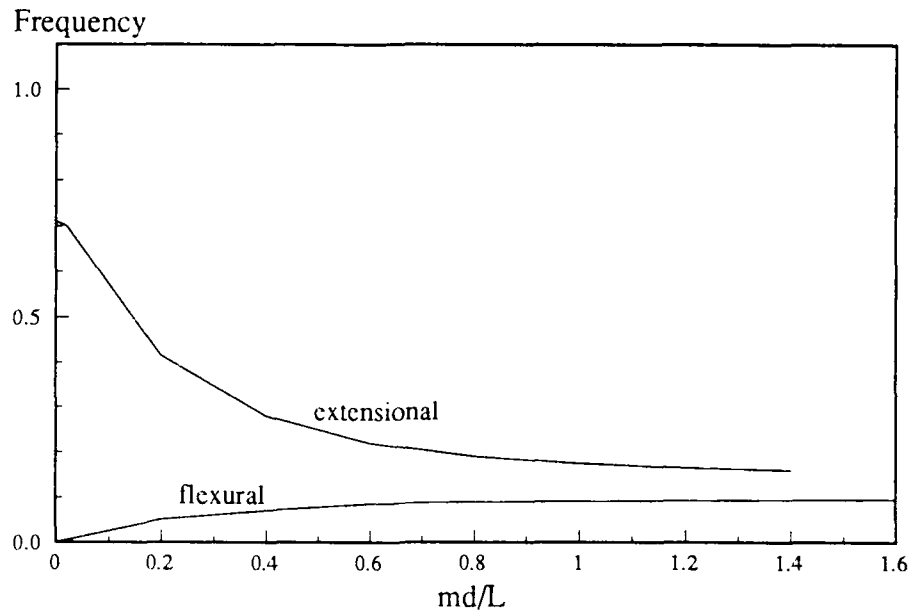
Similar trends are seen in the data from the nonsymmetric case provided in Figure 4.11b. The higher-order element does a good job modeling the "flexural" response of the composite, but does not faithfully reproduce the "extensional" response seen in the solution from [17]. In general, the finite element solutions for this case appear to be more flexible as the result of coupling induced by the lack of symmetry in the composite. This flexibility allows the finite element results to follow

the curve for extensional response more closely, but significant differences still develop after  $md/L$  acquires a value of 0.6. Once again, the limitations of the Bernoulli-Euler element become apparent for both kinds of response as  $md/L$  increases.



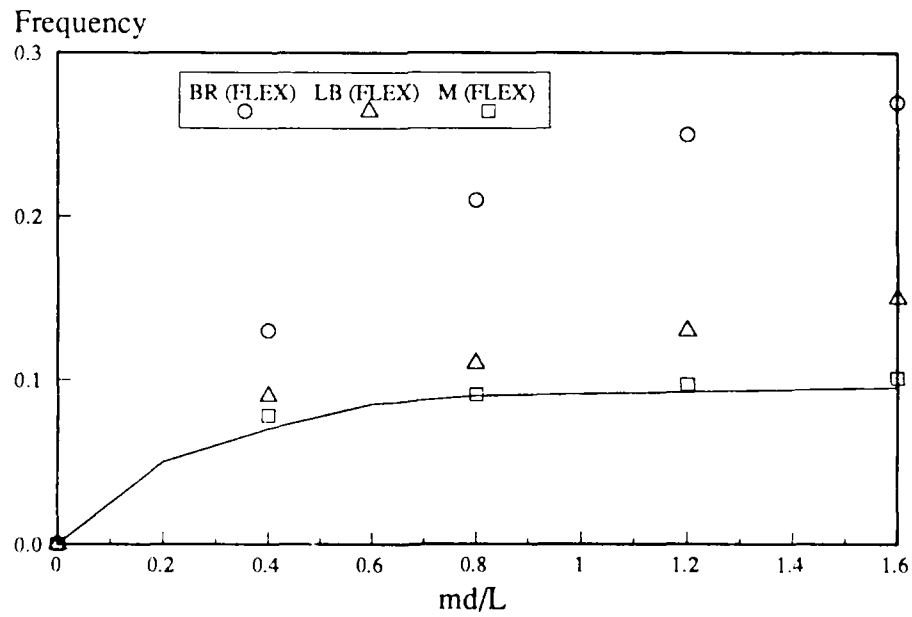
(a) Case A1-L2-J1.

Fig. 4.12 Comparison with Jones [16].



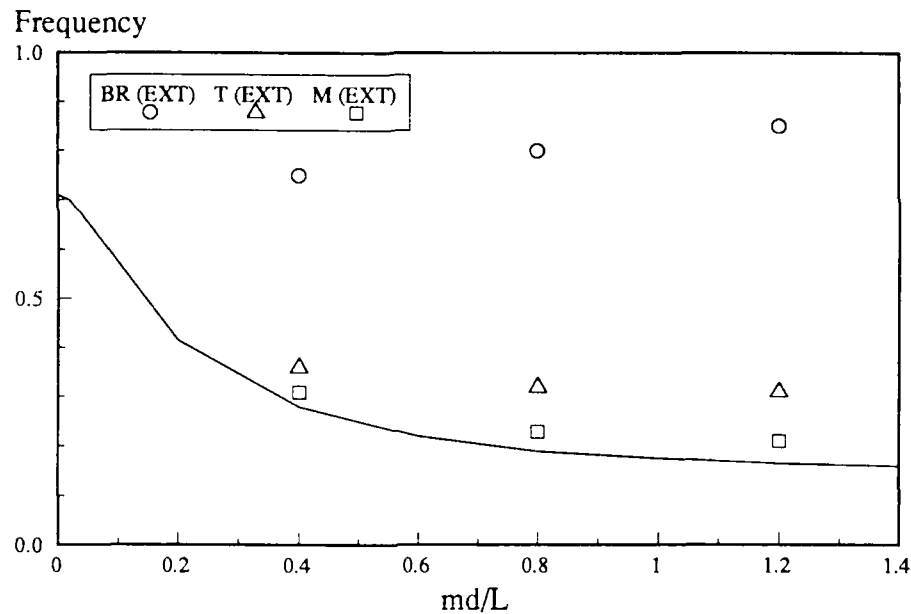
(b) Case A1-L2-J2, elasticity solution.

Fig. 4.12 Continued.



(c) Case A1-L2-J2, flexural response.

Fig. 4.12 Continued.



(d) Case A1-L2-J2, extensional solution.

**Fig. 4.12 Concluded.**

Comparisons with the solutions of Jones [16] given in Figure 4.12 reveal much the same thing. These comparisons extend the maximum value of  $md/L$  30% beyond the maximum value seen in the work of Kulkarni and Pagano.

As in Figure 4.11, only the results obtained using the Bernoulli-Euler and simple third-order element are provided in Figure 4.12a for the mildly orthotropic case. The third-order element yields results which are in excellent agreement with the exact solution for the “flexural” response. Once again, ignoring Poisson’s effect and transverse normal strain does not seem to have much impact on the performance of the third-order element, even for modes or  $L/d$  ratios in which the depth of the beam exceeds the wavelength of flexural vibration.

Agreement for the “extensional” mode appears to be better than that observed in Figure 4.11, but it is still poor for large values of  $md/L$ . As expected, the range of the Bernoulli-Euler element is limited to fairly low values of  $md/L$  (0.2 or less).

Data presented in Figures 4.12b-d provide the severest test of the finite elements discussed so far since the material involved in this case possesses a high degree of orthotropy as characterized by the high ratio of Young's modulus in the longitudinal direction to the transverse shear modulus. Data from the Levinson-Bickford and simple third-order elements are included in the comparison for the flexural response since these data bound the results obtained from finite element calculations made with higher-order elements.

The maximum error for the simple third-order element is about 10% and occurs at a value of  $md/L$  which is quite large. This error is attributed mainly to ignoring the effect of transverse normal strain since accounting for this strain should make the elements more flexible, and hence lower the natural frequencies obtained from them. Even in this extreme condition, the simple third-order element is capable of first-order accuracy. The data in Table 4.14 reveal that the corrected Timoshenko and simple third-order element have accuracy comparable to that of the stacked elements, a trend seen in the composite-beam case considered in the convergence study of Section 4.1.1.

The Levinson-Bickford beam is not as robust as these other higher-order elements. It seems to get stiffer and stiffer as the value of  $md/l$  increases. The maximum error associated with this element relative to the exact solution for the bending response is about 60%. Although this element is out performed by the other higher-order elements, it is obviously better than the Bernoulli-Euler element for this case.

Higher-order results for the extensional response are bounded by the corrected Timoshenko element ( $k = 5/6$ ) and the stacked third-order element. The latter element yields data which follow the dispersion curve for this response fairly faithfully, although a maximum error of about 15% is observed at large values of  $md/L$ . The Timoshenko element is much stiffer, perhaps because it is unable to account for the effects of shear deformation on the axial response of the beam. However, it is obviously superior to the Bernoulli-Euler element in this case.



In summary, comparing results generated by the elements developed in this effort with the exact elasticity solutions found in [17] and [16] reveals that the shear-deformable elements can estimate bending frequencies quite well in most cases considered. The generally good performance of these elements indicates that they do not seem to be unduly hampered by ignoring Poisson's effect and transverse normal strain. However, they are not as good at predicting the axial response in the cases considered.

#### 4.3.2. Higher-Order Theories

This section evaluates the performance of the finite elements developed in this effort against data obtained from higher-order beam theories. Theories considered include Levinson's beam theory [56,57], the sandwich beam theory of Yan and Dowell [86], and the finite element formulation of Kao and Ross's [89] theory for multilayer sandwich plates implemented by Khatua and Cheung [126]. The material properties, geometric properties, and boundary conditions for all cases considered in this portion of the evaluation study are summarized in Table 4.15.

In [57], Levinson compares the performance of his theory against exact solutions from Bernouli-Euler theory (no rotary inertia) and Timoshenko theory. Several correction factors are selected for the Timoshenko solutions. As seen in Table 4.15, this comparison involves a homogeneous aluminum beam with clamped-free or clamped-clamped boundary conditions.

Table 4.16 compares some of these data for the first and fourth modes of these beams with results obtained using the simple Timoshenko beam ( $k = 5/6$ ) and third-order elements as well as the Levinson-Bickford element developed in this study. Several trends are evident in the data presented in this table. First, the Timoshenko element estimates natural frequencies which are in close agreement with the exact Timoshenko calculations of Levinson. Although the agreement is better for the cantilever beam than for the clamped-clamped beam and for the first mode than the fourth, the largest error seen is still less than 0.1%.

Second, all finite element calculations yield natural frequencies which are higher than those associated with the exact Levinson solution. It should be noted that the discrepancies between the Levinson-Bickford element and the exact Levinson solution are due to the energy formulation used in the former method and the direct approach taken to develop the theory associated with the latter (see [58,59]). The differences between Levinson's results and the finite element estimates become more pronounced as the mode number increases or as the freedom of the ends of the beam becomes more restricted.

Levinson was motivated to develop his beam theory, in part, by a desire to avoid having to calculate the shear correction factor associated with Timoshenko's beam theory. But it appears that he was also motivated, as was Krishna Murty [51], by a desire to match the experimental data of Traill-Nash and Collar [42] and Kordes and Kruszewski [43] more closely. In comparison with these experimental data, Timoshenko beam theory with  $k = 5/6$  appears to be too stiff in that it estimates natural frequencies slightly greater than those obtained in the experiments.

Therefore, both Levinson and Krishna Murty sought theories which yield natural frequencies below those estimated by Timoshenko beam theory with  $k = 5/6$ . In addition, Krishna Murty [51] criticized the work of Cowper [45], since in general it leads to a higher correction factor and consequently a higher estimate of natural frequency. This trend runs counter to what appears to be required in the experimental results found in [42] and [43].

However, the comparisons presented in Section 4.1.1 indicate that, in general, Timoshenko beam theory with  $k = 5/6$  yields natural frequencies which are actually below those calculated using an exact elasticity solution. Therefore, higher values of the correction factor are indeed required to bring the results from Timoshenko theory more in line with those obtained using the more exact theory of elasticity.

The fact that Timoshenko beams with a correction factor of  $5/6$  appear to be too stiff in comparison to beams used in experiments, but too soft relative to the exact elasticity solution may indicate that some mechanism not accounted for by either Timoshenko beam theory or elasticity theory is responsible for the lower frequencies observed in testing. For example, compliance of the beam's supports or damping are two mechanisms which can reduce the natural frequency of a beam. If so, the theories of Levinson and Krishna Murty may appear to give better results, but for the wrong reason.

Table 4.15 reveals that the beam associated with the Yan and Dowell [86] calculations contains a layer of concrete sandwiched between two layers of steel. Calculations for this case were actually reported originally by Miller in [130]. The results from this reference as well as the finite element calculations required for the present evaluation are summarized in Table 4.17. As can be seen in these data, values obtained with the present Bernoulli-Euler element are identical to those of Yan and Dowell when shear deformation is ignored. In addition, these results are either identical or very close to the natural frequencies obtained by Miller [130] using a different finite element model.

Further comparison reveals that the Timoshenko element is more flexible than the Bernoulli-Euler element, but not as flexible as the beam associated with the solution of Yan and Dowell which accounts for shear. All other elements generate natural frequencies lower than those of Yan and Dowell. Comparison with the exact elasticity solution, which ignores Poisson's effect and transverse normal strain, shows these lower values to be more accurate. Therefore, the higher-order elements appear to be superior to the solution technique of Yan and Dowell in this case with the best performance coming from the stacked elements. The Levinson-Bickford and simple third-order elements are capable of second-order accuracy for the first mode, but only first-order accuracy for the fourth mode. This is still better than the 13% error present in the Yan and Dowell solution for the fourth mode.

The work of Khatua and Cheung [126] includes an evaluation of their sandwich-beam finite element against data from an analytical solution obtained by extending the static technique of Kao and Ross [89] to vibration problems. The evaluation of [126] examines the natural frequencies of the five-layer sandwich beam described in Table 4.15. Results from this previous evaluation effort along with finite element and elasticity solutions from the present effort are presented in Table 4.18. As usual, the elasticity solution ignores Poisson's effect as well as transverse normal strain.

The results summarized in Table 4.18 reveal that the solution of Kao and Ross and the finite element results of Khatua and Cheung agree very favorably with the exact elasticity solution. In addition, the stacked elements of the present effort enjoy third-order accuracy relative to the elasticity solution and yield natural frequencies very close to the analytical and finite element results presented in [126]. However, the simple elements are incapable of even first-order accuracy for the first mode and generate answers off by about 200% for the fifth mode. This trend is similar to the one seen in the sandwich-beam case used in the convergence study discussed in Section 4.1.1.

#### 4.3.3. Experimental Data

Experimental results used in this evaluation are taken from the works of Shoua [160] and Leibowitz and Lifshitz [161]. Both of these experimental efforts were undertaken to examine the damped vibration of cantilever sandwich beams. Table 4.19 summarizes properties for the beams investigated in these efforts which are of interest in the present evaluation. These beams include the sandwich beam composed of fiberglass facings with a fiberglass core tested by Shoua [160] and the three-layer aluminum-neoprene beams used in the experiments of Leibowitz and Lifshitz [161]. The sandwich beam of interest to Shoua contains facings which are relatively thin compared with the thickness of the core, whereas the beams tested in [161] have facings and cores of comparable thickness. In addition, both symmetric and nonsymmetric configurations are considered in [161].

Natural frequencies obtained from these experimental efforts are compared with finite element estimates of these frequencies in Tables 4.20 and 4.21. Also included in Table 4.21 are estimates obtained by Leibowitz and Lifshitz using the analytical method of Mead and Markus discussed in [83]. As can be seen in Table 4.20, all elements developed in the present study are able to estimate the first natural frequency of Shoua's sandwich beam to within 3% of the experimental value. However, for the fourth mode, the Bernoulli-Euler and Timoshenko elements are limited to first-order accuracy or less with all higher-order elements generating errors about an order of magnitude less than those produced by the lower-order elements. The stacked elements do not seem to offer any real advantage in accuracy over the simple elements in this case for either the first or the fourth modes.

However, stacked elements enjoy a decided advantage in the cases investigated by Leibowitz and Lifshitz [161]. In fact, reasonable estimates of the natural frequencies of the aluminum-neoprene sandwich beams considered in [161] cannot be obtained with any of the simple elements. For both the symmetric and nonsymmetric cases, all the simple elements produce comparable errors which range from about 120% for the first mode of the nonsymmetric beam to approximately 200% for the second mode of the symmetric beam.

In sharp contrast to these results, the stacked elements generate amazingly small errors ranging from a minimum of 0.3% for the first mode of the nonsymmetric beam to a maximum of 6% for the first mode of the symmetric beam. In the case of the nonsymmetric beam, the finite element results are quite a bit better than the estimates obtained using the method of Mead and Markus [83]. The same is true for the second natural frequency of the symmetric beam. However, the stacked elements do not outperform the analytical technique for the first mode of this beam. However, in all cases, the stacked elements provide at least first-order accuracy, a capability not demonstrated by the analytical technique of Mead and Markus in every case considered in Table 4.19.

In summary, the finite elements developed in the present study produce estimates of natural frequency which compare very favorably with data available in the literature. Of course, the elements based on the lower-order Bernoulli-Euler and Timoshenko theories have a more limited range of applicability than do the higher-order elements. Even so, the Timoshenko element enjoys a fairly wide range of application provided the proper shear correction factor is chosen.

Since the accuracy of the Levinson-Bickford and simple third-order elements is not governed by the choice of such a factor, these elements appear to be more robust than the Timoshenko element and may be more attractive alternatives as a result. In addition, these elements are very competitive with the stacked elements in most cases considered in the convergence and evaluation studies. The only cases in which these elements are not adequate involve very short beams made of materials possessing a high degree of orthotropy and some sandwich beams composed of significantly dissimilar materials. In the former case, the Levinson-Bickford element becomes too stiff as the beam becomes quite short relative to its depth (see Figure 4.12b). In the latter case, stacked elements may be the only elements able to calculate natural frequencies accurately. The conditions in which stacked elements are required are examined in detail in Section 4.4.

#### **4.4. Conditions Requiring Stacked Elements**

The purpose of this portion of the evaluation effort is to identify conditions under which stacked elements must be used to estimate natural frequencies with adequate accuracy. A review of the data available in Sections 4.1 through 4.3 reveals that, in general, these elements are not required in the case of fiber-reinforced composite beams of laminated construction, but are essential in some cases involving sandwich beams. Therefore, this study starts with a sandwich beam whose natural frequencies can be estimated accurately only with stacked elements. Then properties of this beam are changed in an attempt to find under what conditions stacked elements are no longer essential.

The baseline chosen for this study is the sandwich beam used in the convergence calculations discussed in Section 4.1. The salient features of this baseline case are summarized in Table 4.22. Variations to the baseline considered in this study are also detailed in Table 4.22. Both the simple and stacked third-order elements were used to obtain estimates of first natural frequency for all cases listed in Tables 4.22.

All finite element calculations were performed using four-element models of the sandwich beams. The exact elasticity solution ignoring coupling due to Poisson effects and transverse normal strain provides the standard against which the performance of the finite elements is measured. By comparing the results from the simple and stacked elements against this standard, it is possible to identify the conditions under which stacked elements are required to obtain a reasonable estimate of the natural frequency of sandwich beams. Table 4.23 tabulates the data necessary to make these comparisons.

As can be seen, merely reducing the ratio of Young's modulus in the facing to Young's modulus in the core ( $E_f/E_c$ ) does not result in a condition amenable to simple-element analysis. In fact, the reduction in this ratio results in a deterioration of the results obtained using the simple element, perhaps caused by the increasing degree of orthotropy produced in the core by increasing its Young's modulus while holding its shear modulus constant. In addition, changing only the density ratio appears to have no effect on the ability of simple elements to model the response of sandwich beams.

However, increasing the shear modulus of the core improves the performance of the simple element dramatically. In cases EG-1 and EG-2, the ratios of  $E_c/G_c$  are changed to 10 and 2, respectively, while the ratio of  $E_f/E_c$  is held at 28.6. A steady improvement in the performance of the simple element can be seen in data from these cases. In case EG-2, the stacked element produces error about two orders of magnitude less than the simple element, but the first-order accuracy of the latter element should be adequate for most engineering purposes.

Even better performance is obtained from the simple element for the same ratios of  $E_c/G_c$  with the ratio of  $E_f/E_c$  reduced to 10 (EG-3 and EG-4) and finally to 1 (EG-5 and EG-6). In case EG-6, the simple element provides accuracy equal to that of the stacked element. However, it is not clear if the improved performance of the simple element is due to a decrease in the degree of orthotropy of the core or if it is caused by a reduction in the mismatch between the shear moduli in the facings and in the core. Data from cases EG-7 through EG-10 help to resolve this problem.

In cases EG-7 and EG-8,  $E_c/G_c$  ratios of 10 and 2, respectively, are obtained by decreasing  $E_c$ , rather than by increasing  $G_c$ . This approach allows the ratio of  $G_f/G_c$  to remain at 247 while decreasing the degree of orthotropy in the core material. For cases EG-9 and EG-10, the  $E_c/G_c$  ratio is held constant at 23.3 while  $G_f/G_c$  is reduced first to 20 and then to 2. These combinations are obtained by increasing both  $E_c$  and  $G_c$  so that their ratio remains the same as the one seen in the baseline.

The results in Table 4.23 reveal that reducing the ratio of  $E_c/G_c$  while holding  $G_f/G_c$  constant produces a marginal improvement in the ability of the simple element to estimate natural frequency, whereas decreasing the ratio of  $G_f/G_c$  while holding  $E_c/G_c$  constant yields the dramatic improvement in the performance of the simple element evident in cases EG-1 through EG-6.

Although it can be argued that the ratio of  $E_f/E_c$  is also decreased in cases EG-9 and EG-10, cases E-1 and E-2 reveal that simply lowering this ratio does not improve the ability of simple elements to estimate natural frequency. Therefore, the improvement in simple-element performance seen in cases EG-9 and EG-10 is attributed to the reduction in the mismatch between the shear moduli in the facings and the core.

This finding indicates that one of the conditions which must be present to render simple elements inadequate for calculating the natural frequency of composite beams is a large difference



in the shear modulus of various layers in the beam. This explains why simple elements are adequate for most situations involving fiber-reinforced composite beams since the mismatch in the shear moduli of adjacent laminae is usually quite small, but cannot be used to analyze some sandwich beams where the mismatch in shear moduli is severe.

Another condition which leads to the requirement for stacked elements can be identified by comparing the data from cases T-1 and T-2 to the baseline case. As can be seen, the need for stacked elements diminishes as the thickness of the facing relative to the total thickness of the beam decreases. This indicates that stacked elements are required only if the facings in a sandwich beam have adequate thickness relative to the core to prevent the strain energy of the core from dominating the response of the beam. This requirement may explain the ability of the simple elements to model the response of the cantilever beam tested by Shoua [160], although it is possible that the beam's  $G_f/G_c$  ratio of about 65 may be too small to be in the range in which stacked elements are required to analyze natural frequencies.

In summary, it can be said that stacked elements are required to calculate the natural frequencies of composite beams when large disparities in shear moduli for the various layers of the beam exist, and when each layer is thick enough to make significant contributions to the overall response of the beam. Simple elements should be capable of generating reasonable results in most other situations. However, as pointed out at the end of Section 4.1.1, this discussion considers the ability of finite elements to calculate natural frequency only. In vibration problems where stresses are of interest, the higher-order kinematic constraints associated with stacked elements may be necessary to estimate these stresses accurately even in situations where simple elements prove adequate for the analysis of natural frequency.

## 5. SUMMARY AND CONCLUSIONS

As stated in Chapter 1, the goal of this investigation is to develop shear-deformable finite elements which can be used to analyze the dynamic response of composite beams. This goal has been achieved by pursuing the objectives established in Section 1.3 to guide this effort. The first objective of this effort is to derive the mass and stiffness matrices for the shear-deformable elements and incorporate them into computer programs which can be used to ascertain the natural frequencies of composite beams in free vibration. The second objective is to evaluate the performance of these elements to determine when elements based on higher-order kinematic constraints must be used to account for the effects of shear deformation on the dynamic response of composite beams. Both objectives have been met.

The shear-deformable elements developed in this study include simple elements associated with the beam theories of Timoshenko [12,29], Levinson [56,57] and Bickford [58], and the general third-order theory of Yuan and Miller [63], as well as stacked versions of the Timoshenko and third-order elements. In addition, a Bernoulli-Euler beam which accounts for rotary inertia is included in the study to show what happens when shear deformation is not accounted for.

Chapter 2 discusses the theories associated with these elements in detail; Chapter 3 focuses on the finite element formulation of these theories. The evaluations made to fulfill the second objective of this effort are discussed in Chapter 4. This chapter summarizes the results and conclusions of this effort.

### 5.1. Summary

Section 5.1.1 reviews the features of the present elements to show how they are different from other elements discussed in the literature and to highlight the improvement in analytical capability made possible by these new elements. Section 5.1.2 summarizes the findings presented in Chapter

4 to show the relative merits of each of the present elements.

#### 5.1.1. Uniqueness of Present Elements

The elements developed in this effort possess a unique combination of features. For one thing, all elements are capable of modeling composite-beam constitutive relations. In addition, kinematic constraints for each element include terms for both axial and bending modes of response. The governing equations associated with these material properties and kinematic constraints account for dynamic response, including the coupling of the axial and bending responses possible in nonsymmetric composites. Finally, the finite element formulation of each composite-beam theory employs a consistent set of shape functions. This allows the elements to avoid locking in a straightforward manner while retaining the property of bounded, monotonic convergence guaranteed for complete, conforming elements.

Although finite elements similar to the ones developed in this study are discussed in the literature, none has been found which possesses features identical to the combination just described. The Timoshenko beam element of Nickel and Secor [106] bears a strong resemblance to the simple Timoshenko element of the present study in that it also uses a consistent set of shape functions; however, it is formulated for homogeneous beams only. The element of Heyliger and Reddy [115] is based on the same kinematic constraint as the present Levinson-Bickford element, but it is also limited to homogeneous beams. In addition, it employs an inconsistent set of shape functions. Even so, the authors claim the element should not lock.

The element of Kant and Gupta [64] is based on a kinematic constraint similar to the one used in the simple third-order element of this study. However, their element accounts for transverse normal strain, but ignores the even-ordered terms contained in the kinematic constraint of the present third-order element. Also, the formulation of the element discussed in [64] does not include

composite-beam constitutive relations. Finally, the linear shape functions used to interpolate each displacement variable in the element give the element a very slow rate of convergence relative to elements in the present study, especially in the thin-beam limit.

In [65], Kant and Manjunath discuss a composite-beam element based on a kinematic constraint identical to the one for the third-order element of the present study. However, the element is limited to static problems. In addition, reduced integration is used to obtain the shear-related terms in the stiffness matrix for this element, as opposed to the exact integration used for all beams developed in this study.

Of course, the simple third-order element derived in this effort is closely related to the one developed by Yuan and Miller in [63], but the element discussed in [63] is different from the present element in two important respects. First, the stiffness matrix of the present element accounts for composite-beam behavior, including the coupling of axial and bending response modes characteristic of nonsymmetric beams. Second, the present element is capable of modeling the dynamic behavior of composite beams.

The stacked elements represent a natural extension of the work of Yuan and Miller [127,128] from static composite-beam elements to dynamic elements for composite beams. In addition, the performance of these elements is similar to that of the sandwich-beam element developed by Khatua and Cheung [126]. However, as with most theories for sandwich beams, this element ignores shear deformation in the facings as well as axial and bending deformations in the cores. Therefore, the stacked elements developed in this study should have a wider range of application since they are not limited by such assumptions. Finally, the stacked third-order element is based on what appears to be the highest-order kinematic constraint discussed in the literature to date.

The comparison of finite element results against the exact elasticity solutions of Kulkarni and Pagano [17] and Jones [16] reveals that all the shear-deformable elements are capable of estimating

the natural frequencies of very short, orthotropic composites accurately as long as the degree of orthotropy is not too large. This indicates that ignoring transverse normal strain and the coupling of longitudinal and lateral motions associated with Poisson effects does not adversely affect the performance of these elements in cases where this restriction is satisfied. However, as the ratio of  $E/G$  gets large, the performance of these elements deteriorates, implying that some attention must be paid to Poisson effects or transverse normal strain as the degree of orthotropy increases.

In general, all finite elements examined in this investigation provide results which are as good as or superior to those which can be obtained from other higher-order theories. The simple Timoshenko element appears to be as accurate as the elements developed by Archer [101], Kapur [103], Nickel and Secor [106], Thomas, et al. [111], and Carnegie, et al. [159]; however, it has a slower rate of convergence than the elements of Archer and Thomas, et al. Even so, the performance of the present Timoshenko element appears to improve relative to these other two elements as the span-to-depth ratio of the beam decreases and as the fixity of the ends of the beam increases.

Comparisons made with results obtained from Levinson's beam theory [56,57] reveal that the Levinson-Bickford element of the present study estimates natural frequencies higher than those obtained by Levinson himself. The differences are attributed to the fact that Levinson developed his theory using a strength of materials approach, whereas the present element is obtained from an energy formulation. The performance of the present Levinson-Bickford element in other cases considered in Chapter 4 in which the exact elasticity solution is available reveals that this element can be quite accurate. Therefore, it is possible that Levinson's theory underpredicts the natural frequencies of beams.

As stated above, the present elements enjoy a faster rate of convergence than does the element of Kant and Gupta [64], even though this element is based on a third-order kinematic constraint. In addition, the accuracy of the present elements appears to be better.

The simple Levinson-Bickford and third-order elements, as well as the stacked elements, also seem to offer an improvement over the analytical technique of Yan and Dowell [86], especially for cases involving short beams or higher modes of vibration. In addition, the stacked elements appear to be slightly more accurate than the theory of Kao and Ross [89] and the finite element of Khatua and Cheung [126].

Finally, the present elements performed well in the comparison with experimental data. Evaluations made using data generated by Leibowitz and Lifshitz [161] also reveal that the stacked elements are quite competitive with the analytical technique of Mead and Markus [83], even though the elements ignore viscoelastic damping and the analytical technique does not.

#### 5.1.2. Relative Merits of Present Elements

As expected, the Bernoulli-Euler element is limited to situations where shear deformation is not important. These conditions usually include the lower modes of long, slender beams made of homogeneous, isotropic material. However, it should be noted that the results from the comparison made with experimental data obtained by Shoua [160] reveal that this element can also be used to analyze the response of a composite beam as long as the beam is quite long relative to its depth and only the lowest response modes are of interest.

The simple Timoshenko beam element turns out to be a very accurate element as long as the proper shear correction factor is chosen. The simplicity of this element makes it a very powerful tool in the hands of an experienced analyst. However, both the Levinson-Bickford element and the simple third-order element are capable of generating highly accurate results without resorting to the use of a correction factor. Therefore, using these elements properly does not require as much engineering judgment as does using a Timoshenko element.

Of the Levinson-Bickford element and the simple third-order element, the former offers the advantage of a faster rate of convergence. In fact, this rate of convergence is even slightly faster than that of the simple Timoshenko element. However, the Levinson-Bickford element is not as robust as the simple third-order element in that it appears to be too stiff in cases involving composite beams made out of highly orthotropic materials. The same is true for the simple third-order element, but this element does not suffer as great a loss in accuracy in these cases as does the Levinson-Bickford element. Also, the Levinson-Bickford element cannot be stacked as the Timoshenko and third-order elements can.

In addition, the  $C^1$  continuity required in the lateral displacement of the Levinson-Bickford element leads to other possible disadvantages. First, as pointed out by Thomas, et al. [111], this continuity requirement prevents the element from being able to model discontinuities in shear strain, should the need arise. In addition, developing a conforming plate element by extending this beam theory to plates may prove difficult. However, the possible limitations associated with the requirement for  $C^1$  continuity posed no problems in the present effort and this element is recommended as an alternative in cases where the shear correction factor required by Timoshenko beam theory is not readily available.

For the cases considered in this investigation, the simple third-order element is always the most accurate simple element not requiring a shear correction factor. However, it achieves this level of performance by employing a greater number of degrees of freedom than do the other simple elements. Therefore, its use must be governed by evaluating the tradeoff between the accuracy of this element and the cost of using it.

Stacked elements are required when there is a large mismatch in the shear moduli of adjacent layers in a composite beam, and when the thickness of adjacent layers is large enough to prevent any one layer from dominating the internal strain energy of the beam. This combination usually comes into play in the case of sandwich beams whose facings are thick enough to contribute strain

energy comparable to that of the core. Obviously, the stacked third-order element is more accurate than the stacked Timoshenko beam. However, the latter is probably accurate enough for most engineering purposes, and attains this accuracy with far fewer degrees of freedom.

It should be pointed out that in cases where stacked elements are not essential, the simple third-order element outperforms the stacked Timoshenko element, indicating that in these cases it is better to impose a higher-order constraint on the entire beam than to impose an independent, lower-order constraint on separate layers within the beam.

It should also be noted that the above remarks apply only to calculations aimed at finding the natural frequencies of composite beams. It is expected that the merits of the simple and stacked third-order elements become even more apparent in cases where stress distributions are of interest (e.g., in the case of forced vibrations).

## 5.2. Conclusions

In conclusion, it can be said that the goal of this effort has been achieved. The elements developed in this effort provide a means of estimating the natural frequencies of composite beams in cases where the effects of shear deformation are expected to be significant. In addition, each element offers some combination of accuracy and efficiency which should make it attractive in certain situations.

The Bernoulli-Euler element is the element of choice in cases where shear deformation is not important. When this is not the case, the simple Timoshenko element can be used effectively if the analyst is able to choose an appropriate value for the shear correction factor. If this factor is not available, the Levinson-Bickford element can be used with confidence as long as the degree of orthotropy is not too high. As the degree of orthotropy increases, the analyst will be forced to use the simple third-order element in order to attain an adequate level of accuracy.



Finally, stacked elements must be used in the analysis of sandwich beams when the shear modulus of the facings is much larger than the shear modulus of the core as long as the facings are thick enough to contribute significantly to the total strain energy of the beam. In these cases, the stacked Timoshenko beam should provide adequate accuracy for most engineering purposes.

## APPENDIX

This appendix contains the tabular data generated for the evaluation efforts documented in Chapter 4.

Table 4.1 Labels used in Finite Element Evaluation.

Class of Calculations	Label	Description of Calculation
Accuracy (and Convergence)	C1-IS	Homogeneous, isotropic beam
	C1-OR	Homogeneous, orthotropic beam
	C1-L3	3-layer laminated composite beam
	C1-S3	3-layer sandwich beam
	C2-IA	Steel beam [111], $L/d = 14.4$
	C2-IB	$L/d = 5.8$
	C3-IA	Same as C1-IS, [64]. $L/d = 10$
	C3-IB	$L/d = 2$
Shear Locking	SL-I-X	Same as C1-IS, $L/d = X$ (i.e., 10,100,1000 or 10,000)
	SL-O-X	Same as C1-OR
	SL-L3-X	Same as C1-L3
	SL-S3-X	Same as C1-S3

Table 4.1 Concluded.

Class of Calculations	Label	Description of Calculation
Accuracy (Comparison with Published Data)	A1-L3-KP	3-layer Symmetric Composite [17]
	A1-L2-KP	2-layer Nonsymmetric composite [17]
	A1-L2-J1	2-layer composite, low degree of orthotropy [16]
	A1-L2-J2	2-layer composite, high degree of orthotropy [16]
	A2-IA	Cantilever steel beam [57]
	B	3-layer clamped-clamped steel beam [57]
	A2-S3	Steel-concrete sandwich beam
	A2-S5	5-layer sandwich beam
	A3-S3-1	3-layer fiberglass sandwich beam [160]
	A3-S3-2A	3-layer symmetric aluminum-neoprene sandwich beam [161]
	-2B	nonsymmetric beam
Stacked Elements	SE-S3-B	Baseline, same as C1-S4
	E1,2	Changes in $E_f/E_{cc}$
	R1,2	Changes in $\rho_f/\rho_c$
	EG1-EG10	Changes in $E_c/G_c$ and $G_f/G_c$
	T1,2	Changes in $t_f/d$

Table 4.2 Abbreviations used in Finite Element Evaluations.

Category	Abbreviation	Meaning
Boundary conditions	F	Free
	S	Simply supported
	P	Pinned
	C	Clamped
Finite elements	BR	Bernoulli-Euler with rotary inertia
	T1	Timoshenko, $k = 1$
	T	Timoshenko, $k = 5/6$ unless otherwise specified
	L	Levinson-Bickford
	M	Third-order
	TS	Stacked Timoshenko
	MS	Stacked third-order
Exact solutions	EB	Bernoulli-Euler
	EBR	Bernoulli-Euler with rotary inertia
	ET1	Timoshenko, $k = 1$
	ET	Timoshenko, $k = 5/6$ unless otherwise specified
	EE	Elasticity
	EL	Levinson (direct method)

Table 4.3 Properties for Accuracy Calculations, Cases C1-XX.

Case	Remarks	$E$ (psi)	$G$ (psi)	$\rho$ (lb-s <sup>2</sup> /in <sup>4</sup> )	$d$ (in)	$L$ (in)	Boundary Conditions
C1-IS	Aluminum	$10 \times 10^6$	$3.7 \times 10^6$	$2.6 \times 10^{-4}$	1	10	PS
C1-OR	Graphite-Epoxy	$20 \times 10^6$	$0.6 \times 10^6$	$1.55 \times 10^{-4}$	1	10	PS
C1-L3	Graphite-Epoxy Laminate					10	PS
	Layer 1	$20 \times 10^6$	$0.6 \times 10^6$	$1.55 \times 10^{-4}$	0.333		
	Layer 2	$1 \times 10^6$	$0.5 \times 10^6$	$1.55 \times 10^{-4}$	0.334		
	Layer 3	$20 \times 10^6$	$0.6 \times 10^6$	$1.55 \times 10^{-4}$	0.333		
C1-S3	Aluminum-Balsa Sandwich					10	PS
	Layer 1	$10 \times 10^6$	$3.7 \times 10^6$	$2.6 \times 10^{-4}$	0.1		
	Layer 2	$350 \times 10^3$	$15 \times 10^3$	$8.67 \times 10^{-6}$	0.8		
	Layer 3	$10 \times 10^6$	$3.7 \times 10^6$	$2.6 \times 10^{-4}$	0.1		

Table 4.4 Accuracy Data for Case C1-IS.

Mode	Element or Solution	No. of Elements	No. of DOF <sup>1</sup>	Natural Frequency (Hz)	$\Delta_e(\%)$	$\Delta(\%)$
1	EE	—	—	874.258	—	—
	EBR	—	—	885.654	1.30	—
	ET1	—	—	876.124	0.21	—
	ET	—	—	874.254	-0.0005	—
	BR	1	4	982.950	12.4	11.0
		2	8	889.145	1.70	0.39
		4	16	885.884	1.33	0.03
		8	32	885.668	1.31	0.002
		12	48	885.657	1.30	0.0003
		16	64	885.655	1.30	0.0001
	T1	1	7	970.138	11.0	10.7
		2	14	879.508	0.60	0.39
		4	28	876.347	0.24	0.03
		8	56	876.139	0.22	0.002
		12	84	876.127	0.21	0.0003
		16	112	876.125	0.21	0.0001
	T	1	7	967.634	10.7	10.7
		2	14	877.617	0.38	0.38
		4	28	874.476	0.02	0.03
		8	56	874.268	0.001	0.002
		12	84	874.258	0.0	0.0005
		16	112	874.256	-0.002	0.0002

<sup>1</sup>DOF = Degrees Of Freedom

Table 4.4 Continued.

Mode	Element or Solution	No. of Elements	No. of DOF	Natural Frequency (Hz)	$\Delta_e(\%)$	$\Delta(\%)$
L		1	7	967.640	10.7	
		2	13	877.622	0.38	
		4	25	874.480	0.03	
		8	49	874.272	0.002	
		12	73	874.261	0.0003	
		16	97	874.260	0.0002	
M		1	13	967.640	10.7	
		2	24	877.621	0.38	
		4	46	874.480	0.03	
		8	90	874.261	0.002	
		12	134	874.261	0.0003	
		16	178	874.259	0.0001	
TS		1	13	968.901	10.8	
		2	24	878.574	0.49	
		4	46	875.422	0.13	
		8	90	875.214	0.13	
		12	134	875.203	0.11	
		16	178	875.201	0.11	
MS		1	31	967.640	10.7	
		2	54	877.621	0.38	
		4	100	874.480	0.03	
		8	192	874.272	0.002	
		12	284	874.261	0.0003	
		16	376	874.259	0.0	

Table 4.4 Continued.

Mode	Element or Solution	No. of Elements	No. of DOF	Natural Frequency (Hz)	$\Delta_e(\%)$	$\Delta(\%)$
5	EE	—	—	16,608	—	
	EBR	—	—	20,248	21.9	
	ET1	—	—	17,082	2.86	
	ET	—	—	16,589	-0.11	
	BR	1	4	—		
		2	8	—		
		4	16	22,820	37.4	12.7
		8	32	20,433	23.0	0.92
		12	48	20,287	22.2	0.19
		16	64	20,260	22.0	0.06
	T1	1	7	71,021	328	316
		2	14	39,513	138	131
		4	28	18,584	11.9	8.79
		8	56	17,193	3.53	0.65
		12	84	17,105	3.00	0.14
		16	112	17,090	2.90	0.05
	T	1	7	65,561	295	295
		2	14	36,077	117	117
		4	28	17,960	8.14	8.27
		8	56	16,690	0.49	0.61
		12	84	16,610	0.01	0.13
		16	112	16,596	-0.07	0.04



Table 4.4 Concluded.

Mode	Element or Solution	No. of Elements	No. of DOF	Natural Frequency (Hz)	$\Delta_e(\%)$	$\Delta(\%)$
L		1	7	65,216	293	
		2	13	59,685	259	
		4	25	17,992	8.34	
		8	49	16,712	0.63	
		12	73	16,630	0.14	
		16	97	16,616	0.05	
M		1	13	65,194	293	
		2	24	39,513	138	
		4	46	17,990	8.33	
		8	90	16,710	0.62	
		12	134	16,629	0.13	
		16	178	16,614	0.04	
TS		1	13	67,781	308	
		2	24	39,513	138	
		4	46	18,290	10	
		8	90	16,954	2.1	
		12	134	16,870	1.6	
		16	178	16,854	1.5	
MS		1	31	65,177	292	
		2	54	39,513	138	
		4	100	17,989	8.3	
		8	192	16,710	0.62	
		12	284	16,629	0.13	
		16	376	16,614	0.0004	

Table 4.5 Accuracy Data for Case C1-OR.

Mode	Element or Solution	No. of Elements	No. of DOF	Natural Frequency (Hz)	$\Delta_s(\%)$	$\Delta(\%)$
1	EE			1410.283	—	
	EBR			1622.183	15.03	
	ET1			1439.356	2.06	
	ET			1409.638	-0.05	
	BR	1	4	1800.393	27.7	11.0
		2	8	1628.583	15.5	0.39
		4	16	1622.604	15.1	0.03
		8	32	1622.209	15.0	0.002
		12	48	1622.188	15.0	0.0003
		16	64	1622.184	15.0	0.0001
	T1	1	7	1562.006	10.8	8.52
		2	14	1443.844	2.38	0.31
		4	28	1439.651	2.08	0.02
		8	56	1439.375	2.06	0.001
		12	84	1439.360	2.06	0.0003
		16	112	1439.358	2.06	0.0001
	T	1	7	1524.693	8.11	8.16
		2	14	1413.856	0.25	0.30
		4	28	1409.915	-0.03	0.02
		8	56	1409.656	-0.04	0.001
		12	84	1409.642	-0.05	0.0003
		16	112	1409.640	-0.05	0.0001

Table 4.5 Continued.

Mode	Element or Solution	No. of Elements	No. of DOF	Natural Frequency (Hz)	$\Delta_e(\%)$	$\Delta(\%)$
L		1	7	1525.712	8.18	
		2	13	1414.560	0.30	
		4	25	1410.587	0.02	
		8	49	1410.327	0.003	
		12	73	1410.313	0.002	
		16	97	1410.310	0.002	
M		1	13	1525.688	8.2	
		2	24	1414.529	0.30	
		4	46	1410.574	0.02	
		8	90	1410.314	0.002	
		12	134	1410.300	0.001	
		16	178	1410.297	0.001	
TS		1	13	1543.933	9.5	
		2	24	1429.260	1.3	
		4	46	1425.185	1.1	
		8	90	1424.917	1.0	
		12	134	1424.903	1.0	
		16	178	1424.900	1.0	
MS		1	31	1525.674	8.2	
		2	54	1414.521	0.30	
		4	100	1410.566	0.02	
		8	192	1410.306	0.002	
		12	284	1410.292	0.0006	
		16	376	1410.289	0.0004	

Table 4.5 Continued.

Mode	Element or Solution	No. of Elements	No. of DOF	Natural Frequency (Hz)	$\Delta_e(\%)$	$\Delta(\%)$
5	EE			13,710		
	EBR			37,086	171	
	ET1			14,506	5.80	
	ET			13,391	-2.33	
	BR	1	4	—		
		2	8	—		
		4	16	41,797	205	12.7
		8	32	37,426	173	0.92
		12	48	37,158	171	0.19
		16	64	37,110	171	0.06
	T1	1	7	56,154	310	287
		2	14	20,667	50.7	42.5
		4	28	14,857	8.37	2.42
		8	56	14,527	5.96	0.14
		12	84	14,510	5.83	0.03
		16	112	14,507	5.81	0.007
	T	1	7	54,343	296	306
		2	14	18,869	37.6	40.9
		4	28	13,688	-0.16	2.22
		8	56	13,408	-2.2	0.13
		12	84	13,394	-2.3	0.02
		16	112	13,392	-2.3	0.007

Table 4.5 Concluded.

Mode	Element or Solution	No. of Elements	No. of DOF	Natural Frequency (Hz)	$\Delta_e(\%)$	$\Delta(\%)$
L		1	7	54,233	296	
		2	13	31,129	127	
		4	25	14,405	5.07	
		8	49	13,972	1.93	
		12	73	13,947	1.73	
		16	97	13,943	1.70	
M		1	13	54,226	296	
		2	24	20,660	50.7	
		4	46	14,142	3.15	
		8	90	13,790	0.58	
		12	134	13,771	0.44	
		16	178	13,768	0.42	
TS		1	13	55,070	302	
		2	24	20,664	51	
		4	46	14,545	6.1	
		8	90	14,199	3.6	
		12	134	14,181	3.4	
		16	178	14,178	3.4	
MS		1	31	54,221	77	
		2	54	20,660	51	
		4	100	14,071	2.6	
		8	192	13,735	0.18	
		12	284	13,717	0.05	
		16	376	13,714	0.03	

Table 4.6 Accuracy Data for Case C1-L3.

Mode	Element or Solution	No. of Elements	No. of DOF	Natural Frequency (Hz)	$\Delta_e(\%)$	$\Delta\%$
1	EE			1376.110	—	
	EBR			1593.214	15.8	
	ET1			1410.432	2.49	
	ET			1380.835	0.35	
	BR	1	4	1768.242	28.5	11.0
		2	8	1599.500	16.2	0.39
		4	16	1593.628	15.8	0.03
		8	32	1593.240	15.8	0.002
		12	48	1593.219	15.8	0.0003
		16	64	1593.216	15.8	0.0001
	T1	1	7	1530.051	11.2	8.48
		2	14	1414.809	2.81	0.31
		4	28	1410.719	2.51	0.02
		8	56	1410.450	2.50	0.001
		12	84	1410.436	2.49	0.0003
		16	112	1410.433	2.49	0.0001
	T	1	7	1492.933	8.49	8.12
		2	14	1384.946	0.64	0.30
		4	28	1381.105	0.36	0.02
		8	56	1380.852	0.34	0.001
		12	84	1380.839	0.34	0.0003
		16	112	1380.836	0.34	0.0001

Table 4.6 Continued.

Mode	Element or Solution	No. of Elements	No. of DOF	Natural Frequency (Hz)	$\Delta_e(\%)$	$\Delta\%$
L		1	7	1487.805	8.12	
		2	13	1380.687	0.33	
		4	25	1376.855	0.05	
		8	49	1376.604	0.04	
		12	73	1376.590	0.03	
		16	97	1376.588	0.03	
M		1	13	1487.776	8.11	
		2	24	1380.638	0.33	
		4	46	1376.823	0.05	
		8	90	1376.572	0.03	
		12	134	1376.589	0.03	
		16	178	1376.557	0.03	
TS		1	13	1505.125	9.38	
		2	24	1394.693	1.35	
		4	46	1390.766	1.07	
		8	90	1390.508	1.05	
		12	134	1390.494	1.05	
		16	178	1390.491	1.05	
MS		1	31	1487.241	8.08	
		2	54	1380.195	0.30	
		4	100	1376.383	0.02	
		8	192	1376.132	0.002	
		12	284	1376.119	0.0006	
		16	376	1376.116	0.0004	

Table 4.6 Continued.

Mode	Element or Solution	No. of Elements	No. of DOF	Natural Frequency (Hz)	$\Delta_e(\%)$	$\Delta\%$
5	EE			13,215		
	EBR			36,424	176	
	ET1			14,116	6.81	
	ET			13,029	-1.42	
	BR	1	4	—		
		2	8	—		
		4	16	41,051	211	12.7
		8	32	36,758	178	0.92
		12	48	36,494	176	0.19
		16	64	36,447	176	0.06
	T1	1	7	54,930	316	289
		2	14	20,084	52.0	42.3
		4	28	14,454	9.37	2.40
		8	56	14,136	6.96	0.14
		12	84	14,120	6.84	0.03
		16	112	14,117	6.83	0.0001
	T	1	7	53,182	302	308
		2	14	18,337	38.8	40.7
		4	28	13,314	0.75	2.19
		8	56	13,044	-1.29	0.12
		12	84	13,031	-1.39	0.02
		16	112	13,029	-1.41	0.0



Table 4.6 Concluded.

Mode	Element or Solution	No. of Elements	No. of DOF	Natural Frequency (Hz)	$\Delta_e(\%)$	$\Delta\%$
L		1	7	52,374	296	
		2	13	29,582	124	
		4	25	13,796	4.39	
		8	49	13,395	1.36	
		12	73	13,372	1.19	
		16	97	13,368	1.16	
M		1	13	52,271	296	
		2	24	20,076	51.9	
		4	46	13,614	3.01	
		8	90	13,275	0.45	
		12	134	13,257	0.31	
		16	178	13,254	0.30	
TS		1	13	52,468	297	
		2	24	20,079	51.9	
		4	46	13,976	5.75	
		8	90	13,641	3.22	
		12	134	13,624	3.09	
		16	178	13,621	3.07	
MS		1	31	51,860	292	
		2	54	20,076	51.9	
		4	100	13,567	2.66	
		8	192	13,239	0.18	
		12	284	13,222	0.05	
		16	370	13,219	0.03	

Table 4.7 Accuracy Data for Case C1-S3.

Mode	Element or Solution	No. of Elements	No. of DOF	Natural Frequency (Hz)	$\Delta_e(\%)$	$\Delta(\%)$
1	EE			689.244	—	
	EBR			1316.547	91.0	
	ET1			1282.738	86.1	
	ET			1276.277	85.2	
	BR	1	4	1461.086	112	11.0
		2	8	1321.739	91.8	0.39
		4	16	1316.889	91.1	0.03
		8	32	1316.569	91.0	0.002
		12	48	1316.552	91.0	0.004
		16	64	1316.549	91.0	0.0004
	T1	1	7	1415.850	105	10.4
		2	14	1287.544	86.8	0.37
		4	28	1283.054	86.2	0.02
		8	56	1282.758	86.1	0.002
		12	84	1282.742	86.1	0.0003
		16	112	1282.739	86.1	0.0
	T	1	7	1407.286	104	10.3
		2	14	1281.011	85.8	0.37
		4	28	1276.588	85.2	0.02
		8	56	1276.297	85.2	0.002
		12	84	1276.281	85.2	0.0003
		16	112	1276.278	85.2	0.0

Table 4.7 Continued.

Mode	Element or Solution	No. of Elements	No. of DOF	Natural Frequency (Hz)	$\Delta_e(\%)$	$\Delta(\%)$
L		1	7	1145.679	66.2	
		2	13	1072.383	55.6	
		4	25	1069.741	55.2	
		8	49	1069.569	55.2	
		12	73	1069.559	55.2	
		16	97	1069.558	55.2	
M		1	13	993.794	44.2	
		2	24	943.295	36.9	
		4	46	941.463	36.6	
		8	90	941.344	36.6	
		12	134	941.338	36.6	
		16	178	941.337	36.6	
TS		1	13	711.887	3.29	
		2	24	690.127	0.13	
		4	46	689.351	0.02	
		8	90	689.302	0.008	
		12	134	689.299	0.008	
		16	178	689.299	0.008	
MS		1	31	711.835	3.28	
		2	54	690.073	0.12	
		4	100	689.296	0.008	
		8	192	689.247	0.0004	
		12	284	689.245	0.0001	
		16	376	689.244	0.0	

Table 4.7 Continued.

Mode	Element or Solution	No. of Elements	No. of DOF	Natural Frequency (Hz)	$\Delta_e(\%)$	$\Delta(\%)$
5	EE			4519.0	—	
	EBR			27,505	509	
	ET1			20,608	356	
	ET			19,669	335	
	BR	1	4	—		
		2	8	—		
		4	16	30,952	585	12.5
		8	32	27,755	514	0.91
		12	48	27,558	510	0.19
		16	64	27,523	509	0.07
	T1	1	7	49,287	991	139
		2	14	37,409	728	81.5
		4	28	21,950	386	6.51
		8	56	20,708	358	0.48
		12	84	20,629	356	0.10
		16	112	20,615	356	0.03
	T	1	7	46,021	918	134
		2	14	34,164	656	73.7
		4	28	20,827	361	5.89
		8	56	19,755	337	0.43
		12	84	19,687	336	0.09
		16	112	19,675	335	0.03

Table 4.7 Concluded.

Mode	Element or Solution	No. of Elements	No. of DOF	Natural Frequency (Hz)	$\Delta_e(\%)$	$\Delta(\%)$
L		1	7	27,745	514	
		2	13	13,435	197	
		4	25	9184.4	103	
		8	49	8980.6	98.7	
		12	73	8969.6	98.5	
		16	97	8967.8	98.4	
M		1	13	26,155	479	
		2	24	9844.0	118	
		4	46	7221.2	59.8	
		8	90	7016.2	55.3	
		12	134	7004.8	55.0	
		16	178	7003.0	55.0	
TS		1	13	24,918	451	
		2	24	5913.6	30.9	
		4	46	4720.7	4.46	
		8	90	4547.0	0.62	
		12	134	4537.2	0.40	
		16	178	4535.5	0.37	
MS		1	31	24,918	451	
		2	54	5912.3	30.8	
		4	100	4698.1	3.96	
		8	192	4531.0	0.27	
		12	284	4521.6	0.06	
		16	376	4520.0	0.02	

Table 4.8 Properties for Accuracy Calculations, Cases C2-XX and C3-XX.

Case	Remarks	$E$ (psi)	$G$ (psi)	$\rho$ (lb-s <sup>2</sup> /in <sup>4</sup> )	$d$ (in)	$L$ (in)	Boundary Conditions
C2-IA	Steel, $k = 2/3$ [111]	$30 \times 10^6$	$11.3 \times 10^6$	$7.25 \times 10^{-4}$	1	14.4	CF
C2-IB	Steel, $k = 0.65$ [111]	$30 \times 10^6$	$11.5 \times 10^6$	$7.25 \times 10^{-4}$	2.49	14.4	CF
C3-IA	Aluminum [64]	$10 \times 10^6$	$3.7 \times 10^6$	$2.6 \times 10^{-4}$	1	10	PS
C3-IB	Aluminum [64]	$10 \times 10^6$	$3.7 \times 10^6$	$2.6 \times 10^{-4}$	1	2	PS

Table 4.9 Convergence Data for Cases C2-IA and B [111].

Case	Mode	Element or Solution <sup>1</sup>	No. of Elements	No. of DOF	Natural Frequency (Hz)	$\Delta\%$
C2-IA	3	ET			2588.991	
		T	1	5	6617.355	156
			2	10	3087.754	19.3
			3	15	2619.154	1.17
			4	20	2606.775	0.69
			6	30	2593.157	0.16
			8	40	2590.373	0.05
C2-IB	3	ET			5015.466	
		T	1	5	7161.914	42.8
			2	10	5632.801	12.3
			3	15	5060.769	0.90
			4	20	5038.169	0.45
			6	30	5020.639	0.10
			8	40	5017.168	0.03

<sup>1</sup> Values from [64] obtained from a graph

Table 4.10 Accuracy Data for Cases C3-IA and B [64].

Case	Mode	Element or Solution <sup>2</sup>	No. of Elements	No. of DOF	Natural Frequency (Hz)	$\Delta\%$
C3-IA	1	EE			874.256	
		[64]	2	10	—	
			4	18	1690	94
			8	34	1130	29
			16	66	920	5.7
			32	130	890	1.7
		BR			See Case C1-IS	
		T1			"	
		T			"	
		L			"	
		M			"	
C3-IB	1	EE			16,598	—
		EE1	(No Transverse Normal Strain)		16,608	0.06
		[64]	2	10	23,500	42
			4	18	18,500	12
			8	34	16,900	2
			16	66	16,900	2
		BR	1	4	22,448	35.2
			2	8	20,327	22.5
			4	16	20,253	22.0
			8	32	20,248	22.0
			12	48	20,248	22.0

<sup>2</sup> Values from [64] obtained from a graph

Table 4.10 Concluded.

Case	Mode	Element or Solution	No. of Elements	No. of DOF	Natural Frequency (Hz)	$\Delta\%$
	T1		1	7	18,361	10.6
			2	14	17,129	3.20
			4	28	17,085	2.93
			8	56	17,082	2.92
			12	84	17,082	2.92
	T		1	7	17,754	6.97
			2	14	16,632	0.20
			4	28	16,592	-0.04
			8	56	16,589	-0.06
			12	84	16,589	-0.06
	L		1	7	17,784	7.15
			2	13	16,652	0.33
			4	25	16,611	0.08
			8	49	16,609	0.06
			12	73	16,609	0.06
	M		1	13	17,783	7.14
			2	24	16,651	0.32
			4	46	16,611	0.08
			8	90	16,608	0.06
			12	134	16,608	0.06



Table 4.11 Data for Study of Shear Locking.

Case	Mode	Element or Solution	Natural Frequency (Hz)	$\Delta\%$
SL-IS-10	1	EBR	885.654	—
		EE	874.258	0.99
		BR	885.668	1.00
		T1	876.139	0.99
		T	874.268	0.99
		L	874.272	0.99
		M	874.272	
-100	1	EBR	8.89252	—
		EE	8.89133	1.00
		BR	8.89266	1.00
		T1	8.89168	1.00
		T	8.89148	1.00
		L	8.89148	1.00
		M	8.89148	1.00
-1000	1	EBR	0.0889288	—
		EE	0.0889286	1.00
		BR	0.0889303	1.00
		T1	0.0889313	1.00
		T	0.0889293	1.00
		L	0.0889302	1.00
		M	0.0889305	1.00
-10,000	1	EBR	$8.89288 \times 10^{-4}$	—
		EE	$8.89289 \times 10^{-4}$	1.00
		BR	$8.89303 \times 10^{-4}$	1.00
		T1	$9.38573 \times 10^{-4}$	1.06
		T	$8.73952 \times 10^{-4}$	0.98
		L	$9.64814 \times 10^{-4}$	1.08
		M	Negative eigenvalue	—

Table 4.11 Continued.

Case	Mode	Element or Solution	Natural Frequency (Hz)	$\Delta\%$
SL-0R-10	i	EBR	1622.183	—
		EE	1410.283	0.87
		BR	1622.209	1.00
		T1	1439.375	0.89
		T	1409.656	0.87
		L	1410.327	0.87
		M	1410.314	0.87
-100	1	EBR	16.2877	—
		EE	16.2609	1.00
		BR	16.2880	1.00
		T1	16.2657	1.00
		T	16.2613	1.00
		L	16.2613	1.00
		M	16.2613	1.00
-1000	1	EBR	0.162884	—
		EE	0.162880	1.00
		BR	0.162887	1.00
		T1	0.162884	1.00
		T	0.162884	1.00
		L	0.162884	1.00
		M	0.162885	
-10,000	1	EBR	$1.62884 \times 10^{-3}$	—
		EE	$1.62891 \times 10^{-3}$	1.00
		BR	$1.62887 \times 10^{-3}$	1.00
		T1	$1.62402 \times 10^{-3}$	1.00
		T	$1.63613 \times 10^{-3}$	1.00
		L	$1.62169 \times 10^{-3}$	1.00
		M	$1.37656 \times 10^{-3}$	0.85

Table 4.11 Continued.

Case	Mode	Element or Solution	Natural Frequency (Hz)	$\Delta\%$
SL-L3-10	1	EBR	1593.214	—
		EE	1376.110	0.86
		BR	1593.240	1.00
		T1	1410.450	0.89
		T	1380.852	0.87
		L	1376.604	0.86
		M	1376.572	0.86
		TS	1390.508	0.87
		MS	1376.132	0.86
-100	1	EBR	15.9969	—
		EE	15.9691	1.00
		BR	15.9971	1.00
		T1	15.9748	1.00
		T	15.9703	1.00
		L	15.9696	1.00
		M	15.9695	1.00
		TS	15.9717	1.00
		MS	15.9695	1.00
-1000		EBR	0.159975	—
		EE	0.159972	1.00
		BR	0.159978	1.00
		T1	0.159976	1.00
		T	0.159975	1.00
		L	0.159975	1.00
		M	0.159973	1.00
		TS	0.159975	1.00
		MS	0.159996	1.00

Table 4.11 Continued.

Case	Mode	Element or Solution	Natural Frequency (Hz)	$\Delta\%$
-10,000	1	EBR	$1.59975 \times 10^{-3}$	—
		EE	$1.59959 \times 10^{-3}$	1.00
		BR	$1.59978 \times 10^{-3}$	1.00
		T1	$1.60667 \times 10^{-3}$	1.00
		T	$1.60546 \times 10^{-3}$	1.00
		L	$1.60347 \times 10^{-3}$	1.00
		M	$1.55007 \times 10^{-3}$	0.97
		TS	$1.57945 \times 10^{-3}$	0.99
		MS	$1.36868 \times 10^{-3}$	0.86
SL-S3-10	1	EBR	1316.547	—
		EE	689.244	0.52
		BR	1316.569	1.00
		T1	1282.758	0.97
		T	1276.297	0.97
		L	1069.569	0.81
		M	941.344	0.72
		TS	689.302	0.52
		MS	689.247	0.52
-100	1	EBR	13.2843	—
		EE	13.1058	0.99
		BR	13.2846	1.00
		T1	13.2809	1.00
		T	13.2802	1.00
		L	13.2494	1.00
		M	13.1061	0.99
		TS	13.1060	0.99
		MS	13.1060	0.99

Table 4.11 Concluded.

Case	Mode	Element or Solution	Natural Frequency (Hz)	$\Delta\%$
-1000	1	EBR	0.132855	—
		EE	0.132837	1.00
		BR	0.132858	1.00
		T1	0.132858	1.00
		T	0.132857	1.00
		L	0.132854	1.00
		M	0.132850	1.00
		TS	0.132837	1.00
		MS	0.133496	1.00
-10,000	1	EBR	$1.32856 \times 10^{-3}$	—
		EE	$1.32854 \times 10^{-3}$	1.00
		BR	$1.32858 \times 10^{-3}$	1.00
		T1	$1.34268 \times 10^{-3}$	1.01
		T	$1.34950 \times 10^{-3}$	1.02
		L	$1.32827 \times 10^{-3}$	1.00
		M	Negative eigenvalue	
		TS	Negative eigenvalue	
		MS	Negative eigenvalue	

Table 4.12 Properties for Accuracy Calculations, Cases A1-XX-XX.

Case	Remarks	$E$	$G$	$\rho$	$L$	$d$	Boundary Conditions
A1-L3-KP	Symmetric laminate [17]			1	10		SS
	Layer 1	4	0.6			0.333	
	Layer 2	2	0.5			0.334	
	Layer 3	4	0.6			0.333	
A1-L2-KP	Nonsymmetric laminate [17]						
				1	10		SS
	Layer 1	4	0.6			0.5	
	Layer 2	2	0.5			0.5	
A1-L2-J1	Nonsymmetric laminate [16]			1	10		SS
	Layer 1	4	1			1	
	Layer 2	1	1			1	
A1-L2-J2	Nonsymmetric laminate [16]			10	10		SS
	Layer 1	40	1			1	
	Layer 2	1	1			1	

Table 4.13 Accuracy Data for Cases from Kulkarni &amp; Pagano [17].

Case	Element	$md/L$	Nondimensional Natural Frequency	
			Flexural	Extensional
A1-L3-KP	BR	0	0	-
		0.2	0.17	0.87
		0.4	0.33	0.87
		0.6	0.46	0.87
		0.8	0.56	0.87
		1.0	0.65	0.87
		1.2	0.71	0.87
	T	0	0.15	-
		0.2	0.23	0.87
		0.4	0.27	0.87
		0.6	0.29	0.87
		0.8	0.30	0.87
		1.0	0.31	0.87
		1.2	0	0.87
	L	0	0	-
		0.2	0.15	0.87
		0.4	0.23	0.87
		0.6	0.27	0.87
		0.8	0.29	0.87
		1.0	0.30	0.87
		1.2	0.31	0.87
	M	0	0	-
		0.2	0.15	0.87
		0.4	0.23	0.86
		0.6	0.27	0.86
		0.8	0.29	0.85
		1.0	0.30	0.84
		1.2	0.31	0.83

Table 4.13 Continued.

Case	Element	$md/L$	Nondimensional Natural Frequency	
			Flexural	Extensional
A1-L2-KP	TS	0	0	-
		0.2	0.15	0.87
		0.4	0.23	0.86
		0.6	0.27	0.86
		0.8	0.29	0.86
		1.0	0.30	0.85
		1.2	0.31	0.84
	MS	0.2	0.15	0.87
		0.6	0.27	0.84
		1.2	0.31	0.79
	BR	0	0	-
		0.2	0.15	0.87
		0.4	0.28	0.87
		0.6	0.39	0.88
		0.8	0.48	0.88
		1.0	0.54	0.89
		1.2	0.59	0.90
	T	0	0	-
		0.2	0.14	0.86
		0.4	0.22	0.84
		0.6	0.26	0.81
		0.8	0.28	0.79
		1.0	0.29	0.77
		1.2	0.30	0.76



Table 4.13 Concluded.

Case	Element	$md/L$	Nondimensional Natural Frequency	
			Flexural	Extensional
L	L	0	0	-
		0.2	0.15	0.86
		0.4	0.22	0.84
		0.6	0.26	0.81
		0.8	0.29	0.78
		1.0	0.30	0.77
		1.2	0.31	0.76
M	M	0	0	-
		0.2	0.14	0.86
		0.4	0.22	0.84
		0.6	0.26	0.81
		0.8	0.28	0.78
		1.0	0.30	0.76
		1.2	0.31	0.75
TS	TS	0	0	-
		0.2	0.14	0.86
		0.4	0.22	0.84
		0.6	0.27	0.81
		0.8	0.30	0.79
		1.0	0.31	0.77
		1.2	0.32	0.76
MS	MS	0.2	0.13	0.86
		0.6	0.26	0.80
		1.2	0.31	0.74

Table 4.14 Accuracy Data for Cases from Jones [16].

Case	Element	$md/L$	Nondimensional Natural Frequency	
			Flexural	Extensional
A1-L2-J1	BR	0	0	-
		0.4	0.23	0.81
		0.8	0.38	0.84
		1.2	0.45	0.87
		1.6	0.49	0.90
		2.0	0.51	0.92
	T	0	0	-
		0.4	0.19	0.73
		0.8	0.26	0.64
		1.2	0.29	0.60
		1.6	0.30	0.58
		2.0	0.31	0.57
	L	0	0	-
		0.4	0.19	0.72
		0.8	0.27	0.63
		1.2	0.30	0.59
		1.6	0.32	0.57
		2.0	0.34	0.56
	M	0	0	-
		0.4	0.19	0.72
		0.8	0.26	0.62
		1.2	0.29	0.58
		1.6	0.31	0.55
		2.0	0.32	0.54

Table 4.14 Continued.

Case	Element	$md/L$	Nondimensional Natural Frequency	
			Flexural	Extensional
A1-L2-J2	TS	0	0	-
		0.4	0.19	0.74
		0.8	0.27	0.65
		1.2	0.30	0.59
		1.6	0.32	0.56
		2.0	0.33	0.54
	MS	0.4	0.19	0.72
		1.2	0.29	0.57
		2.0	0.32	0.53
	BR	0	0	-
		0.4	0.13	0.75
		0.8	0.21	0.80
		1.2	0.25	0.85
		1.6	0.27	0.89
		2.0	0.28	0.91
	T	0	0	-
		0.4	0.08	0.36
		0.8	0.10	0.32
		1.2	0.10	0.31
		1.6	0.10	0.31
		2.0	0.10	0.30
	L	0	0	-
		0.4	0.09	0.34
		0.8	0.11	0.29
		1.2	0.13	0.28
		1.6	0.15	0.28
		2.0	0.16	0.28

Table 4.14 Concluded.

Case	Element	$md/L$	Nondimensional Natural Frequency	
			Flexural	Extensional
	M	0	0	-
		0.4	0.08	0.31
		0.8	0.09	0.23
		1.2	0.10	0.21
		1.6	0.10	0.19
		2.0	0.10	0.18
	TS	0	0	-
		0.4	0.08	0.33
		0.8	0.09	0.23
		1.2	0.10	0.20
		1.6	0.10	0.18
		2.0	0.11	0.17
	MS	0.4	0.08	0.29
		1.2	0.10	0.19
		2.0	0.10	0.17

Table 4.15 Properties for Accuracy Calculations, Cases A2-XX.

Case	Remarks	$E$ (psi)	$G$ (psi)	$\rho$ (lb-s <sup>2</sup> /in <sup>4</sup> )	$d$ (in)	$L$ (in)	Boundary Conditions
A2-IA	Steel Beam	$30.45 \times 10^6$	$11.71 \times 10^6$	$7.34 \times 10^{-4}$	4.92125	19.685	CF
A2-IB	"	"	"	"	"	"	CC
A2-S3	Steel- Concrete-Steel Sandwich					100	PS
	Layer 1	$30 \times 10^6$	$12 \times 10^6$	$7.25 \times 10^{-4}$	1		
	Layer 2	$3 \times 10^6$	$1.2 \times 10^6$	$2.25 \times 10^{-4}$	5		
	Layer 3	$30 \times 10^6$	$12 \times 10^6$	$7.25 \times 10^{-4}$	1		
A2-S5	5-Layer Sandwich					20	PS
	Layers 1,3,5	$10 \times 10^6$	$3.7 \times 10^6$	1.0	0.02		
	Layers 2,4	$12.5 \times 10^3$	$5 \times 10^3$	0.25	0.4		

Table 4.16 Accuracy Data for Cases from Levinson [57].

Case	Mode	Element or Solution	Natural Frequency (Rad/s)		$\Delta\%$
			Levinson [57]	FE	
A2-IA	1	T <sup>1</sup>	2505	2505	0
		L	2480	2508	1.13
		M	2480	2506	1.05
	4	T	46,698	46,727	0.06
		L	46,095	47,788	3.68
		M	46,095	47,157	2.30
A2-IB	1	T	12,284	12,289	0.04
		L	11,985	12,468	4.03
		M	11,985	12,350	3.05
	4	T	61,782	61,843	0.10
		L	60,848	64,809	6.51
		M	60,848	62,949	3.45

<sup>1</sup>  $k = 5/6$

Table 4.17 Accuracy Data for Case A2-S3 from Miller [130].

Mode	Element or Solution	Natural Frequency	$\Delta\%$
1	EE	71.8	-
	[86] without shear	74.1	3.2
	[86] with shear	72.8	1.4
	[130]	74.1	3.2
	BR	74.1	3.2
	T1	73.4	2.2
	T	73.3	2.1
	L	72.3	0.7
	M	72.1	0.4
	TS	71.8	0.0
	MS	71.8	0.0
4	EE	819	-
	[86] without shear	1140	39
	[86] with shear	923	13
	[130]	1160	42
	BR	1140	39
	T1	1010	23
	T	994	21
	L	873	6.6
	M	854	4.3
	TS	821	0.2
	MS	820	0.1

Table 4.18 Accuracy Data for Case A2-S5 from Khatua and Cheung [126].

Mode	Element or Solution	No. of Elements	Natural Frequency (Rad/s)	$\Delta\%$
1	EE		10.912	-
	Kao and Ross	[89]	10.888	-0.22
	Khatua and Cheung	[126]	10.912	0
	BR		12.897	18.2
	T1		12.847	17.7
	T		12.837	17.6
	L		12.828	17.6
	M		12.823	17.5
	TS		10.914	0.02
	MS		10.912	0
5	EE		97.629	-
	Kao and Ross	[89]	97.593	-0.04
	Khatua and Cheung	[126]	98.475	0.87
	BR		317.07	225
	T1		291.77	199
	T		287.39	194
	L		283.92	191
	M		281.62	188
	TS		97.678	0.05
	MS		97.678	0.05



Table 4.19 Properties for Accuracy Calculations, Cases A3-XX-XX.

Case	Remarks	$E$ (psi)	$G$ (psi)	$\rho$ (lb-s <sup>2</sup> /in <sup>4</sup> )	$d$ (in)	$L$ (in)	Boundary Conditions
A3-S3-1	3-Layer Fiberglass Sandwich					20	CF
	Layers 1,3	$3.68 \times 10^6$	$1.47 \times 10^6$	$2.52 \times 10^{-4}$	0.02		
	Layer 2	$56.3 \times 10^3$	$22.5 \times 10^3$	$6 \times 10^{-6}$	0.5		
A3-S3-2A	3-Layer Aluminum Neoprene Sandwich					7.09	CF
	Layer 1,3	$10.3 \times 10^6$	$3.87 \times 10^6$	$2.6 \times 10^{-4}$	0.157		
	Layer 2, mode 1	545	218	$1.17 \times 10^{-4}$	0.118		
	mode 2	730	292				
A3-S3-2B	3-Layer Aluminum Neoprene Sandwich					7.09	CF
	Layer 1	$10.3 \times 10^6$	$3.87 \times 10^6$	$2.6 \times 10^{-4}$	0.197		
	Layer 2, mode 1	545	218	$1.17 \times 10^{-4}$	0.118		
	mode 2	730	292				
	Layer 3	$10.3 \times 10^6$	$3.87 \times 10^6$	$2.6 \times 10^{-4}$	0.0787		

Table 4.20 Accuracy Data for Case A3-S3-1 from Shoua [160].

Mode	Element or Solution	Natural Frequency (Hz)	$\Delta\%$
1	[160]	38.5	-
	BR	39.7	3.1
	T1	39.7	3.1
	T	39.7	3.1
	L	39.5	2.6
	M	39.5	2.6
	TS	39.5	2.6
	MS	39.5	2.6
4	[160]	1198	-
	BR	1353	13
	T1	1319	10
	T	1313	9.6
	L	1212	1.2
	M	1209	0.9
	TS	1191	-0.6
	MS	1191	-0.6

Table 4.21 Accuracy Data for Cases from Leibowitz and Lifshitz [161].

Case	Mode	Element or Solution	Natural Frequency (Hz)	$\Delta\%$
A3-S3-2A	1	[161]	115.5	-
		[83]	111.7	-3.3
		BR	296.5	157
		T1	295.8	156
		T	295.6	156
		L	295.3	156
		M	295.2	156
		TS	108.7	-5.9
		MS	108.7	-5.9
	2	[161]	612.0	-
		[83]	658.0	7.5
		BR	1849	202
		T1	1817	197
		T	1811	196
		L	1798	194
		M	1793	193
		TS	606.8	-0.8
		MS	606.6	-0.9

Table 4.21 Concluded.

Case	Mode	Element or Solution	Natural Frequency (Hz)	$\Delta\%$
A3-S3-2B	1	[161]	115.0	-
		[83]	119.2	3.7
		BR	255.0	122
		T1	254.5	121
		T	254.4	121
		L	254.3	121
		M	254.3	121
		TS	114.7	-0.3
		MS	114.7	-0.3
	2	[161]	631.0	-
		[83]	712.0	12.8
		BR	1592	152
		T1	1571	149
		T	1567	148
		L	1563	148
		M	1560	147
		TS	651.2	3.2
		MS	651.2	3.2

Table 4.22 Properties for Stacked-Element Study.

Case	$E_f/E_c$	$G_f/G_c$	$E_f/G_f$	$E_c/G_c$	$\rho_f/\rho_c$	$t_f/d$
Baseline	28.6	247	2.70	23.3	30	0.1
SE-S3-E1	10			66.7		
-E2	1			667		
-R1					3	
-R2					1	
-EG1		106		10		
-EG2		21.1		2		
-EG3	10	37		10		
-EG4	10	7.4		2		
-EG5	1	3.7		10		
-EG6	1	0.74		2		
-EG7	66.7			10		
-EG8	333			2		
-EG9	2.32	20				
-EG10	0.232	2				
-T1						0.01
-T2						0.333

Table 4.23 Data for Stacked-Element Study.

Case	Element or Solution	Natural Frequency for First Mode (Hz)	$\Delta_e(\%)$
SE-S3-E1	EE	691.61	-
	M	950.12	37
	MS	691.66	0.01
-E2	EE	705.32	-
	M	1017.53	44
	MS	705.48	0.02
-R1	EE	480.47	-
	M	656.74	37
	MS	480.50	0.01
-R2	EE	328.31	-
	M	444.92	37
	MS	328.33	0.01
-EG1	EE	900.04	-
	M	1029.46	14
	MS	900.15	0.01
-EG2	EE	1187.98	-
	M	1206.72	1.6
	MS	1188.23	0.02
-EG3	EE	1135.58	-
	M	1176.69	3.6
	MS	1135.79	0.02
-EG4	EE	1303.64	-
	M	1307.84	0.3
	MS	1303.96	0.02

Table 4.23 Concluded.

Case	Element or Solution	Natural Frequency for First Mode (Hz)	$\Delta_e(\%)$
-EG5	EE	1769.39	-
	M	1770.93	0.09
	MS	1769.81	0.02
-EG6	EE	1833.43	-
	M	1833.91	0.03
	MS	1833.90	0.03
-EG7	EE	688.42	-
	M	938.61	36
	MS	688.47	0.01
-EG8	EE	687.89	-
	M	936.85	36
	MS	687.95	0.01
-EG9	EE	1350.88	-
	M	1371.79	1.6
	MS	1351.15	0.02
-EG10	EE	2823.93	-
	M	2827.11	0.11
	MS	2824.59	0.02
-T1	EE	949.23	-
	M	959.91	1.1
	MS	949.39	0.02
-T2	EE	554.96	-
	M	1021.52	84
	MS	555.02	0.01

## LIST OF REFERENCES

1. Timoshenko, S.P., *History of Strength of Materials*, McGraw-Hill Book Co., Inc., New York, 1953, pp. 7-36.
2. Timoshenko, S.P., and Goodier, J.N., *Theory of Elasticity*, 3rd Ed., McGraw-Hill Book Co., New York, 1970.
3. Love, A.E.H., *A Treatise on the Mathematical Theory of Elasticity*, 4th Ed., Dover Publications, New York, 1944, p. 129.
4. Lekhnitskii, S.G., *Theory of Elasticity of an Anisotropic Elastic Body*, translated from the Russian by P. Fern, Holden-Day, Inc., San Francisco, 1963, pp. 89-94.
5. Little, R.W., *Elasticity*, Prentice-Hall, Inc., Englewood Cliffs, N.J., 1973, pp. 107-143.
6. Neou, C.Y., "A Direct Method for Determining Airy Polynomial Stress Functions," *Journal of Applied Mechanics*, Trans. ASME, Sept. 1957, pp. 387-390.
7. Hashin, Z., "Plane Anisotropic Beams," *Journal of Applied Mechanics*, Trans. ASME, June 1967, pp. 257-262.
8. Schile, R.D., "A Nonhomogeneous Beam in Plane Stress," *Journal of Applied Mechanics*, Trans. ASME, Sept. 1962, pp. 582-583.
9. Pagano, N.J., "Exact Solutions for Composite Laminates in Cylindrical Bending," *Journal of Composite Materials*, Vol. 3, July 1969, pp. 398-411.
10. Pagano, N.J., "Exact Solutions for Rectangular Bidirectional Composites and Sandwich Plates," *Journal of Composite Materials*, Vol. 4, Jan. 1970, pp. 20-34.
11. Pagano, N.J., and Hatfield, S.J., "Elastic Behavior of Multilayered Bidirectional Composites," *AIAA Journal*, Vol. 10, No. 7, July 1972, pp. 931-933.
12. Timoshenko, S.P., "On the Transverse Vibrations of Bars of Uniform Cross Section," *Philosophical Magazine*, Series 6, Vol. 43, No. 253, Jan. 1922, pp. 125-131.
13. Cooper, G.R., "On the Accuracy of Timoshenko's Beam Theory," *Journal of the Engineering Mechanics Division*, Proc. ASCE, EM6, Dec. 1968, pp. 1447-1453.
14. Srinivas, S., Joga Rao, C.V., and Rao, A.K., "An Exact Analysis for Vibration of Simply-Supported Homogeneous and Laminated Thick Rectangular Plates," *Journal of Sound and Vibration*, Vol. 12, No. 2, 1970, pp. 187-199.
15. Srinivas, S., and Rao, A.K., "Bending, Vibration and Buckling of Simply Supported Thick Orthotropic Rectangular Plates and Laminates," *International Journal of Solids and Structures*, Vol. 6, 1970, pp. 1463-1481.
16. Jones, A.T., "Exact Natural Frequencies for Cross-Ply Laminates," *Journal of Composite Materials*, Vol. 4, Oct. 1970, pp. 476-491.



17. Kulkarni, S.V., and Pagano, N.J., "Dynamic Characteristics of Composite Laminates," *Journal of Sound and Vibration*, Vol. 23, No. 1, 1972, pp.127-143.
18. Noor, A.K., "Free Vibrations of Multilayered Composite Plates," *AIAA Journal*, Vol. 11, No. 7, July 1973, pp. 1038-1039.
19. Langhaar, H.L., *Energy Methods in Applied Mechanics*, John Wiley and Sons, Inc., New York, 1962.
20. Reinfield, L.W., and Murthy, P.L.N., "Toward a New Engineering Theory of Bending: Fundamentals," *AIAA Journal*, Vol. 10, No. 5, May 1982, pp.693-699.
21. Suzuki, S., "Stress Analysis of Short Beams," *AIAA Journal*, Vol. 24, No. 8, Aug 1986, pp. 1396-1398.
22. Popov, E.P., *Mechanics of Materials*, 2nd Ed., Prentice-Hall, Inc., Englewood Cliffs, N.J., 1978.
23. Timoshenko, S.P., "Analysis of Bi-Metal Thermostats," *Journal of the Optical Society of America*, Vol. 11, Sept. 1925, pp. 233-255.
24. Allen H.G., *Analysis and Design of Structural Sandwich Panels*, Pergamon Press, Oxford, 1969.
25. Jones, R.M., *Mechanics of Composite Materials*, Hemisphere Publishing Corp., New York, 1975.
26. Timoshenko, S.P., Young, D.H., and Weaver, W., Jr., *Vibration Problems in Engineering*, 4th Ed., John Wiley and Sons, New York, 1974.
27. Rayleigh, Lord, *Theory of Sound*, 1st Ed., 1877, 2nd Ed., Dover Publications., New York, 1945, pp. 293-294.
28. Pister, K.S., "Flexural Vibration of Thin Laminated Plates," *Journal of the Acoustical Society of America*, Vol. 31 , No. 2, Feb. 1959, pp. 233-234.
29. Timoshenko, S.P., "On the Correction for Shear of the Differential Equation for Transverse Vibrations of Prismatic Bars," *Philosophical Magazine*, Series 6, Vol. 41, 1921, pp. 744-746.
30. Rankine, W.J.M., *A Manual of Applied Mechanics*, 1st Ed., London, 1858, 17th Ed., Charles Griffin and Co., Ltd., London, 1904, pp. 342-344.
31. Bresse, M., *Cours de Mechanique Applique*, 1st Ed., Mallet Bachelier, Paris, 1859, 3rd Ed., Gauthier-Villars, Paris, 1880, pp. 362-368.
32. Todhunter, I., and Pearson, K., *A History of the Theory of Elasticity*, Vol. 2, Pt. 1, Cambridge, 1893, (Dover Reprint, 1960), pp. 366-368.
33. Anderson, R.A., "Flexural Vibrations in Uniform Beams According to the Timoshenko Theory," *Journal of Applied Mechanics*, Trans. ASME, Dec. 1953, pp. 504-510.
34. Dolph, C.L., "On the Timoshenko Theory of Transverse Beam Vibrations," *Quarterly of Applied Mathematics*, Vol. 12, No. 2, 1954, pp. 175-187.

35. Huang, T.C., "The Effect of Rotary Inertia and of Shear Deformation on the Frequency and Normal Mode Equations of Uniform Beams with Simple End Conditions," *Journal of Applied Mechanics, Trans. ASME*, Dec. 1961, pp. 579-584.
36. Brunelle, E.J., "The Statics and Dynamics of a Transversely Isotropic Timoshenko Beam," *Journal of Composite Materials*, Vol. 4, July 1970, pp. 404-416.
37. Downs, B., "Transverse Vibration of a Uniform Simply Supported Timoshenko Beam without Transverse Deflection," *Journal of Applied Mechanics, Trans. ASME*, Dec. 1976, pp. 671-674.
38. Mindlin, R.D., and Deresiewicz, H., "Timoshenko's Shear Coefficient for Flexural Vibrations of Beams," *Proc., 2nd U.S. Congress of Applied Mechanics*, Ann Arbor, Michigan, June 1954, pp. 175-178.
39. Mindlin, R.D., "Influence of Rotary Inertia and Shear on Flexural Motions of Isotropic, Elastic Plates," *Journal of Applied Mechanics, Trans. ASME*, March 1951, pp. 31-38.
40. Yang, P.C., Norris, C.H., and Stavsky, Y., "Elastic Wave Propagation in Heterogeneous Plates," *International Journal of Solids and Structures*, Vol. 2, 1966, pp. 665-684.
41. Whitney, J.M., and Pagano, N.J., "Shear Deformation in Heterogeneous Anisotropic Plates," *Journal of Applied Mechanics, Trans. ASME*, Dec. 1970, pp. 1031-1036.
42. Traill-Nash, R.W., and Collar, A.R., "The Effects of Shear Flexibility and Rotary Inertia on the Bending Vibrations of Beams," *Quarterly Journal of Mechanics and Applied Mathematics*, Vol. 6, Pt. 2, 1953, pp. 186-222.
43. Kordes, E.E., and Kruszewski, E.T., "Experimental Investigation of the Vibrations of a Built-Up Rectangular Box Beam," NACA TN-3618, National Advisory Committee for Aeronautics, Washington, D.C., Feb. 1956.
44. Gere, J.M., and Timoshenko, S.P., *Mechanics of Materials*, 2nd Ed., Brooks/Cole Engineering Division, Monterey, California, 1984, pp. 660-666.
45. Cowper, G.R., "The Shear Coefficient in Timoshenko's Beam Theory," *Journal of Applied Mechanics, Trans. ASME*, June 1966, pp. 335-340.
46. Bert, C.W., "Simplified Analysis of Static Shear Factors for Beams of Nonhomogeneous Cross Section," *Journal of Composite Materials*, Vol. 7, Oct. 1973, pp. 525-529.
47. Whitney, J.M., "Shear Correction Factors for Orthotropic Laminates Under Static Load," *Journal of Applied Mechanics, Trans. ASME*, March 1973, pp. 302-304.
48. Basset, A.B., "On the Extension and Flexure of Cylindrical and Spherical Thin Elastic Shells," *Philosophical Transactions of the Royal Society of London*, Vol. 181, 1890, pp. 433-480.
49. Wang, J.T.S., and Dickson, J.N., "Elastic Beams of Various Orders," *AIAA Journal*, Vol. 17, No. 5, May 1979, pp. 535-537.
50. Suzuki, S., "Approximate Analysis of Deflections and Frequencies of Short Beams," *AIAA Journal*, Vol. 25, No. 11, Nov. 1987, pp. 1530-1532.

51. Krishna Murty, A.V., "Vibrations of Short Beams," *AIAA Journal*, Vol. 8, No. 1, Jan. 1970, pp. 34-38.
52. Krishna Murty, A.V., "Analysis of Short Beams," *AIAA Journal*, Vol. 8, No. 11, Nov. 1970, pp. 2098-2100.
53. Krishna Murty, A.V., "Vibrations of Laminated Beams," *Journal of Sound and Vibration*, Vol. 36, No. 2, 1974, pp. 273-284.
54. Krishna Murty, A.V., "Toward a Consistent Beam Theory," *AIAA Journal*, Vol. 22, No. 6, June 1984, pp. 811-816.
55. Krishna Murty, A.V., "On the Shear Deformation Theory for Dynamic Analysis of Beams," *Journal of Sound and Vibration*, Vol. 101, No. 1, 1985, pp.1-12.
56. Levinson, M., "A New Rectangular Beam Theory," *Journal of Sound and Vibration*, Vol. 74, No. 1, 1981, pp. 81-87.
57. Levinson, M., "Further Results of a New Beam Theory," *Journal of Sound and Vibration*, Vol. 77, No. 3, 1981, pp. 440-444.
58. Bickford, W.B., "A Consistent Higher Order Beam Theory," *Developments in Theoretical and Applied Mechanics*, Vol. 11, edited by T.J. Chung and G.R. Karr, University of Alabama, Huntsville, Alabama, 1982, pp. 137-150.
59. Levinson, M., "Consistent and Inconsistent Higher Order Beam and Plate Theories: Some Surprising Comparisons," *Refined Dynamical Theories of Beams, Plates and Shells and Their Applications*, Proc. on Euromech-Colloquium 219, edited by I. Elishakoff and H. Irretier, Springer-Verlag, New York, 1987, pp. 122-130.
60. Levison, M., "An Accurate Simple Theory of the Statics and Dynamics of Elastic Plates," *Mechanics Research Communications*, Vol. 7, No. 6, 1980, pp. 343-350.
61. Reddy, J.N., "A Simple Higher-Order Theory for Laminated Composite Plates," *Journal of Applied Mechanics, Trans. ASME*, Vol. 51, Dec. 1984, pp. 745-752.
62. Reddy, J.N., and Khdir, A.A., "Buckling and Vibration of Laminated Composite Plates using Various Plate Theories," *AIAA Journal*, Vol. 27, No. 12, Dec. 1989, pp. 1808-1817.
63. Yuan, F.G., and Miller, R.E., "Higher-Order Finite Element for Short Beams," *AIAA Journal*, Vol. 26, No. 11, Nov. 1988, pp.1415-1417.
64. Kant, T., and Gupta, A., "A Finite Element Model for a Higher-Order Shear-Deformable Beam Theory," *Journal of Sound and Vibration*, Vol. 125, No. 2, 1988, pp. 193-202.
65. Kant, T., and Manjunath, B.S., "Refined Theories for Composite and Sandwich Beams with C<sup>0</sup> Finite Elements," *Computers and Structures*, Vol. 33, No. 3, 1989, pp. 755-764.
66. Lo, K.H., Christensen, R.M., and Wu, E.M., "A Higher-Order Theory of Plate Deformation, Part 1: Homogeneous Plates; and Part 2: Laminated Plates," *Journal of Applied Mechanics, Trans. ASME*, Dec. 1977, pp. 663-676.

67. Reissner, E., "On Bending of Elastic Plates," *Quarterly of Applied Mathematics*, Vol. 5, No. 1, April 1947, pp. 55-68.
68. Reissner, E., "On the Theory of Bending of Elastic Plates," *Journal of Mathematics and Physics*, Vol. 23, 1944, pp. 184-191.
69. Reissner, E., "The Effects of Transverse Shear Deformation on the Bending of Elastic Plates," *Journal of Applied Mechanics, Trans. ASME*, Vol. 12, June 1945, pp. A69-A77.
70. Hoff, N.J., and Mautner, S.E., "Bending and Buckling of Sandwich Beams," *Journal of the Aeronautical Sciences*, Dec. 1948, pp. 707-720.
71. Yu, Y.Y., "A New Theory of Elastic Sandwich Plates -- One-Dimensional Case," *Journal of Applied Mechanics, Trans. ASME*, Sept. 1959, pp. 415-421.
72. Kimel, W.R., Raville, M.E., Kirmser, P.G., and Patel, M.P., "Natural Frequencies of Vibration of Simply Supported Sandwich Beams," Proc., 4th Midwest Conference on Solid and Fluid Mechanics, Austin, Texas, Sept. 1959, pp. 441-456.
73. Raville, M.E., Ueng, E.S., and Lei, M.M., "Natural Frequencies of Vibration of Fixed-Fixed Sandwich Beams," *Journal of Applied Mechanics, Trans. ASME*, Sept. 1961, pp. 367-371.
74. Cheng, S., "On the Theory of Bending of Sandwich Plates," Proc., 4th U.S. National Congress of Applied Mechanics, University of California, Berkeley, California, June 18-21, 1962, pp. 511-518.
75. Krajinovic, D., "Sandwich Beam Analysis," *Journal of Applied Mechanics, Trans. ASME*, Sept. 1972, pp. 773-778.
76. Krajinovic, D., "Vibrations of Laminated Beams," Proc., 13th Structures, Structural Dynamics, and Materials Conference, San Antonio, Texas, April 10-12, 1972, pp. 1-9.
77. DiTaranto, R.A., "Static Analysis of a Laminated Beam," *Journal of Engineering for Industry, Trans. ASME*, Aug. 1973, pp. 755-761.
78. Rao, D.K., "Static Response of Stiff-Cored Unsymmetric Sandwich Beams," *Journal of Engineering for Industry, Trans. ASME*, May 1976, pp. 391-396.
79. Rubayi, N.A., and Charoenree, S., "Natural Frequencies of Vibration of Cantilever Sandwich Beams," *Computers and Structures*, Vol. 6, 1976, pp. 345-353.
80. Kerwin, E.M., Jr., "Damping of Flexural Waves by a Constrained Viscoelastic Layer," *Journal of the Acoustical Society of America*, Vol. 31, No. 7, July 1959, pp. 952-962.
81. DiTaranto, R.A., "Theory of Vibratory Bending for Elastic and Viscoelastic Layered Finite-Length Beams," *Journal of Applied Mechanics, Trans. ASME*, Dec. 1965, pp. 881-886.
82. DiTaranto, R.A., and Blasingame, W., "Composite Damping of Vibration Sandwich Beams," *Journal of Engineering for Industry, Trans. ASME*, Nov. 1967, pp. 633-638.

83. Mead, D.J., and Markus, S., "The Forced Vibration of a Three-Layer, Damped Sandwich Beam with Arbitrary Boundary Conditions," *Journal of Sound and Vibration*, Vol. 10, No. 2, 1969, pp. 163-175.
84. Nicholas, T., "The Effects of Rotary Inertia and Shear Deformation on the Flexural Vibrations of a Two-Layered Viscoelastic-Elastic Beam," *Shock and Vibrations Bulletin*, Vol. 38, No. 3, 1968, pp. 13-28.
85. Yan, M.J., and Dowell, E.H., "Governing Equations for Vibrating Constrained-Layer Damping Sandwich Plates and Beams," *Journal of Applied Mechanics, Trans. ASME*, Dec. 1972, pp. 1041-1046.
86. Yan, M.J., and Dowell, E.H., "Elastic Sandwich Beam or Plate Equations Equivalent to Classical Theory," *Journal of Applied Mechanics, Trans. ASME*, June 1974, pp. 526-527.
87. Sadisiva Rao, Y.V.K., and Nakra, B.C., "Vibrations of Unsymmetrical Sandwich Beams and Plates with Viscoelastic Cores," *Journal of Sound and Vibration*, Vol. 34, No. 3, 1974, pp. 309-326.
88. Liaw, B.D., and Little, R.W., "Theory of Bending Multilayer Sandwich Plates," *AIAA Journal*, Vol. 5, No. 5, Feb. 1967, pp. 301-304.
89. Kao, J.S., and Ross, R.J., "Bending of Multilayer Sandwich Beams," *AIAA Journal*, Vol. 6, No. 8, Aug. 1968, pp. 1583-1585.
90. Roske, V.P., and Bert, C.W., "Vibrations of Multicore Sandwich Beams," *Shock and Vibrations Bulletin*, Vol. 40, Pt. 5, Dec. 1969, pp. 277-284.
91. DiSciuva, M., "Bending, Vibration and Buckling of Simply Supported Thick Multilayered Orthotropic Plates: An Evaluation of a New Displacement Model," *Journal of Sound and Vibration*, Vol. 105, No. 3, 1986, pp. 425-442.
92. Reddy, J.N., *An Introduction to the Finite Element Method*, McGraw-Hill, Inc., New York, 1984.
93. Logan, D.L., *A First Course in the Finite Element Method*, PWS-Kent Publishing Co., Boston, 1986.
94. Argyris, J.H., "Energy Theorems and Structural Analysis," *Aircraft Engineering*, Feb. 1955, pp. 42-58.
95. Argyris, J.H., and Kelsey, S., *Energy Theorems and Structural Analysis*, Butterworth's Scientific Publications, London, 1960, Plenum Press Reprint, New York, 1968.
96. Melosh, R.J., "A Stiffness Matrix for the Analysis of Thin Plates in Bending," *Journal of the Aerospace Sciences*, Vol. 28, No. 1, Jan. 1961, pp. 34-42.
97. Turner, M.J., Clough, R.W., Martin, H.C., and Topp, L.J., "Stiffness and Deflection Analysis of Complex Structures," *Journal of the Aeronautical Sciences*, Vol. 23, No. 9, Sept. 1956, pp. 805-854.
98. Archer, J.S., "Consistent Mass Matrix for Distributed Mass Systems," *Journal of the Structural Division, Proc. ASCE*, ST 4, Aug. 1963, pp. 161-178.

99. Leckie, F.A., and Lindberg, G.M., "The Effect of Lumped Parameters on Beam Frequencies," *Aeronautical Quarterly*, Aug. 1963, pp. 224-240.
100. Coulter, B.A., and Miller, R.E., "Vibration and Buckling of Beam-Columns Subjected to Non-Uniform Axial Loads," *International Journal for Numerical Methods in Engineering*, Vol. 23, 1986, pp. 1739-1755.
101. Archer, J.S., "Consistent Matrix Formulations for Structural Analysis," *AIAA Journal*, Vol. 3, No. 10, Oct. 1965, pp. 1910-1918.
102. Przemieniecki, J.S., *Theory of Matrix Structural Analysis*, McGraw-Hill Book Co., New York, 1968, pp. 72-82 and 292-297.
103. Kapur, K.K., "Vibrations of a Timoshenko Beam, Using Finite-Element Approach," *Journal of the Acoustical Society of America*, Vol. 40, No. 5, 1966, pp. 1058-1063.
104. Severn, R.T., "Inclusion of Shear Deflection in the Stiffness Matrix for a Beam Element," *Journal of Strain Analysis*, Vol. 5, No. 4, 1970, pp. 239-241.
105. Pian, T.H.H., "Derivation of Element Stiffness Matrix by Assumed Stress Distributions," *AIAA Journal*, Vol. 2, No. 7, July 1964, pp. 1333-1336.
106. Nickel, R.E., and Secor, G.A., "Convergence of Consistently Derived Timoshenko Beam Finite Elements," *International Journal for Numerical Methods in Engineering*, Vol. 5, 1972, pp. 243-252.
107. Prathap, G., and Bhashyam, G.R., "Reduced Integration and the Shear-Flexible Beam Element," *International Journal for Numerical Methods in Engineering*, Vol. 18, 1982, pp. 195-210.
108. Prathap, G., and Ramesh Babu, C., "Field-Consistent Strain Interpolations for the Quadratic Shear Flexible Beam Element," *International Journal for Numerical Methods in Engineering*, Vol. 23, 1986, pp. 1973-1984.
109. Egle, D.M., "Approximate Theory for Transverse Shear Deformation and Rotary Inertia Effects in Vibrating Beams," NASA CR-1317, National Aeronautics and Space Administration, Washington, D.C., May 1969.
110. Davis, R., Henshell, R.D., and Warburton, G.B., "A Timoshenko Beam Element," *Journal of Sound and Vibration*, Vol. 22, No. 4, 1972, pp. 475-487.
111. Thomas, D.L., Wilson, J.M., and Wilson, R.R., "Timoshenko Beam Finite Elements," *Journal of Sound and Vibration*, Vol. 31, No. 3, 1973, pp. 315-330.
112. Narayanaswami, R., and Adelman, H.M., "Inclusion of Transverse Shear Deformation in Finite Element Displacement Formulations," *AIAA Journal*, Vol. 12, No. 11, Nov. 1974, pp. 1613-1614.
113. Thomas, J., and Abbas, B.A.H., "Finite Element Model for Dynamic Analysis of Timoshenko Beam," *Journal of Sound and Vibration*, Vol. 41, No. 3, 1975, pp. 291-299.
114. Dawe, D.J., "A Finite Element for the Vibration Analysis of Timoshenko Beams," *Journal of Sound and Vibration*, Vol. 60, No. 1, 1978, pp. 11-20.

115. Heyliger, P.R., and Reddy, J.N., "A Higher-Order Beam Finite Element for Bending and Vibration Problems," *Journal of Sound and Vibration*, Vol. 126, No. 2, 1988, pp. 309-326.
116. Pryor, C.W. Jr., and Barker, R.M., "A Finite-Element Analysis Including Transverse Shear Effects for Applications to Laminated Plates," *AIAA Journal*, Vol. 9, No. 5, May 1971, pp. 912-917.
117. Epstein, M., and Glockner, P.G., "Nonlinear Analysis of Multilayered Shells," *International Journal of Solids and Structures*, Vol. 13, 1977, pp. 1081-1089.
118. Epstein, M., and Glockner, P.G., "Deep and Multilayered Beams," *Journal of the Engineering Mechanics Division*, Proc. ASCE, EM6, Dec. 1981, pp. 1029-1037.
119. Epstein, M., and Huttelmaier, H.P., "A Finite Element Formulation for Multilayered and Thick Plates," *Computers and Structures*, Vol. 16, No. 5, 1983, pp. 645-650.
120. Pinsky, P.M., and Kim, K.O., "A Multi-Director Formulation for Nonlinear Elastic-Viscoelastic Layered Shells," *Computers and Structures*, Vol. 24, No. 6, 1986, pp. 901-913.
121. DiSciua, M., "Development of an Anisotropic, Multilayered Shear-Deformable Rectangular Plate Element," *Computers and Structures*, Vol. 21, No. 4, 1985, pp. 789-796.
122. Chaudhuri, R.A., and Seide, P., "Triangular Element for Analysis of Perforated Plates Under Inplane and Transverse Loads," *Computers and Structures*, Vol. 24, No. 1, 1986, pp. 87-95.
123. Chaudhuri, R.A., and Seide, P., "Triangular Element for Analysis of a Stretched Plate Weakened by a Part-Through Hole," *Computers and Structures*, Vol. 24, No. 1, 1986, pp. 97-105.
124. Chaudhuri, R.A., and Seide, P., "Triangular Finite Element for Analysis of Thick Laminated Plates," *International Journal for Numerical Methods in Engineering*, Vol. 24, 1987, pp. 1203-1224.
125. Chaudhuri, R.A., and Seide, P., "An Approximate Semi-Analytical Method for Prediction of Interlaminar Shear Stresses in an Arbitrarily Laminated Thick Plate," *Computers and Structures*, Vol. 25, No. 4, 1987, pp. 626-636.
126. Khatua, T.P., and Cheung, Y.K., "Bending and Vibration of Multilayer Sandwich Beams and Plates," *International Journal for Numerical Methods in Engineering*, Vol. 6, 1973, pp. 11-24.
127. Yuan, F.G., and Miller, R.E., "A New Finite Element for Laminated Composite Beams," *Computers and Structures*, Vol. 31, No. 5, 1989, pp. 737-745.
128. Yuan, F.G., and Miller, R.E., "A Higher Order Finite Element for Laminated Beams," *Composite Structures*, Vol. 14, 1990, pp. 125-150.
129. Miller, R.E., "Reduction of the Error in Eccentric Beam Modelling," *International Journal for Numerical Methods in Engineering*, Vol. 15, 1980, pp. 575-582.
130. Miller, R.E., "Dynamic Aspects of the Error in Eccentric Beam Modelling," *International Journal for Numerical Methods in Engineering*, Vol. 15, 1980, pp. 1447-1455.

131. Gupta, A.K., and Ma, P.S., "Error in Eccentric Beam Formulation," *International Journal for Numerical Methods in Engineering*, Vol. 11, 1977, pp. 1473-1477.
132. Balmer, H.A., "Another Aspect of the Error in Eccentric Beam Formulation," *International Journal for Numerical Methods in Engineering*, Vol. 12, 1978, pp. 1761-1763.
133. Pian, T.H.H., and Tong, P., "Basis of Finite Element Methods for Solid Continua," *International Journal for Numerical Methods in Engineering*, Vol. 1, 1969, pp. 3-28.
134. Melosh, R.J., "Basis for Derivation of Matrices for the Direct Stiffness Method," *AIAA Journal*, Vol. 1, No. 7, July 1963, pp. 1631-1637.
135. Fraeijs de Veubeke, B.M., "Upper and Lower Bounds in Matrix Structural Analysis," AGARDograph 72, Pergamon Press, Oxford, 1964, pp. 165-201.
136. Tong, P., and Pian, T.H.H., "A Variational Principle and the Convergence of a Finite-Element Method Based on Assumed Stress Distribution," *International Journal of Solids and Structures*, Vol. 5, 1969, pp. 463-472.
137. Reissner, E., "On a Variational Theorem in Elasticity," *Journal of Mathematics and Physics*, Vol. 29, No. 2, July 1950, pp. 90-95.
138. Washizu, K., *Variational Methods in Elasticity and Plasticity*, Pergamon Press, Oxford, 1968, pp. 31-38.
139. Hellinger, E., "Die allgemeinen Ansätze der Mechanik der Kontinua," *Encyklopadie der Mathematischen Wissenschaften*, Vol. 4, Pt. 4, 1914, pp. 601-694.
140. Hu, H.C., "On Some Variational Principles in the Theory of Elasticity and Plasticity," *Scientia Sinica*, Vol. 4, No. 1, March 1955, pp. 33-54.
141. Washizu, K., "On the Variational Principles of Elasticity and Plasticity," ASRL-TR-25-18, Aeroelastic and Structures Research Laboratory, Massachusetts Institute of Technology, Cambridge, Massachusetts, March 1955.
142. Zienkeiwicz, O.C., and Lefebvre, D., "Three-field Mixed Approximation and the Plate Bending Problem," *Communications in Applied Numerical Methods*, Vol. 3, 1987, pp. 301-309.
143. Oliveira, E., "Theoretical Foundation of the Finite Element Method," *International Journal of Solids and Structures*, Vol. 4, 1968, pp. 929-952.
144. Oliveira, E., "Completeness and Convergence in the Finite Element Method," Proc., 2nd Conference on Matrix Methods in Structural Mechanics, Air Force Institute of Technology, Wright-Patterson Air Force Base, Ohio, 15-17 Oct. 1968, (published as AFFDL-TR-68-150, Air Force Flight Dynamics Laboratory, Wright-Patterson Air Force Base, Ohio, Dec. 1969) pp. 1061-1089.
145. Zienkeiwicz, O.C., *The Finite Element Method in Engineering Science*, McGraw-Hill Publishing Co. Ltd., London, 1971.
146. Cook, R.D., *Concepts and Applications of Finite Element Analysis*, 2nd Ed., John Wiley and Sons, New York, 1981, pp. 421-422.



147. Zienkiewicz, O.C., Taylor, R.L., and Too, J.M., "Reduced Integration Technique in General Analysis of Plates and Shells," *International Journal for Numerical Methods in Engineering*, Vol. 3, 1971, pp. 275-290.
148. Hughes, T.J.R., Taylor, R.L., and Kanoknukulchai, W., "A Simple and Efficient Finite Element for Plate Bending," *International Journal for Numerical Methods in Engineering*, Vol. 11, 1977, pp. 1529-1543.
149. Hughes, T.J.R., Cohen, M., Haroun, M., "Reduced and Selective Integration Techniques in the Finite Element Analysis of Plates," *Nuclear Engineering and Design*, Vol. 46, 1978, pp. 203-222.
150. Hughes, T.J.R., *The Finite Element Method*, Prentice-Hall, Inc., Englewood Cliffs, New Jersey, 1987.
151. Malkus, D.S., and Hughes, T.J.R., "Mixed Finite Element Methods - Reduced and Selective Integration Techniques: A Unification of Concepts," *Computer Methods in Applied Mechanics and Engineering*, Vol. 15, 1978, pp. 63-81.
152. Zienkiewicz, O.C., and Lefebvre, D., "A Robust Triangular Plate Bending Element of the Reissner-Mindlin Type," *International Journal for Numerical Methods in Engineering*, Vol. 26, 1988, pp. 1169-1184.
153. Pinsky, P.M., and Jasti, R.V., "A Mixed Finite Element Formulation for Reissner-Mindlin Plates Based on the Use of Bubble Functions," *International Journal for Numerical Methods in Engineering*, Vol. 28, 1989, pp. 1677-1702.
154. *IMSL Math/Library User's Manual*, Vol. 1, IMSL, Inc., Houston, TX, 1987, pp. 295-297.
155. Biggs, J.M., *Introduction to Structural Dynamics*, McGraw-Hill Book Co., New York, 1964, p. 201.
156. Beer, F.P., and Johnston, E.R., Jr., *Mechanics of Materials*, McGraw-Hill Book Co., New York, 1981, p. 584.
157. Whitney, J.M., and Sun, C.T., "Transient Response of Laminated Composite Plates Subjected to Transverse Dynamic Loading," *Journal of the Acoustical Society of America*, Vol. 61, No. 1, Jan. 1977, pp. 101-104.
158. Khdeir, A.A., and Reddy, J.N., "Exact Solutions for the Transient Response of Symmetric Cross-Ply Laminates Using a Higher-Order Plate Theory," *Composites Science and Technology*, Vol. 34, 1989, pp. 205-224.
159. Carnegie, W., Thomas, J., and Dokumaci, E., "An Improved Method of Matrix Displacement Analysis in Vibration Problems," *The Aeronautical Quarterly*, Nov. 1969, pp. 321-332.
160. Shoua, E.D., "The Composite Damping Capacity of Sandwich Cantilever Beams," *Experimental Mechanics*, July 1968, pp. 300-308.
161. Leibowitz, M., and Lifshitz, J.M., Experimental Verification of Modal Parameters for 3-Layered Sandwich Beams, *International Journal of Solids and Structures*, Vol. 26, No. 2, 1990, pp. 175-184.

## VITA

Stephen Robert Whitehouse was born on May 1, 1954, at [REDACTED]

He was graduated from the United States Air Force Academy in May 1978 with a Bachelor of Science Degree in Engineering Mechanics and a commission as a second lieutenant in the United States Air Force. He then attended Columbia University as a Guggenheim Fellow, receiving a Master of Science Degree in Engineering Mechanics in May 1979. Following graduation from Columbia University, he served as a research structural engineer in the Civil Engineering Research Division of the Air Force Weapons Laboratory in Albuquerque, New Mexico, from June 1979 to June 1984. After this assignment, he taught in the Department of Engineering Mechanics at the United States Air Force Academy from June 1984 to August 1987. Subsequently, he attended the University of Illinois from August 1987 to August 1990 as a graduate student in the Department of Theoretical and Applied Mechanics. While at the University of Illinois, he was inducted into the Phi Kappa Phi Honorary Society. Major Whitehouse's publications include:

"MX Structural Dynamics Modeling Document," AFWL-TR-82-93, Air Force Weapons Laboratory, Kirtland Air Force Base, New Mexico, April 1983 (S.R. Whitehouse, principal author, with 6 others).

"An Evaluation of Simple Equipment-Response Models Against Data from the Multi-Unit Structures Test (MUST) Series," *Proceedings*, International Symposium on the Interaction of Conventional Munitions with Protective Structures, Mannheim, Germany, March 9-13, 1987.

"The Feasibility of Using Scale Models to Determine the Natural Frequencies of Large Shock-Isolated Structures," *Proceedings*, 58th Shock and Vibrations Symposium, Huntsville, Alabama, October 13-15, 1987.

"Single-Degree-of-Freedom Structural Response Model Accounting for Soil-Structure Interaction," *Proceedings*, 7th American Society of Civil Engineers Structures and Pacific Rim Engineering Congress, San Francisco, California, May 1-5, 1989.